UNIVERSITEIT VAN PRETORIA
UNIVERSITY OF PRETORIA
YUNIBESITHI YA PRETORIA

SKELETAL MORPHOLOGY OF THE HUMAN HAND AS APPLIED IN FORENSIC ANTHROPOLOGY

NADIA NAVSA

Thesis submitted in fulfillment of the requirements for the degree PhD Anatomy

In the Faculty of Health Sciences, University of Pretoria, Pretoria

2010

DECLARATION

I declare that this thesis is my own unaided work. It is being submitted for the degree of Doctor of Philosophy in Anatomy at the University of Pretoria, Pretoria. It has not been submitted before for any degree or examination in any other University.

……....

Nadia Navsa

……day of ……2010

TABLE OF CONTENTS

List of figures

List of tables

ABSTRACT

The lack of detailed descriptions makes positive identification of individual bones of the human hand difficult. In some instances, labelled photographs and line diagrams depicting a few anatomical features are available in the literature while in other cases, unlabelled photographs and diagrams are provided. Textbooks generally describe each hand bone as having a head, shaft and base. The morphology of metacarpals is more commonly described than that of the phalanges. Thus, identification and siding of hand bones are rare, which excludes them from use in many forensic cases. Forensic anthropological studies also include the determination of demographic characteristics such as stature and sex. Parts of the human skeleton that are accurate predictors in determining stature and sex include the skull, pelvis, femur and tibia. Hand bones are often excluded from such studies due to their relatively small size and poor preservation. The aims of this study were firstly, to provide detailed morphological descriptions of metacarpals and phalangeal bones of the human hand; secondly, to develop regression formulae for stature using the hand bones and thirdly, to develop discriminant function formulae in which the hand bones can be used to determine the sex of an unknown individual. The study comprised 200 sets of hands of South African individuals. The results indicate that there are morphological features of individual bones of the human hand that can be used to identify and side them. Regression formulae have been devised whereby the length of a hand bone can be regressed to that of a long bone, which in turn can then be used to determine stature. The sexing accuracy, using the bones of the hand, is high for males and females. Average accuracies recorded were more than 80% in most cases, and more than 75% in all cases. Analyses of human hand bones can thus add valuable information when assessing skeletons of unknown individuals.

OPSOMMING

Weens die gebrek aan uitvoerige beskrywings, is dit moeilik om afsonderlike beentjies van die menslike hand positief te identifiseer. Soms is daar geannoteerde foto's en lyndiagramme in die literatuur beskikbaar, wat 'n paar anatomiese eienskappe uitbeeld, maar in ander gevalle is die fotos en lyndiagramme onbenoem. In handboeke word elke handbeentjie gewoonlik beskryf as synde met 'n kop, skag en basis. Die morfologie van die metakarpaalbene word meer dikwels beskryf as dié van die falankse. Identifikasie en die kant bepaling van handbeentjies is dus skaars en so word hulle van baie forensiese gevalle uitgesluit. Forensiese antropologiese studies sluit ook die bepaling van demografiese eienskappe soos liggamslengte en geslag in. Die skedel, bekken, femur en tibia van die menslike skedel is akkurate aanduiders by die bepaling van statuur en geslag. Handbeentjies word dikwels van sulke studies uitgelaat omdat hulle relatief klein en swak bewaar is. Die doel van hierdie studie was ten eerste die voorsiening van gedetailleerde morfologiese beskrywings van metakarpale en falankse van die menslike hand, tweedens, die ontwikkeling van omskakelingsformules vir statuur met aanwending van die handbeentjies en derdens, die ontwikkeling van diskriminante funksie formules waarby die handbeentjies gebruik kan word om die geslag van 'n onbekende individue te bepaal. Die studie het bestaan uit 200 stelle handbeentjies van Suid-Afrikaanse individu. Die resultate dui aan dat daar benige landmerke is om elke handbeen te identifiseer en te onderskei tussen links en regs. Die onderskeie beentjies van die menslike hand se lengte kan gebruik word om dié van 'n langbeen te bepaal, wat op sy beurt gebruik kan word om statuur te bedien. Akkuraatheid van geslagsbepaling deur middel van handbeentjies is hoog vir mans en vrouens. Gemiddelde betroubaarheid was meer as 80%. Ontleding van menslike handbeentjies kan dus 'n waardevolle bydrae lewer by die ondersoek van skelette van onbekende individue.

ACKNOWLEDGEMENTS

This subject was a difficult and rare one, especially the descriptive aspect. Nevertheless, I have found it most heartening and it has taken great pains to bring out this work with the help of the Almighty.

My first encounter with Prof M Yasar İşcan and the many discussions we had concerning the problems facing forensic scientists in identifying and siding hand bones gave me the strong incentive to do a PhD on the skeleton of the hand. The statistical analysis was a great task indeed and would not have been possible without the assistance of Prof MY İşcan's and Dr SAS Olorunju from the Biostatistics Unit at the University of Pretoria and Prof M Steyn's motivation. I am grateful to Prof M Steyn who encouraged me to pursue the questions as a PhD student and gave me guidance and support throughout. I am most grateful to Prof JH Meiring for allowing me access to the dissection cadavers and Pretoria Bone Collection.

For the technical assistance, I would like to thank Mr Erik Marakalla, who assisted in the maceration of the skeletons and to Mrs Louisa Hutten who made the gruelling task of photographing each hand bone appear so easy. I thank her for the patience and skill she exercised in this task. I am grateful to Mrs Marinda Pretorius for all the line diagrams, to Mrs AM Du Plessis, Mrs Santie Swarts and Marius Loots for their advice in formatting the entire document. Thanks to the library staff, especially Mrs Janice de Wee and Mrs Kabelo Nzima, who were most helpful with obtaining all the references I needed.

My gratitude is extended to the students who volunteered to read the descriptive chapters. A word of thanks to Leona Vorster, Susan Gaigulo, and Chantal Van Roey for assisting with refworks and editing of the references. My thanks also goes to the Anatomy staff and the many friends who always passed a word of encouragement throughout this period. There are a number of people that I have not mentioned but that I hold dear to my heart for their words of wisdom.

This thesis would not have been possible without the help, patience, encouragement from my family especially my mother, Rita (Ruwayda) Angela Marrian. To my nieces, Naseemah and

Nazeerah Mia, and my sisters Naeema Mia and Bedelia Anastasia Padiachy, there will be more free time now to spend with you.

It is said that there are two kinds of knowledge, the knowledge of religions and the knowledge of the body. I pray that I have fulfilled both of these in an attempt to better understand the design of each bone of the hand with the wisdom given to me by the Almighty Insha Allaah Ameen.

CHAPTER 1

INTRODUCTION

1.1 General introduction

Anatomy textbooks provide very little information regarding descriptions of individual bones of the human hand. The metacarpals are more readily described than the phalanges. This is because metacarpals are asymmetrical in their morphology which allows them to be easily distinguished from each other. The identification of phalanges, on the other hand, poses a problem in that they are symmetrical in their morphology which makes it almost impossible not only to distinguish them from each other, but also to side them. A further problem arises when looking at the morphology of the three phalangeal series of hand bones. Proximal and middle phalanges have similar morphological features while distal phalangeal bones differ from those of the proximal and middle rows in that they are not only relatively smaller, but the distal end has a non-articulating surface (Romanes 1991, Bass 1995, Moore & Dalley 2006).

The availability of human hands from skeletal collections and cadavers obtained from dissections has provided the opportunity for detailed morphological analyses of these hands. This information may complement analyses of skeletal elements from other parts of the human body used in various anthropological and forensic cases. It may also allow for an indirect assessment of hand function (Ricklan 1987). Analyzing form and structure of human hand bones from juveniles, has led Scheuer and Elkington (1993) to suggest that it is possible to derive distinguishing features which could be used not only to identify, but also to side individual hand bones. No studies, providing such detailed descriptions of the morphology of hand bones of the South African population, have been carried out.

The asymmetry of human hand morphology and human variation in general, is derived from various sources, including biological inheritance. One of the important aspects of physical anthropology is to identify and assess various aspects of human variation which is governed by mutations, genetic drift, natural selection, social and cultural environment (Nishihara *et al*. 2003, Singh 1959). During this assessment, attempts are made to discover factors that cause

similarities as well as differences. Such factors may arise from human evolution, impact of the environment, sociocultural variation, wars and mass disasters.

Skeletons or skeletal remains are often discovered commingled. This makes it difficult to identify victims, not to mention putting parts of the skeleton together based on age, sex, population affinity and stature (Krogman & İşcan 1986). Forensic anthropology, which is a speciality within forensic medicine and a branch of physical anthropology, involves the assessment of such human skeletonized remains and their environments (Krogman & İşcan 1986). To the qualified specialist in the area of identifying human skeletal remains, a thorough knowledge on various fields such as comparative osteology, human osteology, craniometry, osteometry and racial morphology, is crucial in order to carry out these assessments (Krogman & İşcan 1986). The assessment of stature from skeletal remains contributes greatly to the identification process. Long bones are commonly used to determine stature (Black 1978, Dayal 2002, De Mendonca 2000).

The high homicide rate in South Africa has resulted in considerable growth in the field of forensic science and forensic anthropology (Steyn & İşcan 1997). Forensic cases present with bodies in an advanced or complete stage of decomposition where only the skeleton is discernable. In these forensic cases, as much information as can be gathered is required in order to identify individuals. The surge in research in this country is thus devoted primarily to devising standards that are specific for its population. This is because available skeletal forensic identification standards are based on North American and European samples which cannot be applied to South African studies or any other population (Steyn & İşcan 1999).

The aim behind these projects is to establish sufficient data that would assist in medico-legal investigations in South Africa (Franklin *et al*. 2006). Alongside the establishment of stature estimation methods for the South African population, a steady increase in research on the determination of sex for this population group occurred. While various aspects of the human skeleton have been used to determine sex for the South African population (e.g., De Villiers 1968, Kieser *et al*. 1992, Loth & Henneberg 1996, Steyn & İşcan 1997, 1998, 1999, Asala 2001, Asala 2002, Bidmos & Asala 2003, Bidmos & Dayal 2003, 2004, Asala *et al*. 2004,

Bidmos & Asala 2004, Dayal & Bidmos 2005, Barrier 2007, Barrier & L'Abbé 2008, Franklin *et al*. 2006, 2008, Patriquin *et al*. 2003, 2005), no studies on the use of hands to determine the sex or height of an unknown individual has been done. Thus, no discriminant function or regression formulae using the hand bones are available for this population group.

Exploration of the hands in sexually dimorphic studies, has received very little attention in the past. This has now changed as current research has shown that the epiphyseal regions of long bones are more susceptible to damage than the smaller long bones of the hands and feet which are often found to be complete. This motivates for their use in establishing differences between males and females (Scheuer & Elkington 1993, Lazenby 1994, Falsetti 1995, Smith 1996). The use of the skeletal elements of the hands as an aid in identifying the sex of an unknown individual in South Africa is lacking. Thus, no discriminant function formulae for the hand bones have been devised for this population group.

1.2 Aims

The aim of this investigation is to analyse the metacarpals and phalanges of the human hand. In this analysis, the following aspects will be addressed:

A. The development of methods and descriptions that would enable researchers to identify these bones as far as their side and number are concerned.

B. To determine the length of a specific long bone by the length of a specific hand bone. The value obtained can then be inserted into regression formulae devised by Lundy and Feldesman (1987) and Dayal *et al*. (2008) for final estimation of stature.

C. Various measurements will be taken in order to assess sex differences using metacarpals and phalanges. From these measurements, discriminant function formulae will be devised.

1.3 Hypotheses

The information and data obtained from aim A above, will then be used to verify or nullify the following hypotheses:

1. The lengths of the metacarpals and phalanges of the human hand can be used to estimate the length of a long bone which in turn can be used to determine stature of an unknown individual, through the use of regression equations. This hypothesis will be accepted if the standard errors of the equations are of similar magnitude than those obtained for other long bones of the body.
2. The dimensions of the metacarpals and phalanges of the human hand can be used to determine the sex of an unknown individual through the use of discriminant function formulae. This hypothesis will be accepted if more than 80% of the individuals in the sample are correctly assigned.

CHAPTER 2

LITERATURE REVIEW - MORPHOLOGY OF THE HAND BONES

2.1 Introduction and general anatomical descriptions

The internal skeleton serves as a basic framework for the human body. Within this framework are a number of individual bones including the skeletal elements of the hand. Modern humans use their hands primarily for object manipulation with each digit designed to carry out a particular function (Tocheri *et al*. 2003). Based on its function, each digit displays variation in its structure. One of the important aspects of physical anthropology is to identify and assess not only human differences, but also those variations that may exist in hand morphology. During this assessment, there are attempts to discover factors that would cause similarities as well as differences in morphological structure. Such factors may arise from human evolution (Aiello 1992), impact of the environment and sociocultural variation (Nishihara *et al*. 2003).

Human osteology, which is the study of the human skeletal system, is one discipline that is used to gain this knowledge. Textbooks on human osteology have provided brief descriptions on various parts of the skeleton. To the qualified specialist in the field of identifying human skeletal remains, a thorough knowledge on various fields are crucial, including knowledge of human osteology, osteometry and morphology (İşcan 2000, 2004).

It has been suggested that the shape of a bone is determined largely by intrinsic factors with extrinsic factors playing a minor role. Intrinsic factors are primarily involved in molding a bone to its unique shape which would firstly, reflect its ability to perform certain functions and secondly, provide it with the strength to resist certain stresses. Extrinsic factors such as pressure of adjacent structures and the force of pull that a muscle exerts on a bone, brings about a secondary molding of the bone. This is then followed by secondary markings which can be identified on the bone. An example of this occurs when a muscle attaches to a relatively large surface area and it results in a smooth region of the bone. Secondary markings may also form as prominences on a bone. In such cases the terms tuberosity, protuberance

and tubercle are used. If the bone markings are more linear, then the terms used to describe them would be a ridge, crest or line (Leeson & Leeson 1989). Thus, a detailed description of the final shape and morphology of adult hand bones is important in order to relate structure to function and perhaps even to the evolutionary history of this part of the skeleton.

Osteology of the hand, however, has been confined or limited to a single paragraph in major anatomy textbooks (Bass 1995, Romanes 1991). These textbooks do not provide detailed descriptions on identification of hand bones. There is little information regarding variations of individual bones of the human hand, except for the occasional reference to the presence or absence of a medial facet on either the third metacarpal base or lateral side of the fourth metacarpal base (Bass 1995, Romanes 1991). Information regarding side differences is also lacking in these sources. Thus, no conclusive method has been described in anatomy textbooks to identify the various metacarpals and phalanges of the human adult hand as far as their side and number is concerned.

To identify, distinguish and side bones of the human hand, especially the phalanges which occur in three series, is an exceptionally difficult task. This may explain why very few studies have been conducted on the skeletal elements of the hand for forensic anthropological purposes. It is clear from the literature, that identification and variation of individual adult hand bones, as well as variations in side and number, has received the least attention. Yet, the hand is perhaps the most important part of the body that opens the brain to the world and vice versa, by its assessment of the three dimensional environment.

From a functional perspective, the human hand has been adapted in such a way so as to allow an individual to manipulate its environment. Some of these functional movements include grasping, squeezing and pinching. The muscles which carry out these movements must exert a certain force on the bones, resulting in morphological changes which should be evident visually.

Ossification of metacarpals takes place from two centers, one for the body and one for the distal extremity. The first metacarpal differs from adjacent bones in the series in that it has an ossification center for the body and one for the base rather than for the distal extremity.

This has led anatomists to consider the thumb as being made up of three rather than of two phalanges and a metacarpal. The phalanges, on the other hand, are each ossified from two centers, one for the body and one for the proximal extremity (Williams *et al*. 1989). The ossification process in hands is often accompanied by notches seen at the radial and ulnar margins of non-epiphyseal ends of the bones (Levine 1972).

To carry out a study on hands, whether it is metrical or non-metrical in nature requires a reliable sample. As early as 1931, Ashley-Montagu realised the importance of carrying out skeletal measurements on hands obtained from a reliable sample. In order to achieve this, he emphasized that there should be full control over the manner in which the sample is collected, cleaned and labelled.

2.2 Literature review

Before providing reviews on individual bones of the hand, it may be worthwhile mentioning the use of different anatomical terms for hand bones in textbooks. In general, anatomical terminologies have been standardised worldwide to maintain consistency in textbooks.Terms that are used to describe relationships of certain parts of the human body in the anatomical position, are usually arranged in pairs. An example of this includes the terms superior and inferior. Sometimes a combination of terms may relate to the intermediate positional arrangement of structures and these may include words such as inferomedial or superolateral. Terms such as proximal and distal indicate direction or position (Moore & Agur 2002).

Terminologies of orientation in the hand, for example, may differ from one author to the next. Examples of this include the following: palmar (Williams *et al.* 1989, Romanes 1991) instead of volar (Scheuer & Black 2000), anterior (Moore & Dalley 2006) instead of palmar (Gray 1959, Williams *et al.* 1989), radial and ulnar (Hollinshead & Jenkins 1981, Williams *et al.* 1989) instead of lateral and medial (Moore & Dalley 1989) and superior (Gray 1959) instead of proximal (Romanes 1991). In some instances, terminologies used to describe bony landmarks may not always be specific. For example, reference may be made to the presence of a

tubercle on the shaft without clarifying whether it is laterally or medially positioned at either the proximal or distal end of the bone (Romanes 1991). While there appears to be numerous terms used by various authors, this does not affect the description of the individual bones of the hand.

2.2.1 Metacarpals (Figure 2.1)

Naming of individual metacarpal bones differs slightly in the various textbooks. Generally, the five metacarpals (Figure 2.1) are commonly written down using Roman numerals, namely, metacarpal I, II, III, IV and V. Some anatomical textbooks simplify the naming system even further. For example, a textbook may refer to the first, second, third, fourth and fifth metacarpals (Williams *et al*. 1989). The numerous ways of naming metacarpals does not confuse the reader from knowing which bone is being described.

To date, the most comprehensive description of the human hand is that of the developmental juvenile individual, where detailed descriptions of each metacarpal are given (Scheuer & Black 2000). While this detail is lacking in metacarpal descriptions of the human adult hand, numerous anatomy textbooks have attempted to describe or at least mention, certain visible landmarks on these bones. On the other hand, descriptions on metacarpals are given in slightly greater depth than for the phalanges (Bass 1995, Romanes 1991). This is because each metacarpal has distinctly visible features, especially at the base, which allows them to be easily identified. Williams *et al*. (1989), in their 37th edition of Gray's Anatomy, provides detailed descriptions of the metacarpals and phalanges. The latest issue of Gray's Anatomy (2005), as is the case with many current anatomical texts (Moore & Dalley 2006), is more clinically based resulting in loss of detailed anatomical descriptions.

Where hand bones are described, their orientation is crucial. When teaching anatomy of the upper limb region, which includes the hands, the body is generally placed in the anatomical position. In other words, the palm of the hand faces anteriorly with the dorsal aspect directed posteriorly. In this way, the thumb is described as the most lateral digit and the

little finger as the most medial digit (Gray 1959, Williams *et al*. 1989, Scheuer & Black 2000). These terms of orientation are also applicable to anthropological and forensic cases where individual hand bones may be recovered amongst the rest of the skeletal elements of an unknown individual.

Textbooks generally describe each metacarpal as having a head, shaft, and base (Gray 1959, Williams *et al*. 1989, Romanes 1991). The presence of a neck on metacarpals may sometimes also be mentioned (Marrero *et al*. 2007). Usage of common names may be used to refer to a region of a bone. For example, Gray (1959) refers to the metacarpal head as a knuckle, which contributes to the formation of the metacarpophalangeal joint. Metacarpals two to four, sometimes also referred to as the medial four metacarpal bones (Williams *et al*. 1989), is often described as running parallel to each other. These four medial bones are described as diverging from each other in a proximal distal direction when the fingers are abducted (Williams *et al*. 1989).

Metacarpals may be discussed in conjunction with the proximal phalanges and distal row of carpal bones because of their close association with them. For example, the proximal end of the first metacarpal, which is the most mobile of the metacarpal series of bones, articulates with the trapezium, the second with the trapezium and trapezoid, the third with the capitate, and the fourth and fifth with the hamate (Williams *et al.* 1989, Moore & Dalley 2006, Marrero *et al*. 2007). The head of each metacarpal in turn ariculates with the proximal phalanx that corresponds to each digit (Moore & Dalley 2006).

A survey of the literature indicates that metacarpals are often described in terms of their function. One such study is that carried out by Tubiana (1981), where the position of each digit is related to a specific function. For example, the position of the thumb allows it greater mobility in terms of opposition when compared to adjacent metacarpals. The index finger is listed by Tubiana (1981) as second in priority because of its close proximity to the thumb. Its function is the inherent ability to carry out abduction movements efficiently as is needed during pinch and key grip movements. In such activities, the function of the index finger is not isolated from that of the thumb. Tubiana (1981) relates the strength that this digit has in flexion,

precision and power grip movements, to its relative length. Tubiana also describes the function of the ring finger in terms of its distance from the thumb. The strength of this digit is observed during flexion movements, however, the strength of flexion is far less when compared to that of the index and middle finger. The position of the little finger with respect to the thumb is given the least priority (Tubiana 1981).

The advantage that the little finger has over the thumb, with respect to its position in the hand, is its greater range of abduction which is far more than what can be achieved by any of the adjacent digits in the same series. In terms of function, this advantage enables an individual to hold objects firmly against the hypothenar eminence with a certain force. This force is also brought about by the muscles associated with the little finger. The force exerted by these muscles may leave an impression on the bone which may be visible to the naked eye. Such impressions on the bone should assist not only in identifying but also in siding a bone (Tubiana 1981). The location of the little finger thus provides a point of stability, which is of functional importance. This stability, however, may be at the expense of mobility, a function preserved for the thumb.

From this perspective, suggestions have been put forward that many of the noted morphological features of the human hand can be traced back to evolutionary development, and in particular to the amount of stress placed on it (Susman & Creel 1979, Marzke 1983, Marzke & Marzke 1987). The base of the first metacarpal and its contribution to the carpo-metacarpal joint, is designed primarily to allow for increased range of thumb movement (Marzke 1983). The second metacarpal is thought to provide various patterns of evolutionary changes (Lazenby 1998). The presence of a styloid process on the third metacarpal (Williams *et al*. 1989) may provide for stability of this bone in the palm, and its absence may be linked to ligamentous changes which are crucial for stability at the wrist joint (Marzke 1983, 1992a). It would seem that the human hand has undergone a prolonged process of evolutionary change. During this period, the individual skeletal elements of the hand were remodelled, adapting itself for function.

2.2.2 Phalanges (Figures 2.2 to 2.4)

Unlike the metacarpals, which are allocated roman numerals or in some cases called metacarpals 1 to 5 in order to identify them, the phalanges are not numbered at all. Instead, they are merely referred to as the proximal, middle and distal phalanges belonging to the thumb, index, middle, ring and little finger respectively (Matshes *et al*. 2005, El-Najjar & Mc Williams 1978). This form of identifying individual phalanges makes it easy to associate them with a particular finger.

The phalanges are sometimes referred to as miniature long bones with a broad base proximally and a head distally (Romanes 1991). This description does not differentiate the proximal, middle and distal phalanges from each other and cannot be used to identify nor side one series of phalanges from the other. The phalanges of the thumb are basically described as being the shortest and broadest bones when compared to the corresponding bones of adjacent fingers (Romanes 1991). Furthermore, in order to differentiate phalanges of the various digits in one hand, those of the middle finger are regarded as the longest, the little finger as the shortest while those of the ring and index fingers are considered to be of relatively equal length (Romanes 1991).

Descriptions of the phalanges, when compared to those of the metacarpals, are even fewer (Gray 1959, Tubiana 1981, Romanes 1991, Scheuer & Black 2000). The group of phalanges that is perhaps the most difficult to distinguish are the distal bones in this series. Very little, if any, morphological traits are given for the distal phalanges. Some authors have attempted siding techniques by carrying out a blind test using hand bones supplied by anatomical companies and refining the descriptions by comparing it to those of a skeletal collection. Once landmarks were identified by these authors, the bones were then field tested on protohistoric samples (Case & Heilman 2006). In this way, Case and Heilman (2006) developed a method for siding phalanges of the human hand. These authors used some of the features devised by Ricklan (1987, 1988) on hominids as no standardized technique existed for phalanges of the human hand. Case and Heilman's technique for siding the phalanges is seen in Tables 2.1 and 2.2 and illustrated in Figures 2.5 and 2.6.

The thumb, which presents with only two phalanges, may pose less of an identification problem. This is because the distal phalanx of the thumb is relatively bigger in size than the corresponding bone of adjacent fingers in the same hand. Other than this form of identification, the literature does not provide specific morphological traits to identify or side phalanges of the thumb. The first metacarpal may actually be a proximal phalanx as epiphyseal growth is present at the proximal end, similar to that seen in proximal phalanges of adjacent fingers. Attempts have been made by various authors to study the reduction in number of the phalanges in animals with very little success in order to explain the reduced number of phalanges in the first digit (Galis *et al.* 2001).

The few descriptions on phalanges make positive identification of an individual phalanx difficult. Even in studies on the juvenile hand, observations of the phalanges have been restricted to general morphological descriptions of the proximal, middle and distal phalanx as this presents with very few problems (Scheuer & Black 2000). Ligaments and muscles which attach to various bony sites on the phalanges may also be listed with descriptions of these bones In other words, there should be an imprint left on each hand bone as evidence of soft tissue forces placed on a specific area of these bones. The attachment sites of the dorsal and palmar interossei on the phalanges differ, thus creating different forces on these bones. It is assumed that various forces of pull on each phalanx will, over time, present with a bony landmark that can be used not only to identify but also to side the proximal phalanges of the various digits (Scheuer & Black 2000).

Some descriptions of the shaft are given in terms of their curvatures. For example, the shaft of proximal phalanges are said to have a convex dorsal and concave palmar surface. The relative length of a hand bone may also be used for identification purposes. An example of this is the proximal phalanx of the thumb, which is said to be the shortest bone while the middle finger is considered as the longest bone. The proximal phalanges of the remaining digits are then listed in order of increasing length, namely, the fifth, second and fourth digit (Scheuer & Black 2000).

The shape of the proximal phalangeal base is said to be dictated by the shape of the metacarpal bone which it articulates with. The shape of a bone is often used in joint classification systems. For example, the metacarpophalangeal joint is classified either as an ellipsoidal or bicondylar joint (Scheuer & Black 2000). The articular surface of the proximal phalangeal base is considered to have a single concave oval facet which is relatively longer in width than in a dorsopalmar aspect (Scheuer & Black 2000). The heads of the proximal phalanges are described as being bicondylar with the medial and lateral condyles varying in relative size for each proximal phalanx (Scheuer & Black 2000). For example, the medial condyle is said to be larger than the lateral one in proximal phalanges of second and third digits while the lateral condyle is seen to be relatively larger in proximal phalanges of digits one, four and five respectively (Scheuer & Black 2000). Often the condyles are simply described as being small with no reference to their difference in size (Bass 1995).

The only descriptions provided for the middle phalanges is that they are the second row of bones in the phalangeal series with a head, base and shaft (Bass 1995). Distal phalanges have previously been referred to as ungual phalanges because of their claw-like appearance at the distal end. These bones are not described in detail in any anatomy textbook, except to state that it also has a base, shaft and head. What is described is the triangular shape of this bone with a wide base and tapered distal end. The distal phalanx of the thumb can be distinguished from those of adjacent digits based on relative size, as it is the longest and most robust bone in this series. It is also the only row of phalanges that has a non-articular distal extremity (Scheuer & Black 2000).

The literature records various degrees of robusticity for the distal phalanges of digits two to five (Scheuer & Black 2000). In order of decreased robusticity they are listed as the first, third, second, fourth and fifth distal phalanx (Scheuer & Black 2000). The base (proximal end) of a distal phalanx articulates with the head (distal end) of a middle phalanx in the case of digits two to five, forming the distal interphalangeal joint. In the thumb, the distal phalanx articulates with the distal end of a proximal phalanx forming an interphalangeal joint (Scheuer & Black 2000).

Two articular facets have been recorded on the articular surface of the distal phalangeal base in the juvenile infant (Scheuer & Black 2000). The dorsal surface is smooth except for an area at the proximal end of the dorsal surface which serves for attachment of the tendon of extensor pollicis longus in the thumb and the tendons of extensor digitorum in the adjacent digits (Scheuer & Black 2000). At the distal end of the dorsal surface, the distal phalanx is smooth. This is part of the bone deep to the fingernail. The palmar surface, in contrast, is rough and flattened at the proximal end owing to the attachment of soft tissue structures (Gray 1959, Scheuer & Black 2000).

Figure 2.1: Dorsal (A) and palmar (B) view of metacarpals (MC) 1 to 5 of the right (R) hand.

Figure 2.2: Dorsal (A) and palmar (B) view of proximal phalanges (PP) 1 to 5 of the right (R) hand.

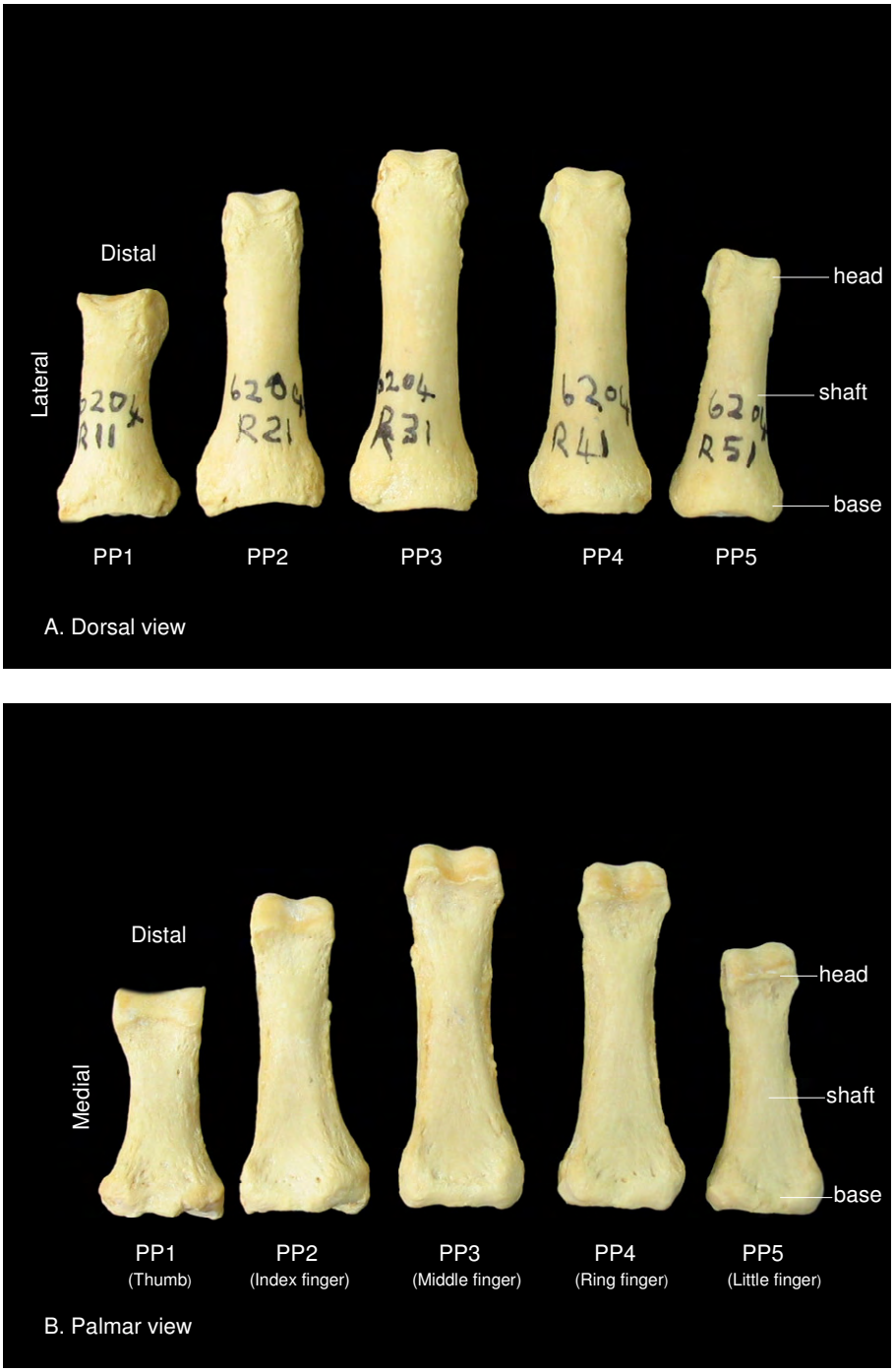

Figure 2.3: Dorsal (A) and palmar (B) view of middle phalanges (MP) 2 to 5 of the right (R) hand.

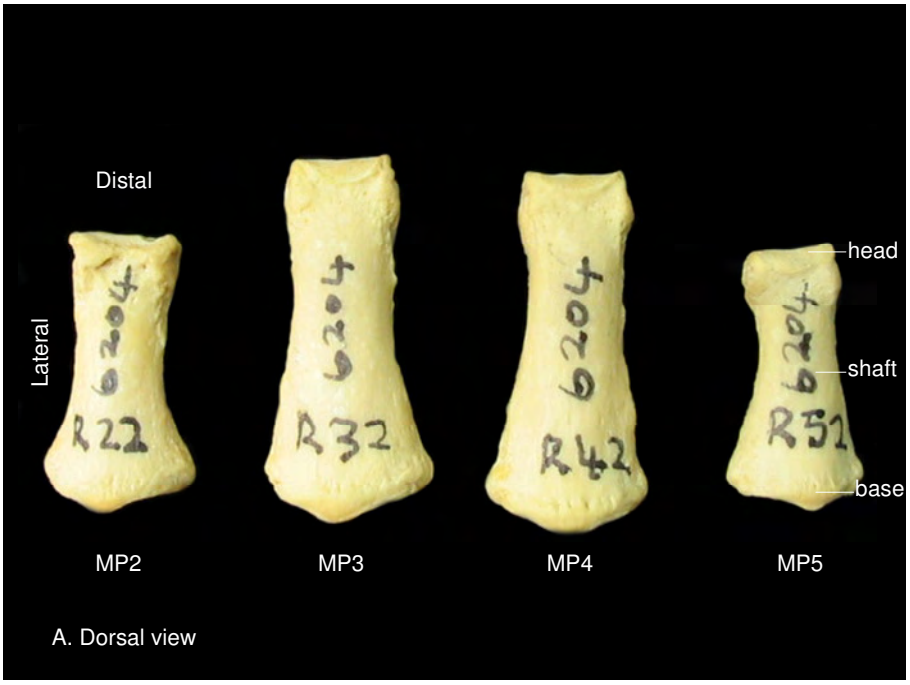

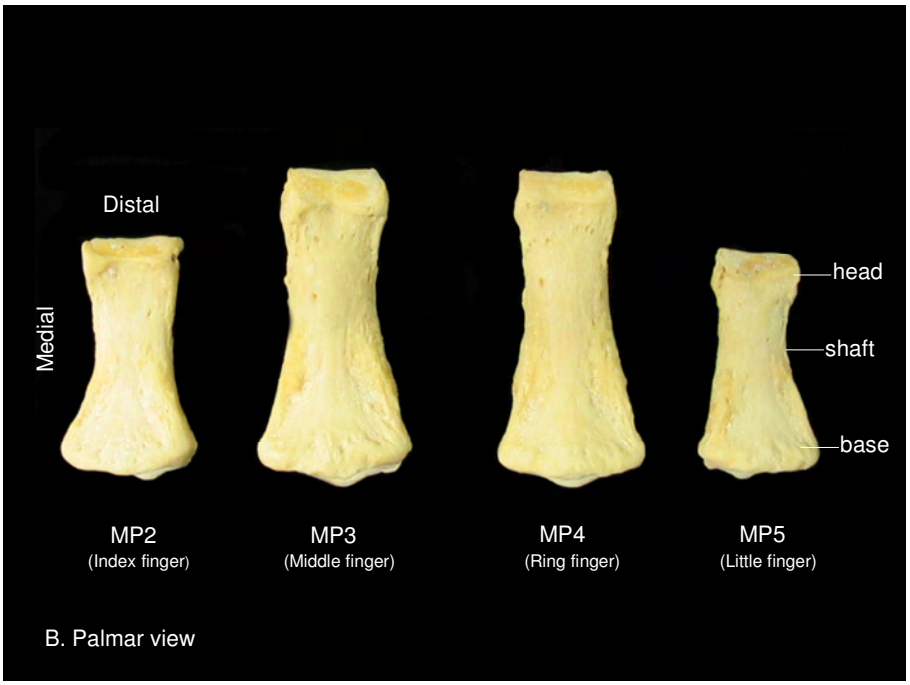

Figure 2.4: Dorsal (A) and palmar (B) view of distal phalanges (DP) 1 to 5 of the right (R) hand.

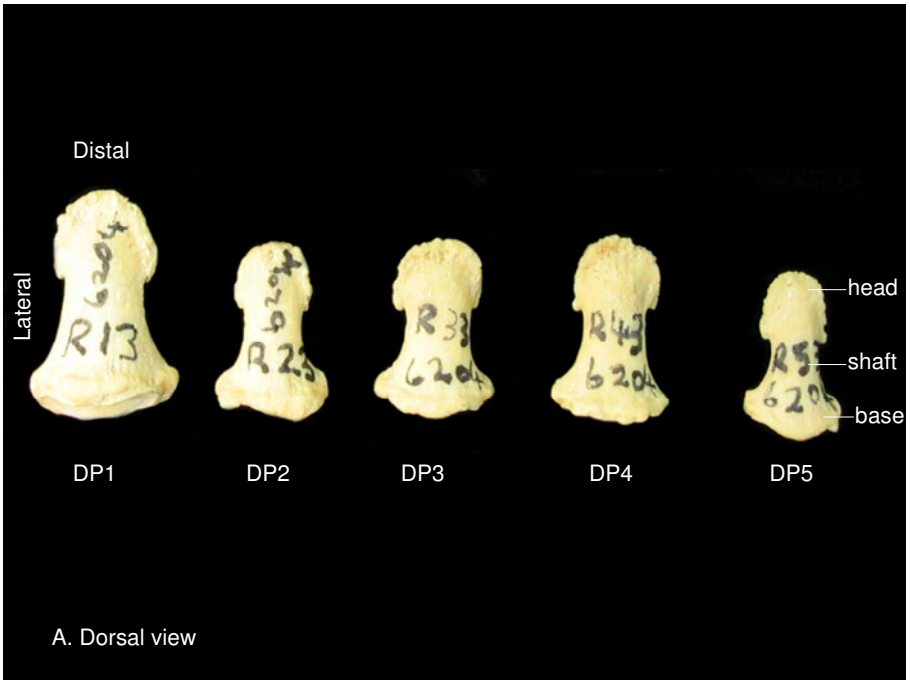

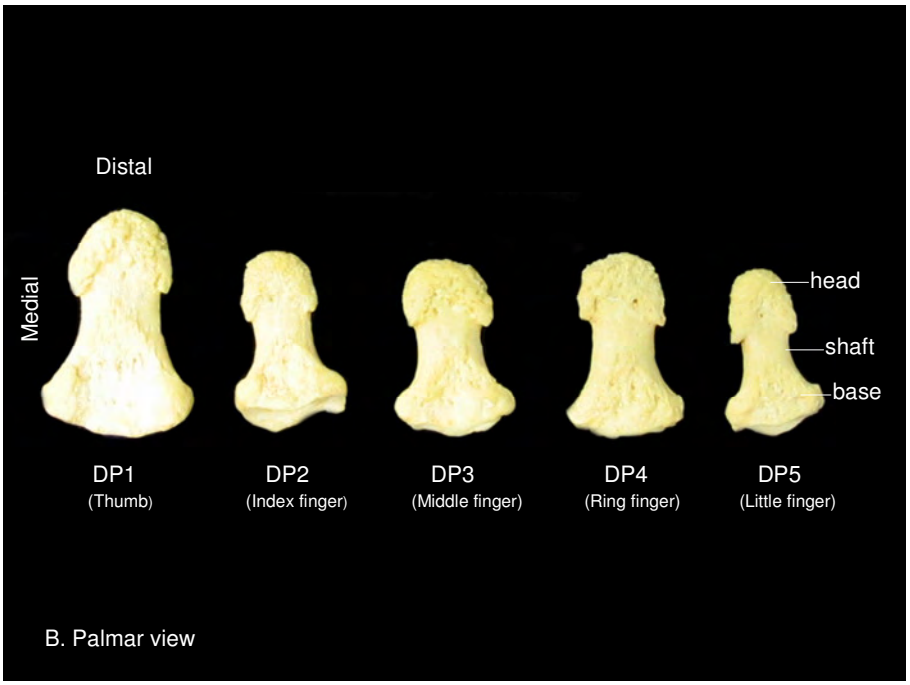

Figure 2.5: Siding techniques for the manual proximal (1-5) and intermediate (2-3) phalanges [Taken from Case DT and Heilman J 2006. International Journal of Osteoarchaeology 16: 338-346 Copyright: 2006 John Wiley & Sons, Ltd.]

Bone and View (Accuracy)	**Left Side**	**Right Side**	**Siding Techniques**
Proximal Phalanx I (100%)	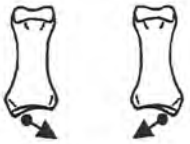		PP1: The lateral edge of the proximal facet Palmar faces toward the opposite side the bone is from. Additionally look for the most proximal point to be on the side the bone is from.
Proximal Phalanx 2 Palmar (96%)	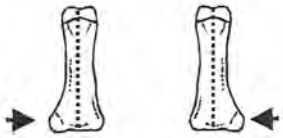		PP2: The mass of the proximal end is greater on the side the bone is trom. Additionally, look for the most distal point on the bone to be opposite the side the bone is from.
Proximal Phalanx 3 Palmar	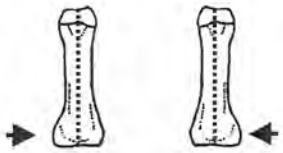		PP3: The mass of the proximal end is greater on the side the bone is from. Additionally, look for the most distal point on the bone to be opposite the side the (94%)bone is from.
Proximal Phalanx 4 Proximal (94%)			PP4: With the bone on its dorsal urface the greatest vertical height on the proximal end is found on the side the bone is from. Use finger pressure on the shaft to keep the bone from rolling. The bone also tends to roll toward the side the bone is from.
Proximal Phalanx 5 Dorsal (88%)	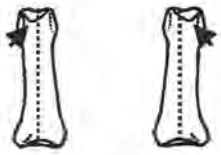		PP5: The margin of the superodistal facet extends more proximal1y on the side the bone is from. Additionally, look for the most distal point on the bone to be opposite the side the bone is from.
Intermediate Phalanx Dorsal (96%)	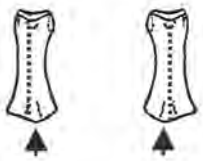		IP2: The projection of the superior margin of the proximal facet is off-center opposite the side the bone is from.
Intermediate Phalanx Dorsal (96%)	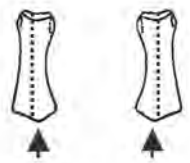		IP3: The projection of the superior margin of the proximal facet is off-center opposite the side the bone is from.

Figure 2.6: Siding techniques for the manual intermediate (4-5)and distal phalanges (1-5) [Taken from Case DT and Heilman J 2006. International Journal 0f Osteoarchaeology 16: 338-346 Copyright: 2006 John Wiley & Sons, Ltd.]

Bone and View (Accuracy)	Left Side	Right Side	Siding Techniques
Intermediate Phalanx 4 Dorsal (78%)	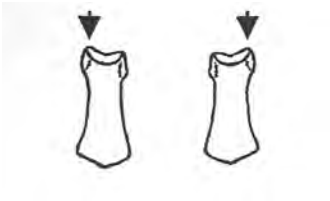		IP4: The most distal point on the bone is on the side the bone is from. Additionally, the shaft of the bone exhibits deeper curvature opposite the side the bone is from.
Intermediate Phalanx 5 Dorsal (98%)	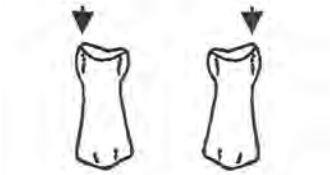		IP5: The most distal point on the bone is on the side the bone is from. Additionally, the shaft of the bone exhibits deeper curvature opposite the side the bone is from.
Distal Phalanx 1 Dorsal (94%)	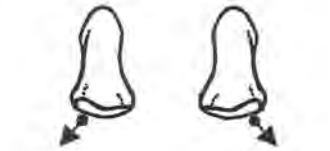		DP I: One half of the proximal face partially faces toward the side the bone is from. Additionally, the most proximal point on the bone is opposite the side the bone is from.
Distal Phalanx 2 Proximal (52%)			DP2: Looking at the proximal facet with the palmar aspect down, the smaller of the two facets is on side the bone is from. Additionally, look for the facet height to narrow more on the side the bone is from.
Distal Phalanx 3 Proximal (66%)			DP3: Looking for the proximal facet with the palmar aspect down, the smaller of the two facets is on the side the bone is from. Additionally, look for the facet height to narrow more on the side the bone is from.
Distal Phalanx 4 Proximal (68%)	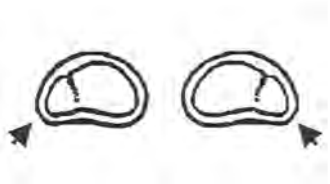		DP4: Looking at the proximal facet with the palmar aspect down, the smaller of the two facets is on the side the bone is from. Additionally, look for the facet height to narrow more on the side the bone is from.
Distal Phalanx 5 Dorsal (78%)	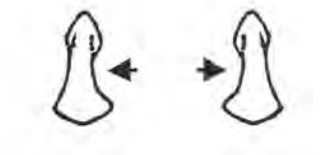		DP5: The shaft of the bone exhibit deeper curvature opposite the side the bone is from.

Table 2.1: Additional siding techniques for the manual phalanges by Case and Heilman (2006) (PP=proximal phalanx, IP-intermediate phalanx)

Bone	Accuracy	Description
PP1	96%	Distal view: Place the bone on a flat surface on its palmar aspect, holding the proximal end down firmly. The distal end does not contact the flat surface opposite the side the bone is from
PP2	94%	Distal view: Place the bone on a flat surface on its palmar aspect, holding the proximal end down firmly. The distal end does not contact the flat surface on the side the bone is from
PP5	82%	Dorsal view: The mass of the proximal base is greater on the side the bone is from
IP2	90%	Proximal view: Lay the bone on a flat surface on its dorsal aspect. The side of the proximal base highest above the flat surface is on te side the bone is from
IP3	90%	Proximal view: Lay the bone on a flat surface on its dorsal aspect. The side of the proximal base highest above the flat surface is on the side the bone is from
IP5	96%	Dorsal view: The degree of curvature of the shaft margin is greater on the lateral side, which is opposite the side the bone is from

Table 2.2: Additional siding techniques for the manual phalanges by Ricklan (1988) (PP=proximal phalanx, IP=intermediate phalanx, DP=distal phalanx)

Bone	Accuracy	Description
PP1	83%	Distal view: With the palmar aspect down, the largest part of the distal articular surface is on the side the bone is from
PP2	82%	Distal view: With the palmar aspect down, the largest part of the distal articular surface is opposite the side the bone is from
PP3	80%	Distal view: With the palmar aspect down, the largest part of the distal articular surface is opposite the side the bone is from
PP5	98%	Palmar view: The most distal point on the bone is on the side the bone is from
IP2	93%	Proximal view: Loking at the proximal facet with the palmar aspect down, the larger of the two facet area is on the side the bone is from
IP3	85%	Proximal view: Looking at the proximal facet with the palmar aspect down, the larger of the two facet areas is on the side the bone is from
DP2	91%	Palmar view: A line tangent to the medial- and lateral-most edges of the proximal articular surface trends distally opposite the side the bone is from
DP3	77%	Palmar view: A line tangent to the medial- and lateral- most edges of the proximal articular surface trends distally opposite the side the bone is from
DP4	57%	Palmar view: A line tangent to the medial- and lateral- most edges of the proximal articular surface trends distally on the side the bone is from
DP5	89%	Palmar view: A line taget to the medial- and lateral- most edges of the proximal articular surface trends distally on the side the bone is from

CHAPTER 3

LITERATURE REVIEW - STATURE DETERMINATION

3.1 Introduction

In many forensic cases, the soft tissue of human remains recovered at a crime scene, has often degenerated to such a point that demographics such as population affinity, age, sex and living height cannot be ascertained with accuracy. Most often, only skeletal parts are recovered, rather than the entire skeleton, which then serves as the only available resource to estimate the height of an unknown person. The role of the forensic anthropologist, in such cases, is to then determine and assess the characteristics of such remains through various methods of analyses in order to establish the identity of an unknown individual. One such characteristic is that of height measurement.

Stature is a unique biological entity in that it can be estimated not only in the living individual, but also from a skeleton long after the death of a person (Ryan & Bidmos 2007). In order to assess height from human remains, an understanding of it in a living person is crucial. Stature has been shown to steadily increase from infancy to adulthood. It remains stable throughout middle age and then decreases with old age (Sjøvold 2000). Ageing is not the only factor that causes a reduction in height. In fact, in a living individual, it has been shown to decrease by approximately 2 cm per day. This is from the time a person wakes up and carries out their various daily activities throughout the course of the day, to the time that an individual goes back to sleep at night. This reduction in height that occurs with continuous postural changes is ascribed to loss of elasticity in the intervertebral discs. This happens to such an extent that there is compression of the cartilages with resultant approximation of adjacent vertebrae (Sjøvold 2000).

Due to the variability in height, various approaches to the study of human growth and development have evolved. These methods may be theoretical, non-theoretical, descriptive or quantitative. Data on growth and development obtained by statistical analyses on a human population sample can be and is used to derive standard references for parameters such as

height. These standard references are designed into equations which are then used to assess growth, development, nutritional status, social and cultural circumstances of an individual or a population (Tanner 1981, Bogin 1988, Malina *et al*. 2004).

Gigantism or dwarfism is said to occur when there is a 20 percent deviation of height from the average. The problem in such instances is to establish what the average is for an individual in a particular population (Bogin 1988, Kottak 1997, Steyn & Smith 2007). It has been suggested that adult height in males or females of a particular ethnic group should follow a normal distribution pattern (Bogin 1988).

Bogin (1988) reported that on average, men are taller than women and that growth in height tends to come to a halt when the growing end of a long bone, namely the epiphysis, fuses with the diaphysis (shaft) of the bone. At this point, the long bone is said to have reached its peak length.

While stature is an entity that is seen to vary in the living individual, its inherent characteristic makes it an important contribution to the identification process (Krogman & İşcan 1986). Estimation of antemortem or living stature from a skeleton forms an important part of the forensic analyses. It must therefore be estimated in a way that adjustments can be made as closely as possible to that measured on the living individual (Trotter 1970). The actual height measured from an individual or cadaver is often referred to as the biological stature and is more accurate than forensic stature (Ousley 1995). The latter is an estimate rather than the actual recording of an individual's height. Such estimates of stature are often encountered when relatives report the height of an individual as short, medium or tall (Kottak 1997, Saferstein 2004, Rich *et al*. 2005, Steyn & Smith 2007).

Intact long bones recovered amongst human remains, is ideal to reconstruct stature of an unidentified individual. However, this is not always possible in many forensic cases as fragments of long bones are often encountered. In order to assist with identification of such forensic cases, researchers have formulated regression equations from the skull (Chiba & Terazawa 1998, Patil & Mody 2005, Ryan & Bidmos 2007), metacarpals (Musgrave & Harneja 1978, Meadows & Jantz 1992), long bone fragments (Steele & McKern 1969, Mysorekar *et al*.

1980, Simmons *et al*. 1990, Holland 1992, Ozaslan et al. 2003, Chibba & Bidmos 2007), hand and foot dimensions and shoe prints (Ozden *et al*. 2003, Krishan & Sharma 2007) and metatarsals (Byers *et al*.1989, Robling & Uberlaker 1997).

In circumstances where bodies have been recovered from mass disasters or at the scene of a crime, or in cases where the corpse has been severely mutilated, decomposed or fragmented, stature can only be determined by measuring parts of the skeleton that are available (Sjøvold 2000). The height of the individual is often related to the relative size of the skeletal bone or fragment under study. In other words, the larger the bone, the taller the individual is expected to be (Sjøvold 2000). The aim of forensic anthropologists is to put together as many systematic studies in order to identify fragmented and dismembered human remains as accurately as possible (Ozaslan *et al*. 2003).

Another problem added to the identification process is that of variation in a single bone or in the entire skeleton as well as in skeletons of a larger sample. Knowledge of this variation is essential to forensic anthropologists as it interferes with the identification process (Krogman and İşcan 1986). Studies on assessing human variation carried out by a number of physical anthropologists have contributed to forensic cases (Bogin 1988, Kottak 1997, Malina *et al*. 2004). Due to the existence of these variations, the likelihood of errors occurring when determining stature is inevitable, not only in a single skeleton but also in a population. To overcome the problem of variation, a correlation analysis needs to be carried out. The higher the correlation between bone measurements and stature, the more accurate the estimation of stature is likely to be. The opposite is true in cases where the correlation is low (Sjøvold 2000).

Population differences in stature have drawn great interest worldwide. The ability to allocate skeletal remains as accurately as possible to a specific population depends on whether such a group exists as well as on the availability of the sample which represents the specific population (Brickley & Fellini 2007). In fact, differences in height as well as the rate of growth between different populations have been ascribed to various hereditary and environmental factors (Trotter & Gleser 1951, Bogin 1988). Bogin (1988) showed that young adult males and females from the Netherlands are relatively the tallest people when compared

to Americans, Turkana pastoralists, Japanese, Guatemalan Indians and Bolivian Indians with the African Mbuti pygmy being the shortest people.

One other factor that has also received attention is the effect of secular trends on height. Tobias (1975) was one of the first authors to illustrate the existence of a secular trend towards an increase in adult stature and stated that it did not always have a positive effect. A negative or absent trend can exist in various populations (Tobias 1975, 1985, Tobias & Netscher 1977, Cameron *et al*. 1989).

3.2 Literature review

3.2.1 Historical background

The determination of the individuality of a skeleton involves an in-depth understanding of the skeletal biology, related anomalies, pathology, health and disease status (Krogman & İşcan 1986). Demographic factors such as age, sex and race need to be established when identifying human remains. Once these characteristics have been confirmed, the stature of the individual is then recorded.

The concept of determining stature from long bones is said to have developed as early as the 1700's where maximum length of bones was first recorded by a French anatomist on foetuses and adults (Steele 1970). This interest in stature continued into the 1800's with emphasis on differences between cadaver height and living stature (Steele 1970). To address these differences, the relationship between stature and long bone length was attempted by British researchers whose methods differed slightly from those of the French. These researchers made adjustments for measurements of the femur and multiplied the length of this long bone by a given number. A mathematical method was thus established towards the end of the 1800's (Steele 1970).

Various methods were approached to measure the length of bones. In 1859, a French medical anthropologist, Paul Broca, designed an osteometric board in order to accurately measure bone lengths. His successor, Paul Topinard, published a series of papers between

the period of 1885 and 1888 which included mathematical methods regarding the ratio of long bones to stature (Steele 1970).

In 1888, Rollet compared lengths of long bones from male and female cadavers which were measured before and after maceration. This he did to establish whether different values would be obtained in fresh and dried bones (Trotter & Gleser 1952, Steele 1970, Krogman & İşcan 1986). This study was probably also the first to mention sexual dimorphism. Rollet's results showed a difference of about 2 mm between fresh and dried bones (Krogman & İşcan 1986). Studies on cadavers have shown that the drying process following maceration, causes shrinkage of the skeleton and that a 2 mm difference could affect calculation of stature by as much as 4-6 mm (Trotter & Gleser 1952).

In 1893, Rollet's data was re-evaluated by Manouvrier who recommended that this 2 mm difference should be added to the dried bone length. Thereafter, 20 mm should be subtracted from the cadaver stature to obtain living stature. It was only 50 years later that regression formulae for accurate stature estimation for males and females were established (Trotter & Gleser 1951, 1952, Steele 1970, Lundy 1983, Krogman & İşcan 1986, Lundy & Feldesman 1987, Dayal 2002).

Since these earlier years, many studies emerged regarding the incorporation of these regression equations into various human population studies. Problems that arose from later studies are that many of these equations were applied across populations. This brought into question the accuracy of recorded data from studies which used the Trotter and Gleser regression equations and applied it to populations far removed from those for whom the equations were initially intended for (Trotter & Gleser 1951, 1952). Regression equations are population specific and one should be careful when using these formulae in different groups (Lundy 1983). An example of using equations across populations is the study carried out by Stevenson in 1929, where this author used Pearson's regression formula for a Chinese cadaver sample which yielded unfavourable results for this population (Steele 1970).

Equations that were devised by Trotter and Gleser in the early 1950's for Americans were being continuously revised using data from different sources. In 1977, they proposed new

equations using the radius and ulna. These equations were applied to forensic cases where results proved unsuccessful. The conclusions drawn from the methods used to derive the Trotter and Gleser equations, included inconsistency as it was not clear from published papers as to whether the malleolus of the tibia had been included or excluded in the measurements (Jantz 1992, Jantz *et al*. 1994, 1995).

3.2.2 Studies on prehistoric material

Stature, in humans, has contributed to various aspects of hominid development (Pilbeam & Gould 1974, Blumenberg 1984). Regression equations established for modern populations have been used to estimate stature of fossil hominids. However, these have been shown to be unreliable, presenting with numerous problems (Musgrave & Harneja 1978, Himes & Roche 1982).

Hens *et al*. (1998) encountered difficulties when attempting to predict stature or body length in a modern and fossil hominid sample using the same regression formulae. The inverse calibration method is used by researchers carrying out archaeological and forensic studies (Hens *et al*. 1998). In a sample where one assumes that equal allometries exists, it has been suggested that the classical calibration be used especially if extrapolating the study to larger or smaller animal (Hens *et al*. 1998). In fossil studies, researchers are often faced with the problem of not knowing whether allometries between the reference sample and a sample of isolated or commingled bones does exist or not (Hens *et al*. 1998).

Allometric techniques have been used to compare weight and stature in Plio-Pleistocene hominids and modern humans with the aim of being able to predict these parameters with a certain degree of accuracy (Aiello 1992). In such studies, the argument may arise as to which allometric technique would be the best to estimate the functional relationship between two variables under study. Studies by Trotter and Gleser (1951, 1952) were not excluded from prehistoric studies. Their regression equations for human populations have found their way into studies on Plio-pleistocene hominids (McHenry 1974).

Hens *et al*. (1998), in their study on determining body length from femur length, employed five commonly used statistical methods to a sample of humans and thereafter applied it to the African ape. In the first instance, they regressed body length to long bone length which is an inverse calibration. Secondly, they regressed long bone length to body length which they referred to as a classical calibration. Thirdly, they computed the major axis regression of body length on long bone length. Fourthly, they calculated reduced major axis regression of body length on long bone length and finally, they used the ratio of long bone to body length.

Attempts by palaeoanthropologists to reconstruct stature of fossil hominids, using the Trotter and Gleser equation, proved unsuccessful as the results overestimated height (Lovejoy & Heiple 1970, McHenry 1974). Even the use of classical formulae or equations developed from a population that closely resembles the height of, for example Australopithecines, resulted in marked differences (Olivier 1976). Other researchers have used regression formulae from various postcranial elements on prehistoric Native Americans to regress stature (Sciulli & Giesen 1993). The disadvantage of any study attempting to determine stature in a prehistoric sample is that the actual stature will never be known. Mathematical methods derived are only able to provide some idea of what the actual height may have been.

3.2.3 Bones used to estimate stature

Ideally, a complete skeleton is preferred when determining stature. While this may not always be possible in many forensic cases, single intact or fragmented bones of the skeleton are used. Of all the bones available for the estimation of stature, the human femur, being the largest and most robust long bone in the skeleton, makes it the bone of choice when reconstructing stature (Trotter & Gleser 1958, Genoves 1967, Lundy 1985). Besides being the largest and most robust bone, the intact femur also has the highest correlation to stature and is thus widely used to derive regression equations (Bidmos 2008). Research has shown that the relationship of femoral length to stature is constant and population but not sex specific

(Feldesman 1992, Sjøvold 2000). The contribution of the femur to total stature is 26.75% while the stature/femur ratio has been calculated as 3.74 for all populations (Sjøvold 2000).

Numerous other studies have also used long bones, namely, the humerus, radius, ulna, femur, tibia, and fibula, for estimating stature (e.g., Telkka *et al*. 1962, Genoves 1967, Olivier *et al*. 1978). Some studies have excluded measurements of dried bones such as the tibia, as it yields unsuccessful results when compared to that of living stature (Allbrook 1961). Estimation of stature in Asiatic Indians (Singh & Sohal 1952, Jit & Singh 1956) using the clavicle, computed standard error of estimates as high as 32 cm. Such a high error value would exclude the clavicle from being used in forensic cases. Similar attempts to use the scapula in estimating stature, proved unsuccessful (Musgrave & Harneja 1978).

In the 1800's, the vertebral column was not used at all in studies on stature determination, as the absence of one or more vertebrae could render a study invalid and unreliable. The earliest study carried out on stature using the spine, was in 1894 by Dwight (Tibbetts 1981). While the results from this study indicated that the spine can be used to estimate stature, it cannot readily be used in forensic cases as it needs to be in the fresh intact state (Tibbetts 1981). In 1960, Fully and Pineau used the lengths of thoracic and lumbar vertebrae of white European males to devise regression formulae for estimate the length of the vertebral column (Tibbetts 1981). A similar study was carried out on American blacks by Tibbetts (1981), who reported standard errors in the estimates ranging from 67.89 to 54.72 mm for males and 68.22 to 53.09 mm for females. Tibbetts concluded that while the vertebral column can be used to estimate stature, the high errors obtained indicate that it is not the best variable when compared to the low standard error estimates from long limb bones lengths. Jason and Taylor (1995) estimated stature from the lengths of cervical, thoracic, and lumbar segments of the spine in American whites and blacks. Pelin *et al*. (2005) measured dimensions of the sacrum and coccyx from magnetic resonance images of 42 male adults. Statistical analyses of this study indicated that a combination of the sacrococcygeal variables proved to be better predictors for stature than equations derived from individual vertebrae. Furthermore,

the equations for the combined variables proved to be better predictors than that given for the foot and head but worse than equations based on long bone lengths.

Celbis and Agritmis (2005) estimated stature using the length of the radius and ulna recorded from a Turkish corpse sample. While recording measurements from corpses is not a standard anthropological method, these authors acknowledge that their study is applicable to accurate determination of antemortem stature and that their regression formulae may need adjustments. Furthermore, these authors report that the lengths of the radius and ulna are 30 mm longer in males than in the females. They obtained correlation values of 0.62 and 0.64 in males and 0.76 and 0.85 in females for the ulna and radius respectively. These authors concluded that dried bone measurements are better estimates of stature than recently deceased individuals. Byers *et al*. (1989) used the lengths of metatarsals to calculate stature.

In their study on Japanese cadavers, Chiba and Terazawa (1998) recorded the diameter of the skull, its circumference as well as the sum of the two variables. The skull measurements were regressed to the length of the cadaver. These authors reported correlation values ranging from 0.32 to 0.53 with a range of the standard error of estimates being 6.59 to 8.59. Patil and Mody (2005) recorded the skull length from lateral cephalometric radiographs to derive at a regression equation for stature. Ryan and Bidmos (2007) reported moderate correlation values ranging from 0.40 to 0.54 with standard error of estimates of 4.37 and 6.24 for their indigenous South African sample. Ryan and Bidmos suggested that while the skull can be used in estimating stature, caution be exercised when it comes to its use in forensic cases. They reiterated the use of long limb bones if available, rather than the skull, to identify human remains.

While conventional methods of estimating stature are dependent on the use of long bones, fragmented bones may be the only available parts of human remains presented to forensic anthropologists. The main problem with using fragments of bone, is the difficulty in identifying landmarks on these samples (Simmons *et al*. 1990, Steele & McKern1969, Steele 1970).

Simmons *et al*. (1990) developed new regression equations for the Terry Collection. These equations were not only for estimating maximum femoral length for stature, but also for three well-defined segments of the femur, namely, the proximal, middle and distal ends. At the proximal end, they measured the vertical diameter of the femoral head and neck and upper breadth. In the midshaft, they recorded the minimum transverse diameter while at the distal end, the parameters were height dimensions of the medial and lateral condyles. By using a fragment of the femur, these authors were able to regress it to maximum femoral bone length. The maximum femoral length in turn was then regressed to stature. The standard error of the estimates, however, was also increased. The proximal femoral breadth yielded the highest correlation value (0.587) in males, while the lateral condyle height in females gave the highest correlation (0.677). Generally, their results showed correlations which were not higher than 0.65. These authors acknowledged that the relationship of bone fragments to stature present with lower prediction accuracies and higher standard errors in comparison to long limb bones.

Holland (1992) estimated stature from fragmented tibia. Five measurements of the proximal tibial end was used, namely, length and width of the lateral and medial tibial condyles as well as bicondylar width. Standard errors for this study ranged from 3.69 to 5.92 cm.

Numerous studies on estimating stature from hand and finger length recorded on living subjects have been carried out (Saxena 1984, Tyagi *et al*. 1999, Jasuja & Singh 2004). In their study of the Indian population, Jasuja and Singh (2004) recorded correlation values ranging from 0.215 to 0.681 in males and 0.279 to 0.622 in females. Standard errors for this group were given as a range from 4.033 to 4.82 in males and 5.061 to 5.127 in females. Radiographic studies have also been taken from living subjects to estimate stature from the length of hand bones (Himes *et al*. 1977).

Musgrave and Harneja (1978) used the length of metacarpals from radiographs to estimate stature. They recorded the inter-articular (physiological) length which was adjusted to compensate for radiographic enlargement. These radiographs were taken from adult male and female patients. The results of their linear regression analysis, where stature was regressed on the length of each metacarpal bone, gave correlation values ranging from 0.53 to 0.67 in males

with standard errors of 5.49 to 6.30 cm. In their female group, correlation values ranged from 4.71 to 8.15 with standard errors of 4.70 to 8.14.

Meadows and Jantz (1992) studied the relationship between the length (mm) of a metacarpal and stature (cm) in American white and black males and females. They recorded measurements from the middle of the proximal articular surface to the middle of the distal tip. These authors reported correlation values for males ranging from 0.565 to 0.828 with standard errors from 4.68 to 5.96 cm. Correlation values for their female group ranged from 0.61 to 0.79 with standard errors of 4.68 to 5.96. According to Byers (2005), the standard errors reported by Meadow and Jantz (1992) are large and suggested that metacarpals should not be used for estimating stature when long limb bones are present. Standard error of estimates reported for fragmented femora, were higher than those given for the metacarpals (Simmons et al. 1990). This led Meadows and Jantz (1992) to conclude that metacarpals are preferred to long bone fragments when estimating stature. Grieshaber (2001) stated that standard errors using metacarpals to estimate stature is higher than from long bones.

3.2.4 Methods used in estimating stature

The ideal stature to measure is that of a living individual. This is more useful than measuring skeletal or cadaveric stature, as it records the actual height of the living individual. Stature recorded on a drivers license (forensic stature), is one piece of information that contributes to data which can identify a living individual. However, its accuracy has been questioned (Ousley 1995). Willey and Falsetti (1991) showed that the heights recorded in a drivers license does not differ significantly from the measured heights. On the other hand, these authors suggested that the height in a driver's license is not accurate, as it is not updated on a regular basis to account for subsequent growth changes. Giles and Hutchinson (1991) compared measured stature to self-reported stature and found that taller people often overestimate their stature. From these studies, Giles and Hutchinson concluded that forensic stature was not a precise measure. Numerous other studies have reported similar findings (Snow & Williams 1971, Musgrave & Harneja 1978, Sjøvold 2000).

In the forensic context, however, reconstructing stature from human remains is not easy when compared to that of living stature. Forensic anthropologists are often involved in excavation of human remains from graves (Ta'ala *et al*. 2006). Irrespective of the trials and errors in methods used in estimating living or ante-mortem stature, this characteristic trait forms an intergral component in the analyses of unknown individuals. When human remains are found by the police, the task of the forensic anthropologist is to measure the long bones and apply it to linear regression equations. These equations, which are population specific, are developed to estimate stature from known living or cadaver stature. The estimated stature is then compared to recorded as well as reported stature of missing individuals. Estimates of living stature together with characteristics such as age, sex and race, is then used to draw up a profile of the unknown individual (Krogman & İşcan 1986).

A method for estimating stature, using a complete skeleton, was first introduced by Dwight in 1894 (Ryan & Bidmos 2007). This first attempt was improved upon by Fully's method, commonly referred to as Fully's anatomical method .Fully's technique (1956), involves calculating total skeletal height (TSH) from the sum of the following parts of the skeleton, namely, basibregmatic height of the skull, C2 to S1 vertebral body heights, femoral length, tibial length, articulated talo-calcaneal height. Fully's method also incorporates a correction factor for soft tissues in males and females, which is included in calculating total skeletal height. This method brings estimated stature very close to that of living stature. The disadvantage of this technique, however, is that it is time consuming and requires a complete skeleton which is not always available in forensic cases.

Various other methods for estimating stature have been devised by forensic anthropologists. Some of the earlier research in this field includes the work carried out by Trotter and Gleser (1951, 1952) and Trotter (1970). These authors devised regression formulae for estimating stature which were based on data from World War II male casualties of African American and Euro American descent. These authors measured living stature as well as long bone lengths from skeletonized remains. Trotter and Gleser (1958) re-evaluated their original formulae using casualties from the Korean War. This sample contained a more

ethnically diverse group of individuals. A number of problems were still encountered with the measured statures reported by Trotter and Gleser including the fact that their formulae were population specific (Jantz *et al*. 1994).

Some authors have used a number of methods to estimate stature in the same sample. For example, Konigsberg *et al*. (1998) compared five different methods, namely, regression stature on a long bone length, regressing long bone length on stature, major axis regression of stature on long bone length, reduced major axis regression of stature on long bone length and the ratio of long bone to stature. According to Komar and Buikstra (2008), regression of stature on long bone length is the method of choice if these remains are from the same "stature distribution as the reference sample" (p. 149). If this assumption cannot be made with certainty, then it is preferable to regress long bone length to stature. Various computer programs provide different combinations of long bone measurements in order to assist forensic anthropologists in estimating stature (Ubelaker 1998).

The aim of devising regression equations is that it should enable the researcher to predict with a certain degree of accuracy the stature of a deceased individual, or to at least estimate stature from the skeletal remains in a forensic case. Some studies have restricted stature estimation to simple percentages while others have used the least squares method of factor analysis to calculate regression formulae (Steele & McKern 1969). Numerous sets of regression equations have been developed and these have been revised for different samples (Trotter & Gleser 1952, 1958, Trotter 1970). Not only has regression equations been used across populations but they have also been employed in prehistoric studies, as discussed earlier on, with poor results (Trotter & Gleser 1958).

Statistical errors than can occur during stature estimation is said to be as much as 10 cm (Mysorekar *et al*. 1980). On the other hand, it has been suggested that a 1 mm difference in the measurement of the total length of a long bone, should not affect the regression equation employed (Mysorekar *et al*. 1984).

Fully's revised anatomical method was incorporated into a study carried out by Raxter *et al*. (2006) whose findings resulted in 95 percent of their samples being correctly estimated to

within 4.5 cm. Furthermore, these authors emphasized consistency when carrying out any measurements on bones. They also concluded that the mathematical method was not able to account for disproportionate individuals when compared to the anatomical method. These authors also proposed new formulae for soft tissue value additions.

3.2.5 Effect of age on stature

The height of an individual, irrespective of race and sex, is at its maximum at the age of 21 years (Trotter & Gleser 1951). Thereafter, the height decreases notably after 30 years (Trotter & Gleser 1951), 35 years (Boas 1940) or 40 years according to Büchi (Trotter & Gleser 1951). This reduction in length is said to be as much as 0.06 cm (Trotter & Gleser 1951) or 1cm per year over the age of 50 (Galloway 1988, Himes & Roche 1982). Galloway (1988) was confident that age was the overriding parameter in estimating stature and that the major decline in stature according to him did not begin until the age of 45 years after which the rate of loss in stature was then very rapid. Giles and Hutchinson (1991) suggest a decrease in stature of Americans in their midforties, which in males is 1 mm per year compared to 1.25 mm per year for females.

Statistical analyses carried out by Pearson (1899) proved that shrinkage of bones with ageing does not appear to alter the correlation. Studies in 1951 (Trotter & Gleser) proved otherwise. Negative correlations between stature and age, and in some cases between bone length and age, were reported to occur. Regression formulae which were devised by Trotter and Gleser (1951), adjusted for the effects of aging on stature. The only problem with the proposed formulae is that the sample recorded height of a young military group and did not include those of older individuals.

Friedlander *et al.* (1977) reported that a reduction in stature, associated with an increase in age, is brought about primarily by changes in the vertebral column. In 2006, Raxter *et al.* attempted to address the issue of age correction of stature in their skeletal sample aged between 21 to 85 years. In their observations, these authors noted changes within the

individual vertebrae which they incorporated into the anatomical technique of Fully. These authors also reported an age adjustment of 0.04 cm per year in comparison to the 0.06 cm per year recommended by Trotter and Gleser (1951, 1952). The adjustment of age proposed by Trotter and Gleser (1951, 1952) has been questioned by a number of authors (Galloway 1988, Cline *et al*. 1989, Chandler & Bock 1991, Giles 1991). The debate reigns on the fact that firstly, age reduction is nonlinear and secondly, that a decline of stature in males and females follows different patterns. Thus, a gradual loss in height during the fourth decade would be difficult to identify without long term longitudinal data. Melton and Cooper (2001) reported greater height loss in females than in males which predisposes them to vertebral fractures.

Due to anatomical variations in individuals, the age at death is always given as a range (Bass 1995). In order to overcome these problems in forensics, Raxter *et al*. (2006) devised regression equations for estimating living stature from skeletal height which excluded the age correction factor. This adjustment was done so that their equations would be applicable to forensic cases. Furthermore, their study produced slightly lower correlations and higher standard errors of estimates when compared to the results where the age correction factor was included.

3.2.6 Living stature versus cadaver stature

The height of a human being is a measure of how tall or short a person is and this can be defined from a forensic (drivers licence) or biological (cadaver or living individuals) perspective (Ousley 1995). Living stature is measured in the living person, while cadaver stature is measured directly from an embalmed body. The outcome of measuring cadaver stature is to ultimately reach an estimate of living stature. Methods employed to derive at living stature thus differs which may also bring about certain advantages and disadvantage with each method used.

One example is that of reported heights in living individuals. This method is commonly used as it is easy to guess how tall or short a person is.The disvadantage is that forensic anthropologists need accurate information for identification purposes. Reports on living stature

in black, coloured and white South Africans of both sexes were provided by Steyn and Smith in 2007. Their measurements were based on the definition of ISO 7250. They recorded the vertical distance from the standing surface to the highest point of the head (vertex) with their subjects in the erect standing position. These authors classified their subjects as short (for results in the lower 25% of stature distribution), tall (upper 25% of stature distribution) and average or medium in height (middle 50% of stature distribution). These authors proposed that their fndings for estimating ante-mortem stature in South Africans be included in forensic reports.

Methods used on cadavers also differ. Some authors have measured hanging stature while others have recorded supine stature on cadavers in an attempt to accurately record stature. Byers *et al*. (1989) used a correction factor devised by Trotter and Gleser (1951) to account for differences between hanging cadaver stature and living stature. A correction factor is necessary as hanging stature is said to be 2.5 cm greater than living stature (Trotter & Gleser 1951).

According to Dupertuis and Hadden (1951) very little difference occurs between supine cadaver stature and living stature to warrant the use of a correction factor. They applied their formula to a cadaver sample belonging to American negroid and white groups, whereby standing statures of cadavers were measured with ice tongs inserted into the ear holes and the bodies suspended so that the soles of the feet were in contact with the ground (Dupertuis & Hadden 1951). Such methods have been criticized as they do not reflect the true stature of these cadavers. Various authors have shown that measurements of living stature as opposed to that recorded on cadavers differ by as much as two and a half centimeters (Telkka 1962, Trotter & Gleser 1952).

In conclusion, while discrepancies in methods used to record living and cadaver stature are known to occur, the heights of cadavers kept in records at medical schools also needs to be checked as it may lead to biased results. This was the case in the present study where cadaver heights were found to be inaccurate or missing and could thus not be used for stature estimation. This resulted in the indirect approach of stature estimation being adopted.

3.2.7 South African studies

Numerous studies on estimating stature have been initiated in South Africa (Lundy 1983, 1985, 1988a, Lundy & Feldesman 1987, İşcan & Steyn 1999, Dayal 2002, Bidmos & Asala 2004, Bidmos 2006, Chibba & Bidmos 2007, Steyn & Smith 2007, Ryan & Bidmos 2007, Bidmos 2008). The earliest recordings of stature in the Southern African population, according to Tobias (1972), goes back to 1910, where unpublished data by Dr WH Brodie was taken over by Dr GA Turner who added to the original data. At this stage, no regression formulae for samples from the African continent were available. In 1983, Lundy devised, for the first time, regression equations for estimating living stature from long limb bones in the South African "Negro". His sample comprised 177 male and 125 female South African "Negroes" between the ages of 18 and 65 years. His sample was obtained from the Raymond Dart Collection of Human Skeletons, housed at the University of the Witwatersrand. As living stature and cadaver lengths of his samples were not known, Lundy used the anatomical method described by Fully in 1956, to estimate total skeletal height. Once he had calculated the skeletal height using the humerus, radius, ulna, femur, tibia and spine, a correction factor was added for the soft tissues. He added 10 cm for heights of 153.3 or less, 10.5 cm for heights ranging between 153.6 to 165.4 cm and 11.5 cm for heights of 165.5 cm and above. For individuals over 60 years, 0.06 cm was subtracted for every year over the age of 30 years.

In 1987, Lundy and Feldesman revised Lundy's regresson equations which were published in 1983 due to five cases, which were excluded from the original study, being accidently included in the calculations. Lundy and Feldesman used Fully's original anatomical technique protocol of 1983, in re-computing skeletal height and lengths of the humerus, radius, ulna, femur, tibia and fibula.The revised results yielded higher correlations with lower standard errors than those reported in 1983. Comparison of results given for the final computed living stature and actual living stature showed a difference of approximately 2.0 cm. Lundy and Feldesman listed the femur as the best single bone to estimate stature in males and females. The best predictor using a number of bones in their study was the combined lengths of the femur, tibia and lumbar vertebral segment. These results were similar to that reported by

Lundy in 1983. The research carried out by Lundy and Feldesman, prompted further studies on stature estimation in the South African population.

To estimate stature in a South African white population, Dayal *et al*. (2008) calculated total skeletal height on a sample of 169 skeletons (98 males and 71 females) using Fully's anatomical method (Fully 1956, Lundy 1985). To obtain regression formulae for total skeletal height, Dayal *et al*. (2008) recorded maximum lengths of the humerus, radius, ulna, fibula, femur (physiological length) and tibia (non-malleolar length). Correlation values of 0.92 for males and 0.93 for females were reported. All lower limb bone correlations were higher in females than in males. Correlation values for the upper limbs in females were shown to be equal or slightly less than those for males. Dayal *et al*. (2008) concluded that lower standard error of estimates was seen in males when compared to females as well as with multivariate (combination of bones)

Bidmos and Asala (2005) used calcaneal measurements to estimate stature in South African blacks using the anatomical method devised by Fully (1956) for deriving regression equations. These authors reported the middle breadth as the variable with the highest correlation value of 0.47. Their highest correlations for the sexes were reported as 0.52 and 0.65 for males and females respectively.

Using the calcaneus to reconstruct adult stature in South Africans of European descent, Bidmos (2006) indicated that correlation values were significantly higher ($p<0.05$) in males than in females. Correlations for combined variables in the sexes were 0.76 for males and 0.79 for females while maximum length had the highest correlation (0.75). The results on the calcaneus for the two South African population groups indicate that the correlation values for whites are higher than for blacks.

Chibba and Bidmos (2007) derived regression equations for estimation of stature and maximum tibial length from six measurements of different fragments of the tibia in South Africans of European descent. These authors found that in males, the highest correlation for an individual variable was obtained for proximal breadth (0.58) and for females it was distal breadth (0.54). Their correlation values, when using various combinations of variables, ranged

from 0.58 to 0.61 for males and in females from 0.54 to 0.70. Standard error of estimates for their regression equations in males had values ranging between 6.52 and 6.71 cm and in females they reported a range from 5.20 to 5.94 cm. Their derived regression equations for predicting total skeletal height in females presented with greater accuracies than for males.

The skull has also been used in reconstructing skeletal height in an indigenous South African sample by Ryan and Bidmos (2007). These authors took six measurements of which the basibregmatic height in males showed the highest correlation (0.360) to total skeletal height. In females, the variable selected with the highest correlation with total skeletal height was the maximum bizygomatic breadth (0.606). These authors reported higher correlations for combinations of measurements rather than for individual variable measurements.

Regresssion equations using metatarsals have also been devised for South Africans of European descent and indigenous population groups (Bidmos 2008). Total skeletal height measurements for this sample were calculated according to that described by Fully and Brauer (cited in Bidmos 2008). The number of variables which Bidmos used for the metatarsals included six linear measurements to estimate stature for forensic purposes. These variables were listed as the lengths of metarsals one to four. For the fifth metatarsal, Bidmos recorded the functional and morphological lengths. The highest correlation values for individual variables reported by Bidmos for the indigenous groups were 0.62 for males (metacarpal one) and 0.72 for females (metacarpal one and two). His highest correlation results, for a combination of measurements in the indigenous groups, were recorded as 0.72 in males (all six variables) and 0.76 for females (a combination of firstly, metacarpals one, three and physiological length of the fifth metacarpal and secondly, for metacarpals one, two, three and physiological length of the fifth metacarpal). For the group of European descent, the highest correlation values were reported by Bidmos as 0.72 for males (firstly, metacarpals two, four and both physiological and functional lengths of the fifth metacarpal and secondly, all six variables together) and 0.76 for females (a combination firstly of metacarpals one, two and functional length of the fifth metacarpal and secondly, metacarpals one, two and both length measurements of the fifth

metacarpal). Males were shown to consistently have higher mean values when compared to females ($p<0.0001$) for total skeletal height.

Fragmentary femora have been successfully used to reconstruct stature in South Africans both of European descent and indigenous South Africans (Bidmos 2008). The seven femoral measurements which Bidmos undertook, included the maximum length, upper epicondylar length, vertical neck diameter, epicondylar breadth, bicondylar breadth, medial and lateral condylar length. These measurements were recorded according to definitions given by Bräuer (cited in Bidmos 2008). In males, the upper epicondylar length displayed the highest correlation (0.661) with total skeletal height and the epicondylar breadth the lowest correlation (0.525). In females, the highest and lowest correlations to total skeletal height were the lateral condylar length (0.729) and upper epicondylar length as well as vertical neck diameter (0.562) respectively. Bidmos reported slightly lower correlation values between maximum femoral length and fragmentary femoral measurements. For males, the highest and lowest correlations were given as 0.610 (upper epicondylar length) and 0.400 (epicondylar breadth respectively. For females, Bidmos obtained values of 0.781 (bicondylar breadth) and 0.544 (vertical neck diameter) as the highest and lowest correlations. Generally, Bidmos found the mean values to be significantly higher ($p<0.0001$) in males than in females.

In conclusion it can thus be said that there are South African standards for regressions from whole long limb bones for both black (Lundy & Feldesman 1987) and white (Dayal *et al*. 2008) groups, as well for fragmented tibia and femora, but nohing currently on hand bones for this population.

CHAPTER 4

LITERATURE REVIEW - SEX DETERMINATION

4.1 Introduction

When forensic anthropologists are confronted with decomposed material which is human in nature, great consideration is placed on anatomical detail in order to compile the morphological data of an individual (Rich *et al*. 2005). Together with the determination of age, population affinity, and stature, the establishment of sex from the analysis of human skeletal remains is of vital importance in forensic identification (Krogman & İşcan 1986, Rich *et al*. 2005).

The genetic, morphological and biological difference between males and females of the same species is referred to as sexual dimorphism. These genetic and physiologic differences are extremely marked which makes it possible to establish the sex from the human skeleton (Holman & Bennet 1991, Bass 1995, White & Folkens 2000). The extent to which the human skeleton, or parts thereof, can be used to determine sex with a fair degree of accuracy is of importance to physical anthropologists and forensic scientists (Thieme & Schull 1957).

Sexual dimorphism of the human skeleton has been well documented, with some regions described in greater detail and receiving more attention than others. According to Williams *et al*. (1989), the preference of using a bone relates to its anatomical position in the skeleton and subsequently to its functional role in males and females.

The bones of the skeleton commonly used to establish sexual dimorphism, include the pelvis, skull and long bones, which have been studied either on their own or in combination with other bones. Williams *et al*. (1989) have shown that because the axial skeleton is relatively heavier in males than in females, it creates a force which is carried over to the femur, motivating the use of this bone in comparison to other long limb bones to distinguish between the sexes.

To sex the remains of an unknown adult individual is easier than that of the neonate or juvenile, except in cases where the adult skeleton is incomplete, which makes the task more

daunting and difficult. Working with an intact skeleton, which is the ideal for any researcher, it is possible to obtain ±100 % accuracy in establishing the unknown individual's sex (Krogman & İşcan 1986).

However, skeletal remains may be found poorly preserved and fragmented rather than well preserved and intact (Franklin *et al*. 2008). In practice, the common methods employed by physical anthropologists and forensic scientists are either non-metric (visual of morphological) or metric in nature.

Sex determination based on differences in skeletal morphology has been successfully carried out on the pelvis (Krogman & İşcan 1986), skull (De Villiers 1968, Krogman & İşcan 1986), scapula and humerus (Steele 1970) and, mandible (Loth & Henneberg 1996). These morphological studies have also shown that males tend to be larger and more robust than females (De Villiers 1968, Loth & İşcan 2000). While morphological indicators are useful with intact bones, their value and accuracy is reduced when only bone fragments or an incomplete skeleton is available. This has led to the development of standards for metric sex determination of various parts of the skeleton. In cases where forensic findings need to be defended in court, the accuracy of sexing an unknown individual is often coupled to the metric methods employed in such an investigation.

The earliest recording of the use of metric methods was by Washburn in 1948. He measured lengths of the ischium and pubis and calculated an ischio-pubic index from these bones. From this study, Washburn reported sexing accuracies of 90%.

In 1955, the first assessment of long bones was carried out by Pons, who developed discriminant function formulae for femora and sterna obtained from a skeletal collection in Lisbon. In 1957, Thieme and Schull used several long bone variables on an African American sample taken from the Terry Collection. Their results showed that the maximum length and bicondylar width of the humerus were the best variables to use in assigning sex. They aso reported higher accuracies with a combination of bones when compared to the use of single bones. Standard osteometric methods have since been widely used by numerous authors in

assessing and determining sexual dimorphism (Black 1978, Novotny *et al*. 1993, France 1998, Asala 2001).

Invariably, from a series of measurements recorded on a bone, it may be that one variable is singled out as providing the highest degree of accuracy when establishing sexual dimorphism (Black 1978). This has been shown in the case, for example, where the pubic length has been preferred over and above the ischial length (Washburn 1948, 1949, Hanna & Washburn 1953).

4.2 Literature review

The purpose of this section is to review past and present research directly associated with the use of various aspects of the skeleton in establishing sex as a form of identification. As the literature is so vast, particular emphasis will be placed on previous studies involving the hand, as well as studies on sexual dimorphism in South Africa.

4.2.1 Manifestation of sexual dimorphism in the skeleton

Scientists have attempted to incorporate almost all of the bones of the postcranial skeleton in their investigations on sexual dimorphism (Krogman 1962). Intact and complete skeletons are not always available resulting in studies being carried out on single bones or fragments thereof that have been obtained from excavation expeditions, or from recovered bodies in forensic cases.

The bones of the skeleton receiving a great amount of attention includes the humerus (e.g., Singh & Singh 1972a), radius (e.g., Steel 1963), ulna (e.g., Steel,1963, Singh & Singh 1974), clavicle (e.g., Thieme & Schull 1957, Jit & Singh 1956), sternum (e.g., Thieme & Schull 1957, Jit *et al.*1980), scapula (e.g., Bainbridge & Genoves 1956), pelvis (e.g., Reynolds 1947, Washburn 1948, Kelly 1978, Weaver 1980, Kimura 1982a), sacrum (e.g., Flander 1978, Kimura 1982b, İşcan & Derrick 1984), femur (e.g., Dwight 1905, Pearson 1917-1919, Steel 1963, Singh & Singh 1972b, Black 1978, DiBennardo & Taylor 1979, 1982, İşcan & Miller-

Shaivitz 1984a, Dittrick & Suchey 1986, Steyn & İşcan 1997), tibia (e.g., Dwight 1905, Steel 1963, Singh 1975, İşcan & Miller-Shaivitz 1984b, 1984c; Kieser *et al*. 1992, Steyn & İşcan 1997) and fibula (e.g., Steel 1963, Singh & Singh 1976). These bones have been shown to be accurate predictors in determining sex. In other words, these major long bones have been preferred over other ones. While weight-bearing bones of the skeleton are preferred in studies on sexual dimorphism, non-weight bearing bones can also be sexually dimorphic (MacLaughlin & Bruce 1985).

The impact of the forces received by the pelvis to the femur has resulted in this bone being used extensively in various populations, including the Japanese (Hanihara 1958), Australian aborigines (Davivongs 1963), American blacks, whites, and Indians (Black 1978, DiBennardo & Taylor 1979, 1982, İşcan & Miller-Shaivitz 1984c, 1986), Italians (Pettener 1979), Czechs (Cerny & Komenda 1980), prehistoric Scottish (MacLaughlin & Bruce 1985), Chinese (İşcan & Shihai 1995), and Nigerians (Asala 1998). These studies are all based on an intact femur rather than fragments of the bone.

4.2.2 Manifestation of sexual dimorphism in bones of the human hand

In adults, sexual differences are evident in hand length measurements and in hand width to length ratios (McFadden & Shubel 2002). Observations of the index and ring finger indicate that the second digit in males is shorter than the fourth digit while in females they are either of equal length or it may be that the second digit is slightly longer than the fourth one. In young adults, sexual dimorphism in the diaphyseal diameter of metacarpals appears to be related to differences in body size (Himes & Malina 1977). In other words, at a constant body size and age, diaphyseal measurements of the metacarpals in males are shown to be significantly larger than that in females (Himes & Malina 1977).

With an increase in age, the metacarpals are reported to reduce in size, a feature more prevalent in males than in females (Harris *et al*. 1992). Bone loss in second metacarpals occurs more rapidly in females than in males especially after the fifth decade and then tends to decrease after the sixth decade (Plato & Purifoy 1982). The midshaft of second metacarpals is

particularly prone to earlier bone loss than the rest of the bone, an observation that is age-related (Kimura 1990, Lazenby 1998). The rate of bone loss probably relates to the amount of cortical bone present. Earlier studies have concluded that in males the second metacarpal was longer and composed of more cortical bone than in females (Plato *et al*. 1982).

The weight of an individual is known to place a load on the skeleton which ultimately accounts for sexual differences recorded in the pelvis and lower limb (McFadden & Shubel 2002). It may be assumed that if similar forces were placed on the hands, that these sexual differences may be expressed in the individual bones of the human hand. Research in hominids has shown that the relatively large distal phalanges are due to these bones accommodating increased loads (Smith 1995). On the other hand, there is evidence to indicate that distal phalanges have decreased rather than increased in relative size through time (Smith 1995). This reduction in size has been ascribed to negative selective forces (Smith 2005).

External factors such as culture and environment are also known to have an influence on sexual differences in the human skeleton (Loth & İşcan 2000). The hands are no exception to this influence. In the late 1900's it was shown that metacarpals are poorly preserved and relatively small in size when compared to long bones. For this reason, metacarpals were excluded from studies on sexual dimorphism (Black 1978). Other studies, however, have shown the hands to be as sexually dimorphic as the rest of the skeleton (Garn *et al*. 1973, Meadows & Jantz 1992). In fact, the second metacarpal has contributed to methodologies in forensic anthropology with regard to identification of the sex of an individual. (Falsetti 1995, Scheuer & Elkington 1993). The relatively large size of the second metacarpal may be due to apposition of bone on the outside rather than resorption from the medullary area which influences the width of the second metacarpal (Plato *et al*. 1980).

Scheuer and Elkington (1993) in their cadaveric study of sex differences on metacarpals and first proximal phalanx of 60 white British subjects, described a multiple regression method which yielded accuracies of 74% to 94% with the first metacarpal showing the highest degree of accuracy. They employed combinations of six measurements for each metacarpal in order to generate multiple regression equations (Scheuer & Elkington 1993).

According to these authors, a method used to sex the bones is only useful if it yields an accuracy of at least 80%.

Falsetti (1995) used the data collected by Musgrave in 1970 on the metacarpals of a cadaveric sample at the Royal Free Medical School in London. To this sample he added metacarpals of 212 individuals from the Terry collection at the Smithsonian Institution in Washington and increased his sample with an additional 40 cases from the forensic or donated collection in the Maxwell Museum of Anthropology in New Mexico. Falsetti (1995) used 5 measurements for each metacarpal to generate discriminant functions. Data for the different populations were pooled, so too were the measurements for right and left metacarpals. His results on the collections yielded accuracies of 78.0% to 92% for the second metacarpal, 80.0% to 86% for the fourth metacarpal, and 84.0% to 85.0% for the fifth metacarpal. Furthermore, he concluded that metacarpals 1 and 3 exhibit different levels of sexual dimorphism and great variation in morphology by race and could not be used to develop discriminant functions. Falsetti (1995) also tested for population differences and found that metacarpals 2, 4 and 5 displayed no morphological differences that were population specific.

Wien (1984) was able to show that length and width measurements of metacarpals and phalanges were approximately 90.0% accurate in detecting sexual differences. Scheuer and Elkington (1993) generated their prediction accuracy for correct sex determination which ranged from 78.0% to 94.0% for the metacarpals. In 2003, Burrows *et al.*, rather than devising their own regression formulae, tested equations already developed for different populations groups. They concluded that the percentage accuracies are for the same for all the metacarpals. While some studies prove that metacarpal one is the most accurate in sexing individuals (Scheuer and Elkington 1993), the same bone was found to be the least accurate in another study (Burrows *et al*. 2003). In some cases, authors may report on the same bone as providing the highest accuracies as is the case with the second metacarpal (Falsetti 1995, Burrows *et al*. 2003).

Stojanowski (1999) placed the 4th metacarpal top of his list. What these findings show is that these equations cannot be used across populations as these studies indicate that

different hand bones show different prediction accuracies. Smith (1996) also used the osteological collections incorporating metacarpals and phalanges in order to correctly sex and population affinity. In hand studies most of the focus has been on the use of metacarpals (Scheuer & Elkington 1993, Smith 1996) however, this has changed to include the proximal and distal phalanges as well (Smith 1996, Scheuer & Elkington 1993).

Using metacarpals, Scheuer and Elkington (1993) reported an overall sexing accuracy ranging from 74.0% to 94.0% with the first metacarpal producing the highest degree of correct estimation. Lazenby (1994) reported sexing accuracies ranging from 97.4% to100% for males and 37.5% to 76.8% for females using the right and left second metacarpal. The average sexing accuracy for his total sample was 94.0%. Lazenby concluded that the right second metacarpal was more likely to provide correct identification in males while in females it was the left side.

Smith (1996) reported results for both right and left hands ranging from 87.0% to 89.0% for metacarpals, 76.0% to 79.0% for proximal phalanges, and 81.0% to 83.0% for distal phalanges. Results for the middle phalanges were slightly different in that the left hand yielded average results of 79.0% while the right hand yielded results of 72.0% while another three pairs of models yielded success rates of 2-3%. Smith applied her models for sex determination in reverse and reported success rates of 84-86% for metacarpals. Of all the metacarpals, the second (Kusec *et al.*1988, 1989, Plato 1980), third and fourth metacarpals have received most of the attention (Kusec *et al*. 1988, 1989).

In conclusion, the literature indicates that the hand bone with the highest degree of accuracy differs for each population group. While Thieme and Schull (1957) emphasized the fact that right-left asymmetry has no value when estimating sex, current research clearly indicates that right-left asymmetry does contribute to the sexing process.

4.2.3 Sexual dimorphism in the South African population

While forensic anthropology is known to be one of the fastest growing fields worldwide (İşcan 1988), South Africa, which is located in an interesting geographical part of the world,

may slowly be included in this category in the near future. Its unique position at the tip of Africa has provided opportunities for different populations not only from Africa, but also from the rest of the world to converge and exchange genes. One may assume that the South African population has over the centuries, and with its history, been composed of a gene flow representative from every part of the world (Benjeddou 2006). Besides estimating factors such as race, age and stature, South African forensic anthropologists have also included determination of sex in the identification of unknown remains.

The earliest studies on sexual dimorphism in South Africa were reported by de Villiers (1968) who studied the skulls of the South African black population. This author collected non-metric and linear metric data to establish sexual dimorphism, however, no discriminant function equations were devised for this sample. Later research has seen the development of discriminant equations which has resulted in a considerable surge in the number of standards available for estimating sex in the South African population. Rightmire (1972) reported sexing accuracies using the crania of South African blacks as 90.6%. Franklin *et al*. (2005a, b) also examined crania from indigenous South African groups in order to establish sexual dimorphism. They reported accuracies ranging between 77.0 - 80.0% and listed the facial width as the most accurate trait followed by the cranial length and basi-bregmatic height. Steyn and İşcan (1998) reported sexing accuracies for the cranium in South African whites as 86.0%.

The bones of the feet have not been excluded from such studies. Bidmos and Asala used the calcaneus to discriminate sex in South African whites (2003) and blacks (2004). Mean values for their male sample were significantly higher ($p<0.001$) than for the female sample in both groups. For their white sample the variable with the highest percentage accuracy in the stepwise (91.1%) and direct discriminant (92.1%) analyses was the dorsal articular facet breadth. In testing the validity of the discriminant function equations, Bidmos and Asala reported that 88.0% of their sample was correctly sexed using the stepwise analysis while the direct analysis of all their variables computed an 84.0% accuracy of correct classification. Their findings for the black group showed that the dorsal articular facet length, presented with the highest percentage accuracy using the demarking process (79.3%) and

stepwise analysis (85.3%). Maximum height of the calcaneus was the variable with the highest percentage accuracy (86.2%) in the direct analysis. The percentage of cases correctly classified and cross-validated ranged between 79.3 - to 86.2% for the direct analysis and 79.3 - 85.3% for the stepwise analysis. When compared to the results of the white group, those of their black group had slightly lower average percentage accuracies. Bidmos and Asala concluded that measurements of breadth and length are of greater value than height as sex determinants when using the calcaneus.

Bidmos and Dayal used the talus to establish sexual dimorphism in South African whites (2003) and blacks (2004). Their mean values indicated statistically significant differences ($p<0.05$ for whites and $p<0.001$ for blacks) between males and females. High correlation coefficients ranging from 0.90 to 0.99 were also reported by these authors for both groups. Sexing accuracies for their white group, as computed from the direct analysis were given as 82.0% (talar length) and 80.0% (breadth of the posterior auricular surface). Results for the stepwise analysis indicated that talar length had the highest sexing accuracy of 87.5% (all variables entered) and 85.0% (for all lengths entered) while the breadth of the trochlea had the highest sexing accuracy of 77.5% (for all breadth dimensions entered). The average sexing accuracy for lengths was given as 88.0% as compared to average breadth accuracy of 78.0%. Sexing accuracies for their black sample which was based on the direct analysis, listed the talus head as the variable with the highest average sexing accuracy (85.8%). In their stepwise analysis the average sexing accuracy was 86.7% with an overall length and breadth accuracy of 85.0% and 84.2% respectively. These authors concluded that the talus length for whites and talus head for blacks were the best sex discriminators.

In establishing standard numerical values and demarking points to determine sexual dimorphism, Asala (2001) used the femoral head obtained from a South African white and black skeletal sample. This author established that there were no statistically significant side differences in the vertical and transverse head diameters in both sexes for whites and blacks. On the other hand, the same parameters were found to be significantly higher ($p<0.001$) in males than in females for both groups. A comparison of the two groups showed that the

identification and demarking points in South African whites are higher than in their black counterparts. Asala concluded that the mean head diameter of right and left femora or only the vertical head diameter can be used to establish sex in this population if only a fragment of this bone is available.

Based on his findings in 2001, Asala then looked at the efficiency of the demarking point of the transverse and vertical femoral head diameters as parameters to determine sex (2002). For the white group, this author reported 32.0% cases for three vertical diameters and 18.0% for three transverse diameters that could be accurately sexed using the demarking points. A comparison of the sexes indicated that only 47.0% males and 18.0% females could be accurately sexed. In total, 32.0% of his cases could be accurately sexed using the demarking. For his black sample, Asala reported sexing accuracyof 22.0% (using the vertical diameter) and 31.0% (using the horizontal diameter) when combining the demarking points for right and left sides. The demarking point could also be used to accurately sex 47.0% males and 10.0% females. This author concluded that the overall success rate using the demarking point in South African blacks was the same as for whites, namely, 32.0%.

Fragments of the femur of a South African black population have also been shown to be sexually dimorphic (Asala *et al*. 2004). Percentage accuracies reported by Asala *et al* (2004) for the proximal femoral end ranged between 85.1 - 82.6% compared to 85.1 – 82.6% at the distal end for combined and single variables respectively. These authors concluded that the femoral head was the most important sex discriminator in this population group. Contrary to these findings, Steyn and İşcan (1998) stated that the distal femoral breadth was the best variable selected to discriminate for sex in the South African white population group.

Steyn and İşcan (1997) studied the femur and tibia in South African whites and reported average accuracies ranging from 86 – 91%. Their results for classification accuracy on the humerus in South Africans (1999) were 96.0% (whites) and 95.0% (blacks) which was slightly higher than their earlier study on lower limb bones but nonetheless high. Generally, their accuracies for females were slightly higher than for their male samples except in the case of the humerus where accuracies for black males (95.0%) were slightly higher than black

females (91.0%). These authors concluded that in the humerus, the head and epicondylar diameters in whites and head and maximum length dimensions in blacks as the best discriminators of sex. Kieser *et al*. (1992) reported classification accuracies using the proximal tibial end as ranging between 84.6 - 92.0% for white and black South Africans, results which are similar to that given by Steyn and İşcan (1997).

Franklin *et al*. (2008) used seven standard and two non-standard dimensions of the mandible to establish sexual dimorphism in five (Zulu, Swazi, Xhosa, Sotho and Tswana) local black South African populations. These authors found very little variation in sexing accuracies between the five local population groups and presented results for a pooled sample. Results from their F-statistics analysis, listed four variables that expressed the greatest level of dimorphism. These variables, including their expected sexing accuracies, were given as follows: maximum length (77.3%), height of the ramus (73.8%) and coronoid process (73.3%) and bi-gonion beadth (70.7%). Stepwise analyses results for.the pooled groups, indicated the highest percentage (81.8%) recorded was for the coronoid height. The percentage for sexing accuracy, as computed from the direct analysis of the pooled sample, was 84.0%. Steyn and İşcan (1998) showed that the bizygomatic breadth was the most dimorphic of all the measurements taken with an average accuracy of 80.0%, similar to that given by Loth and Henneberg (2001).

While South African studies mentioned thus far report on sexual dimorphism for whites and blacks, pooling of data of the two groups has also been done. One such study is that carried out by Barrier and L'Abbé (2008). These authors used nine anthropometric measurements of the radius and seven of the ulna, to establish sexual dimorphism in a modern South African sample (n=400). Results for the radius indicate that the minimum midshaft diameter was listed as the single best discriminating variable in males (82.0%) and females (86.0%). Classification accuracies in males ranged from 80.0 - to 86.0% for the radius and 76.0 - 87.0% for the ulna. In females, the accuracies reported varied between 82.0 - 88.0% for the radius and 83.0 - 89.0% for the ulna.

A sesamoid bone such as the patella, which is said to display very few post-mortem changes (Introna *et al*. 1998), was used as a sex determinant in South African blacks with results indicating average classification accuracies ranging between 60.0 - 80.0% (Dayal & Bidmos 2005).

Initial studies on South Africans reported on different groups such as the Zulu, Xhosa and Southern Sotho populations while more current research in the field of sexual dimorphism publish results purely on the South African white and black population group. This is due to the fact that the earlier groups are disappearing (Franklin *et al.* 2006).

It can be concluded that while earlier studies carried out on South Africans presented with numerous problems due to the diverse ethnic origins and mixture of the various populations which occured as a result of urban migration, current research focuses on the South African white and black population groups. Furthermore, diagnostic accuracies for the crania are far less when compared to that obtained from the femur and tibia in the South Africans (Steyn & İşcan 1998). While attempts are made to establish discriminant function equations for various aspects of the skeleton for South Africans, a comprehensive analysis of sexual dimorphism in the hand bones of this population group is lacking.

CHAPTER 5

MATERIALS AND METHODS

5.1 Materials

In order to be able to identify and side individual hand bones, an initial sample of 20 sets of hands from each sex-race group (blacks, whites, males and females) were collected. These hands were obtained from cadavers, aged between 21 and 86 years that had been completely dissected by second year medical and dental students.

To estimate stature and sex of an individual, an additional sample of 30 sets of hand bones from each of the four groups were used. These hands were obtained from skeletons currently housed in the Department of Anatomy at the University of Pretoria. These skeletons are from individuals aged between 21 and 81 years. The entire study thus comprised 50 sets of hands from each sex-race group giving a total sample of 200 individuals.

5.1.1 Pretoria Bone Collection

The Anatomy Department receives on an annual basis approximately 50 to 100 bodies which are either unclaimed or donated. The unclaimed bodies are obtained from local state hospitals in the Tshwane Metropolitan Area (L'Abbé *et al*. 2005). Under the Human Tissues Act, No 65 of 1983, anyone may donate his or her body to science for the purpose of tissue transplants, medical training and research. This act also covers destitute people who die in public hospitals. If these individuals are not claimed within a twenty-four hour period, the body is transferred to the nearest medical school where they are embalmed and stored for about a year. All bodies that are received by the Department of Anatomy at the University of Pretoria, are of known age, sex and population affinity. Additional information regarding the height, weight and cause of death is also known.

These bodies are then dissected by students registered in the Department of Anatomy. After being dissected the bodies undergo a cleaning process which includes maceration and defatting. Complete skeletons are then reserved for the Pretoria Bone Collection and used for

research purposes. The incomplete skeletons are allocated to the Student Collection and used for teaching purposes. The Pretoria Bone Collection currently has approximately 2000 skeletons. The currently appointed director for the Pretoria Bone Collection is EN L'Abbé who can be contacted for any additional information including access to this collection (L'Abbé *et al*. 2005).

5.2 Methods

5.2.1 Preparation of the dissected hand bones for identification and siding (Figures 5.1a-f)

The method for preparation of the hand bones as described by Scheuer and Elkington (1993), were used as a guide for the present study. The right and left hands necessary for purposes of identification were disarticulated from each cadaver after the students had completed dissecting them, removing as much of the soft tissue as possible. These hands were placed into a single calico bag which was divided into two pockets to separate the right and left hand belonging to the same cadaver (Figure 5.1). An aluminium identification label which would not be destroyed by the boiling process was attached to each hand. The calico bags were then placed into a larger linen bag and transferred to a huge drum filled with water. The drum was then positioned over an open fire and the hands were boiled for approximately four days in order to soften the tissue. It should be stressed that if the hands are boiled for a longer period than stipulated, it may soften the tissues to a point where individual hand bones may mix and thus make it difficult to assign them to a digit.

Once the hands were boiled for the specified time period, they were cleaned manually by N Navsa. The cleaning process involved disarticulating the individual hand bones and removing the surrounding soft tissue. Once disarticulated and cleaned, all five metacarpals and 14 phalanges from each hand were placed into specially designed calico bags. Each calico bag was divided into 38 small pockets which were carefully sewn to accommodate and isolate the 19 hand bones from each hand of one cadaver. Each pocket was labelled exactly

the same way as for each finger bone. The metacarpals were each assigned a single digit number, namely, 1 for thumb, 2 for index finger, 3 for middle finger, 4 for ring finger and 5 for little finger. Each phalangeal bone was assigned two numbers. The first number indicated the bone associated with a specific finger, namely, the number 1 (thumb), 2 (index finger), 3 (middle finger), 4 (ring finger) and 5 (little finger). The second number would indicate the row that the bone belongs to, namely, 1 for proximal phalanx, 2 for middle phalanx and 3 for distal phalanx. As an example, the phalanges belonging to the index finger are numbered as 21, 22 and 23 for proximal, middle and distal phalanges respectively, those for the middle finger as 31, 32 and 33, etc.

In the final stages of preparation, the labelled calico bags containing the hand bones were boiled in Trichloroethylene solution for 24 hrs in order to remove all traces of fat. The hands were then removed from the individual pockets, air-dried on racks and labelled as mentioned above. All 80 sets of hand bones from each of the four groups, including both right and left hands, were prepared by N Navsa. In this way, each bone was correctly assigned to the appropriate digit.

The individual bones were carefully examined and characteristic features recorded for identification purposes. Various anatomical textbooks were used to assist in compiling detailed descriptions of each hand bone. Unique features of individual hand bones were used to assign them to either the right or left hand. These unique features were listed at the end of the descriptions of each hand bone. Right and left hands were cleaned and employed in the identification and siding process, however, only the bones from the left hand were used for the rest of this study. For purposes of orientation, the following terms were used with the hand in the anatomical position, namely, dorsal, palmar, medial, lateral, articular end of the head and articular end of the base. To make the descriptions easy to follow, numbers are placed next to each bony landmark identified. These numbers coincide with the numbers on the corresponding figure.

5.2.2 Problems which arose throughout the preparation of the dissected hand bones for identification and siding

Once the maceration process was complete, the hands were laid out on tables and hand diagrams were then made to record morphological features. In the process of noting landmarks, asymmetries were observed, not only in a series of bones, but also between corresponding bones of the right and left hand. The characteristic features noted for identification purposes were also used for siding the hand bones. Once a list of identifying and siding features had been put together, the question arose as to the presentation of this information. Line diagrams were attempted but these did not bring out detail that was required. Photographs of each hand bone were taken and these were redone on a few occasions so that the morphology of each bone could be clearly seen. Each photograph was then re-looked and it was decided to highlight certain features with a thick broken line to emphasize the bony landmark. During the entire process, terminologies had to be standardized which meant that labelling on photographs of each hand had to be checked to maintain consistency throughout.

Photographs of the individual hand bones were re-done on many occasions in order to enhance key morphological traits that were described in the text. While terminologies of the metacarpals in most anatomy textbooks proved to be limited for descriptive purposes, the phalanges, especially the distal row in this series of hand bones, lacked an adequate description in most anatomy textbooks. In these cases, new terminologies were introduced which best represented characteristic features of each bone. A shortfall in the use of new terminologies is that different persons may view bony landmarks differently. For example, a tubercle to one researcher may be considered to be a tuberosity to another.

5.2.3 Measurements of the hand bones (Figures 5.2 to 5.17)

Only left hands from a total sample of 200 (50 white males, 50 white females, 50 black males and 50 black females) individuals were measured. A total of seven measurements, as opposed to six used by Scheuer and Elkington (1993), were taken on each hand bone, namely, length, dorsal palmar and medial lateral width of the base, dorsal palmar and medial

lateral width of the head and dorsal palmar and medial lateral width of the midshaft region. All measurements were recorded to the nearest 0.01 mm, using a digital caliper.

Length measurement:

Maximum length was measured as opposed interarticular length used by Scheuer and Elkington (1993). The reason for taking the maximum length is that proximal and distal articular ends of each bone varied in shape and this may affect accurate length measurements. Maximum length was recorded by placing the digital caliper on the lateral aspect of the bone. All length measurements were taken along the longitudinal axis of the bone from the proximal to the distal end (illustrated in Figures 5.2, 5.4, 5.6, 5.8, 5.10, 5.12, 5.14 and 5.16).

Base measurements:

The maximum medial-lateral measurements were always taken from the most medial to the most lateral point on the base of each hand bone (Figures 5.2, 5.4, 5.6, 5.8, 5.10, 5.12, 5.14, and 5.16). Maximum diameters were also recorded from the most dorsal to the most palmar point (Figures 5.3, 5.5, 5.7, 5.9, 5.11, 5.13, 5.15, and 5.17). This was done to overcome the morphological variation which exists at the proximal end of each of these bones. This variation was more marked in the metacarpals than in the phalanges. All measurements were carried out using a caliper which was always positioned in the medial lateral and dorsal palmar plane.

Head measurements:

Maximum medial-lateral (Figures 5.2, 5.4, 5.6, 5.8, 5.10, 5.12, 5.14, and 5.16) and dorsal-palmar (Figures 5.3, 5.5, 5.7, 5.9, 5.11, 5.13, 5.15, and 5.17) measurements of the head were also recorded. Unlike the base, the morphology of the distal ends of each hand bone displayed fewer variations which made it easy to record the maximum dimensions. All measurements of the head were also recorded with a calliper positioned in the medial lateral and dorsal palmar plane.

Midshaft measurements:

Scheuer and Elkington (1993) used a single measurement for the midshaft, namely, the maximum dimension. In the present study, the midshaft was found to have a maximum medial-lateral (Figures 5.2, 5.4, 5.6, 5.8, 5.10, 5.12, 5.14, and 5.16) as well as a maximum dorsal-palmar (Figures 5.3, 5.5, 5.7, 5.9, 5.11, 5.13, 5.15, and 5.17) dimension. The midshaft of each hand bone was established by noting the halfway mark of the maximum length recorded. The midshaft region for all hand bones was found to be the narrowest part of the shaft. Both diameters of the midshaft region were recorded with a caliper which was positioned in the medial-lateral and dorsal-palmar plane.

5.2.4 Measurements of the humerus, radius, ulna, femur and tibia

The length of the bones most commonly used for stature estimation, namely, humerus, radius, ulna, femur, and tibia, had to be measured. This dimension was needed as the length of each hand bone had to be regressed to that of a long bone. Only long bones belonging to the left side of the skeleton were used and these long limb bones came from the same cadavers and skeletons as the hand bones. The maximum length of each of the five long bones was recorded using an osteometric board (Figures 5.18 to 5.22).

5.3 Statistical analysis

A data file was created using Statistical Product and Service Solutions (SPSS®, version 11.5). All variables used in this study were defined according to the measurements recorded on each hand bone. All data collected were subsequently entered separately for black males, black females, white males and white females into the SPSS spreadsheet. Once entered and before any analyses was done, screening and cleaning of the data was done. In this way any errors in the data was checked and corrected. In other words, any value/s that fell outside the range of possible values for a variable was checked and corrected. All minimum and maximum values were looked at to see if they were within the range of possible scores for

that variable. Valid and missing cases were also screened for any errors that may have occurred when entering the data. A paired *t*-test for inter- and intraobserver test was carried out to test for repeatability of the measurements.

To test for intra-observer repeatability in the metric analysis, hand bones from 36 individuals were randomly selected from a total sample of 200. These bones were the metacarpal, proximal, middle, and distal phalanges of the thumb and little finger. All seven hand bone dimensions recorded on the initial sample of 200, were re-measured on this random sample after all the initial data was collected. The repeated metric data was statistically compared to the original data set using a one-way analysis of variance (ANOVA).

To test for inter-observer repeatability in the metric analysis, a PhD student in Anthropology was asked to re-measure the randomly select left hand bones from the 36 individuals. The student was not involved in this study at all. The metric data collected by this student was statistically compared to the original set of data also using a one-way ANOVA.

Once the data were screened for errors and the repeatability test was carried out, a basic statistical analysis was done to establish whether the 7 hand bone dimensions were significantly different firstly between whites and blacks, and secondly, between males and females. To do this an independent sample T-test was carried out and the descriptive statistical analysis which was calculated included the means, standard deviations, and ranges. The independent samples T-test will indicate whether there is a statistically significant difference in the mean scores for the 7 dimensions carried out on the hand bones (metacarpals and phalanges) and the length dimensions of long bones (humerus, radius, ulna, femur and tibia). That is, it will establish whether the hand and long limb bone dimensions differ firstly, between whites and blacks and secondly, between males and females of the South African population.

5.3.1 Stature determination

The mean values of hand and long limb bone measurements in the descriptive statistics indicated few statistically significant differences between whites and blacks, the data was thus pooled. In order to reconstruct the length of a long bone, a correlation was established between the metacarpals and phalanges to each of the five long limb bones, namely, the humerus, radius, ulna, femur, and tibia. A correlation analysis is done to indicate the strength and direction of the linear relationship between the hand bones to each of the long limb bones, otherwise it will not be possible to use them for linear regressions. The Pearsons correlation test was chosen for this analysis.

As most of the skeletons lacked documented cadaver lengths and the reliability of documented cadaver lengths when present, was questionable, it was decided to regress the length of a hand bone to that of a long limb bone. The length of a long bone is frequently used when determining stature of an unknown individual.

Generally, for stature estimation both univariate and multivariate analyses in a direct and stepwise manner is carried out. In the present study, a univariate analysis was done where the hand bones were regressed against each of the long bones of the upper (humerus, radius, and ulna) and lower (femur and tibia) limbs. Multivariate analyses of these variables were not carried out because of the numerous combinations possible, which would have been beyond the scope of this thesis. It was thus decided to carry out only a single variable analysis. From the regression analyses, the correlation coefficient (r) standard error of estimate (SEE), slope and intercept were obtained.

The value obtained from this analysis could then be inserted into a second formula such as that devised by Lundy and Feldesman (1987) and Dayal *et al*. (2008) in order to estimate final stature. The statistical analysis is discussed further under the chapter of stature estimation.

5.3.2 Sex determination

As the intention of this analysis was to provide sex discriminant functions, it was necessary to determine whether or not levels of sexual dimorphism varied between the white and black groups. An analysis of variance (ANOVA) was then carried whereby a detailed description of data for males, females, whites, and blacks was generated. From the ANOVA analysis, data for whites and blacks were pooled and a discriminant function was run on the pooled data.

Discriminant function analysis is primarily used to sort binomial characteristics (e.g. sexual dimorphism) between two groups (e.g. males and females). This method identifies those variables that are competent at separating groups, selects variables which perform equally well and it also selects variables with similarities and differences. Discriminant analysis provides a predictive model for group membership (e.g. males or females) based on the observed characteristics (e.g. measurements) of each case. The statistical output generates a discriminant function for the two groups or a set of discrimant functions if there are more than two groups. These functions are generated from a sample of cases for which group membership is known and then applied to new cases with the available measurements where group membership is unknown (Pallant 2001, Tabachnick & Fidell 2007).

The accuracy of the discriminant function is expressed by an F-ratio and Wilks Lambda value. The F-ratio is used to assess whether the differences between the groups are statistically significant, with higher F-scores indicating a stronger significance. Wilk's Lambda identifies the contribution each variable had in distinguishing between the sexes and defines the order in which dimension will appear in the discriminant function formula. If a score=1 it means that the groups are equal. Smaller Lambda values indicate increased variability between the groups (Pallant 2001, Tabachnick & Fidell 2007). After the stepwise analysis was calculated, the variable that appeared to best distinguish between the sexes, was selected and subjected alone to direct discriminant analysis so as to develop a formula for determing sex from fragmented remains.

Classification accuracies were then tested. A “leave one out classification” procedure was employed to measure the effectiveness of the discriminant function. This method of analysis classified each specimen from the functions derived from all the other cases. The results were then cross-validated to determine whether or not specimens were correctly assigned to either the male or female group.

Discriminant function statistics explore the predictive ability of a set of independent variables on a single categorical dependent measure. In other words, it takes the measured seven dimensions of each hand bone and uses them to predict the sex (male or female) of an individual with a certain degree of accuracy. The use of linear discriminant analysis for deriving classification functions is dependent on the assumption of multivariate normality of the data and equality of variance-covariance matrices (Tabachnick & Fidell 2007). In other words, the distribution of each variable within each of the classes must be normal. Studies have shown that the level of sexual dimorphism varies within the skeleton by population (Garn *et al*. 1973, Meadows & Jantz 1957).

Figure 5.1: Paired hands in calico bags for boiling (a), hand after boiling (b), disarticulation and cleaning of individual bones (c), calico bag with 30 pockets for individual bones ready for defatting process (d), hand bones being air-dried (e), labelling of individual bones (f).

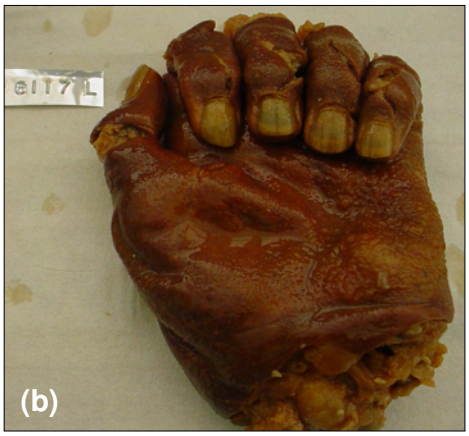

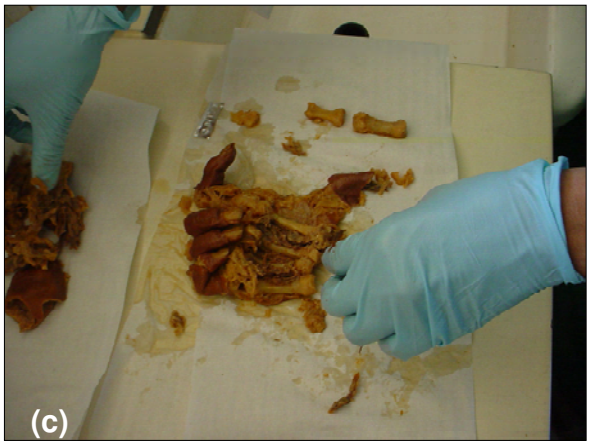

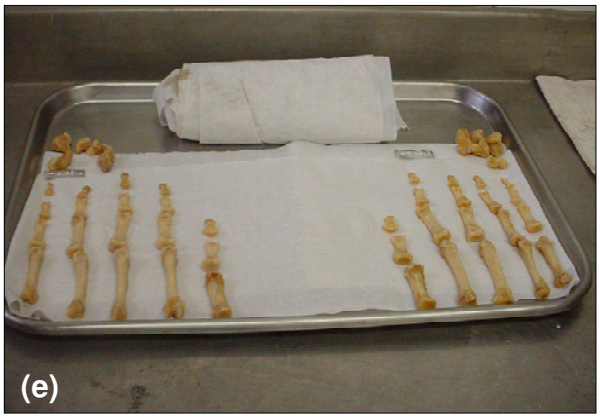

Figure 5.2: Palmar view of metacarpal I - thumb (m-l = medial lateral measurement)

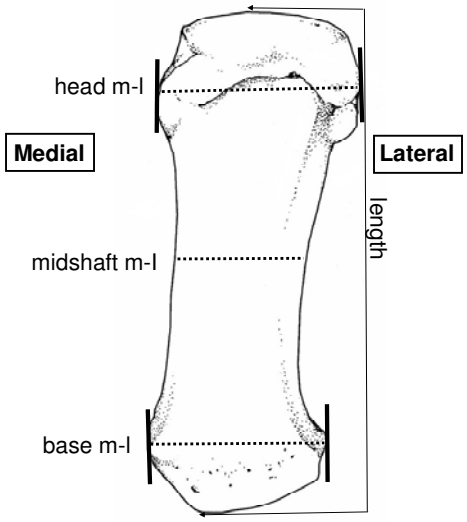

Figure 5.3: Lateral view of metacarpal I - thumb (d-p = dorsal palmar measurement)

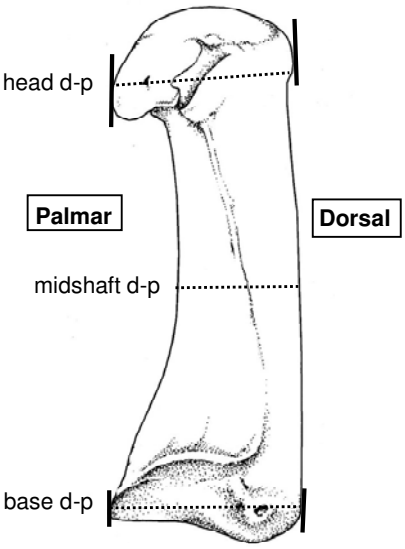

Figure 5.4: Palmar view of metacarpal II - index finger (m-l = medial lateral measurement)

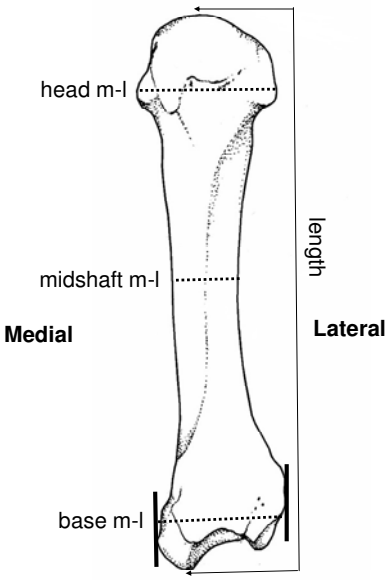

Figure 5.5: Lateral view of metacarpal II - index finger (d-p = dorsal palmar measurement)

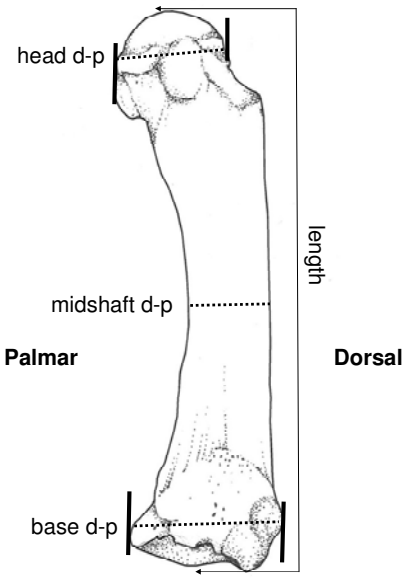

Figure 5.6: Palmar view of metacarpal III - middle finger (m-l = medial lateral measurement)

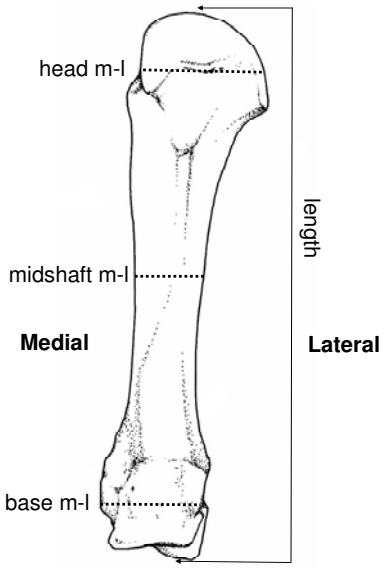

Figure 5.7: Lateral view of metacarpal III - middle finger (d-p = dorsal palmar measurement)

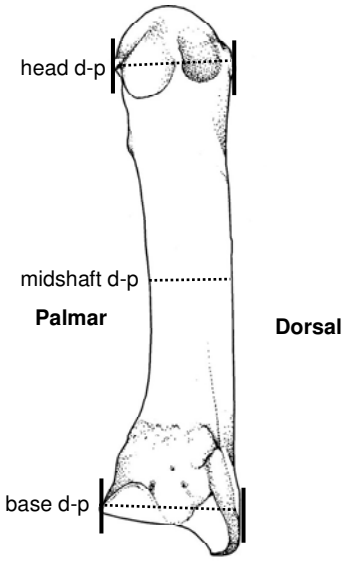

Figure 5.8:Palmar view of metacarpal IV - ring finger (m-l = medial lateral measurement)

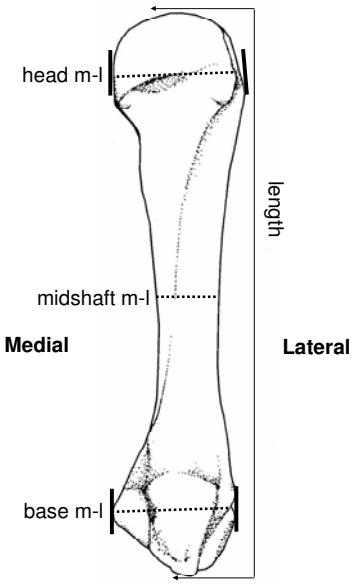

Figure 5.9: Lateral view of metacarpal IV - ring finger (d-p = dorsal palmar measurement)

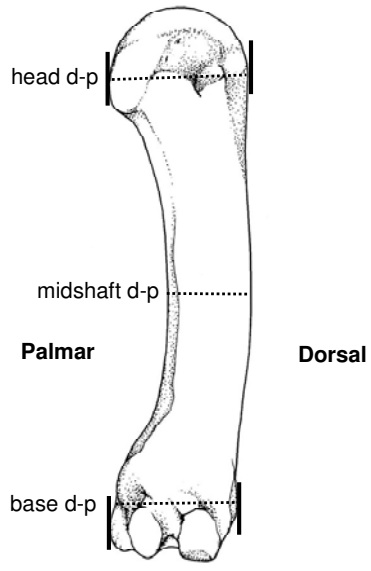

Figure 5.10: Palmar view of metacarpal V - little finger (m-l = medial lateral measurement)

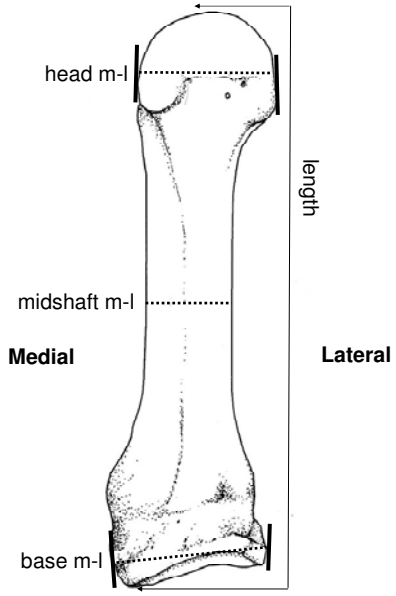

Figure 5.11: Lateral view of metacarpal V - little finger (d-p = distal palmar measurement)

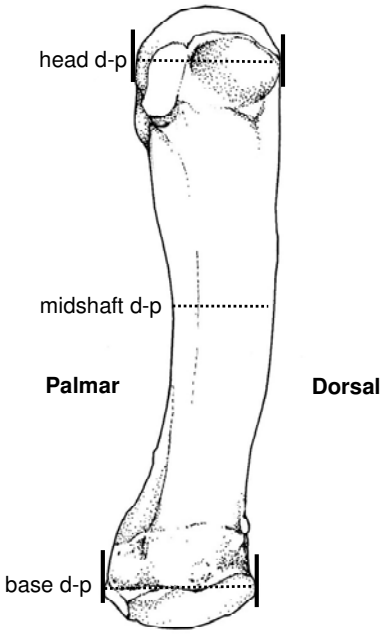

Figure 5.12: Palmar view of proximal phalanx - index finger (m-l = medial lateral measurement)

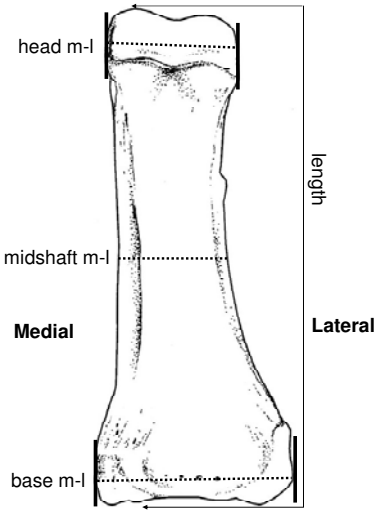

Figure 5.13: Lateral view of proximal phalanx - index finger (d-p = distal palmar measurement)

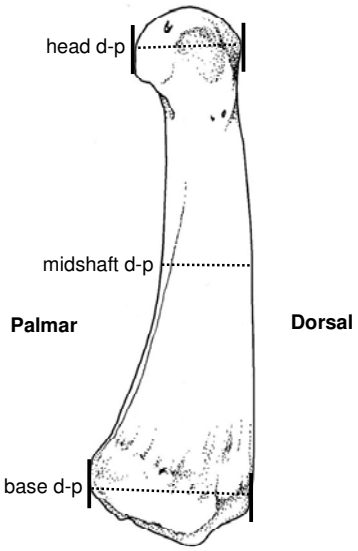

Figure 5.14: Palmar view of middle phalanx - index finger (m-l = medial lateral measurement)

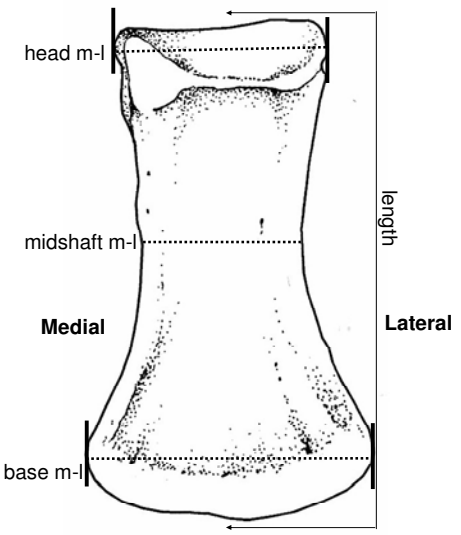

Figure 5.15: Lateral view of middle phalanx - index finger (d-p = dorsal palmar measurement)

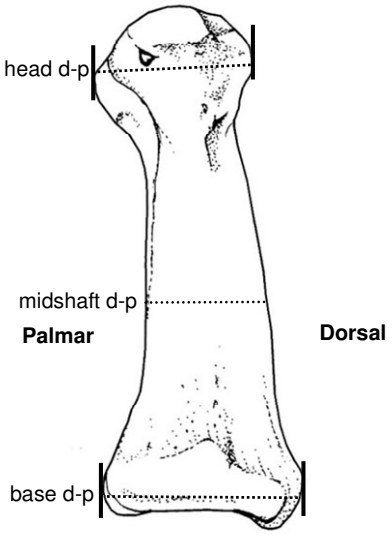

Figure 5.16: Palmar view of distal phalanx - index finger (m-l = medial lateral measurement)

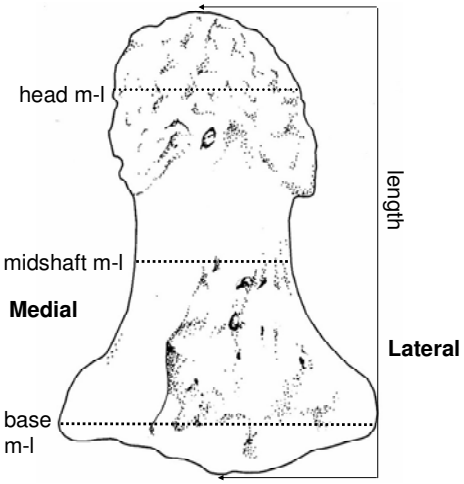

Figure 5.17: Lateral view of distal phalanx - index finger (d-p = dorsal palmar measurement)

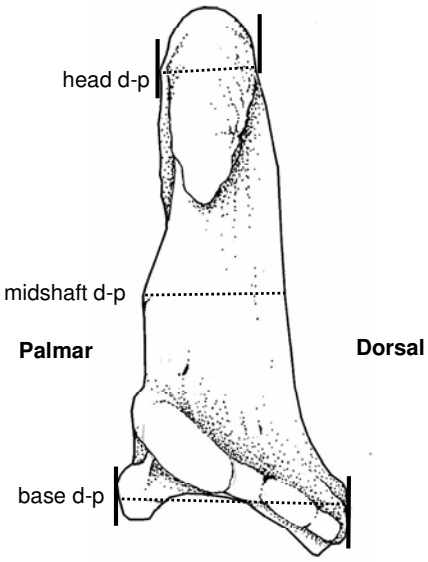

Figure 5.18: Maximum length measurement of the left humerus

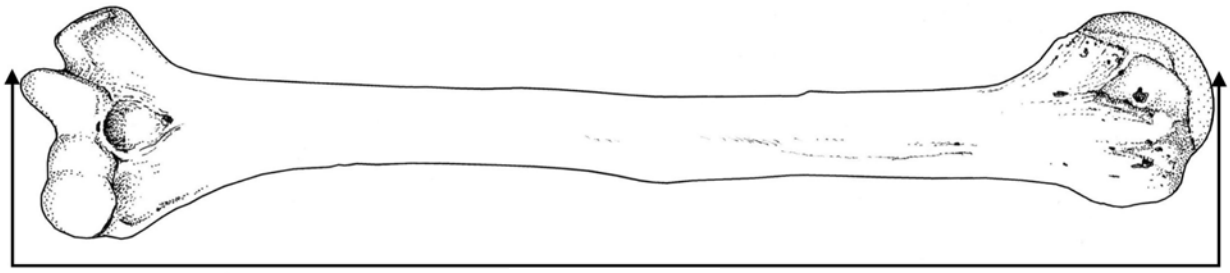

Figure 5.19: Maximum length measurement of the left radius

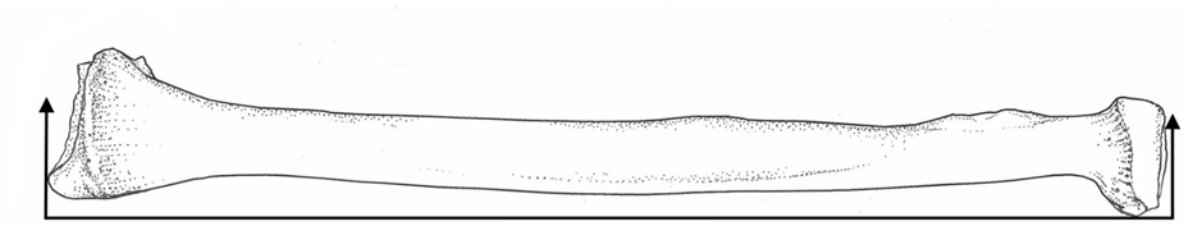

Figure 5.20: Maximum length measurement of the left ulna

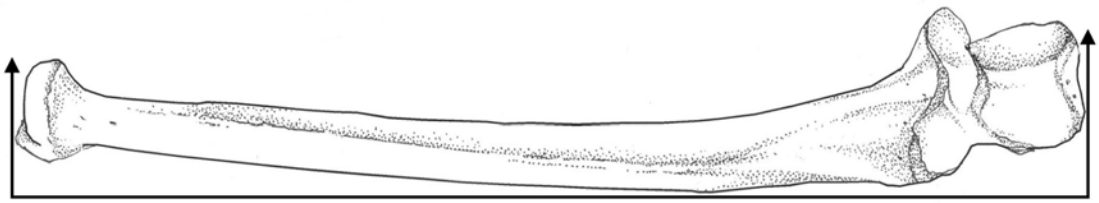

Figure 5.21: Maximum length measurement of the left femur

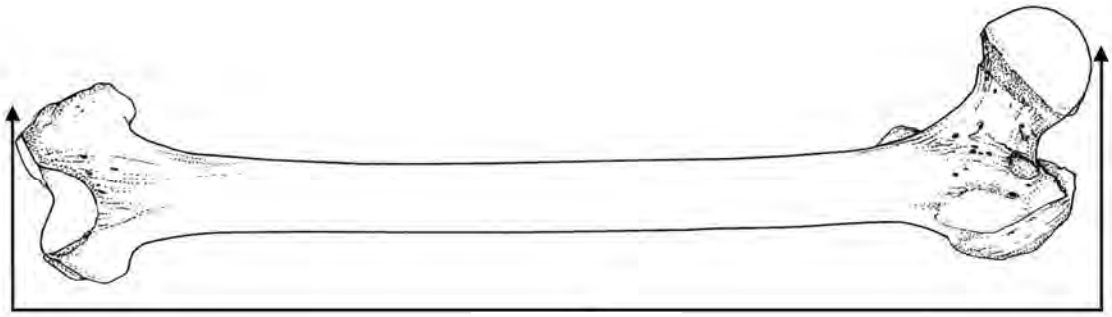

Figure 5.22: Maximum length measurement of the left tibia

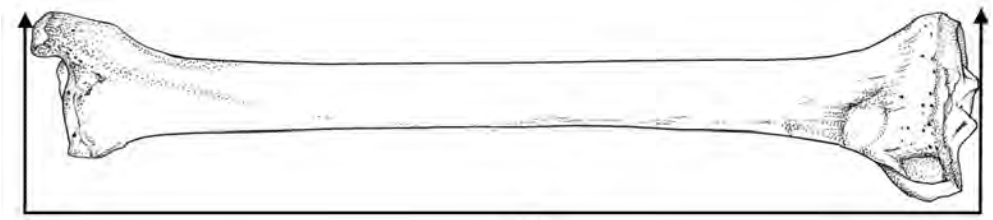

CHAPTER 6

RESULTS - MORPHOLOGY OF THE HAND BONES

6.1 General introduction

In this section, a description of the morphology and siding of the metacarpals and phalanges will be given. The basic descriptions of these bones will come from the literature, to which additional features found in this study will then be added. These additional features will be indicated by a number in brackets which corresponds to the number on the relevant figure. A description of each bone will be provided under the headings of shaft, head and base.

The metacarpals in the literature are described in greater detail than the phalanges. For this reason, there is an introduction before each metacarpal bone and not for the phalanges in this study.

6.2 Morphology of the first metacarpal (Figures 6.1a-f)

6.2.1 Introduction

The first metacarpal is the most lateral digit in the anatomically positioned hand (Matshes *et al*. 2005). It is often described as being the shortest and most robust when compared to adjacent metacarpals (Gray 1989, 1995, Matshes *et al*. 2005, Scheuer & Black 2000). The first metacarpal articulates with the trapezium proximally and the first proximal phalanx distally (Matshes *et al*. 2005, Scheuer & Black 2000).

The shape of the shaft is described from two aspects, namely, the transverse and longitudinal plane. In the transverse plane it is said to have a flattened dorsal and convex palmar surface. In the longitudinal plane, the shaft is described as being concave on the palmar aspect (Scheuer & Black 2000).

Surface markings on the palmar aspect of the shaft include a round ridge which divides the palmar aspect into a larger lateral area for attachment of opponens pollicis and a smaller medial surface for attachment of the lateral head of the first dorsal interosseous muscle (Scheuer & Black 2000).

Nutrient foramina have been identified on the dorsal (Patake & Mysorekar 1977) and medial palmar surface of the distal end of the shaft (Scheuer & Black 2000). At the proximal end of the shaft, tubercles are evident on the lateral and medial ends. These tubercles serve for attachment of abductor pollicis longus laterally and first palmar interosseous medially (Scheuer & Black 2000). The head is described as being large and round and tilted in a palmar direction (Bass 1995).

Scheuer and Black (2000) describe the base as being concavo-convex, thus creating two surfaces separated by a less prominent ridge for articulation with the saddle-shaped trapezium. This ridge is said to be continuous with the medially directed styloid process on the palmar aspect of the base (Scheuer & Black 2000). The first metacarpal is considered to be the most dimorphic bone in the series of metacarpals which relates to its function as a power grip digit.

Gray (1959) describes the shaft of the first metacarpal as a longitudinal curve with three surfaces, namely, medial, lateral and dorsal. He also describes the distal two-thirds as smooth dorsally, triangular in form and flattened. He lists two small tubercles on either side of the distal extremity which converge proximally to form a centrally located ridge and describes the medial margin of the shaft seen from the volar (palmar) surface, as concave from superior to inferior and divided by a rounded ridge into a larger anterolateral and a smaller anteromedial surface. He notes the presence of a large lateral and a small medial articular eminence which provides a surface for gliding of the sesamoid bones. The dorsal surface is described by this author as rotated laterally.

Identification and siding of a metacarpal to a particular ray is said to be easier when the base is present. Difficulties arise in cases when bone fragments or only the head or distal segment is present (Ricklan 1987). For the purpose of the present study, bony landmarks as well additional features not mentioned in textbooks, will be noted and described under the headings of shaft, head and base as seen from a dorsal, palmar, lateral, medial, superior and inferior view. This should make it easy to identify and side any part of this bone.

6.2.2 Shaft or body (Figures 6.1a-d)

A dorsal view of the shaft (Figure 6.1a) shows a medial margin (3 - dotted line) that is straight in the central part. As this margin is followed through to the distal end it curves slightly medially, forming an obtuse angle before merging with the dorsal medial tubercle (2). This tubercle is evident only from the medial and dorsal aspect. At the proximal end, the medial margin forms another angle as it projects outward. In contrast, the lateral margin (8 - dotted line) is concaved laterally throughout its course and becomes less prominent distally before merging with the dorsal lateral tubercle of the head (7). At the proximal end the lateral margin forms a prominent outward projection which tends to curl laterally, forming a rounded tip as it merges with dorsal lateral articular margin of the base (10). The dorsal surface is flattened from proximal to distal and has greater width distally than proximally.

From a palmar view (Figure 6.1b) a centrally positioned palmar median ridge of the shaft (13) can be identified. The ridge creates two surfaces, namely, the palmar lateral (9) and palmar medial (16) surfaces of the shaft. If followed through to the proximal end, this ridge merges with the proximal palmar tubercle of the shaft (17).

A lateral view of the shaft (Figure 6.1c) depicts the dorsal lateral tubercle (7) with a prominent lateral margin (8) extending from it in a proximal direction. The lateral margin is rough in its distal half and smooth in the proximal half where it deviates onto the dorsal surface of the shaft. A line demarcating the junction between the base and the proximal end of the shaft (21) is evident. This line is slightly distal to the lateral articular margin of the base (22). The palmar lateral surface of the shaft (9) can be seen from this view.

A medial view of the shaft (Figure 6.1d) shows a round and smooth medial margin (3) compared to the rough lateral margin. The dorsal surface is flattened compared to the concave palmar surface. The palmar medial surface of the shaft (16) can be identified as a slight concavity.

6.2.3 Head (Figures 6.1a-e)

The head is described in the literature as being large and round (Romanes 1991, Bass 1995), asymmetrical and projecting more towards the palmar than towards the dorsal aspect (Scheuer & Black 2000). It is broader medial laterally and less convex than that of adjacent metacarpals (Gray 1932, Scheuer & Black 2000). The enlarged lateral and medial angles are referred to as articular eminences for sesamoid bones that will develop within the tendons of adductor pollicis longus and the first palmar interosseous muscles medially and the flexor pollicis brevis laterally (Scheuer & Black 2000). Additional features of the head as observed in the present study are discussed below.

From a dorsal view, the head, which is located at the distal end of the shaft (Figure 6.1a), shows greater width than height. The dorsal articulating margin of the head (1) which separates the head from the shaft runs from the dorsal medial tubercle (2) to the dorsal lateral tubercle of the head (7). The dorsal lateral tubercle is positioned more distally than the dorsal medial tubercle.

While very little of the head is seen from the dorsal aspect, the palmar view shows more detail (Figure 6.1b). The palmar articular margin (11) which separates the head from the shaft extends from the palmar lateral tubercle (12) to the palmar medial tubercle (15) of the head. The head is not as wide from this view when compared to the dorsal view, making it possible to identify the dorsal medial tubercle (2) and the dorsal lateral tubercle of the head (7). Not only are these palmar tubercles closer to each other accounting for the smaller width of the head, they are also positioned more distally than the dorsal tubercles. The palmar tubercles tend to have sharper end points than the more rounded ends of the dorsal tubercles. A comparison of the palmar tubercles shows that the palmar lateral tubercle is relatively larger and projects more proximally than the palmar medial tubercle.

From a lateral view (Figure 6.1c) the dorsal lateral tubercle (7) and palmar lateral tubercle (12) are separated from each other by the lateral intertubercular fossa (20). The palmar lateral tubercle is elongated and projects downward or proximally when compared to the relatively smaller, round dorsal palmar tubercle.

Landmarks from a medial view of the head (Figure 6.1d) are similar to that seen from a lateral view except that different terminologies are used. From a medial view, the dorsal medial tubercle (2) is separated from the palmar medial tubercle (15) by a medial intertubercular fossa (23). Both these tubercles are relatively smaller and less prominent when compared to those on the lateral side. This is especially true for the palmar medial tubercle (15) which is not as elongated as the palmar lateral tubercle (12).

While bony landmarks of the first metacarpal head are described from each view described above, the head as seen from a superior view (Figure 6.1e) is rhomboidal in shape. From this view, the greater width dorsally is due to the outward extensions of the dorsal lateral and dorsal medial tubercles. The articulating margin (Figure 6.1e, dotted line) forms the boundary of the articular surface. The lateral intertubercular fossa (20) lies medial to the dorsal lateral tubercle (7) while the medial intertubercular fossa (23) lies lateral to the dorsal medial tubercle (2).

6.2.4 Base (Figures 6.1a-d and f)

The outline of the base of the first metacarpal is described as being cubical (Romanes 1991) or rhomboidal in shape while the articulating surface is saddle-shaped (Hollinshead & Rosse 1985) for articulation with the greater multangular bone (Gray 1932), trapezium (Hollinshead & Rosse 1985) and the scaphoid bone (Gray 1932, Hollinshead & Rosse 1985, Romanes 1991). In the present study, the base was observed to be oval to square in shape. The articular surface of the base is described as concavo-convex (Gray 1932). According to Gray, there are no articulating facets on the lateral aspect of the base, except for the presence of a tubercle located laterally. Additional features of the base as observed in the present study is described below and shown in Figures 6.1a to d and f.

From a dorsal view (Figure 6.1a) the articulating margin appears to be round. On closer observation, the articular margin has two slopes, namely, a shorter straight dorsal medial

articular margin (4) and a longer curved dorsal lateral articular margin (10). The point where these two margins meet is called the dorsal apex of the base (6).

The palmar view (Figure 6.1b) of the base is very similar to that observed from a dorsal aspect. The two slopes forming the articular margin are the palmar lateral articular margin (14) and palmar medial articular margin (18). The point where these two margins meet is referred to as the palmar apex of the base (19) which is more medially than laterally positioned.

On the lateral view (Figure 6.1c) a line differentiating the base from the rest of the shaft (21) is located distal to the lateral articular margin of the base (22). This articular margin has a relatively longer slope running in a palmar direction when compared to the dorsal slope. The lateral articular margin (22) is also at a higher or more distal level than that on the medial side (25). Part of the concavo-convex articulating surface of the base can be seen from this view.

The medial surface (Figure 6.1d) of the base is different from the lateral view. The articular margin is set at a lower or more proximal level compared to that on the lateral side (25). Furthermore, the line between the base and shaft is straight and not curved as seen from a lateral side.

The articular surface of the base (Figure 6.1f) is divided into two articular surfaces by an interarticular ridge (26) which runs from lateral to medial. These two surfaces are called the dorsal (28) and palmar (27) articular surfaces of the base. The articular surfaces are surrounded by an articular margin. The latter is labelled according to the view that it is observed from, namely, lateral (22), medial (25), dorsal lateral (10), dorsal medial (4), palmar lateral (14) and palmar medial (16). The terminology used for the articular margin makes it easy to identify and side this bone.

6.2.5 Siding

In order to differentiate the right first metacarpal from the corresponding one on the left side, most authors have orientated the bone in such a way that the palmar surface faces down and the dorsal surface faces up or towards one, while the head is placed at the top end and

the base at the bottom end (Bass 1995, Matshes *et al*. 2005). It has been suggested that the pivot-shaped base will tend to slant more towards the same side (10 and 14) as that to which the bone belongs to (Matshes *et al*. 2005).

Additional landmarks which Matshes *et al*. (2005) list as key identifying features include the large articular facet on the lateral aspect of the base, the most prominent nodular eminence found distally on the palmar aspect, a feature which is called the palmar lateral tubercle (12) in the present study, all of which occurs on the same side as that to which the bone belongs to the oblique metacarpal ridge which starts on the same side of the head as that to which the bone belongs to (Matshes *et al*. 2005).

For the purpose of the present study, a list of bony landmarks on the shaft, head and base of the first metacarpal will now be provided. This is to overcome any problems that may be encountered if only a fragment of the first metacarpal is found amongst skeletal remains.

Shaft

1. Straight medial margin (3) (Figure 6.1a)
2. Curved lateral margin (8) (Figure 6.1a)
3. Smaller palmar medial (16) and larger palmar lateral (9) surface (Figure 6.1b)
4. Palmar medial ridge (13) concave towards the medial surface (Figure 6.1b)

Head

1. Greater width dorsally than on the palmar aspect (Figure 6.1e)
2. Four tubercles:
   a) Dorsal tubercles relatively smaller and rounder (dorsal view) than larger and pointed palmar tubercles (Figure 6.1b)
   b) Palmar lateral tubercle (12) relatively longer than palmar medial tubercle (15) (Figure 6.1b)

Base

1. Dorsal (6) and palmar (19) apices directed more medially (Figures 6.1a and b)

2. Dorsal medial articular margin (4) relatively shorter than the dorsal lateral articular margin (10) (Figure 6.1a)
3. Palmar medial articular margin (18) relatively shorter than the palmar lateral articular margin (14) (Figure 6.1b)
4. Lateral articular margin (22) higher or more distally placed than the medial articular margin (25) (Figures 6.1c and d)

Figure 6.1: Morphology of the right (R) and left (L) first metacarpal

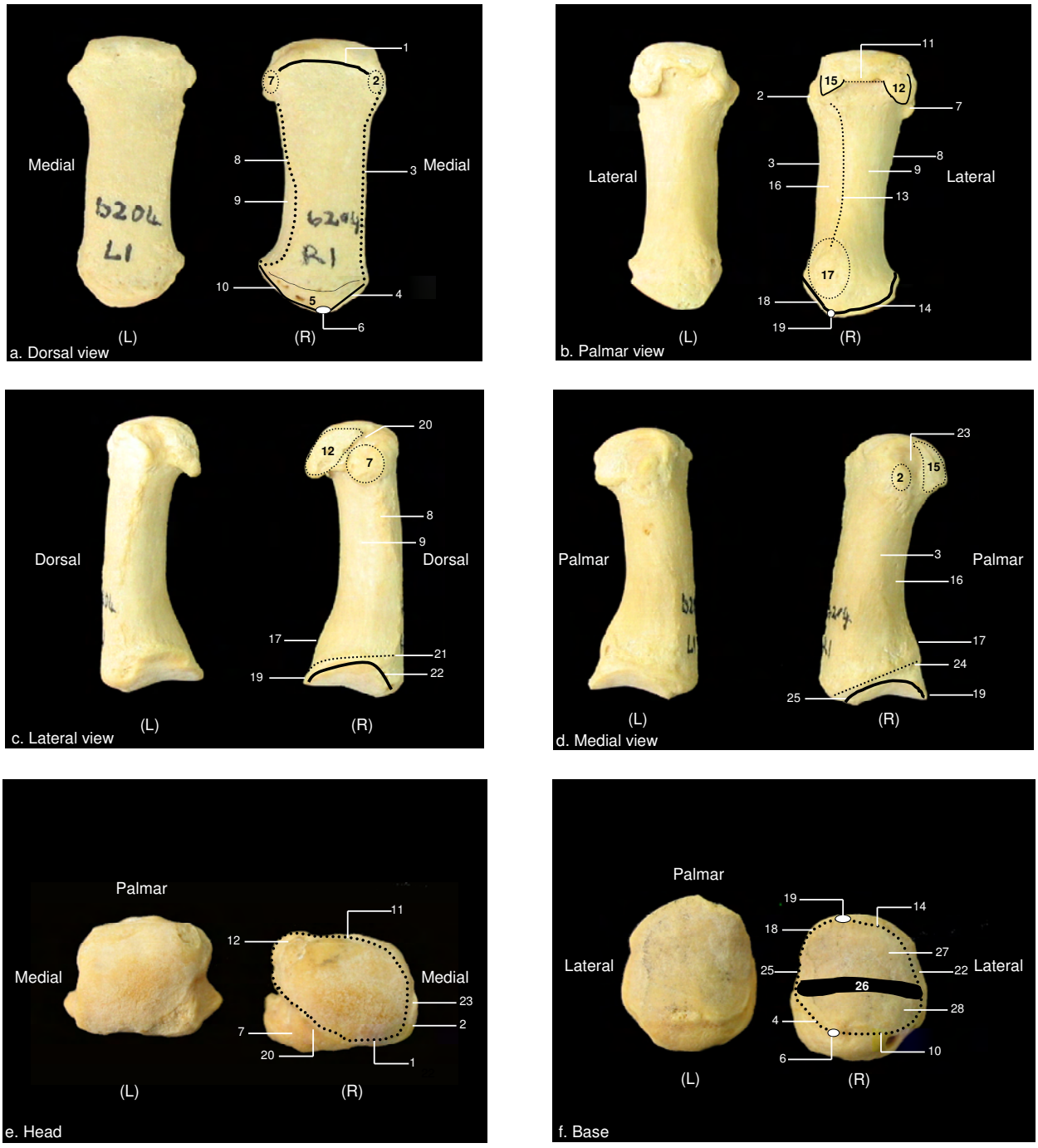

1=dorsal articular margin of the head, 2=dorsal medial tubercle of head, 3=dorsal medial margin of shaft, 4=dorsal medial articular margin of base, 5=dorsal articular surface of base, 6=dorsal apex of base, 7=dorsal lateral tubercle of head, 8=dorsal lateral margin of shaft, 9=palmar lateral surface of shaft, 10=dorsal lateral articular margin of base, 11=palmar articular margin of head, 12=palmar lateral tubercle of head, 13=palmar median ridge of shaft, 14=palmar lateral articular margin of the base, 15=palmar medial tubercle of head, 16=palmar medial surface of shaft, 17=proximal palmar tubercle of shaft, 18=palmar medial articular margin of base, 19=palmar apex of base, 20=lateral intertubercular fossa, 21=lateral junction line between shaft and base, 22=lateral articular margin of base, 23=medial intertubercular fossa, 24=medial junction line between shaft and base, 25=medial articular margin of base, 26=interarticular ridge of base, 27=palmar articular surface of base, 28=dorsal articular surface of base

6.3 Morphology of the second metacarpal (Figures 6.2a-f)

6.3.1 Introduction

The second metacarpal is the bone associated with the index finger. It is medial to the first and lateral to the third metacarpal. The fact that it is adjacent to the thumb which is the most important digit in the hand, places it second on the list of importance (Scheuer & Black 2000). It is considered to play an important biomechanical role in power and precision grip (Scheuer & Black 2000).

The second metacarpal articulates with the distal row of carpal bones which are listed from lateral to medial as the trapezium, trapezoid and capitate. It also articulates with the base of the first and third metacarpal and with the base of the proximal phalanx of the index finger (Matshes *et al*. 2005). Features listed as unique for this bone is that it is the longest in the metacarpal series and the only bone with a wedge-shaped base (Matshes *et al*. 2005). Authors have used this digit in determining bone mass with age, especially with regard to the development of osteoporosis in postmenopausal women (MacLennan & Caird 1973).

A detailed description of the second metacarpal in the present study, under the headings of head, shaft and base as seen from a dorsal, palmar, lateral, medial, superior and inferior view, will now be discussed in conjunction with descriptions given in the literature.

6.3.2 Shaft or body (Figures 6.2a-d)

The shaft of the second metacarpal is described as being convexed dorsally and concaved on its palmar aspect (Matshes *et al*. 2005). The palmar aspect of the shaft is described as having two surfaces, namely a palmar medial and palmar lateral surface separated by a palmar ridge. The medial and lateral surfaces, in turn, are separated from the dorsal aspect by medial and lateral interosseous ridges. The dorsal surface is broad and narrows proximally serving for attachment of the extensor tendons of the index finger. Due to the oblique course of the medial interosseous ridge, the term metacarpal 2 ridge is used (Matshes *et al*. 2005).

The lateral surface provides attachment for the medial head of the first dorsal interosseous muscle while the medial surface gives rise to the second palmar interosseous ventrally and the second dorsal interosseous dorsally (Stack 1962). Although the position of the nutrient foramen is said to vary, it has been suggested that it is always directed proximally (Scheuer & Black 2000) or on the anteromedial and anterolateral surfaces (Patake & Mysorekar 1977). While variations of bony features are known to exist, terminologies used to describe the location of these variations also differ.

In the present study, a dorsal view of the right (R) second metacarpal (Figure 2a) was captured in such a way to illustrate that the proximal end of the shaft is twisted around its longitudinal axis. In this way, two oblique ridges can be seen running across the dorsal aspect of the shaft, namely, the distal oblique dorsal ridge (3) and proximal oblique dorsal palmar ridge (5). The distal oblique dorsal ridge is restricted to the dorsal surface while the proximal oblique dorsal palmar ridge runs from the dorsal to the palmar surface. The distal oblique dorsal ridge runs from the relatively short medial margin in a proximal direction where it terminates at a central point above the base. The dorsal aspect has two surfaces, namely, dorsal lateral (10) and dorsal medial (4). The dorsal lateral surface is rough compared to the smooth dorsal medial surface. It is assumed that the medial and lateral margins observed in the present study are the medial and lateral interosseous ridges mentioned by Scheuer and Black (2000). The medial oblique ridge reported by Matshes *et al*. (2005) relates to the distal oblique dorsal ridge (3) which is an extension of the medial margin.

A palmar view of the second metacarpal (Figure 6.2b), shows a central palmar tubercle (17) at its distal end. A shallow depression is located distal to this tubercle. The central palmar tubercle continues proximally as the central palmar ridge (19) which deviates medially. Three surfaces are present from this view, namely, palmar lateral (18), distal palmar medial (22) and proximal palmar medial (6). The deviation of the central palmar ridge medially increases the relative surface area of the palmar lateral surface.

From a lateral view (Figure 6.2c) the shaft is smooth. Both the palmar lateral (18) and dorsal lateral surfaces (10) can be seen. The palmar surface is concave while the dorsal

surface is convex as is reported in the literature. The central palmar tubercle (17) is seen as a bony prominence at the distal end.

The rotation of the proximal half of the shaft is clearly visible from a medial view (Figure 6.2d). Two ridges are present, namely, distal oblique dorsal ridge (3) and proximal oblique dorsal palmar ridge (5). Three surfaces can be identified, namely, dorsal lateral (10), palmar medial (22) and proximal palmar medial (6).

6.3.3 Head (Figures 6.2a-e)

The head is described as being smooth and round (Romanes 1991). Two tubercles associated with the head are mentioned in the literature, although they are not named (Romanes 1991). The head of the second metacarpal in the juvenile hand is described as asymmetrical. This asymmetry is due to the large attachment site of the metacarpophalangeal ligament in the juvenile (Scheuer & Black 2000). The ridge connecting the two palmar tubercles of the head has been called the palmar articular margin (Romanes 1991). Romanes (1991) described the extension of the head as being much greater on the palmar than on the dorsal aspect which allows for greater flexion at this site. This feature was also observed in the present study.

In the present study, the shape and bony landmarks present on the head was different from various views. For this reason, the discussion will center around the dorsal, palmar, medial, lateral and superior views.

Not much of the head is visible dorsally (Figure 6.2a). This is because a relatively greater part of the head projects in a palmar direction. The head does appear to be round as mentioned in the literature. At the junction line where the head is demarcated from the shaft, two tubercles are found which are not mentioned in the literature, namely, dorsal medial (2) and dorsal lateral (9) tubercles. The former may in some cases be positioned more distally than the latter, but this varies. Another variation is that an elongated region may be found between these tubercles and the head, which has been called the neck (8) in the present

study. The relative length of the neck varied in the samples of the present study as seen in Figure 6.2a. In this figure, the neck is elongated in the right (R) and shortened in the left (L) second metacarpal (Figure 6.2a). This difference in relative length of the neck was observed more frequently in right hands, possibly indicating that it has to do with right or left handedness.

A relatively greater surface area of the head can be seen from a palmar aspect (Figure 6.2b). The head is not only tilted forward, but two extensions are present on either side of the head. These extensions, which project proximally, are referred to as the palmar lateral (16) and palmar medial (15) tubercles connected to each other by palmar articular margin (14). The palmar lateral tubercle is relatively larger and flares out more laterally than the palmar medial tubercle which is relatively smaller and projects proximally.

Nutrient foramina, when present, were located in the shallow concavity just proximal to the palmar articular margin (14).

The tilting of the head forward is clearly seen from a lateral view (Figure 6.2c). Two tubercles can be identified, namely, the dorsal lateral (9) and the palmar lateral (16) tubercles separated from each other by a lateral fossa (24).

A medial view of the head also shows the tilting (Figure 6.2d). The tubercles that can be identified are the dorsal medial (2) and palmar medial (15) tubercles separated by the medial fossa (28).

A superior view (Figure 6.2e) shows a smooth rhomboidal-shaped head. The head has relatively greater length laterally than medially. The lateral tubercles are more prominent than the medial tubercles. The lateral fossa (24) separating the dorsal lateral tubercle (9) from the rest of the head is easily identified.

6.3.4 Base (Figures 6.2a-d and f)

The base is sometimes referred to as the carpal (Bass 1995) or proximal end of the shaft. Matshes *et al*. (2005) listed the presence of nodular eminences on the lateral and medial

styloid processes which are for articulation with the trapezium and capitate carpal bones respectively, as key features for purposes of identification. They described the base as “pivot” or “wedge-shaped”. Gray (1932) describes the inferior facet as a medial facet identified at the tip of a long, narrow ridge. It is assumed that this ridge is the proximal medial articulating margin that distinguishes the two medial articulating facets from the inferior facet in the present study. Gray (1959) describes the four articular facets of the base as follows “Of the facets on the upper surface the intermediate is the largest and is concave from side to side, convex from before backward for articulation with the lesser multangular; the lateral is small, flat and oval for articulation with the greater multangular; the medial, on the summit of the ridge, is long and narrow for articulation with the capitate. The facet on the ulna side, articulates with the third metacarpal” (p. 255).

In reviewing the literature, a more detailed description of the base was found for the juvenile hand as given by Scheuer and Black (2000). Unfortunately, most of the key features listed by them are not depicted in their diagrams. These authors also identified the presence of a deep groove that accommodates the dorsal palmar inclination of the trapezoid. This groove is given the number 32 in the present study (Figure 6.2f). These authors describe the lateral and medial edges as extensions of this deep groove with the medial edge being much longer for articulation with the capitate. They noted the presence of a small quadrilateral facet on the lateral aspect of the base which articulates with the trapezium. This facet is numbered 25 in the present study (Figure 6.2f). On the dorsal aspect they report the presence of lateral and medial tubercles for attachment of the extensor carpi radialis longus and brevis respectively. In the present study, these tubercles were called the lateral (12) and medial (13) styloid processes. These authors also describe the position of the lateral tubercle immediately behind the quadrilateral facet (25) on the dorsal surface. Scheuer and Black (2000) also describe a lateral inclination on the palmar aspect of the base for the attachment of the flexor carpi radialis tendon. The attachment of the oblique head of adductor pollicis they state would be on the medial side on the palmar aspect. The medial side of the base they confirm articulates via a strip-like facet with the base of the third metacarpal. This strip-like facet is often identified as

2 individual facets in the adult hand where it is called the facet for metacarpal 3 (Matshes *et al*. 2005). These authors suggest that the constriction in the centre of the strip-like facet is presumably due to the interosseous ligament. This constriction is numbered 29 in the present study. A more comprehensive study of the base in the adult similar to that described for the juvenile hand by Scheuer and Black (2000) was not found.

Key features of a dorsal view of the base (Figure 6.2a) include a relatively longer medial (13) and a relatively shorter lateral (12) styloid process separated by a deep dorsal groove which continues onto the base (32).

From a palmar aspect (Figure 6.2b), the lateral end of the base extends further proximally than the medial end. The palmar articular margin is not as elevated as that on the dorsal surface. An oval-shaped articular facet is seen on the lateral surface (20).

A lateral view (Figure 6.2c) of the base shows the lateral styloid process (12) as well as parts of the medial styloid process (13). The lateral articular margin (26) is horizontally positioned.

The base from a medial view (Figure 6.2d) presents with a convex articular margin (31). Distal to this articular margin is an articular facet (30) with an adjacent interarticular fossa (29). Two instead of one facet may sometimes be present on the medial aspect.

The base is triangular in shape when seen from the articulating surface (Figure 6.2f). The descriptions of the base as given for the juvenile hand by Scheuer and Black (2000) are also identified in the present study. The only other additional landmark provided, is the lateral articular surface (27).

6.3.5 Siding

In order to differentiate the right second metacarpal from the corresponding one on the left side, most authors orientated the bone in such a way that the palmar surface faces down and the dorsal surface faces up or towards one, while the head is placed at the top end and the base at the bottom end (Bass 1995, Matshes *et al*. 2005).

For the purpose of the present study, a list of bony landmarks for the shaft, head and base of the second metacarpal will now be provided. This is to overcome any problems that may be encountered if only a fragment of the second metacarpal is found amongst skeletal remains.

Shaft

1. Distal oblique dorsal ridge of the shaft (3) (Figure 6.2a)
2. Two surfaces can be identified on the dorsal aspect, namely, a relatively larger dorsal medial (4) and a relatively smaller dorsal lateral (10) surface (Figure 6.2a)
3. Proximal half of shaft rotated or twisted from medial to lateral (Figure 6.2a)
4. Central palmar tubercle (17) located distally (Figure 6.2b)
5. Central palmar ridge (23) deviates medially in the proximal third (Figure 6.2b)

Head

1. Two palmar tubercles, namely, dorsal medial (located more distally) (2) and dorsal lateral (located more proximally) (9) (Figure 6.2b)
2. Two palmar tubercles, namely, a relatively smaller palmar medial (15) and a relatively larger palmar lateral (16) (Figure 6.2b)
3. Rhomboidal-shaped from a superior view with greater length laterally than medially (Figure 6.2e)
4. From a superior view, the dorsal lateral tubercle (9) is relatively larger and flares to the side to a much greater extent than the dorsal medial tubercle (16) (Figure 6.2e)

Base

1. Longer medial styloid process (13) (Figure 6.2a)
2. Dorsal articular margin elevated or raised (7), resulting in a relatively longer medial styloid process (13) and a relatively shorter lateral styloid process (Figure 6.2a)
3. Palmar articular margin less elevated or almost horizontal (21) which slopes to merge with the medial styloid process (Figure 6.2b)
4. Larger bi-concave articular facet medially (27) (Figure 6.2f)

5. Triangular in shape as seen from the articulating surface, with the base at the dorsal end and the apex of the triangle at the palmar end. The articular margin which forms the medial boundary of this triangle (31) is straight compared to the curved lateral articular margin (Figure 6.2f)
6. Quadrilateral articular facet (25) relatively smaller than lateral facet as seen from the articulating surface (Figure 6.2f)
7. Small quadrangular facet (25) located laterally and overlapping onto the lateral surface (Figure 6.2f)
8. Relatively small facet (20) located laterally which is absent on the medial aspect of the base (Figure 6.2c)

Figure 6.2: Morphology of the right (R) and left (L) second metacarpal

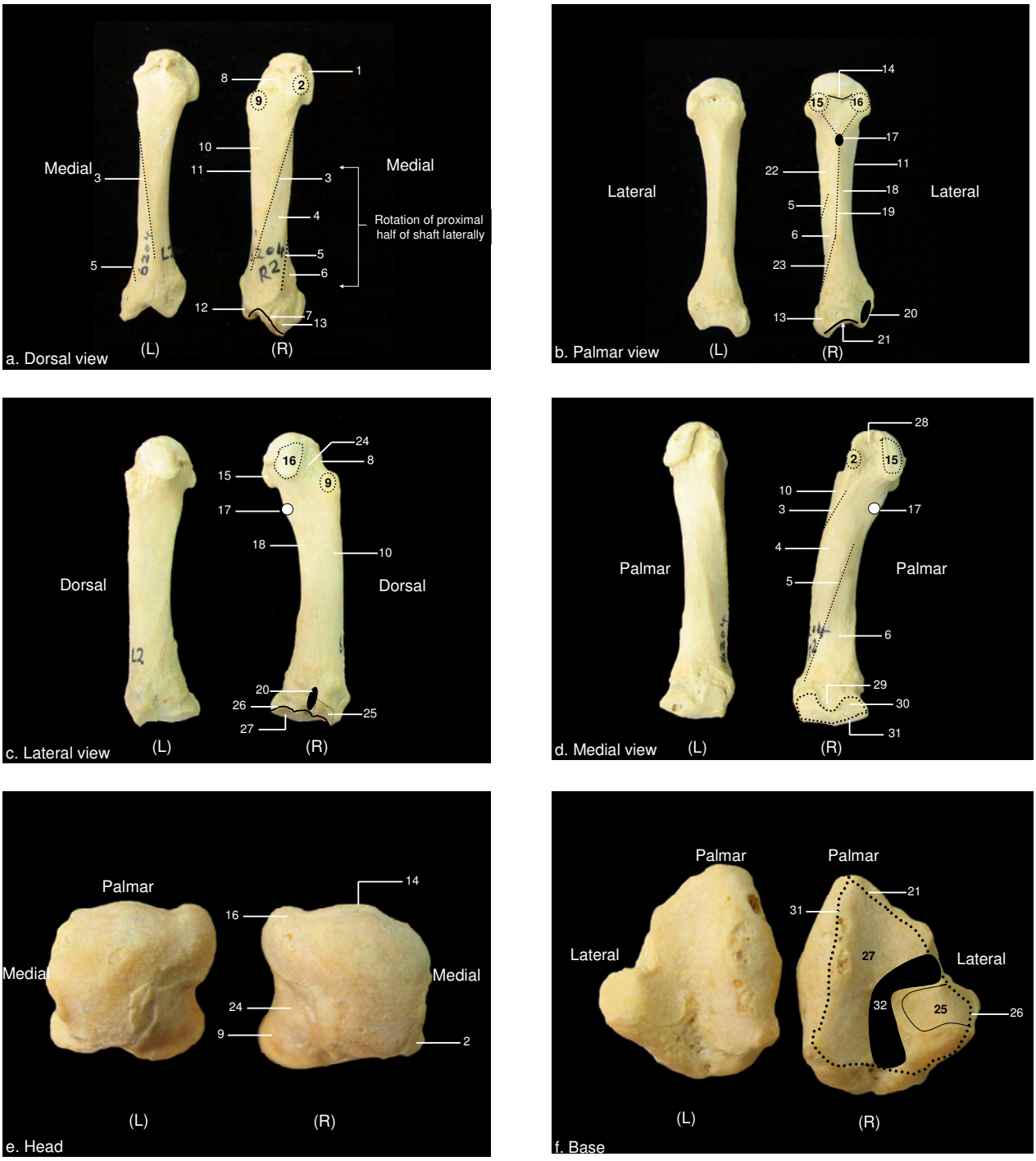

1=medial fossa, 2=dorsal medial tubercle, 3= distal oblique dorsal ridge, 4= dorsal medial surface, 5=proximal oblique dorsal palmar ridge medially, 6= proximal palmar medial surface, 7=dorsal articular margin, 8=neck, 9= dorsal lateral tubercle, 10=dorsal lateral surface, 11=medial margin of shaft, 12=lateral styloid process, 13=medial styloid process, 14=palmar articular margin of head, 15= palmar medial tubercle, 16=palmar lateral tubercle, 17= central palmar tubercle, 18=palmar lateral surface, 19= central palmar ridge, 20=lateral articular facet, 21=palmar articular margin, 22=distal palmar medial surface, 23=medial deviation of central palmar ridge, 24=lateral fossa, 25= quadrilateral facet, 26= lateral articular margin of base, 27=medial articular facet of base, 28=medial fossa, 29=interarticular fossa, 30=medial articular facet of the base, 31=medial articular margin of base, 32=interarticular ridge of base

6.4 Morphology of the third metacarpal (Figures 6.3a-f)

6.4.1 Introduction

The third metacarpal is a bone associated with the middle finger. This unique central position is said to increase the functional efficiency of this bone as a stabiliser during various movements (Scheuer & Black 2000). With regards to the morphology of this bone, the literature provides brief descriptions (Bass 1995). Most of these list soft tissues associated with this bone rather than specific bony landmarks. For example, Gray *et al*. (1932) describe the attachment of the ulnar head of the second dorsal interosseous muscle and radial head of the third dorsal interosseous muscle to the radial and ulna side of the shaft respectively.

A description of the shaft, head and base of the third metacarpal as observed from a dorsal, palmar and lateral, medial view in the present will be discussed. This will be in conjunction with bony landmarks already mentioned in the literature.

6.4.2 Shaft or body (Figures 6.3a-d)

On a dorsal view (Figure 6.3a) the shaft is noticeably wider distally in comparison to the narrowed proximal end. Two ridges can be identified on the dorsal surface, namely, the dorsal medial ridge (2) and dorsal lateral ridge (11). These ridges converge towards the center of the shaft in the proximal third. Three surfaces associated with these ridges are identified as the dorsal medial (4), dorsal (3) and dorsal lateral (12) surfaces. The dorsal surface is rough and serves for attachment of the extensor tendon in comparison to the smooth lateral and medial surfaces which serve for attachment of the second and third dorsal interosseous muscle (Matshes *et al*. 2005).

The shaft, as observed from a palmar aspect (Figure 6.3b), also shows a broader distal and narrowed proximal end. The palmar surface is smooth throughout its entire length. The lateral margin forms an angle at the proximal and distal ends giving this margin a concave shape. The medial margin, on the other hand, is straight. A central palmar ridge (16) serves for attachment of the transverse head of adductor pollicis in the distal third (Matshes *et al*. 2005).

Two surfaces are found on either side of the central palmar ridge namely the palmar lateral (15) and palmar medial (22) surfaces for attachment of the second and third dorsal interosseous muscle (Matshes *et al*. 2005). In the midshaft, this ridge splits into two, namely, the palmar medial ridge (23) and palmar lateral ridge (17) which surrounds a third surface called the proximal palmar surface (18).

From a lateral view (Figure 6.3c), the shaft is smooth. The dorsal surface is straight in comparison to the palmar surface which is concave. Nutrient foramina are reported to occur on the lateral aspect of the shaft (Patake & Mysorekar 1977).

Features from a medial view (Figure 6.3d) are very similar to that seen on a lateral view with regards to the dorsal and palmar surfaces. What is noticeable from this view is that the proximal palmar surface (18) overlaps onto the medial surface.

6.4.3 Head (Figures 6.3a-e)

Not much of the head can be seen from a dorsal view (Figure 6.3a). This is because the head is tilted forward on the shaft. On either side of a line joining the head with the shaft, are two tubercles, namely, the dorsal lateral (10) and dorsal medial (1) tubercles. A ridge of bone extending fom each tubercle joins distally and becomes concave in shape. The palmar lateral tubercle (9) can be seen from this view because of the greater width of the head on the palmar aspect. Between the dorsal lateral and palmar lateral tubercles is a shallow concavity, the lateral fossa (8).

The head also presents with two tubercles on a palmar view (Figure 6.3b). These are called the palmar lateral (9) and palmar medial (21) tubercles. The palmar lateral tubercle is relatively larger, longer and tends to flare outwards and proximally much more than the palmar medial tubercle, which is relatively smaller and shorter. These tubercles are connected to each other by a ridge of bone, also referred to as the palmar articular margin (20). A shallow rough depression is found in the area between these tubercles and the central palmar tubercle.

A lateral view (Figure 6.3c) shows a relatively larger and longer palmar lateral tubercle (9) as opposed to a relatively smaller and shorter dorsal lateral tubercle (10) separated by a lateral fossa (8). The palmar lateral tubercle is more distally positioned in relation to the dorsal lateral tubercle.

The medial view (Figure 6.3d) is similar to the lateral view with exception of the terminologies used. The dorsal medial (1) and palmar medial (21) tubercles are separated from each other by a medial fossa (33).

The head is square in shape from a superior view (Figure 6.3e). The tubercles on the dorsal and palmar aspect can be identified. The dotted line on this figure illustrates the relatively greater palmar width in comparison to the narrower dorsal width.

6.4.4 Base (Figures 6.3a-d and f)

The base presents with a lateral styloid process (13) (Matshes *et al*. 2005) from a dorsal view. Gray (1932) describes the base as follows “A pyramidal eminence is present on the lateral side of the dorsal part of its base and is termed the styloid process” (p. 342). Distal to the styloid process, is a rough area, referred to as a tubercle in third metacarpals of the juvenile hand (Scheuer & Black 2000), which serve as attachment for extensor carpi radialis brevis (Gray 1932). Scheuer and Black (2000) refer to the attachment of extensor carpi radialis brevis to a tubercle on the dorsal lateral aspect. In the present study this was found to be distal to the lateral styloid process (13). Lin and Cardenas (2003) reported that the brachioradialis may attach to the dorsal aspect of the base just deep to extensor carpi radialis brevis. In the present study, this region is located between the styloid process laterally (13) and the smaller medial tubercle (6). The medial tubercle of the base serves for attachment of the interosseous ligament (Scheuer & Black 2005).

In the present study, the base presents with a prominent bony extension which is referred to as the palmar baseplate (19) as seen from a palmar view (Figure 6.3b). This bony projection is directed medially which explains the irregular convex shape of the articulating facet. Due to this deviation, the lateral styloid process can also be identified in the background.

In the present study a lateral view (Figure 6.3c) of the base was seen to present with two facets rather than a single “strip-like” facet (Scheuer & Black 2005). Both the dorsal (27) and palmar (26) lateral facets are convexed distally. A shallow depression (25) is located distal to the constricted point where the two facets meet. The lateral aspect of the base is smooth and has a concave facet for articulation with the second metacarpal (Gray 1932, Matshes *et al*. 2005). It is said that the lateral facet is constricted in the midline as it serves for attachment of the interosseous ligament (Scheuer & Black 2005).

The medial aspect of the base (Figure 6.3f) has two oval facets for articulation with the lateral aspect of the base of the fourth metacarpal (Scheuer & Black 2000). It is said that the palmar facet (31) located medially on the base occurs less frequently and in some cases may even be absent (Scheuer & Black 2000). The other facet was referred to as the dorsal facet located medially (30).

A rectangular-shaped base is clear from an inferior view (Figure 6.3f). The dotted line on this figure illustrates the relatively longer dorsal width represented by the dorsal articular margin (7) in comparison to the narrower palmar width represented by the palmar articular margin (24). The proximal articular facet on the base is concaved dorsally (Gray 1932, Scheuer & Black 2000) where it becomes continuous with the lateral styloid process and convex on the palmar aspect (Scheuer & Black 2000). The proximal facet articulates with the capitate (Gray 1932, Matshes *et al*. 2005, Scheuer & Black 2000), proximal phalanx, second and third metacarpals (Matshes *et al*. 2005).

6.4.5 Siding

In order to differentiate the right third metacarpal from the corresponding one on the left side, the bone is orientated with the palmar surface facing down and the dorsal surface facing up or towards one, while the head is placed at the top end and the base at the bottom end (Bass 1995, Matshes *et al*. 2005).

For the purpose of the present study, a list of bony landmarks for the shaft, head and base of the third metacarpal will now be provided. This is to overcome any problems that may be encountered if only a fragment of the third metacarpal is found amongst skeletal remains.

Shaft

1. Palmar medial ridge (23) extending more medially (Figure 6.3b)
2. Proximal palmar surface (18) deviates medially (Figure 6.3b)

Head

1. Palmar lateral tubercle (9) longer and flares outwards and proximally (Figure 6.3b)
2. Lateral fossa (8) deeper and relatively bigger than medial fossa (33) (Figures 6.3c and d)
3. Head is wider on the palmar than on the dorsal aspect (Figure 6.3e)

Base

1. Longer styloid process located laterally (13) (Figure 6.3a)
2. Palmar foot plate directed medially (19) (Figure 6.3b)
3. Lateral articular margin concave (28) (Figure 6.3c)
4. Medial articular margin oblique (32) (Figure 6.3d)
5. While the base is approximately rectangular in shape as seen from the articulating surface, it is relatively wider dorsally than on the palmar aspect (Figure 6.3f)

Figure 6.3: Morphology of the right (R) and left (L) third metacarpal

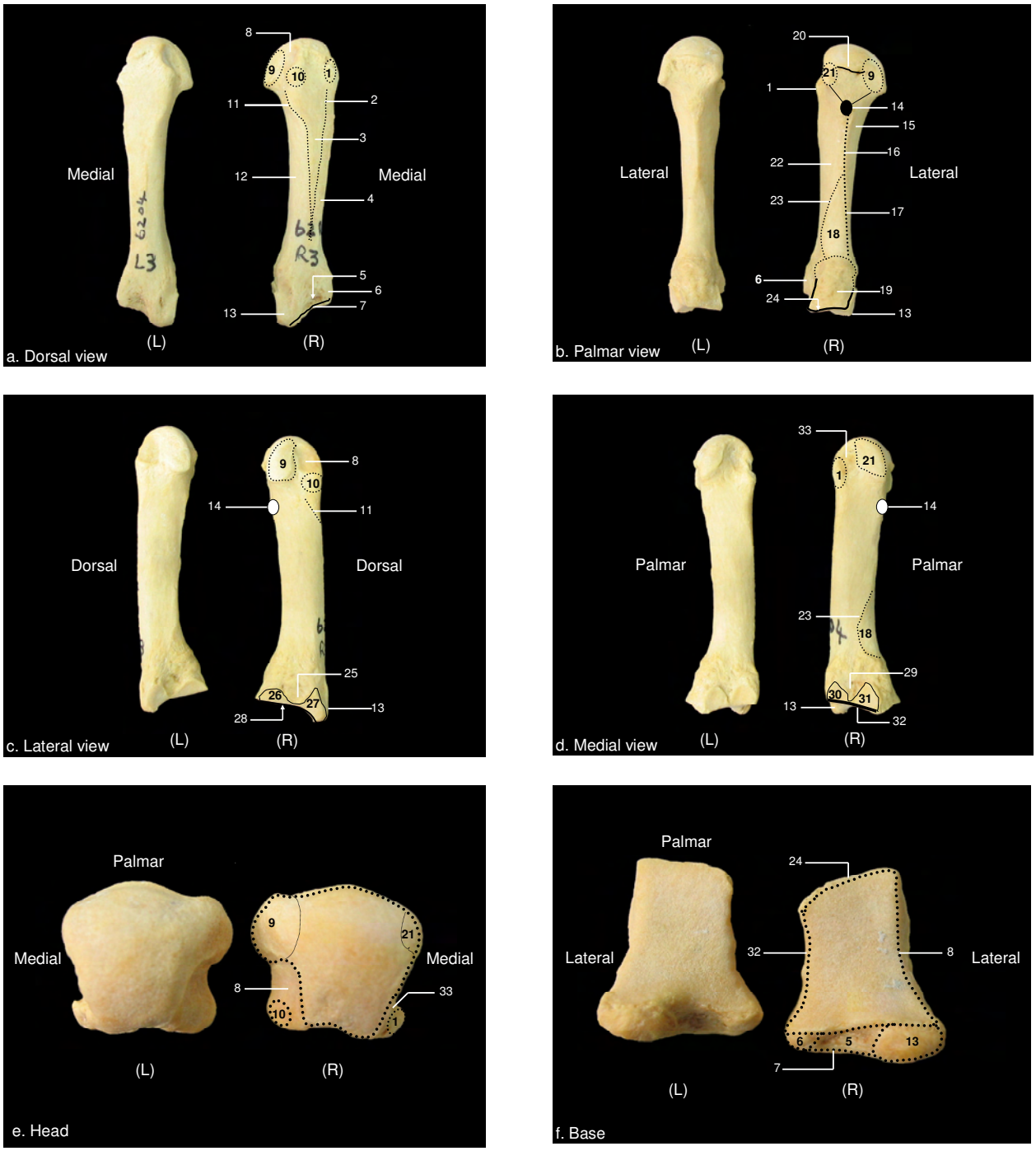

1=dorsal medial tubercle of head, 2=dorsal medial ridge, 3=dorsal surface of shaft, 4=dorsal medial surface of shaft, 5= dorsal concavity of base, 6=dorsal medial tubercle of base, 7=dorsal articular margin of base, 8=lateral fossa of head, 9=palmar lateral tubercle of the head, 10=dorsal lateral tubercle of the head, 11=dorsal lateral ridge, 12=dorsal lateral surface of shaft, 13=styloid process, 14=central palmar tubercle, 15=palmar lateral surface, 16= central palmar ridge, 17=lateral palmar ridge, 18=proximal palmar surface, 19=palmar baseplate, 20=palmar articular margin of head, 21=palmar medial tubercle, 22=palmar medial surface, 23=medial palmar ridge, 24=palmar articular margin of base, 25=lateral interarticular fossa of base, 26-dorsal articular facet of base located laterally, 27=palmar articular facet of base located medially, 28=lateral articular margin of base, 29=medial interarticular fossa of base, 29=dorsal articular facet of base located medially, 30=palmar articular facet of base located medially, 32=medial articular margin of base, 33=medial fossa of head

6.5 Morphology of the fourth metacarpal (Figures 6.4a-f)

6.5.1 Introduction

The fourth metacarpal is described as a miniature (Romanes 1991), long (Bass 1995, Romanes 1991), cylindrical (Bass 1995) bone aligned with the ring finger. This bone is relatively short, (Bass 1995, Matshes *et al*. 2005) slender, (Scheuer & Black 2000) and more gracile (Matshes *et al*. 2005) when compared to the second and third metacarpals. It is, however, relatively longer than the first and fifth metacarpal. The fourth metacarpal articulates with adjacent third and fifth metacarpals, the proximal phalanx distally, the capitate and hamate proximally (Gray 1959, Matshes *et al*. 2005, Romanes 1991). In some textbooks, brief summaries of general features for all metacarpals are given (Hal-Graggs 1985, Moore & Agur 2002). El-Najjar and McWilliams (1978) provide diagrams of the hand but the metacarpals, including the fourth one, are not labelled.

6.5.2 Shaft or body (Figures 6.4a-d)

The shaft is triangular in cross section (Bass 1995, Hollinshead & Rosse 1985) The smooth dorsal surface is broad distally and narrows at the proximal end (Figure 6.4a) In the distal third, the medial (4) and lateral (9) margins run in an oblique manner proximally towards the center of the shaft and merges at a point just distal to the base. Three surfaces can be identified on the dorsal aspect, namely, dorsal medial (5), dorsal (6) and dorsal lateral (10) surfaces.

The palmar surface is concave (Bass 1995, Hollinshead & Rosse 1985) and interrupted by a centrally located palmar ridge (24) (Figure 6.4b). The presence of this ridge creates two surfaces, namely, palmar lateral (18) and palmar medial (25) surfaces. Although the presence of a ridge is recorded in the literature, it does not state whether it is on the dorsal or palmar surface (Scheuer & Black 2000, Matshes *et al*. 2005). Muscle attachments associated with the palmar surfaces are commonly described or labeled on diagrams. For example, the third palmar interosseous and medial head of the third dorsal interosseous muscles attach to the

lateral surface (Scheuer & Black 2000) The medial surface of the shaft, on the other hand, is reserved for attachment of the lateral head of the fourth dorsal interosseous muscle (Scheuer & Black 2000). A nutrient foramen has been identified at the proximal end (Bass 1995) of the lateral surface of the shaft (Scheuer & Black 2000). The shape of the lateral and medial margins as seen from both the dorsal and palmar views, is concave with the medial margin extending further proximally than the lateral margin.

From a lateral view (Figure 6.4c), the dorsal lateral margin (9) extends proximally from the dorsal lateral tubercle (2) and in the midshaft region, it runs across to the dorsal surface. The palmar lateral margin (17) runs proximally and ends at the proximal tuberosity of the shaft (27).

From a medial view (Figure 6.4d), the dorsal medial margin (4) runs from the dorsal medial tubercle (3) to the midshaft region where it then crosses over to the dorsal aspect of the smooth shaft, similar to that observed for the dorsal lateral margin (9). A rough articular surface (30) presents proximally just above the base on the medial surface. The palmar articular margin is straight (31).

6.5.3 Head (Figures 6.4a-e)

The head or distal extremity of the shaft (Bass 1995) articulates with the base of the proximal phalanx (Scheuer & Black 2000). It is large and round (Bass 1995) with the distal articulating margin convexed distally (1). The tilting of the head forward on the shaft may allow for greater flexion than extension at this joint. This forward angulation thus results in a relatively smaller area of the head being visible from a dorsal view (Figure 6.4a). In fact, the head is said to be asymmetrical which allows the fingers to roll into the palm of the hand forming a clenched fist (Bass 1995). Scheuer and Black (2000) describe the head of the fourth metacarpal in juveniles as symmetrical (Scheuer & Black 2000).

The greater surface area of the head visible on a palmar view (Figure 6.4b), also presents with two tubercles. The palmar lateral (16) and palmar medial (15) tubercles are separated from each by a shallow depression. The palmar medial tubercle is directed more

outwards or medially while the palmar lateral tubercle points proximally. The palmar articular margin of the head (14) merges with each tubercle on the sides.

A relatively smaller dorsal lateral tubercle (2) and relatively larger palmar lateral tubercle (16) can be seen on a lateral view (Figure 6.4c). A shallow fossa (26) is located between the two tubercles.

On a medial view (Figure 6.4d) a relatively smaller dorsal medial tubercle (3) and a relatively larger palmar medial tubercle (15) can be seen. A medial fossa (29) separates the two medial tubercles.

The head is rhomboidal in shape as seen from a superior view (Figure 6.4e). The palmar width is greater than the dorsal width. The head is asymmetrical as is seen by the medial deviation of the dorsal margin, resulting in the dorsal lateral tubercle (2) being prominent.

6.5.4 Base (Figures 6.4a-d and f)

The base of the fourth metacarpal is identified as an irregular expansion at the proximal end of the shaft (Hall-Craggs 1985.) This feature allows it greater approximation and thus reduced mobility at the carpo-metacarpal joint (Hall-Craggs 1985). Matshes *et al*. (2005) state that descriptions of facets for articulation with the hamate, third and fifth metacarpals are easily identified bony landmarks. Gray (1973) refers to the presence of a facet and tubercle on the radial and ulna side of the base for articulation with the fifth and third metacarpal respectively.

At the proximal end of the dorsal surface (Figure 6.4a), a relatively small, elongated lateral tubercle (11) forms a sharp point as it runs proximally. On the medial side, the bone which deviates outward is called the styloid process (7). A shallow depression (8) is found between the tubercle and the styloid process.

From a palmar view (Figure 6.4b) the base forms a rounded apex (21) with two articular facets located on its lateral and medial side, namely, palmar lateral articular facet (22) and palmar medial articular facet (20).

A lateral view (Figure 6.4c) shows the presence of two facets, namely, palmar lateral articular facet (22) and dorsal lateral articular facet (12). These articular facets are separated from each other by an interarticular groove (28).

The medial aspect of the base (Figure 6.4d) has a single, relatively large oval facet for articulation with the lateral aspect of the base of the fifth metacarpal (Scheuer & Black 2000).

The articular end of the base (Figure 6.4f) is irregular in shape. The medial articular facet is semilunar (32) in shape while the lateral half presents with two rounded articular facets, namely, the dorsal lateral (12) and palmar lateral (22) facets. Gray (1973) describes the proximal surface of the base as concavo-convex incorporating the entire surface.

6.5.5 Siding

In order to differentiate the right fourth metacarpal from the corresponding one on the left side, the bone is orientated with the palmar surface facing down and the dorsal surface facing up or towards one, while the head is placed at the top end and the base at the bottom end (Bass 1995, Matshes *et al*. 2000).

For the purpose of the present study, a list of bony landmarks for the shaft, head and base of the fourth metacarpal will now be provided. This is to overcome any problems that may be encountered if only a fragment of the fourth metacarpal is found amongst skeletal remains.

Shaft

1. Styloid process located medially at the proximal end (7) (Figure 6.4a)
2. Central palmar ridge (24) runs its course from a central position at the distal end to the medial end of the shaft in the proximal third (Figure 6.4b)

Head

1. Head is wider on the palmar than on the dorsal aspect with the latter deviating slightly medially (Figure 6.4e)
2. The dorsal margin of the head is directed laterally (Figure 6.4e)

Base

1. Long styloid process located medially (7) (Figure 6.4a)
2. Single articular facet medially (20) (Figure 6.4d)
3. Two articular facets laterally (12 & 22) (Figure 6.4c)
4. Medial articular margin slightly concave (31) (Figure 6.4d)
5. A view from the articular surface (Figure 6.4f):
    a. There is a single medially located semilunar facet (32)
    b. There are two laterally located round facets (12 & 22)
    c. The dorsal lateral facet (12) is relatively larger than the palmar lateral facet (22)
6. Lateral articular margin interrupted by the interarticular groove (28) (Figure 6.4f)

Figure 6.4: Morphology of the right (R) and left (L) fourth metacarpal

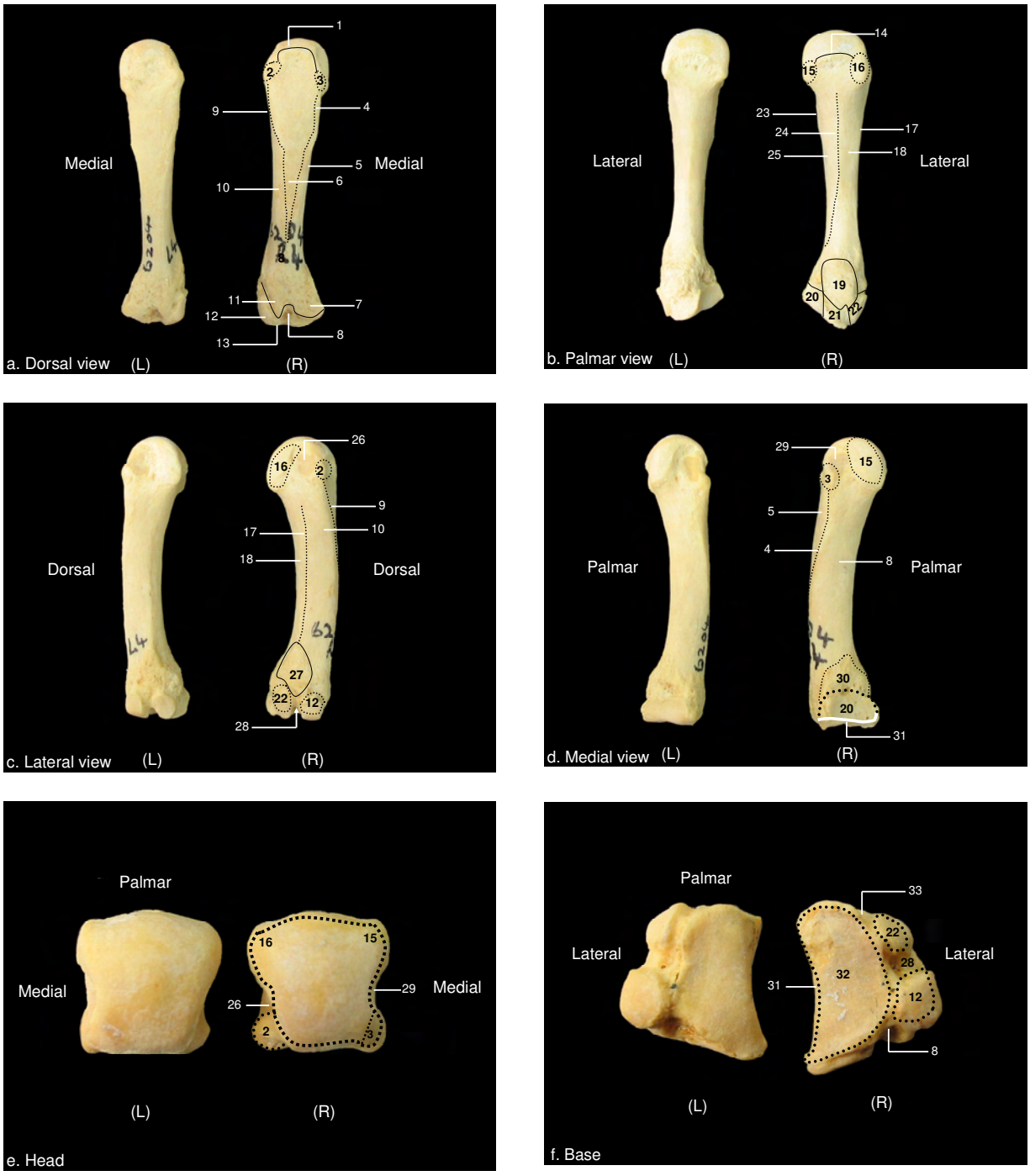

1=dorsal articular margin of head, 2=dorsal lateral tubercle of head, 3=dorsal medial tubercle of head, 4=medial margin of shaft, 5=dorsal medial surface of shaft, 6=dorsal surface of shaft, 7=styloid process, 8=shallow depression of base on the dorsal surface, 9=lateral margin of shaft, 10=dorsal lateral surface of shaft, 11=lateral tubercle of base, 12=dorsal lateral articular facet of base, 13=dorsal articular margin of base, 14=palmar articular margin of head, 15= palmar medial tubercle of head, 16=palmar lateral tubercle of head, 17=palmar lateral margin of shaft, 18=palmar lateral surface of shaft, 19=proximal oval tuberosity on palmar surface of base, 20=medial articular facet of base on lateral surface, 21=proximal footplate of base on palmar surface 22=palmar lateral articular facet of base, 23=palmar medial margin of shaft, 24=central palmar ridge, 25=palmar medial surface of shaft, 26= lateral fossa of head, 27=proximal rectangular tuberosity on lateral surface of base, 28=interarticular groove, 29=medial fossa of head, 30=proximal rough area on medial surface of shaft, 31=medial articular margin of base, 32=lateral articular facet of base, 33=palmar articular margin of base

6.6 Morphology of the fifth metacarpal (Figures 6.5a-f)

6.6.1 Introduction

The fifth metacarpal is the most medially positioned digit in the hand. Its position in the hand dictates the number of articulating facets that it has. For example, it is identified by three articulating facets, namely, a facet on the lateral aspect of the shaft, a facet proximally for the hamate and a facet distally for the proximal phalanx. The medial aspect of the shaft has no articulating facets (Matshes *et al*. 2005).

Generally, the only reference made of the fifth metacarpal in the literature is the division into a head, shaft and base (Hollinshead & Rosse 1985). Sometimes, the fifth metacarpal is mentioned in terms of movement, where it is said to be the least mobile digit when compared to adjacent metacarpals (Hollinshead & Rosse 1985). On the other hand, descriptions of the fifth metacarpal in the juvenile hand, has received much more attention with regards to morphological detail (Scheuer & Black 2000). Descriptions of the adult hand as observed in the present study will be discussed below under the headings of shaft, head and base. The numbers in brackets adjacent to the bony landmark corresponds to the numbers on the appropriate diagrams.

6.6.2 Shaft or body (Figures 6.5a-d)

The dorsal surface presents with an oblique (Gray 1959, Matshes *et al*. 2005), sometimes referred to as a linear (Matshes *et al*. 2005) ridge running from the medial side of the base (Gray 1959, Matshes *et al*. 2005) to the lateral end of the head (Gray 1959, Matshes *et al*. 2005). From the present study, a dorsal view (Figure 6.5a) shows the oblique ridge (6) starting distal to the medial tuberosity of the shaft (8) and running laterally across the shaft in a distal direction where it ends proximal to the dorsal lateral tubercle (3). On either side of the ridge are two surfaces, namely, a dorsal lateral (13) and dorsal medial (5) surface.

At the distal end of the palmar surface of the shaft (Figure 6.5b) is a prominent central palmar tubercle (17). Distal to this tubercle is a rough triangular region. Extending proximally

from this tubercle is a central palmar ridge (23). Two surfaces can also be seen on either side of this ridge, namely, the palmar lateral (19) and palmar medial surfaces (22). At the proximal end of the shaft are the palmar lateral (7) and palmar medial (8) tuberosities of the shaft.

The lateral surface of the fifth metacarpal in the juvenile hand presents with a longitudinal ridge which divides this surface into a dorsal and palmar division (Scheuer & Black 2000). In the present study, (Figure 6.5c) the longitudinal ridge is labelled as the palmar lateral margin of the shaft (18). Most textbooks relate the attachments of the medial head (Scheuer & Black 2000), the fourth dorsal interosseous (Scheuer & Black 2000, Gray 1959) and extensor tendons (Gray 1959) to the lateral surface. Patake and Mysorekar (1977) identified nutrient foramina at the proximal aspect of the lateral surface.

The medial aspect of this surface has been described as being smooth (Gray 1959) and serves for attachment of opponens digiti minimi (Scheuer & Black 2000).
A view of the medial aspect of the shaft in the present study (Figure 6.5d), shows the palmar medial margin of the shaft (21) extending from the proximal tuberosity (25) to the dorsal medial tubercle of the head (4) distally. The proximal end of the dorsal oblique ridge (6) can also be seen to merge with the palmar medial margin of the shaft (21) from this view.

6.6.3 Head (Figures 6.5a-e)

The head or distal end of the fifth metacarpal, articulates with the base of the proximal phalanx (Gray 2005, Matshes *et al*. 2005). It is asymmetrical with a round articulating surface (Romanes 1991). Studies by Scheuer and Black (2000) on the juvenile hand ascribed this asymmetry to a “large attachment site” for the metacarpophalangeal ligament. Two tubercles occur on the head when observed from a dorsal view (Figure 6.5a), namely, the dorsal lateral (3) and dorsal medial (4) tubercles. Scheuer and Black (2000) state that although these tubercles appear to be the same distance from the joint surface, the lateral tubercle is more distally placed than the medial tubercle in the juvenile hand. This feature was also observed in the present study.

Tubercles similar to those observed on the dorsal surface are seen from a palmar aspect (Figure 6.5b). The palmar lateral tubercle (16) appears to project more proximally than the palmar medial tubercle (15). The literature describes the head as being larger on the palmar than on the dorsal aspect. The tendon of abductor digiti minimi attaches to the palmar medial aspect (Scheuer & Black 2000, Hubay 1949).

A relatively larger palmar lateral tubercle (16) is separated from a relatively smaller dorsal lateral tubercle (3) by a lateral fossa (12) seen from al lateral view (Figure 6.5c). When a medial view of the head is observed (Figure 6.5d), a relatively larger palmar medial tubercle (15) is separated from a relatively smaller dorsal medial tubercle (4) by a medial fossa (2) is seen.

From a superior view (Figure 6.5e) the head is rhomboidal in shape. The dorsal and palmar tubercles can be seen from this view.

6.6.4 Base (Figures 6.5a-d and f)

Matshes *et al.* (2005) mention the presence of two facets on the base, namely, one for the hamate and the other for the fourth metacarpal. Gray (1973), on the other hand, gives a more detailed description by stating that the base is concaved-convexed on its proximal surface. Some authors (Gray 1973, Scheuer & Black 2000) mention the facet and tubercle on the radial and ulna sides of the base for articulation with the fourth metacarpal and for attachment of the extensor carpi ulnaris muscle respectively. Gray (2005) tend to provide a general statement by mentioning that the base articulates with the carpal bones and with adjacent metacarpals. Hollinshead and Rosse (1985) describe the base as being flat. El-Najjar and McWilliams (1978) provide diagrams of the hand bones but the metacarpals, including the fifth, one are not labelled.

The dorsal articular margin (11) as seen from a dorsal view (Figure 6.5a), is concave distally, making the articular surface of the base visible from this view (10). The lateral articular facet (9) can be seen from a dorsal view due to rotation of the proximal end of the base in a medial direction.

The concave articulating margin (20) of the base as seen from a palmar view (Figure 6.5b), is at a lower level when compared to the dorsal articular margin.

From a lateral view (Figure 6.6c) the articular margin (24) is convexed proximally. Located distal to the articular margin is an oval-shaped articular facet (9). From a medial view (Figure 6.5d) the articular margin (26) is also convexed proximally. The proximal tuberosity of the shaft (25) is located distal to the medial articular margin.

The concave articular surface of the base (Figure 6.6f) is rectangular-shaped. The lateral margin (24) is relatively longer when compared to the relatively shorter medial margin (26).

6.6.5 Siding

In order to differentiate the right fifth metacarpal from the corresponding one on the left side, the bone is orientated with the palmar surface facing down and the dorsal surface facing up or towards one, while the head is placed at the top end and the base at the bottom end (Bass 1995, Matshes *et al*. 2000).

For the purpose of the present study, a list of bony landmarks for the shaft, head and base of the fifth metacarpal will now be provided. This is to overcome any problems that may be encountered if only a fragment of the fifth metacarpal is found amongst skeletal remains.

Shaft

1. Dorsal oblique ridge (6) runs obliquely from the medial surface of the shaft proximally to the lateral surface of the shaft distally (Figure 6.5a)
2. Proximal third of the shaft is rotated laterally (Figures 6.5a and b)
3. Central palmar ridge (23) deviates medially in the proximal third (Figure 6.5b)

Head

1. Palmar medial tubercle (15) is relatively larger than the palmar lateral tubercle (16) (Figure 6.5b)

Base

1. The concavity of the dorsal articular margin (11) is set more distally than the palmar articular margin (20) (Figures 6.5a and b)
2. Articular margin of the base on the lateral surface is convexed proximally (24) (Figure 6.5c)
3. Articular margin of the base on the medial surface is rounded (26) (Figure 6.5d)
4. Absence of an articular facet on the medial aspect of the base (Figure 6.5f)

Figure 6.5: Morphology of the right (R) and left (L) fifth metacarpal

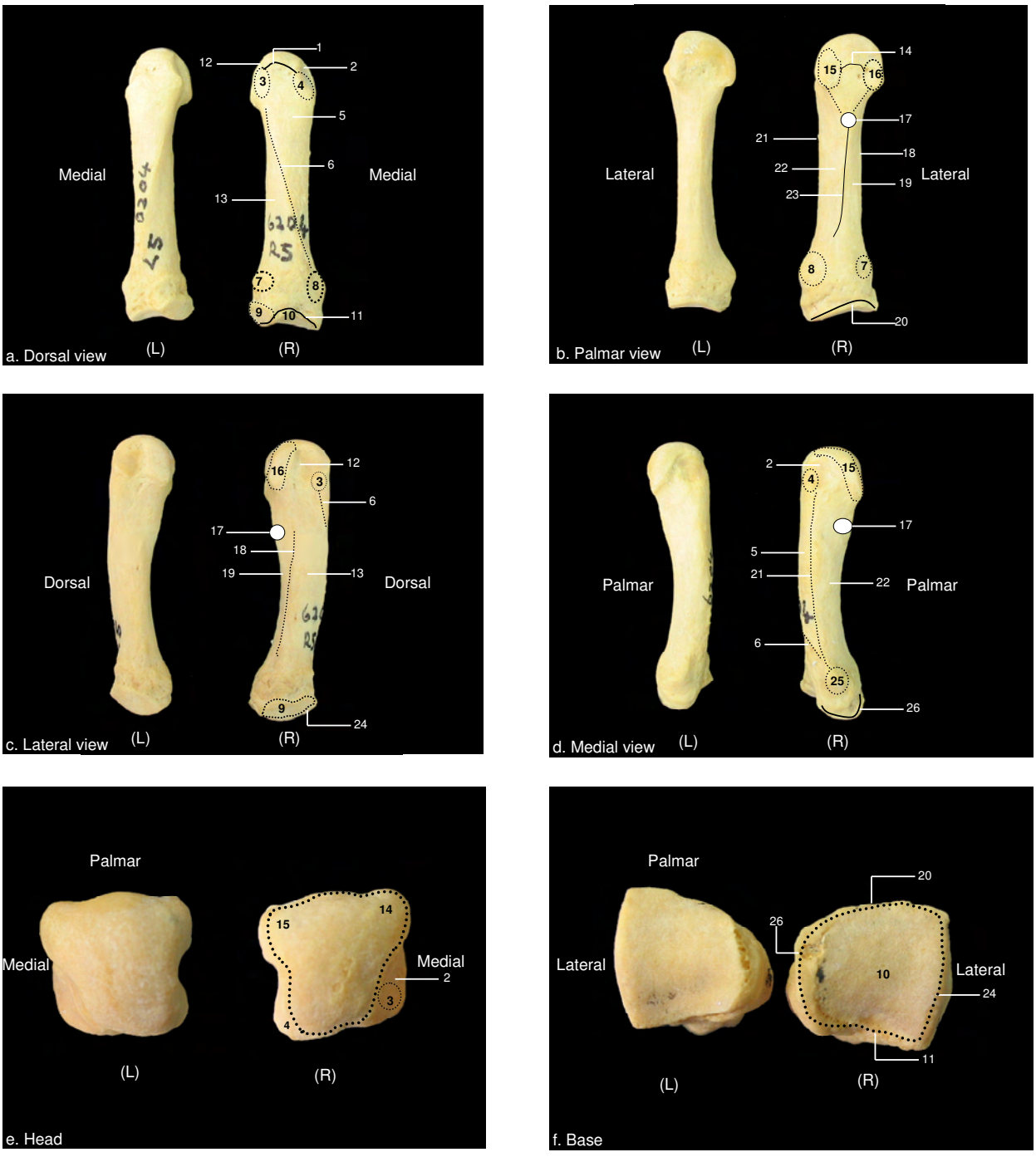

1=dorsal articular margin of head, 2=medial fossa of head, 3=dorsal lateral tubercle of head, 4=dorsal medial tubercle of head, 5=dorsal medial surface of shaft, 6=dorsal oblique ridge of shaft, 7=palmar lateral tuberosity of shaft, 8=palmar medial tuberosity of shaft, 9=lateral articular facet of base, 10=articular facet of base, 11=dorsal articular margin of base, 12=lateral fossa, 13=dorsal lateral surface of shaft, 14=palmar articular margin of head, 15= palmar medial tubercle of head, 16=palmar lateral tubercle of head, 17= distal palmar tubercle of shaft, 18=palmar lateral margin of shaft, 19=palmar lateral surface of shaft, 20=palmar articular margin of base, 21=palmar medial margin of shaft, 22=palmar medial surface of shaft, 23= central palmar ridge, 24=lateral articular margin of base, 25=proximal tuberosity on medial surface of shaft, 26=medial articular margin of base

6.7 Morphology of the first proximal phalanx (Figures 6.6a-f)

6.7.1 Shaft or body (Figures 6.6a-d)

From a dorsal view (Figure 6.6a) the shaft is smooth along its entire length and also wider at the proximal than at the distal end. The lateral margin (10) has a deeper concavity than the medial margin (4). The tilting of the base laterally causes the lateral margin to project further proximally than the medial margin. Where the shaft joins the base, an inverted-V margin is formed (5).

From a palmar view (Figure 6.6b), the proximal half of the shaft is rotated laterally and the distal half rotated medially. This rotation results in the lateral margin projecting forward. The palmar surface is concave from proximal to dorsal. A shallow depression is evident in the distal third (19). Numerous nutrient foramina can be identified in the proximal third (15).

The shaft in the proximal two-thirds is broad and becomes narrow at the distal end when observed from a lateral view (Figure 6.6c). Scheuer and Black (2000) describe the distal end of the shaft as tapered. Nutrient foramina can be identified at the proximal end of the lateral surface. The proximal two-thirds of the palmar surface of the shaft can be seen from a lateral view due to rotation of the shaft laterally. The dorsal surface is flat while the palmar surface is concave.

The medial margin, when observed from a medial view (Figure 6.6d), presents with a steeper slope than the lateral margin. The palmar surface is not visible from the medial aspect.

6.7.2 Head (Figures 6.6a-e)

A dorsal view (Figure 6.6a) shows a relatively small surface area of the head. This is because the head projects more in a palmar than in a dorsal direction. A distinct dorsal articular margin (1) can be seen separating the head from the distal end of the shaft. The rotation of the distal end of the shaft medially causes a simultaneous rotation of the head in the same direction, thus exposing more of the medial fossa (3) than the lateral fossa (9). Although the articular surface, which forms a joint with the base of the middle phalanx is concave, it

tends to tilt more on the medial than on the lateral side. This tilting causes the lateral condyle (8) to be at a lower or more proximal level than the medial condyle (2).

A relatively larger surface area of the head can be seen from a palmar view (Figure 6.6b). The rotation of the head medially together with the distal end of the shaft is obvious. The lateral (8) and medial (2) condyles are convex distally and are separated from each by a shallow concavity. The medial condyle (2) is at a higher level than the lateral condyle (8) which is indicated on the diagram by the solid black line which depicts the inclination of the slope associated with each condyle. The palmar articular margin (14) is concave proximally.

From a lateral view (Figure 6.6c) the rotation of the head medially on the shaft is seen. The head is round in shape and surrounds the lateral fossa (9).

Features of the head from a medial view (Figure 6.6d), is similar to that observed from a lateral view. The medial condyle (2) surrounds the medial fossa (3). The rotation of the head medially enables one to identify both the lateral (8) and medial (2) condyles from this view.

From a superior view (Figure 6.6e) the head is rectangular in shape. The dorsal articular margin (1) is convex in shape compared to the concave palmar articular margin (14). The lateral condyle on the palmar surface is relatively bigger and projects more laterally than the relatively smaller medial condyle. This projection of the condyles outwards results in a longer palmar and shorter dorsal margin. The intercondylar groove (23) separates the two condyles.

6.7.3 Base (Figures 6.6a-d and f)

From a dorsal view (Figure 6.6a), the lateral margin (11) of the base tilts proximally and has relatively greater height than the medial margin (6). The dorsal articular margin (7) is slightly concave proximally.

The base as viewed from a palmar aspect (Figure 6.6b) is broad when compared to the rest of the bone. The medial articular margin (18) of the base is an irregular line which is horizontally positioned. Located distal to the palmar articular margin are the lateral (17) and medial (16) tubercles. The medial tubercle is relatively larger than the lateral tubercle. The

lateral rotation of the proximal end of the shaft causes a simultaneous rotation of the base in the same direction.

From a lateral view (Figure 6.6c) the articulating margin (21) tends to slope from the proximal end of the dorsal surface to the lateral tubercle (17) on the palmar surface. A lateral articular facet (12) can be seen on the dorsal surface.

From a medial view (Figure 6.6d) the articulating margin (22) is fairly straight. The medial tubercle (16) occupies a large area at the proximal end of the palmar surface.

The articular surface of the base (Figure 6.6f) is oval in shape. The palmar tubercles are prominent with the palmar medial tubercle (16) relatively larger than the palmar lateral tubercle (17).

6.7.4 Siding

In order to differentiate the right first proximal phalanx from the corresponding one on the left side, the bone is orientated with the palmar surface facing down and the dorsal surface facing up or towards one, while the head is placed at the top end and the base at the bottom end (Bass 1995, Matshes *et al*. 2000).

For the purpose of the present study, a list of bony landmarks on the shaft, head and base of the first proximal phalanx will now be provided. This is to overcome any problems that may be encountered if only a fragment of the first proximal phalanx is found amongst skeletal remains.

Shaft

1. Proximal end of lateral margin of shaft slopes more proximally (10) than medial margin (Figures 6.6a and b)
2. Lateral margin of shaft longer than the medial margin (Figures 6.6a and d)
3. Lateral margin of shaft has greater depth than medial margin (Figures 6.6a and d)
4. Proximal end of shaft rotated laterally (Figures 6.6a and b)

Head

1. Medial condyle (2) located more distal than the lateral condyle (8) (Figures 6.6a and b)
2. Surface area of medial condyle relatively smaller than lateral condyle (Figure 6.6e)
3. Lateral condyle projects more laterally than the medial condyle (Figure 6.6e)

Base

1. Medial margin of base tilted proximally (6) (Figure 6.6a)
2. Lateral margin tilted distally (11) (Figure 6.6a)
3. Dorsal articular margin slightly concave (7) (Figure 6.6a)
4. Palmar articular margin straight (18) (Figure 6.6b)

Figure 6.6: Morphology of the right (R) and left (L) first proximal phalanx (PP)

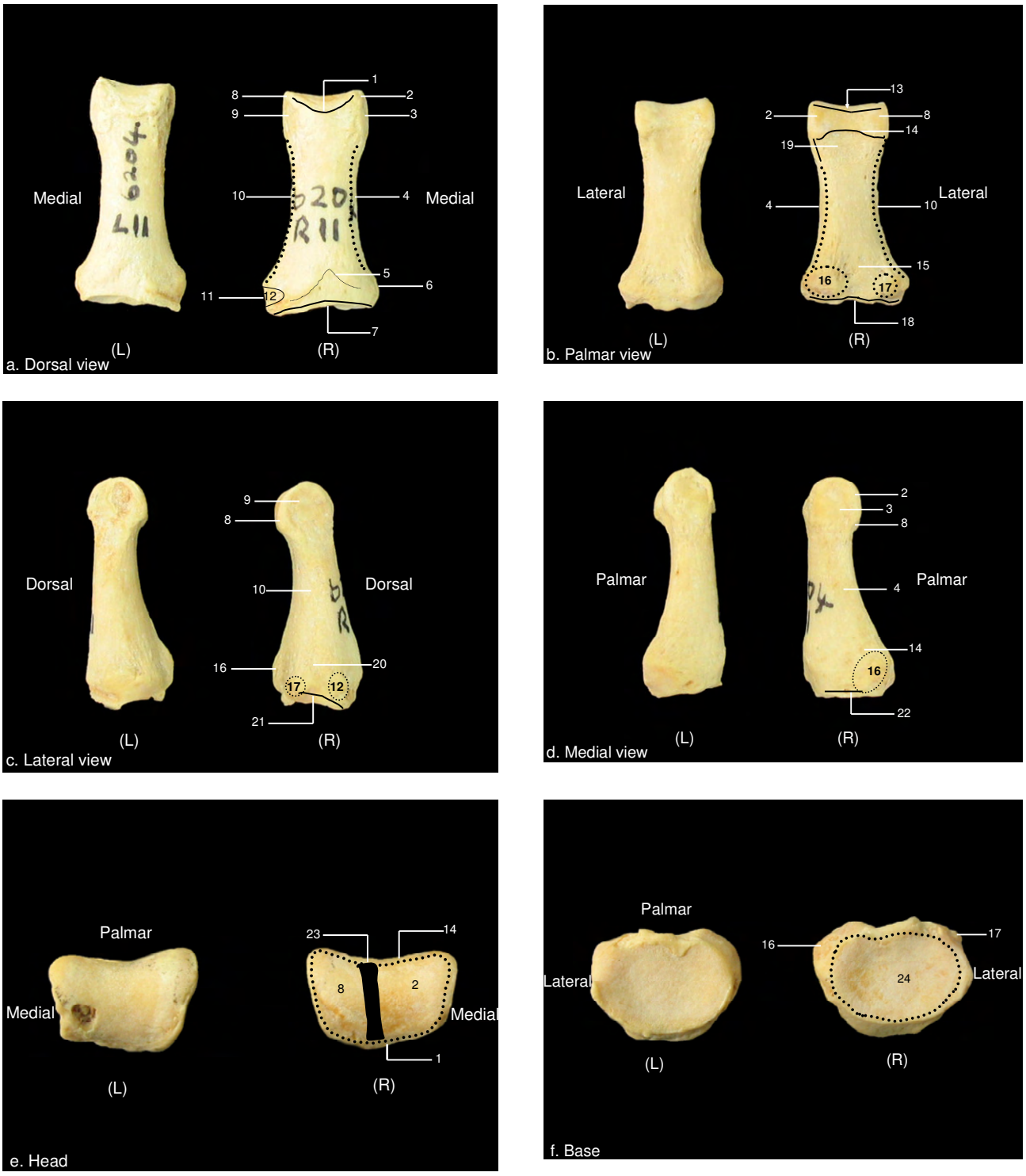

1=dorsal articular margin of the head, 2=medial condyle of head, 3=medial fossa of head, 4=medial margin of shaft, 5=inverted v-shaped space of shaft, 6=medial margin of base, 7=dorsal articular margin of base, 8=lateral condyle of head, 9=lateral fossa of head, 10=lateral margin of shaft, 11=lateral margin of base, 12=proximal dorsal lateral tubercle, 13=slope of articular surface of head, 14=palmar articular margin of head, 15=nutrient foramina on proximal palmar surface of shaft, 16=palmar medial tubercle of base, 17=palmar lateral tubercle of base, 18=medial articular margin of base, 19=distal concavity on palmar surface of shaft, 20=nutrient foramina on lateral surface of shaft, 21=lateral articular margin of base, 22=medial articular margin of base, 23=intercondylar groove, 24=articular facet of base.

6.8 Morphology of the second proximal phalanx (Figures 6.7a-f)

6.8.1 Shaft or body (Figures 6.7a-d)

Detailed analysis of the dorsal view (Figure 6.7a), indicated that the shaft of the second proximal phalanx is relatively longer than the corresponding bone of the thumb. It is also smooth along its entire length. The medial margin (4) is relatively straight along its entire length except for the proximal third where it tends to slope as it approaches the base. The lateral margin (10) is also straight and slopes just proximal to the midshaft region as it approaches the base. This results in the slope of the lateral margin being relatively longer than the slope of the medial margin. At the point where the lateral margin meets the base, a straight margin rather than a convex margin is formed when compared to the medial side.

In a palmar view (Figure 6.7b) the proximal end of the shaft seems to be slightly rotated in a lateral direction while the distal end does not appear to be rotated at all. This lateral rotation is slightly less than that observed in the corresponding bone of the thumb. The margins on either side of the shaft are rough, and referrred to as the lateral (12) and medial (18) ridges. The lateral ridge is more prominent in comparison to the medial ridge. Close observation of the palmar surface shows that the central part of the shaft, called the palmar surface (13), is separated from the lateral and medial marginal ridges by a shallow groove on either side of it.

The lateral view (Figure 6.7c), and medial view (Figure 6.7d) of the shaft are very similar. The lateral ridge (12), medial ridge (18) and palmar surface (13) can be seen. The dorsal surface is straight in comparison to the concave palmar surface. Scheuer and Black (2000) describe the distal end of the shaft as being tapered.

6.8.2 Head (Figures 6.7a-e)

Only a relatively small surface area of the head can be seen on a dorsal view (Figure 6.7a). The dorsal articular margin (1) is convexed towards the shaft. An intercondylar fossa (23) separates the lateral (8) and medial (2) condyles from each other (Figure 6.7e). These

condyles are slightly more prominent when compared to that of the thumb. The medial condyle is set at a higher or more distal level than the relatively smaller lateral condyle. The articular end of the medial condyle not only slopes more distally, it also projects out more medially than the lateral condyle. The rotation of the shaft in a lateral direction exposes the lateral fossa when the head is viewed from a dorsal aspect.

In a palmar view (Figure 6.7b) a relatively greater surface area of the head can be seen. The lateral (8) and medial (2) condyles are clearly seen with the medial condyle being elevated at a slightly higher level than the lateral condyle. The shallow intercondylar groove separating the two condyles is more marked from this view than from the dorsal aspect.

Lateral (Figure 6.7c) and medial (Figure 6.7d) views of the head are similar. The head shows tilting forward in a palmar direction in both views. The lateral condyle (8) surrounds the lateral fossa (9) and the medial condyle condyle (2) surrounds the medial fossa (3).

When viewed from the articular end (Figure 6.7e), the head is rectangular in shape. The medial condyle (2) is relatively bigger than the lateral condyle (8). Both condyles tend to flare out to the sides. The palmar margin of the medial condyle is round in comparison to the pointed palmar margin of the lateral condyle. The intercondylar groove (23) is a shallow cavity located between these condyles.

6.8.3 Base (Figures 6.7a–d and f)

A dorsal view (Figure 6.7a) shows a broad base in comparison with the rest of the bone. This view displays a round and convex medial margin in comparison to a straight lateral margin. The dorsal articular margin (7) is slightly concave in shape. The lateral end of the base is pulled in a proximal direction giving the appearance that the lateral margin (10) is tilted laterally and proximally.

In a palmar view (Figure 6.7b) the articulating margin (16) of the base is represented as an irregular line that is straight in comparison to the concave dorsal articular margin. The

lateral (15) and medial (14) tubercles surrounding a rough central region are located just distal to the palmar articular margin.

A straight articular margin as seen from a lateral view (Figure 6.7c), slopes in a distal direction from the dorsal to the palmar surface. The dorsal lateral (5) and palmar lateral (15) tubercles on either side of a lateral facet (20) can be easily identified.

The articular margin on the medial surface (Figure 6.7d) slopes in a distal direction from the palmar to dorsal surface. This slope is less than that observed on the lateral side. The dorsal medial (6) and palmar medial (14) tubercles are located just distal to the articular margin.

The base as observed from the articular end (Figure 6.7f) is oval in shape. The articular surface (24) is concave. The more prominent palmar medial tubercle (14) projects more medially when compared to the less prominent lateral tubercle (15). The lateral articular facet (20) is a prominent feature on the lateral margin.The dorsal articular margin is smooth in comparison to the irregular palmar articular margin.

6.8.4 Siding

In order to differentiate the right second proximal phalanx from the corresponding one on the left side, the bone is orientated with the palmar surface facing down and the dorsal surface facing up or towards one, while the head is placed at the top end and the base at the bottom end (Bass 1995, Matshes *et al*. 2000).

For the purpose of the present study, a list of bony landmarks for the shaft, head and base of the second proximal phalanx will now be provided. This is to overcome any problems that may be encountered if only a fragment of the second proximal phalanx is found amongst skeletal remains.

Shaft

1. Medial margin (4) straight (Figures 6.7a and b)
2. Lateral margin (10) concave (Figures 6.7a and b)

3. Proximal end of shaft well developed and robust on the lateral side (Figure 6.7c)
4. Proximal end of shaft rotated laterally (Figures 6.7a and b)

Head

1. Surface area of medial condyle relatively larger than the lateral condyle (Figure 6.7e)
2. The palmar margin of the medial condyle is round (Figure 6.7e)
3. The palmar margin of the lateral condyle is pointed (Figure 6.7e)

Base

1. The medial articular margin is straight as seen from the articular end (Figure 6.7f)
2. The lateral articular margin is tapered as seen from the articular end (Figure 6.7f)

Figure 6.7: Morphology of the right (R) and left (L) second proximal phalanx

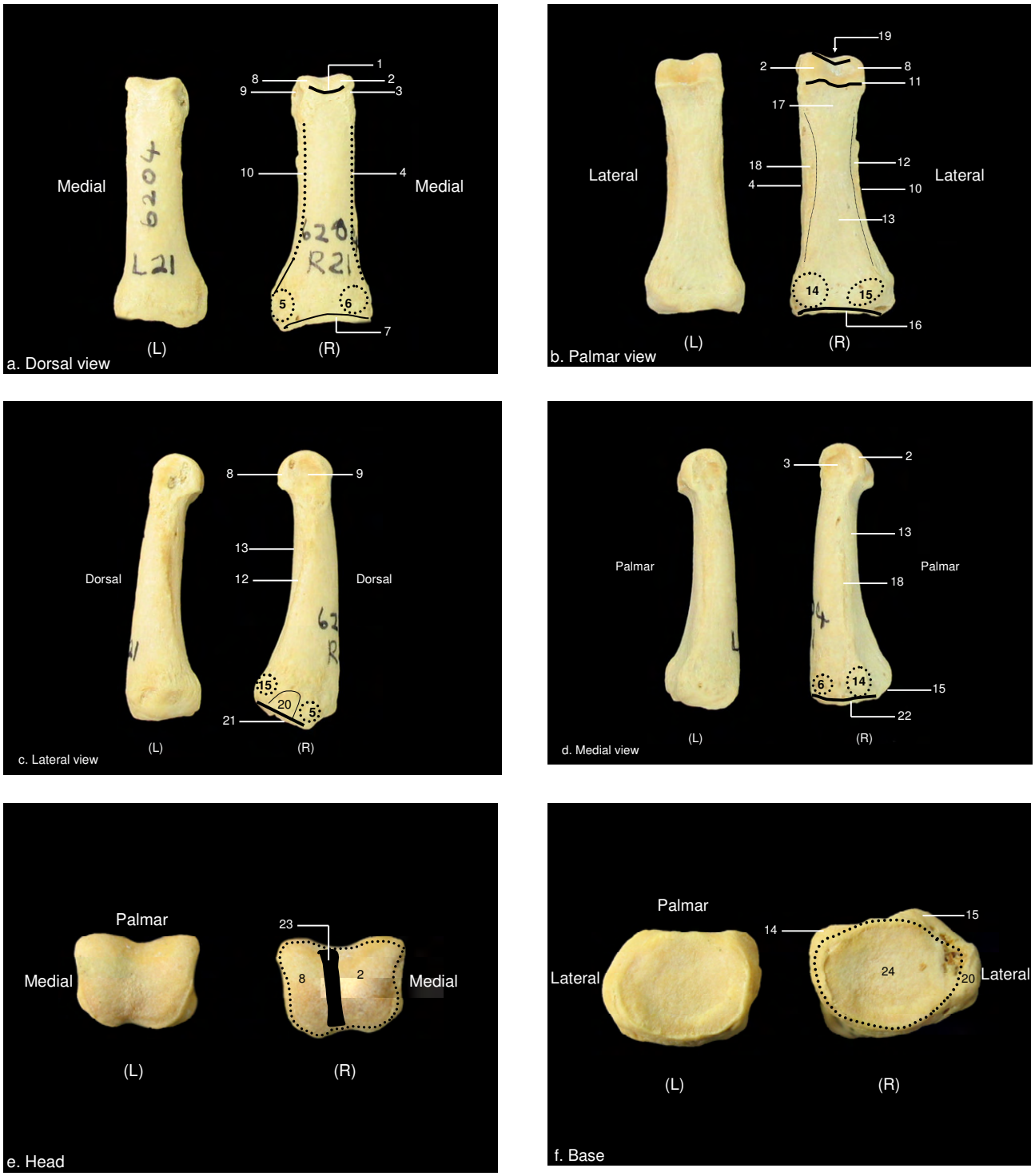

1=dorsal articular margin of head, 2=medial condyle of head, 3=medial fossa of head, 4=medial margin of shaft, 5=dorsal lateral tubercle of base, 6=dorsal medial tubercle of base, 7=dorsal articular margin of base, 8=lateral condyle of head, 9=lateral fossa of head, 10=lateral margin of shaft, 11=palmar articular margin of head, 12=palmar lateral ridge of shaft, 13=palmar surface of shaft, 14=palmar medial tubercle of base, 15=palmar lateral tubercle of base,16=palmar articular margin of base, 17=distal palmar concavity of shaft, 18=palmar medial ridge of shaft, 19=slopes of condyles, 20=lateral articular facet of base, 21=lateral articular margin of base, 22=medial articular margin of base, 23=intercondylar fossa of head, 24=articular surface of base.

6.9 Morphology of the third proximal phalanx (Figures 6.8a-f)

6.9.1 Shaft or body (Figures 6.8a-d)

The literature generally describes the dorsal surface of the shaft as convex (Scheuer & Black 2000). In the present study, the shaft is smooth when observed from a dorsal view (Figure 6.8a), and relatively longer than the proximal phalanges of adjacent fingers. The medial margin is (4) is straight except in the proximal third where it becomes convex. The lateral margin (10) is also straight except for the midshaft region where it forms a slope and at the base it is convex.

The palmar surface (13) of the shaft (Figure 6.8b) is smooth and converges in the midshaft region creating the narrowest part of the bone compared to the broader proximal and distal ends. On either side of the shaft, the bone is rough. These are called the lateral (12) and medial (18) ridges. The concavity between these ridges and the palmar surface (13) is called the lateral (12) and medial (18) grooves. Scheuer and Black (2000) also observed the concave palmar surface in the third proximal phalanx of the juvenile hand.

The lateral surface of the shaft (Figure 6.8c) is interrupted by the rough lateral ridge (12). This ridge, which runs in an oblique manner from the dorsal to the palmar surface, is not present along the entire length of the lateral surface. In the proximal third, the lateral surface is smooth with no evidence of a ridge. The concave palmar and convex dorsal surfaces can be seen from this view. Scheuer and Black (2000) recorded that the shaft had a more flattened surface when viewed from side to side.

Features observed from a lateral view are also seen from a medial view (Figure 6.8d). One observation that is slightly different on the medial side when compared to the lateral view is that the rough medial ridge (18) tends to continue towards the palmar medial tubercle (14). In other words, this ridge is seen along the entire length of the medial surface.

6.9.2 Head (Figures 6.8a-e)

Different features of the head are observed from different views. For example, in a dorsal view (Figure 6.8a) the dorsal articular margin (1) is much more prominent than that

observed for the first and second proximal phalanges. Thick ridges of bone extend from the articular margin to the sides where they surround the lateral and medial fossae respectively. Part of the lateral (8) and medial (2) condyles can be seen on the dorsal surface. The medial condyle is elevated at a slightly higher or more distal level than the lateral condyle.

In a palmar view (Figure 6.8b), the head is tilted laterally which may explain why the medial condyle is elevated at a higher level than the lateral condyle. The convex condyles are separated from each other by an intercondylar groove. A greater surface area of the head overlies the palmar than the dorsal aspect.

The head is not only tilted laterally but also forward on the shaft as seen from a lateral view (Figure 6.8c). The lateral condyle (8) forms a thin plate of bone surrounding the lateral fossa (9).

Features on the head as seen from a medial view (Figure 6.8d) is similar to that observed from a lateral view. The medial condyle (2) also forms a thin plate of bone surrounding the medial fossa (3).

When the head is viewed from the articulating end (Figure 6.8e), it is rectangular in shape. At first glance it may even give the appearance of being butterfly-shaped. The medial condyle (2) is set at a higher level than the lateral condyle (8) as seen from a dorsal and palmar view. The lateral condyle (8), however, is relatively bigger than the medial condyle (2) when viewed from the articular end. Both condyles are convex and tend to flare out to the sides, but the medial condyle does this to a greater extent than the lateral condyle. The intercondylar fossa (21) is a shallow concavity separating the two condyles. Due to the convexity of the condyles and the concavity of the intercondylar groove, the articular surface can be described as being concavo-convex.

6.9.3 Base (Figures 6.8a–d and f)

A dorsal view (Figure 6.8a) shows a broad base in comparison with the rest of the bone. The dorsal lateral (5) and dorsal medial (6) tubercles are located just above the dorsal articular margin (1). Where the base joins the proximal end of the shaft a straight margin is

formed laterally, while on the medial side it is convex or rounded in shape. The dorsal articular margin varies from a horizontal line to one that is slightly curved. The lateral end of the base is pulled in a proximal direction, together with the rest of the lateral margin of the shaft.

From a palmar view (Figure 6.8b) the palmar articular margin (16) of the base also presents as a horizontal line but it is irregular in comparison with the smooth continuous line seen from the dorsal aspect. The palmar lateral (15) and palmar medial (14) tubercles are located on either side of a triangular region at the proximal end of the shaft.

A lateral view (Figure 6.8c) of the base shows the lateral articular margin (19) sloping distally from dorsal to palmar. The dorsal lateral (5) and palmar lateral (15) tubercles can be seen from this view.

In comparison, a medial view (Figure 6.8d) shows the medial articular margin (2) sloping distally from palmar to dorsal. The dorsal medial (6) and palmar medial (14) tubercles are seen from this view.

The articular end of the base (Figure 6.8f) indicates an oval-shaped surface which is concave. The more prominent dorsal medial (6) and less prominent dorsal lateral (5) tubercles can be identified. On the palmar surface, the palmar medial (14) and palmar lateral (15) tubercles are visible.

6.9.4 Siding

In order to differentiate the right third proximal phalanx from the corresponding one on the left side, the bone is orientated with the palmar surface facing down and the dorsal surface facing up or towards one, while the head is placed at the top end and the base at the bottom end (Bass 1995, Matshes *et al.* 2000).

For the purpose of the present study, a list of bony landmarks for the shaft, head and base of the third proximal phalanx will now be provided. This is to overcome any problems that may be encountered if only a fragment of the third proximal phalanx is found amongst skeletal remains.

Shaft

1. Medial ridge (18) straight and becomes convex at the base (Figure 6.8a)
2. Lateral ridge (12) straight in the distal third and concave in the proximal third (Figure 6.8a)
3. Lateral ridge of shaft (12) does not extend to the base (Figure 6.8c)
4. Medial ridge of shaft (18) extends to the base (Figure 6.8d)

Head

1. The medial condyle extends further distally than the lateral condyle (Figures 6.8a and b)
2. Lateral condyle (8) is relatively larger than medial condyle (2) (Figure 6.8e)

Base

1. Dorsal articular margin is straight and smooth (7) (Figure 6.8a)
2. Palmar articular margin is straight and irregular (16) (Figure 6.8b)
3. The medial articular margin is slightly convexed distally (20) (Figure 6.8d)
4. The lateral articular margin is markedly convexed proximally (19) (Figure 6.8c)

Figure 6.8: Morphology of the right (R) and left (L) third proximal phalanx

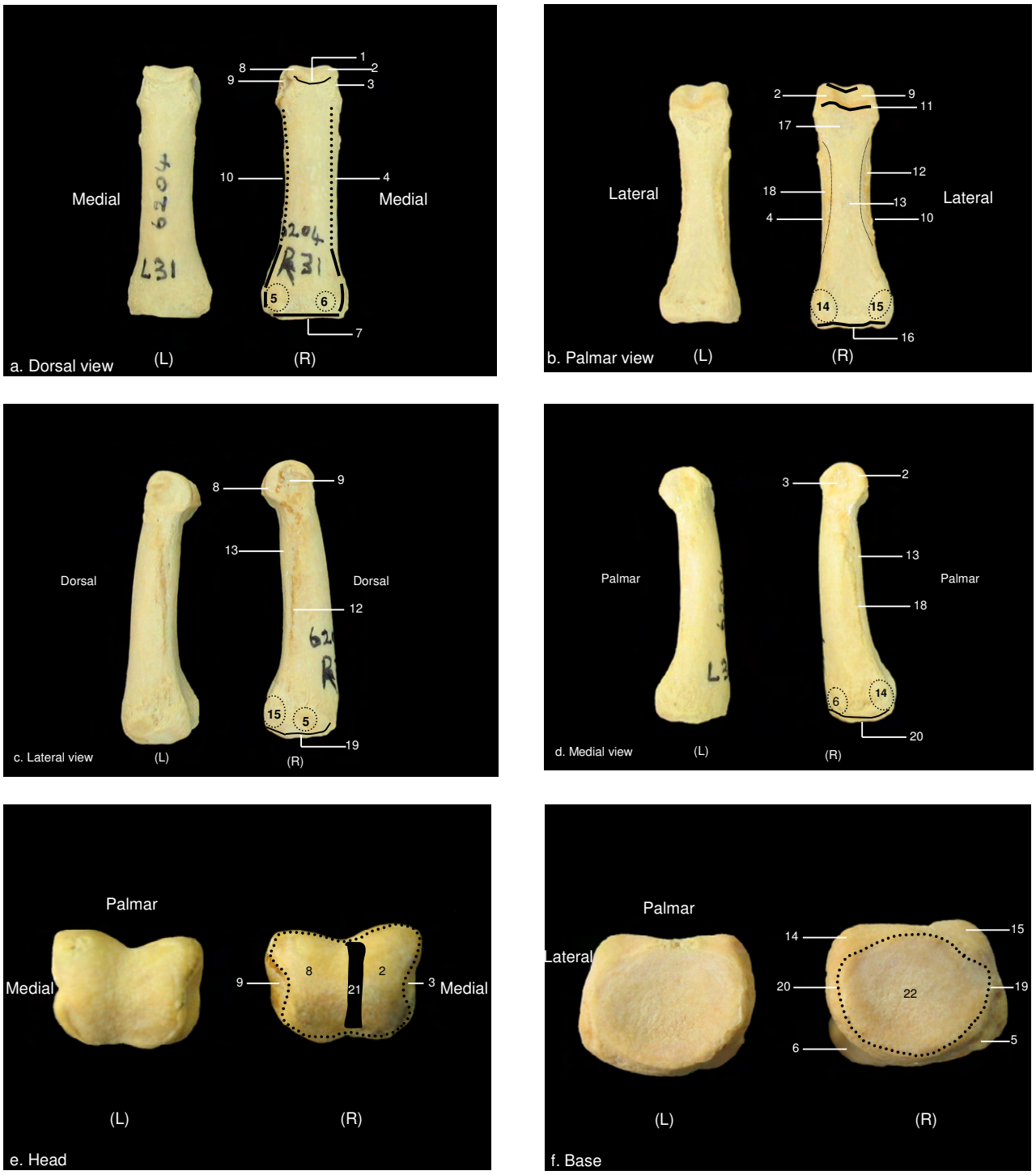

1=dorsal articular margin of head, 2=medial condyle of head, 3=medial fossa of head, 4=medial ridge of shaft, 5=dorsal lateral tubercle of base, 6=dorsal medial tubercle of base, 7=dorsal articular margin of base, 8=lateral condyle of head, 9=lateral fossa of head, 10=lateral ridge of shaft, 11=palmar articular margin of head, 12=palmar lateral ridge of shaft, 13=palmar surface of shaft, 14=palmar medial tubercle of base, 15=palmar lateral tubercle of base, 16=palmar articular margin of base, 17=distal palmar concavity of shaft, 18=palmar medial ridge of shaft, 19=lateral articular margin of base, 20=medial articular margin of base, 21=intercondylar fossa of head, 22=articular surface of base.

6.10 Morphology of the fourth proximal phalanx (Figures 6.9a-f)

6.10.1 Shaft or body (Figures 6.9a-d)

This bone is relatively shorter and more slender when compard to the proximal phalanges of the middle finger but relatively longer than the corresponding bone of the thumb, index and little finger. Observations from a dorsal view (Figure 6.9a), indicate a lateral (10) and medial (4) margins on either side of the shaft. Both margins are straight except for the proximal third where they slope to the respective sides. The slope of the lateral margins, indicated by a solid line on the diagram, is longer and more angulated than the slope of the medial ridge. The dorsal surface of the shaft is smooth along its entire length. At the distal end where the shaft joins the head, the lateral and medial margins are also sloped to the respective sides. These slopes are not as marked as the proximal end. The shaft is rotated at its proximal end to the medial rather than the lateral side. This rotation is a feature similar to that observed in the thumb, index and middle fingers.

Morphological features observed on a palmar view (Figure 6.9b), is similar to that seen in the index and middle finger. The palmar surface (14) is broader proximally than at the distal end and narrowest in the midshaft region. The lateral (10) and medial (4) margins project more forward and ending in rough edges, a feature not observed from a dorsal view. Between the palmar surface and lateral (13) and medial (18) ridges, are the lateral and medial grooves. The central region of the shaft is smooth along its entire length. At the distal end of the shaft, just below the palmar articular margin, is a shallow depression or concavity (12). Numerous foramina are located at the proximal end. The rotation of the distal half of the shaft results in the palmar lateral tubercle (16), which is relatively bigger and set at a higher level than the palmar medial tubercle (15), projecting more forward than the palmar medial tubercle.

From a lateral perspective (Figure 6.9c), the shaft displays a concave palmar and convex dorsal surface. The convexity of the dorsal surface is more marked in the distal than in the proximal region mainly due to the forward tilt of the head on the shaft. In fact, the convexity

at the proximal end becomes a straight line. The lateral ridge (13) is more prominent in the midshaft than at the proximal and distal ends.

Features observed from a lateral view are also seen from a medial view (Figure 6.9d). In other words, the medial ridge (18) separating the dorsal and palmar surfaces from each other can be clearly identified. This ridge is more marked in the midshaft region than at the proximal and distal ends, similar to that observed from a lateral view. The rotation of the proximal end of the shaft medially, exposes more of the palmar surface from a medial view. In other words, the lateral margin is also visible from this view. The palmar surface is concave and the dorsal surface is convex.

6.10.2 Head (Figures 6.9a-e)

In a dorsal view (Figure 6.9a) the head is located at the distal end of the shaft. A well-defined dorsal articular margin (1) separates the distal end of the shaft from the condyles. This articular margin is convexed proximally. The lateral (8) and medial (2) condyles are separated by a shallow intercondylar fossa. The lateral condyle is set at a higher or more distal level than the medial condyle. A lateral (9) and medial (3) fossa can be seen on the lateral and medial sides respectively.

A palmar view of the head (Figure 6.9b) indicates a straight palmar articular margin (11). No sloping of this margin occurs as is the case with the middle finger.The lateral condyle (8) is raised more distally compared to the medial condyle (2). When compared to the dorsal view, a greater surface area of the head can be seen from a palmar view. This is due to the head projecting forward on the shaft. The width of the head from this perspective is relatively greater than the height.

The tilting of the head towards the palmar aspect is much more evident from a lateral view (Figure 6.9c) than from a medial view. The lateral fossa (9) is seen as a shallow depression surrounded by a thin plate of bone, the lateral condyle (8).

A medial view (Figure 6.9d) of the head also shows a shallow medial fossa (3) surrounded by the medial condyle (2).

When viewed from the articular end (Figure 6.9e), the head is butterfly-shaped with the dorsal margin narrow and palmar margin broad. The shape may also be defined as rectangular. Both condyles project outwards to the lateral and medial sides respectively. The lateral condyle (8) has a relatively larger surface area than the medial condyle (2). The intercondylar fossa (21) can be identified between the two condyles.The lateral (9) and medial (3) fossae are visible on the sides.

6.10.3 Base (Figures 6.9a-d and f)

The base from a dorsal view (Figure 6.9a) is broad with convex lateral and medial margins. The dorsal lateral (5) and dorsal medial (6) tubercles are clearly seen. The dorsal articular margin (7) is straight.

Two tubercles can be identified on the palmar surface of the base (Figure 6.9b). These are the palmar lateral (16) and palmar medial (15) tubercles. The palmar lateral tubercle is relatively larger and projects more anteriorly than the palmar medial tubercle. The palmar articulating margin (17) slopes in a proximal direction from the medial to the lateral surface. Nutrient foramina can be seen between the two palmar tubercles.

The lateral surface of the base (Figure 6.9c) shows a relatively smaller dorsal lateral (5) and a relatively larger palmar lateral (16) tubercle. The lateral articular margin (19) tends to slope proximally from the dorsal to the palmar surface.

Two tubercles can also be identified on the medial surface (Figure 6.9d). These are the relatively smaller dorsal medial (6) and relatively larger palmar medial (15) tubercles. The medial articular margin (20) has a slight convexity in a proximal direction.

The articular surface (22) of the base (Figure 6.9f), displays an oval shape. The dorsal margin is convex compared to the bi-convex palmar margin. This bi-convexity is due to the prominence of the palmar lateral (16) and palmar medial (15) tubercles. From this view, the palmar lateral tubercle is seen to be relatively larger than the palmar medial tubercle.

6.10.4 Siding

In order to differentiate the right fourth proximal phalanx from the corresponding one on the left side, the bone is orientated with the palmar surface facing down and the dorsal surface facing up or towards one, while the head is placed at the top end and the base at the bottom end (Bass 1995, Matshes *et al.* 2000).

For the purpose of the present study, a list of bony landmarks on the shaft, head and base of the fourth proximal phalanx will now be provided. This is to overcome any problems that may be encountered if only a fragment of the fourth proximal phalanx is found amongst skeletal remains.

Shaft

1. Medial margin (4) extends further proximally than the lateral margin (Figure 6.9a)
2. Lateral margin (10) more prominent and sharp in the midshaft region when compared to the medial margin (Figure 6.9c)

Head

1. Lateral condyle (8) relatively larger than the medial condyle (2) (Figure 6.9e)
2. Medial border relatively longer than lateral border (Figure 6.9e)
3. Lateral condyle (2) raised at a higher level than the medial condyle (Figures 6.9a and b)

Base

1. Palmar articular margin (17) slopes in a proximal direction from the medial to the lateral surface (Figure 6.9b)
2. Palmar lateral tubercle (16) projects more anteriorly and is relatively larger than the palmar medial tubercle (15) (Figures 6.9b and f)

Figure 6.9: Morphology of the right (R) and left (L) fourth proximal phalanx

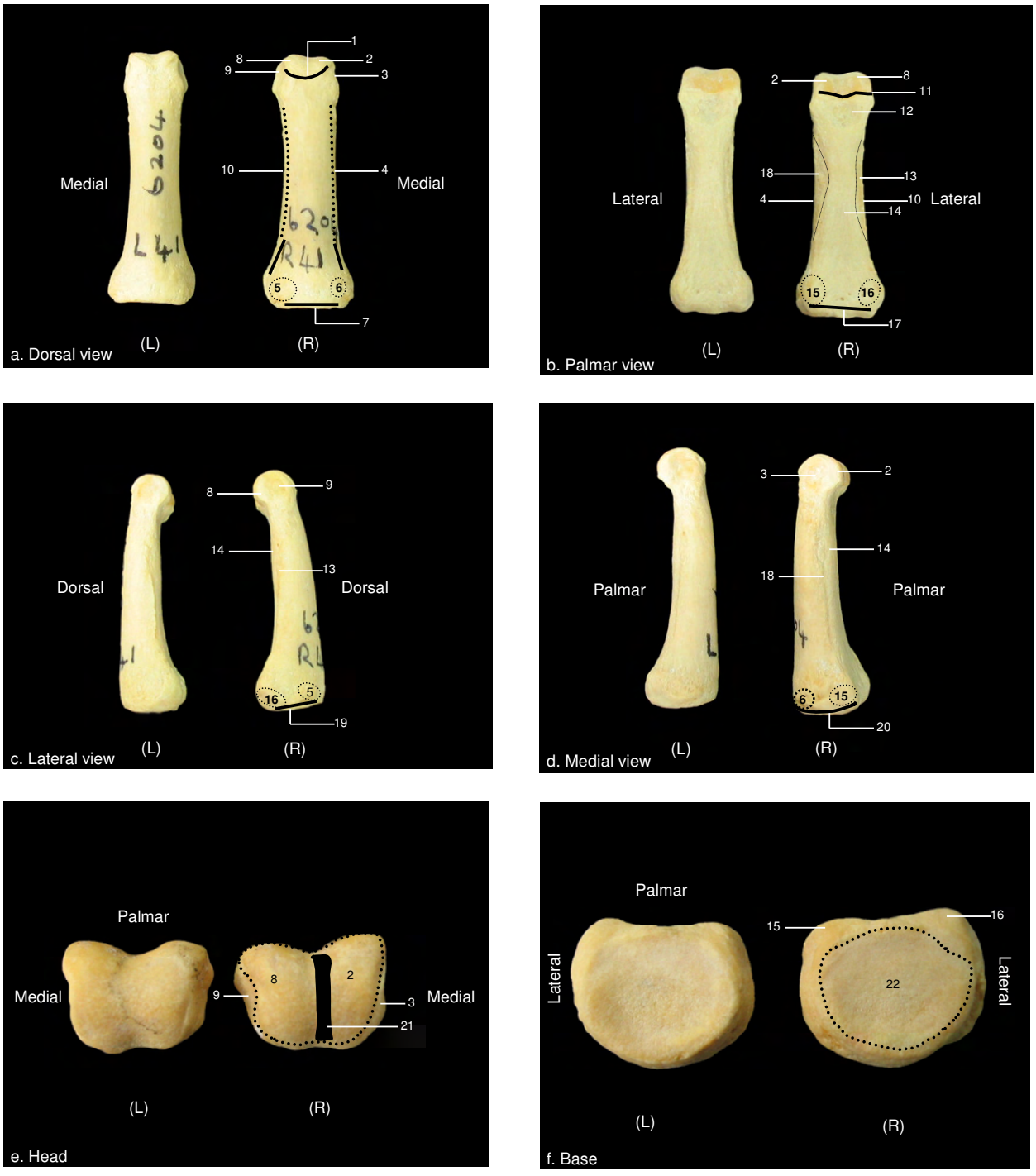

1=dorsal articular margin of head, 2=medial condyle of head, 3=medial fossa of head, 4=medial ridge of shaft, 5=dorsal lateral tubercle of base, 6=dorsal medial tubercle of base, 7=dorsal articular margin of base, 8=lateral condyle of head, 9=lateral fossa of head, 10=lateral ridge of shaft, 11=palmar articular margin of head, 12=distal palmar concavity of shaft, 13=palmar lateral ridge of shaft, 14=palmar surface of shaft, 15=palmar medial tubercle of base, 16=palmar lateral tubercle of base, 17=palmar articular margin of base, 18=palmar medial ridge of shaft, 19=lateral articular margin of base, 20=medial articular margin of base, 21=intercondylar fossa of head, 22= articular surface of base.

6.11 Morphology of the fifth proximal phalanx (Figures 6.10a-f)

6.11.1 Shaft or body (Figures 6.10a-d)

The shaft is described in the literature as being convex on its dorsal aspect and concave along its longitudinal axis on the palmar surface. When viewed from side to side, the shaft is flattened (Scheuer & Black 2000). In the present study, the proximal phalanx of the fifth digit was seen to be shorter and more robust in comparison to the proximal phalanges of the other digits.

From a dorsal view (Figure 6.10a) the lateral margin (8) is straight for most of its course except at the proximal end where it is sloped as it approaches the base. The concave medial margin (4), projects more medially at the proximal end causing the shaft to be tilted slightly medially. The width of the shaft proximally is thus greater than at the distal end. The width at the mishaft and distal regions is approximately the same unlike that observed in the proximal phalanges of adjacent digits, where the midshaft was the narrowest region.

Observations of the palmar surface (Figure 6.10b) confirm the relatively longer straight lateral ridge (8) compared to the relatively shorter concaved medial ridge (4). The distal palmar concavity (15) is a shallow depression proximal to the head. While this concavity was observed in adjacent proximal phalanges, its size in the fifth proximal phalanx is relatively larger. The lateral (10) and medial (16) ridges are rough on the palmar surface when compared to the smooth appearance on the dorsal surface. The grooves located between these ridges and the palmar surface (11), are referred to as the lateral and medial grooves of the shaft. Nutrient foramina can be identified in the proximal third of the shaft.

The lateral surface (Figure 6.10c) of the shaft shows the rough lateral ridge (10) prominent in the midshaft region. The proximal third of this surface is rough compared to the smooth distal two thirds. The dorsal surface is straight while the palmar surface is concave. The broadest part of the shaft is at the proximal end after which the shaft narrows.

Observations of the medial surface (Figure 6.10d) are exactly the same as that identified on the lateral surface, except that the terminologies are different.

6.11.2 Head (Figures 6.10a-e)

The presence of the lateral (6) and medial (2) condyle in this bone is a feature which is also observed on adjacent proximal phalanges. Closer observation of the lateral condyle from a dorsal aspect (Figure 6.10a), indicates that it is set at a higher or more distal level than the medial condyle. The dorsal articular margin (1) converges to the center and has a convex shape in a proximal direction. The lateral and medial condyles form thick ridges on each side of the articular margin, and then continue onto the palmar aspect. Thus, when the head is observed from the lateral or medial side, the condyles appear as complete circles surrounding the lateral and medial fossae.

In a palmar view (Figure 6.10b) the tilting of the head is much more prominent revealing the greater height of the lateral condyle (6) in comparison to the medial condyle (2). The slope formed on the uppermost or distal part of the head is indicated by a solid line in this figure. The palmar articular margin, indicated by the more proximal solid line, has a scalloped edge which slopes in the same direction as the head, namely, medially.

Turning the bone laterally (Figure 6.10c), the lateral condyle (6) can be seen as a complete circle encasing the lateral fossa (7). The head is also tilted forward.

A medial view (Figure 6.10d) the head is similar in comparison to the lateral view. The medial condyle (2) is also a complete circle surrounding the medial fossa (3).

When the head is observed from its articular end (Figure 6.10e), the shape of the articular surface is almost triangular. The lateral and medial articular margins converge but it leaves a relatively short margin on the dorsal surface.The palmar margin is relatively longer than the dorsal margin. The lateral condyle (6) occupies a slightly greater surface area than the medial condyle (2). The amount of flaring of the condyles is slight and not as marked as observed in adjacent proximal phalanges.

6.11.3 Base (Figures 6.10a-d and f)

The dorsal surface of the base (Figure 6.10a) is rough with numerous nutrient foramina. The articular margin (5) is slightly concave in a proximal direction. The medial margin of the base has a greater curvature or convexity than the lateral margin as indicated by the curved solid line on the figure. The palmar articular margin (14) can be seen from a dorsal view because it extends more proximally than the dorsal articular margin (5). The base is greater in width than the rest of the bone.

When viewed from a palmar perspective (Figure 6.10b), two tubercles are visible, namely, a relatively larger palmar lateral (13) and a relatively smaller palmar medial (12) tubercle. The palmar articular margin (14) has a scalloped appearance and the center of this margin extends further proximally making it visible from a dorsal perspective. The base is also much broader than the rest of the bone.

The lateral surface of the base (Figure 6.10c) is also rough with numerous tiny foramina. The palmar lateral (13) tubercle is located anteriorly. The articular margin (17) is relatively straight and forms a slope dorsally. The base is much broader than the rest of the bone. No articular facet is present on the lateral aspect of the base.

The medial surface of the base (Figure 6.10d) is also much broader than the rest of the shaft. The medial articular margin (18) is slightly convex and continues to the dorsal surface. A palmar tubercle (12) can be identified at the anterior end of the base.

When viewed from the articular end (Figure 6.10f), the base is oval in shape with a smooth articular surface (20). The palmar medial tubercle (12) is relatively bigger than the palmar lateral tubercle (13).

6.11.4 Siding

In order to differentiate the right fifth proximal phalanx from the corresponding one on the left side, the bone is orientated with the palmar surface facing down and the dorsal surface

facing up or towards one, while the head is placed at the top end and the base at the bottom end (Bass 1995, Matshes *et al*. 2000).

For the purpose of the present study, a list of bony landmarks on the shaft, head and base of the fifth proximal phalanx will now be provided. This is to overcome any problems that may be encountered if only a fragment of the fifth proximal phalanx is found amongst skeletal remains.

Shaft

1. Lateral margin (8) relatively longer than the medial margin (Figures 6.10a and b)
2. Medial margin (4) relatively short and concave (Figures 6.10a and b)

Head

1. Lateral condyle (6) raised at a higher level than the medial condyle (Figures 6.10a and b)
2. Medial condyle (2) flares out more to the side than the lateral condyle (Figure 6.10b)

Base

1. Medial margin of base has greater height than the lateral margin (Figure 6.10a)
2. Medial margin of base has greater height than the lateral margin (Figures 6.10c and d)
3. Palmar medial tubercle relatively greater in size than the palmar lateral tubercle (Figure 6.10f)

Figure 6.10: Morphology of the right (R) and left (L) fifth proximal phalanx

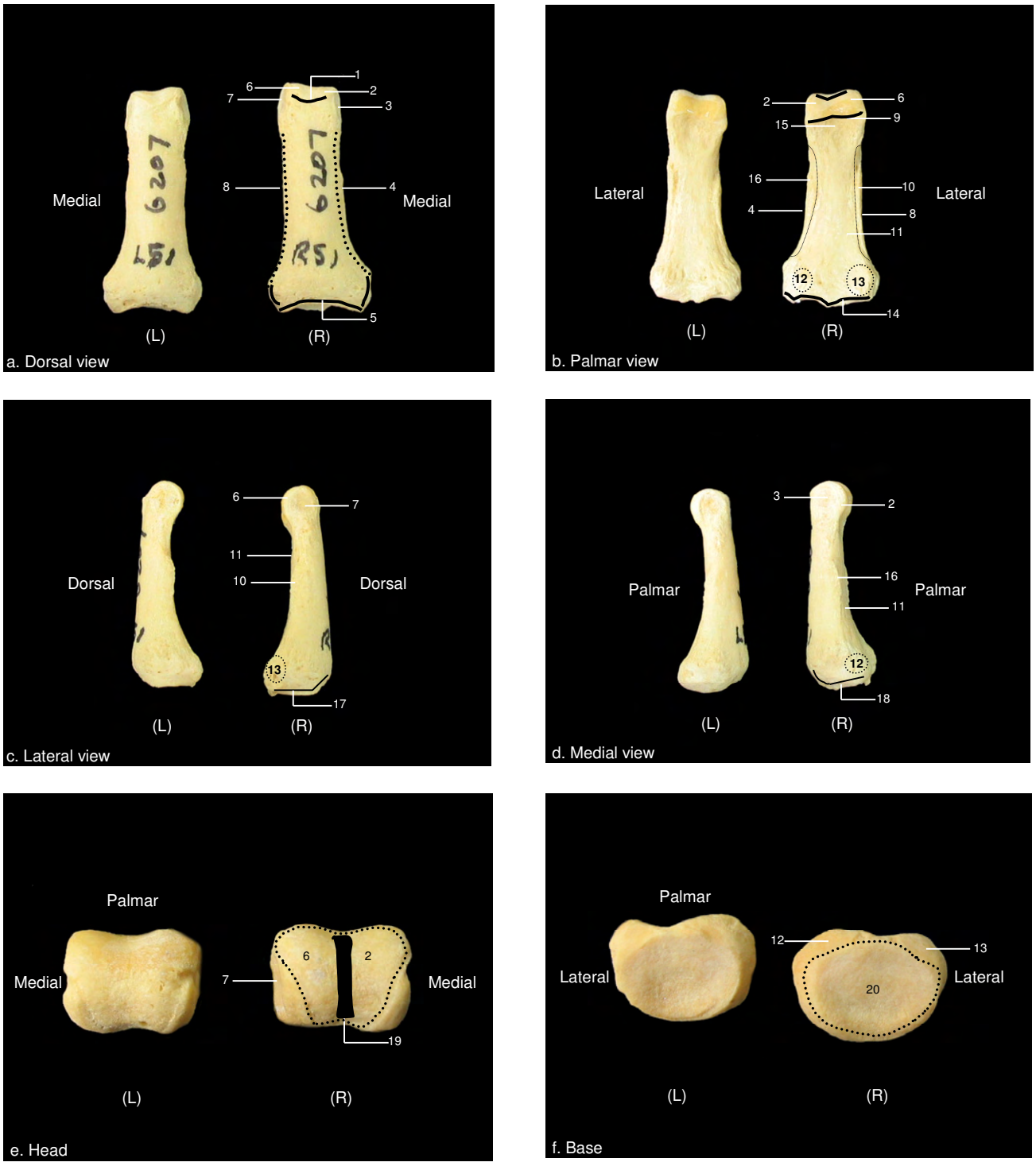

1=dorsal articular margin of head, 2=medial condyle of head, 3=medial fossa of head, 4=medial ridge of shaft, 5=dorsal articular margin of base, 6=lateral condyle of head, 7=lateral fossa of head, 8=lateral ridge of shaft, 9=palmar articular margin of head, 10=palmar lateral groove of shaft, 11=palmar surface of shaft, 12=palmar medial tubercle of base, 13=palmar lateral tubercle of base, 14=palmar articular margin of base, 15=distal palmar concavity of shaft, 16=palmar medial groove of shaft, 17=lateral articular margin of base 18=medial articular margin of base, 19=intercondylar groove of head, 20=articular facet of base.

6.12 Morphology of the second middle phalanx (Figures 6.11a-f)

6.12.1 Shaft or body (Figures 6.11a-d)

A dorsal view (Figure 6.11a) depicts a short and more robust shaft in comparison to the middle phalanges of the adjacent digits. The shaft shows greater width proximally than distally. The lateral and medial margins are concave with the curvature on the lateral aspect being slightly greater than on the medial side. The lateral margin is also relatively longer than the medial margin. The bending of this bone seen in the midshaft region causes the proximal half of the lateral margin not only to extend more laterally but also to tilt in a palmar direction. The shaft is smooth along its entire length. A few randomly located foramina may be seen at the distal end of the shaft.

From a palmar aspect (Figure 6.11b) the middle phalanx of the second digit is seen to be the shortest and most robust, when compared to the middle phalanges of digits three to five. Unlike the entire smooth dorsal surface, the palmar surface has a central area that is smooth (14). On either side of this central area, the lateral (15) and medial (17) palmar ridges located at the midshaft level can be identified. These ridges are distinct from the smooth central area as they appear rough. Few small foramina may be seen scattered randomly at the proximal and distal ends. The proximal half of the shaft is rotated.

The buckling or anterior tilting of the midshaft is more obvious from a lateral view (Figure 6.11c) than from the dorsal and palmar aspects. The dorsal surface is convex and the palmar surface is concave.

Not only is the buckling or anterior tilting of the midshaft clearly seen from a medial view (Figure 6.11d), but medial rotation of the shaft along its longitudinal axis, is more prominent at this angle than from a lateral view.

6.12.2 Head (Figures 6.11a-e)

In this example of the head, the articular surface of the right (R) middle phalanx is worn down compared to the corresponding bone on the left (L) side. Nonetheless, two condyles can

be seen from a dorsal view (Figure 6.11a). These are the lateral (8) and medial (1) condyles, very similar to that identified on the head of the proximal phalanges except that in this instance, they are relatively smaller. The head projects mainly forward, resulting in only a relatively small area being visible on the dorsal aspect. Scheuer and Black (2000) referred to these condyles as the lateral and medial elevations. The dorsal articular margin (3) can be identified as a horizontal line between the two condyles.

A greater surface area of the head can be seen from a palmar view (Figure 6.11b). The palmar articular margin (13) is visible between the two condyles.

When viewed from the lateral side (Figure 6.11c), the lateral condyle (8) forms a complete circle which surrounds the lateral fossa (9). The head is rotated laterally with a slight forward projection. There is great variation in the size and shape of this condyle, not only in different individuals but also between hands of the same individual.

When the bone is turned in such a way that the medial surface (Figure 6.11d) can be seen, the rotation of the head and distal end of the shaft in a lateral direction is more marked than that observed from the lateral view. The medial condyle (1) surrounding the medial fossa (2) can be easily identified. The thick rim of bone identified on the lateral and medial aspects may occur as a result of bone remodeling in these regions.

A superior view (Figure 6.11e) shows a great deal of variability in the shape of the head, not only in different individuals but also in middle phalanges of the right and left hand of the same individual. The shape may vary from rectangular to square. The width on the palmar surface is greater than on the dorsal aspect. Scheuer and Black (2000) refer to the head as the distal metaphyseal surface that is convex from dorsal to ventral. In the present study, this convex surface had a shallow concavity separating the two condyles. Scheuer and Black (2000) go on to describe the slope on the dorsal aspect as being steeper than on the ventral surface. This was not observed on the middle phalanx of the index finger. A feature observed on the articular surface of the head and indicated by a circle (Figure 6.11e), represents a shallow fossa which may be due to erosion or arthritic changes at this end of the bone. In this example, the eroded region was identified on the medial side of both the right and left bones.

6.12.3 Base (Figures 6.11a-d and f)

The articular margin of the base, when observed from a dorsal view (Figure 6.11a), slopes in a proximal direction. These are called the lateral (12) and medial (6) slopes respectively. Where these slopes meet, it is referred to as the apex (7). Scheuer and Black (2003) referred to this central point as a tubercle for attachment of the extensor digitorum muscle. Distal to these slopes at the margins are the lateral (11) and medial (5) tubercles. A striking difference with the articular margin (16) on the palmar surface of the base (Figure 6.11b), is that it is curved rather than sloped.

The shape of the articular margin on the lateral surface (Figure 6.11c) may vary from being straight to concave. If this articular margin is followed through to the dorsal surface, it projects down or proximally together with the apex (7). The oval-shaped lateral tubercle (11) can be located distal to this articular margin.

Similar to a lateral view of the base, the medial view (Figure 6.11d) also shows the medial articular margin (19) as a straight line. It is only at its dorsal end where it runs obliquely in a proximal direction for a short while where it also contributes to the formation of the dorsal apex of the base. The oval-shaped and relatively large medial tubercle (5) extends from dorsal to palmar ends across the medial margin.

The articular surface of the base (Figure 6.11f), takes on an oval shape. The palmar, lateral and medial articular margins tend to be straight. The dorsal articular margin, on the other hand, is convex and longer than the palmar articular margin. The rotation of the base medially is clearly seen from this view. Two shallow depressions can be identified, namely, the relatively smaller lateral (22) and relatively larger medial (21) articular facets, separated by a broad interarticular ridge (23) that is convex.

6.12.4 Siding

In order to differentiate the right second middle phalanx from the corresponding one on the left side, the bone is orientated with the palmar surface facing down and the dorsal surface

facing up or towards one, while the head is placed at the top end and the base at the bottom end (Bass 1995, Matshes *et al*. 2000).

For the purpose of the present study, a list of bony landmarks on the shaft, head and base of the second middle phalanx will now be provided. This is to overcome any problems that may be encountered if only a fragment of the second middle phalanx is found amongst skeletal remains.

Shaft

1. Lateral margin (10) projects more in a palmar direction than the medial margin (4) (Figures 6.11a and b)

Head

1. Head rotated laterally (Figures 6.11a and c)

Base

1. Apex on dorsal surface (7) directed laterally (Figure 6.11a)
2. Dorsal lateral articular slope (12) shorter than dorsal medial articular slope (6) (Figure 6.11a)

Figure 6.11: Morphology of the right (R) and left (L) second middle phalanx

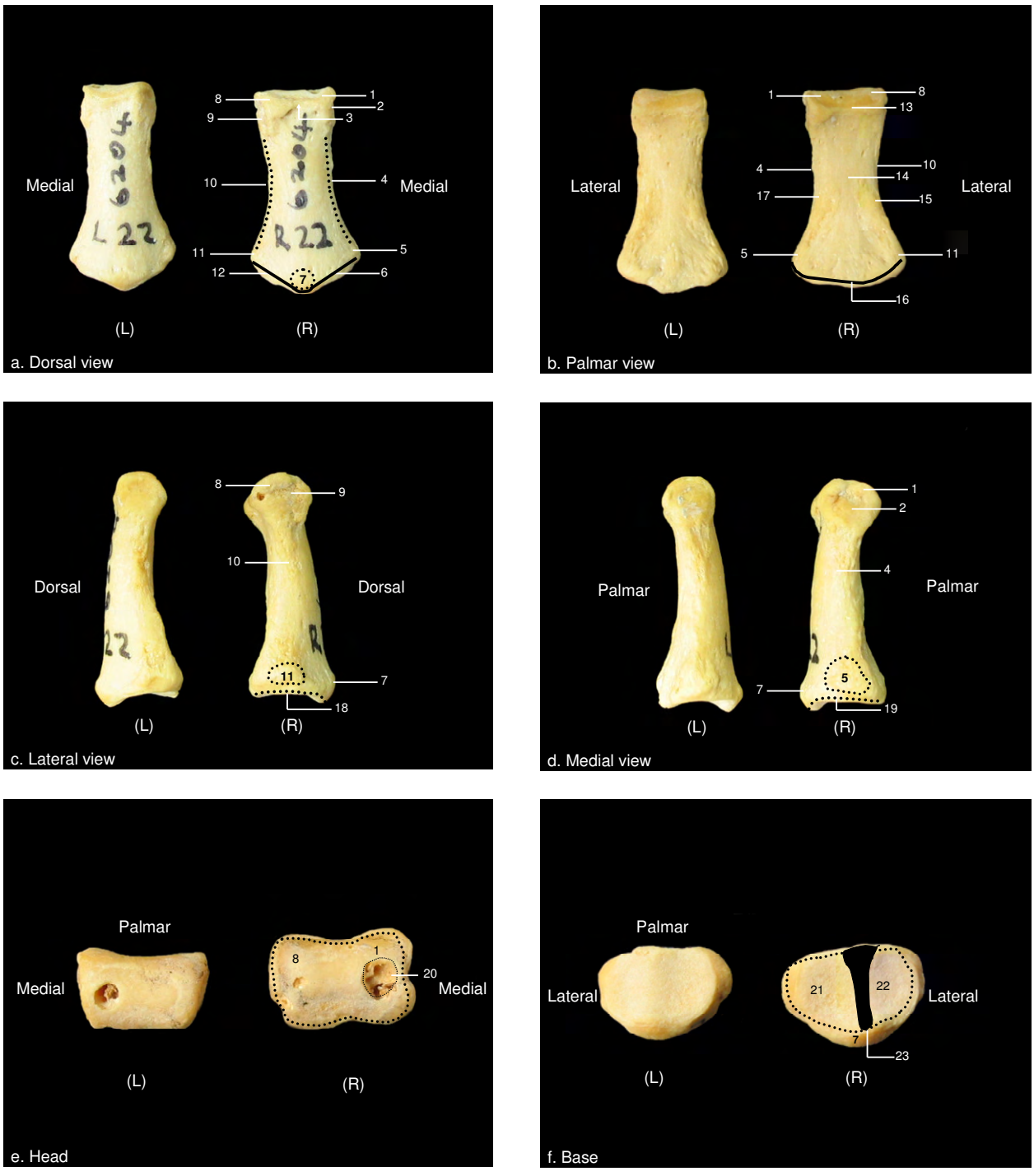

1=medial condyle of head, 2=medial fossa of head, 3=medial articular margin of head, 4=medial margin of shaft, 5=medial tubercle of base, 6=dorsal medial slope of base, 7=dorsal apex of base, 8=lateral condyle of head, 9=lateral fossa of head, 10=lateral margin of shaft, 11=lateral tubercle of base, 12=dorsal lateral slope of base, 13=palmar articular margin of head, 14=palmar surface of shaft, 15=palmar lateral ridge of shaft, 16=palmar articular margin of base, 17=palmar medial ridge of shaft, 18=lateral articular margin of base, 19=medial articular margin of base, 20=artifact on head, 21=medial articular facet of base, 22=lateral articular facet of base, 23=interarticular ridge of base.

6.13 Morphology of the third middle phalanx (Figures 6.12a-f)

6.13.1 Shaft or body (Figures 6.12a-d)

The shaft of this bone is relatively longer and wider than that of the index finger when viewed from the dorsal aspect (Figure 6.12a). The lateral margin (10) is concave whereas the medial margin (4) is straight. The difference in shape of these margins causes the shaft to be tilted in a slightly lateral direction. The surface is relatively smooth with sparsely scattered foramina at the proximal and distal ends.

The bending or anterior tilting in the midshaft region from a palmar aspect (Figure 6.12b), where the lateral margin forms an angle, is more prominent when compared to that observed in the index finger. The lateral palmar ridge (15) is also more prominent and elongated when compared to the less prominent and shorter medial palmar ridge (17). A few sparsely scattered foramina may be seen at the proximal and distal ends of the shaft.

Turning the bone so that the lateral surface is conspicuous (Figure 6.12c), displays a convex dorsal and concave palmar surface. A thin line demarcating the lateral margin (10) can be identified at the midshaft. The rest of the proximal half is taken up by the lateral ridge (15) which is seen as a forward projection of part of the bone. At the distal end of the shaft just below the head, the bone appears rough. The shaft is broader proximally than distally.

A view of the same bone from a medial direction (Figure 6.12d), indicates that the medial margin (4) is rough in the distal third where it is visible. While the medial ridge (17) also projects forward, it is not as prominent as the one observed from the lateral surface. The rest of this surface is similar to the lateral surface.

6.13.2 Head (Figures 6.12a-e)

The lateral (8) and medial (2) condyles appear as thick bony ridges on the dorsal surface of the head (Figure 6.12a). The dorsal articular margin (1) is convexed in a proximal direction. The width of the head is narrower than on the palmar surface making it easy to identify the lateral (9) and medial (3) fossae.

These condyles become more prominent on the palmar surface (Figure 6.12b). The articular margin (13) on this surface of the bone is concave in a proximal direction. Numerous foramina can be located just proximal to this margin. At first glance, the articular surface appears smooth.

From a lateral view, rotation of the distal end of the shaft laterally, causes both condyles to be visible (Figure 6.12c). While only the medial condyle (2) can be identified, both the lateral condyle (8) and the lateral fossa (9) which it encircles can be seen from this view.

A medial view (Figure 6.12d) only reveals the medial condyle (2) which forms a complete circle around the medial fossa (3).

The head is rectangular-shaped as observed from a superior view (Figure 6.12e). The palmar and dorsal margins are relatively greater in length than the lateral and medial margins which are relatively shorter in length. The articular surface is smooth.

6.13.3 Base (Figures 6.12a-f)

A dorsal view of the base (Figure 6.12a) has two slopes similar to that observed in the middle phalanx of the index finger. The point where the short lateral and long medial slopes join is called the apex (7). Distal to each slope, the lateral (11) and medial (5) tubercles are located.

Features on the palmar surface (Figure 6.12b) include an articular margin (16) that slopes in a proximal direction from the lateral to the medial surface. Distal to this articular margin, the base is rough and presents with fine ridges running parallel to each other.

The articular margin (18) on the lateral surface (Figure 6.12c) is sloped in a proximal direction from the palmar to the dorsal surface. An oval-shaped lateral tubercle (11) can be seen proximal to this articular margin.

In contrast, the medial (19) articular margin (Figure 6.12d) runs a straight course from the palmar to the dorsal surface. An oval-shaped medial tubercle (5) is associated with this margin.

The articular surface of the base is oval in shape (Figure 6.12f), with the medial articular facet (22) being relatively larger than the lateral articular facet (20). These facets are separated from each other by an interarticular ridge (21). The medial tubercle (5) is much more prominent than the lateral tubercle (11).

6.13.4 Siding

In order to differentiate the right third middle phalanx from the corresponding one on the left side, the bone is orientated with the palmar surface facing down and the dorsal surface facing up or towards one, while the head is placed at the top end and the base at the bottom end (Bass 1995, Matshes *et al*. 2000).

For the purpose of the present study, a list of bony landmarks on the shaft, head and base of the third middle phalanx will now be provided. This is to overcome any problems that may be encountered if only a fragment of the third middle phalanx is found amongst skeletal remains.

Shaft

1. Lateral margin is angulated (10) (Figures 6.12a and b)
2. Medial margin is concave and straight (4) (Figures 6.12a and b)
3. Shaft tilted laterally (Figures 6.12a and b)
4. Lateral palmar ridge more prominent and elongated (15) (Figure 6.12b)
5. Medial palmar ridge less prominent and short (17) (Figure 6.12b)

Head

1. Head rotated laterally (Figures 6.12a and c)
2. Lateral and medial margins of head slopes medially (Figure 6.12e)

Base

1. Prominent medial tubercle (5) from articular surface (Figure 6.12f)
2. Less prominent lateral tubercle (11) (Figure 6.12f)

Figure 6.12: Morphology of the right (R) and left (L) third middle phalanx

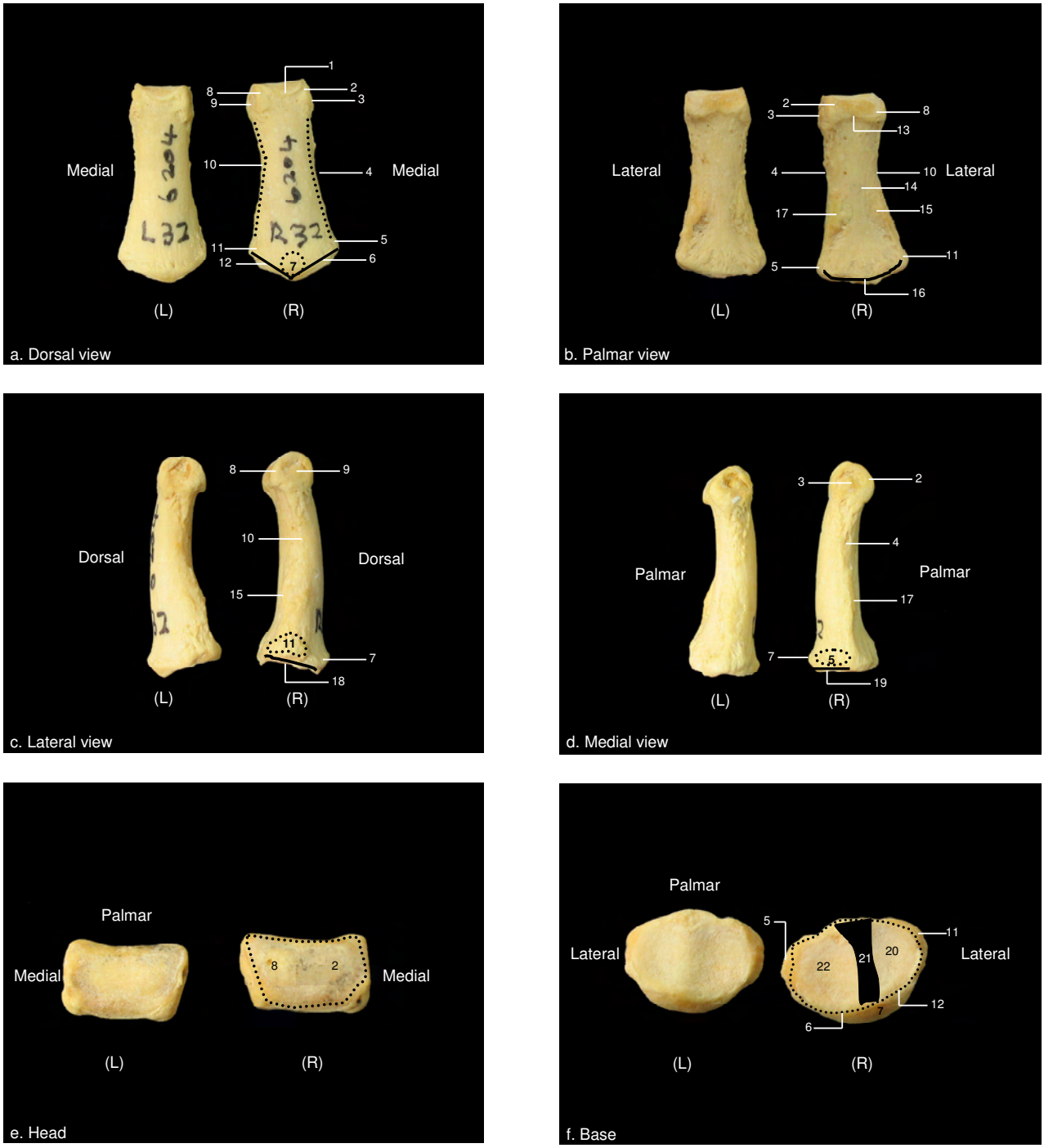

1=dorsal articular margin of head, 2=medial condyle of head, 3=medial fossa of head, 4=medial margin of shaft, 5=medial tubercle of base, 6=dorsal medial slope of base, 7=dorsal apex of base, 8=lateral condyle of head, 9=lateral fossa of head, 10=lateral margin of shaft, 11=lateral tubercle of base, 12=dorsal lateral slope of base, 13=palmar articular margin of head, 14=palmar surface of shaft, 15=palmar lateral ridge of shaft, 16=palmar articular margin of base, 17=palmar medial ridge of shaft, 18=lateral articular margin of base, 19=medial articular margin of base, 20=lateral articular facet of base, 21=interarticular ridge of base, 22=medial articular facet of base.

6.14 Morphology of the fourth middle phalanx (Figures 6.13a-f)

6.14.1 Shaft or body (Figures 6.13a-d)

A dorsal view of this bone (Figure 6.13a), shows angulation of the lateral margin in the midshaft area (Figure 6.13a). A feature similar to that observed in the index and middle fingers but not as marked. It is this angulation that gives the lateral margin (10) a slight concavity. On closer observation, this angulation is actually a slope that is formed by the proximal two-thirds, after which it forms a straight line at the distal third. The concavity of the medial margin (4) is less and in some cases this margin is straight. The broadest part of this bone is the proximal half. The midshaft and distal ends are relatively similar in diameter. The shaft is smooth along its entire length with sparsely scattered foramina at the proximal and distal ends. The distal end of the shaft tends to rotate in a lateral direction.

The palmar view (Figure 6.13b) is very similar to the dorsal view. Some of the differences include the lateral (15) and medial (17) ridges which occur on either side of the smooth palmar surface (14). Nutrient foramina are more prevalent in the distal third.

A lateral view (Figure 6.13c) shows a convex dorsal and a concave palmar surface. Due to the angulation of the shaft, the dorsal surface is tilted slightly forward at its distal end while proximally the shaft is straight. The rough lateral ridge (15) stands out as a sharp bony projection in the proximal half. The width of the shaft is greater at the proximal than at the distal end.

The medial surface (Figure 6.13d) is similar to the lateral surface. In other words, the distal end of the shaft is angulated forward while the proximal end is straight. The rough medial ridge (17) appears as a sharp bony projection in the proximal half of the shaft.

6.14.2 Head (Figures 6.13a-e)

The surface area of the head, when viewed dorsally (Figure 6.13a), is relatively small. The difference in height of the lateral (8) and medial (2) condyles is responsible for the slope seen at the articular end. In other words, the medial condyle extends more distally than the

lateral condyle. The opposite was true for the middle finger. The dorsal articular margin (1), which is convexed proximally, is clearly demarcated from the lateral (8) and medial (2) condyles, which continue onto the lateral and medial surfaces.

A greater surface area of the head can be seen from a palmar aspect (Figure 6.13b). The straight articular margin (13) is relatively longer than the corresponding one on the dorsal surface. The condyles are convexed distally with a shallow depression separating them.

Due to the distal end of the shaft rotating more laterally than the rest of the bone, both the lateral and medial aspects of the head can be seen from a lateral view (Figure 6.13c). The head extends forward on the shaft. The lateral condyle (8) can be identified as a circular rim of bone surrounding the lateral fossa (9).

Due to the distal half of the shaft rotating more laterally than medially, only the medial (2) and not the lateral (8) condyle can be identified (Figure 6.13d). From this view, the head extends forward on the shaft and the medial condyle (2) is seen as a circular rim of bone surrounding the medial fossa (3).

The head is rectangular in shape as seen from the articular end (Figure 6.13e) with the dorsal and palmar margins being relatively longer than the shorter medial and lateral margins. The lateral margin runs obliquely from the dorsal to the palmar aspect, while the medial margin tends to be straight. Similar to the index and middle fingers, the lateral condyle in the ring finger forms a sharp edge and projects more laterally on the palmar surface when compared to the more rounded medial condyle.

6.14.3 Base (Figures 6.13a-d and f)

From a dorsal view (Figure 6.13a) the base presents with two slopes of almost equal length, namely, a lateral (12) and medial (6) slope similar to that seen in the index finger. At the point where the lateral and medial slopes meet a round apex is formed. This apex maintains a neutral position unlike that of the index and middle fingers where the apices are medially orientated. The dorsal tubercle (7) is located just above the apex of the base. The

lateral and medial slopes including the apex form a smooth and regular dorsal articular margin of the base. At the sides, the lateral (11) and medial (5) tubercles of the base can be seen as bony protrusions.

Unlike the presence of a medial and lateral slope in the index and middle fingers, a palmar view (Figure 6.13b) of the ring finger shows a single convex palmar articular margin (16). The lateral (11) and medial (5) tubercles are associated with the articular margin at its lateral and medial sides respectively. Similar to the dorsal articular margin, the palmar articular margin is also smooth.

From a lateral view (Figure 6.13c) the lateral articular margin (18) slopes distally from the dorsal to the palmar surface. An oval-shaped lateral tubercle (11) extends from the dorsal to the palmar surface across the lateral margin.

In contrast to the lateral articular margin (Figure 6.13d), the medial articular margin (19) forms a shallow concave margin from dorsal to proximal. An oval-shaped medial tubercle (5) can be seen to extend from dorsal to palmar surfaces across the medial margin.

The articular surface (Figure 6.13f), is oval in shape. The medial articular margin is straight while the lateral articular margin is convex. Two shallow depressions can be seen which represent the relatively larger lateral (22) and relatively smaller medial (23) articular facets separated by a broad interarticular ridge. This is in contrast to the medial facets that were found to be larger in the index and middle fingers. An interesting observation is that if the ring finger is placed on its palmar surface very little if any tilting laterally is seen. If the same bone is placed on its dorsal surface, slight tilting to the medial aspect is seen.

6.14.4 Siding

In order to differentiate the right fourth middle phalanx from the corresponding one on the left side, the bone is orientated with the palmar surface facing down and the dorsal surface facing up or towards one, while the head is placed at the top end and the base at the bottom end (Bass 1995, Matshes *et al*. 2000).

For the purpose of the present study, a list of bony landmarks on the shaft, head and base of the fourth middle phalanx will now be provided. This is to overcome any problems that may be encountered if only a fragment of the fourth middle phalanx is found amongst skeletal remains.

Shaft

1. Lateral margin is angulated (10) (Figures 6.13a and b)
2. Medial margin is concave and smooth (4) (Figures 6.13a and b)
3. Distal end of shaft rotated laterally (Figures 6.13a and b)

Head

1. Lateral condyle (8) extends more distally then the medial condyle (2) (Figures 6.13a and b)

Base

1. Lateral articular margin straight (18) (Figure 6.13c)
2. Medial articular margin concave proximally (19) (Figure 6.13d)

Figure 6.13: Morphology of the right (R) and left (L) fourth middle phalanx

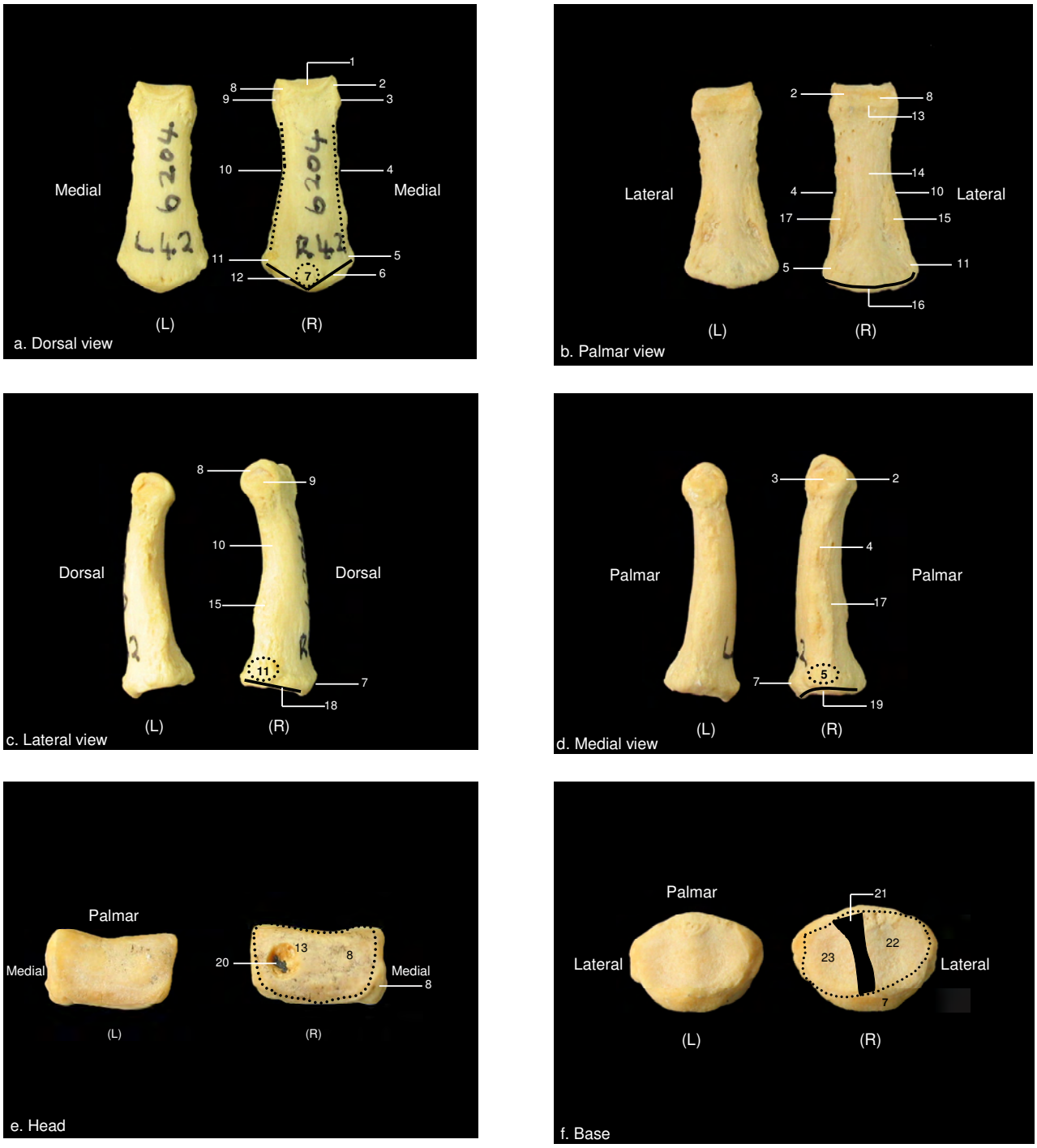

1=dorsal articular margin of head, 2=medial condyle of head, 3=medial fossa of head, 4=medial margin of shaft, 5=medial tubercle of base, 6=dorsal medial slope of base, 7=dorsal tubercle of base, 8=lateral condyle of head, 9=lateral fossa of head, 10=lateral margin of shaft, 11=lateral tubercle of base, 12=dorsal lateral slope of base, 13=palmar articular margin of head, 14=palmar surface of shaft, 15=palmar lateral ridge of shaft, 16=palmar articular margin of base, 17=palmar medial ridge of shaft, 18=lateral articular margin of base, 19=medial articular margin of base, 20=artifact on head, 21=interarticular ridge of base, 22=lateral articular facet of base, 23=medial articular facet of base.

6.15 Morphology of the fifth middle phalanx (Figures 6.14a-f)

6.15.1 Shaft or body (Figures 6.14a-d)

The little finger is the shortest bone in the middle phalangeal series. The shaft is wider proximally than distally. The lateral margin (10) also shows angulation in the midshaft area as seen from a dorsal view (Figure 6.14a), but to a lesser extent when compared to the middle phalanges of the index, middle and ring fingers. The shaft is smooth along its entire length with sparsely scattered foramina at the proximal and distal end. The shaft is rotated slightly laterally in contrast to the medial rotation seen in the middle and ring fingers. A dorsal tubercle (7) is located above the apex which is formed by the union of the dorsal lateral (12) and dorsal medial (6) slopes of the base. The dorsal apex of the base is orientated medially rather than laterally as was the case in the index, middle and to a certain extent in the ring finger. This medial orientation of the apex results in a longer lateral and shorter medial slope of the articular margin of the base.

Features observed on a palmar view (Figure 6.14b) are similar to that identified on a dorsal view. These include the lateral (15) and medial (17) palmar ridges located on either side of the smooth palmar surface (14). The medial palmar ridge is more prominent and elongated than the less prominent, short lateral palmar ridge. The reverse is true for the index, middle and ring fingers.

From a lateral view (Figure 6.14c) the base is convex dorsally and concave on the palmar surface. The lateral margin (10) is smooth except for the rough palmar lateral ridge (15) which projects forward at the proximal end of the shaft. The shaft is also much broader proximally than distally.

Bony landmarks seen from a medial view of the shaft (Figure 16.4d), are similar to that described for the lateral view. In other words, the smooth medial margin (4) is interrupted by a rough palmar medial ridge (17) located at the proximal end of the shaft. The shaft is also relatively broader proximally than distally.

6.15.2 Head (Figures 6.14a-e)

Similar to what was observed on the middle phalanges of adjacent digits, a dorsal view (Figure 6.14a) shows a relatively small surface area of the head. The dorsal articular margin (1), a clearly marked line, converges towards the center. Lying on either side of this articular margin are the lateral (8) and medial (2) condyles. The medial condyle (2) extends further distally than the lateral condyle (8).

A greater surface area of the head can be seen from a palmar aspect (Figure 6.14b). A shallow groove separates the two condyles. The articular margin (13) is longer and straight when compared to the dorsal articular margin.

Due to the distal end of the shaft rotating more medially than the rest of the bone, only the lateral aspects of the head can be seen from a lateral view (Figure 6.14c). The lateral condyle (8) forms a thin rim of bone surrounding the lateral fossa (9).

The lateral and medial aspects of the head can be seen from a medial view (Figure 6.14d) due to rotation of the distal half of the shaft medially. The medial condyle (2) forms a thin rim of bone that surrounds the medial fossa (3).

The head is rectangular in shape from the articular end (Figure 6.14e). The head has greater length on the palmar and dorsal margins in comparison to the shorter medial and lateral margins. The medial condyle (2) stretches out more medially and forms a blunt margin. This tends to create a slope on the palmar margin.

6.15.3 Base (Figures 6.14a-d and f)

From a dorsal view (Figure 6.14a) the base presents with two slopes of different length, namely, a longer lateral (12) and a shorter medial (6) slope. At the point where the lateral and medial slopes meet, a round apex is formed. This apex is medially orientated. The dorsal tubercle (7) is located just above the apex of the base. The lateral and medial slopes, including the apex, form a smooth and regular dorsal articular margin of the base. At the sides, a lateral (11) and medial (5) tubercle of the base can be identified.

Similar to the ring finger, the little finger has a convex palmar articular margin (16) (Figure 6.14b) which is smooth. The lateral (11) and medial (5) tubercles are visible on each side.

From a lateral view (Figure 6.14c) the lateral articular margin (18) is straight from dorsal to palmar surfaces. An oval-shaped lateral tubercle (11) can be seen to extend from the dorsal to the palmar surface.

From a medial view (Figure 6.14d), the medial articular margin (19) also runs as a straight line from the dorsal to the palmar surface. An oval-shaped medial tubercle (5) can be seen to extend from the dorsal to the palmar surface.

The base is oval in shape when looked at from the articular end (Figure 6.14f). Two shallow concavities are visible. They represent the relatively larger lateral (22) and relatively smaller medial (21) articular facets separated by a broad interarticular ridge (20), similar to that observed in the ring finger. In contrast, the medial facet was relatively larger than the lateral facet in the index and middle fingers.

6.15.4 Siding

In order to differentiate the right fifth middle phalanx from the corresponding one on the left side, the bone is orientated with the palmar surface facing down and the dorsal surface facing up or towards one, while the head is placed at the top end and the base at the bottom end (Bass 1995, Matshes *et al*. 2005).

For the purpose of the present study, a list of bony landmarks on the shaft, head and base of the fifth middle phalanx will now be provided. This is to overcome any problems that may be encountered if only a fragment of the fifth middle phalanx is found amongst skeletal remains.

Shaft

1. Lateral margin is angulated (10) (Figures 6.14a and b)

2. Shaft is rotated medially (Figures 6.14a, b and d)

Head

1. Medial condyle (2) extends further distally than the lateral condyle (Figures 6.14a and b)
2. Medial condyle extends further medially and forms a blunt point than the lateral condyle (Figure 6.14e)

Base

1. Larger lateral articular facet (22) (Figure 6.14f)
2. Smaller medial articular facet (21) (Figure 6.14f)
3. Medial condyle more prominent than lateral condyle (Figure 6.14f)

Figure 6.14: Morphology of the right (R) and left (L) fifth middle phalanx

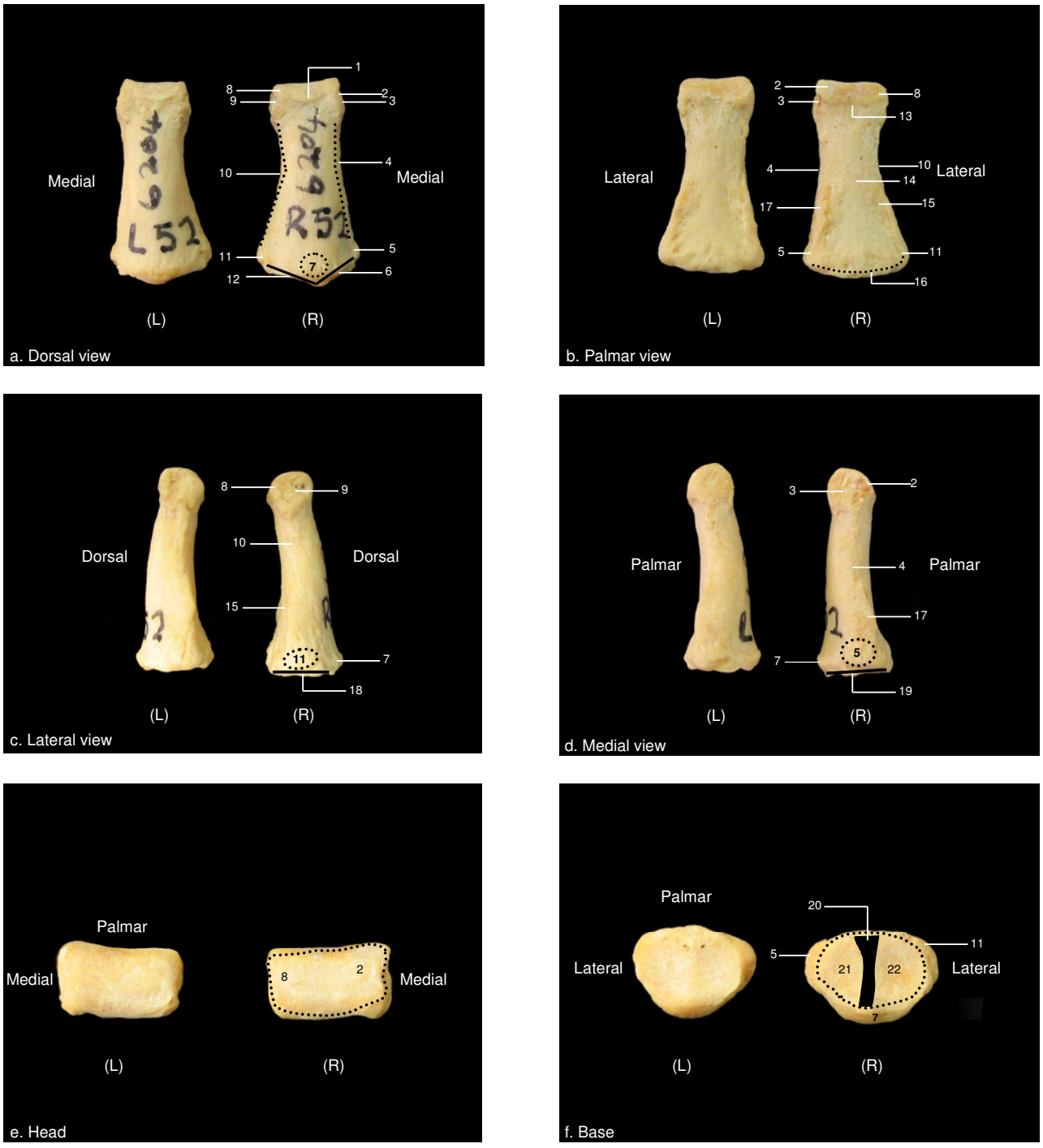

1=dorsal articular margin of head, 2=medial condyle of head, 3=medial fossa of head, 4=medial margin of shaft, 5=medial tubercle of base, 6=dorsal medial slope of base, 7=dorsal tubercle of base, 8=lateral condyle of head, 9=lateral fossa of head, 10=lateral margin of shaft, 11=lateral tubercle of base, 12=dorsal lateral slope of base, 13=palmar articular margin of head, 14=palmar surface of shaft, 15=palmar lateral ridge of shaft, 16=palmar articular margin of base, 17=palmar medial ridge of shaft, 18=lateral articular margin of base, 19=medial articular margin of base, 20=interarticular ridge of base, 21=medial articular facet of base, 22=lateral articular facet of base.

6.16 Morphology of the first distal phalanx (Figures 6.15a-f)

6.16.1 Shaft or body (Figures 6.15a-d)

A dorsal view (Figure 6.15a) shows that the shaft narrows at its distal end. The lateral (6) and medial (2) margins of the shaft are concave. The lateral margin extends further proximally than the medial margin. The latter tends to run obliquely in a palmar direction in the proximal third of the shaft. This gives the impression that the lateral margin is relatively longer than the medial margin. The dorsal surface is smooth except for a rough area at the proximal end of the dorsal surface which serves for attachment of the tendon of extensor pollicis longus (Scheuer & Black 2000). The distal end of the dorsal surface is smooth and deep to the fingernail (Wilkinson 1953). In the present study, numerous nutrient foramina were located at the proximal and distal ends of the shaft.

Unlike the smooth dorsal surface, the palmar surface (Figure 6.15b) is rough due to attachment of soft tissue structures in this region. This surface is also flattened at the proximal end (Wilkinson 1953). This surface presents with two concavities, namely, the smooth distal palmar surface (9) and the rough proximal palmar surface (11). The proximal palmar concavity (11) is for attachment of the flexor digitorum profundus tendon. On either side of the proximal palmar concavity (11) are two ridges located on the lateral and medial side of the shaft respectively. The lateral palmar ridge (10) is broader and extends further proximally than the medial palmar ridge (15).

The lateral surface of the shaft (Figure 6.15c) is broader proximally and tapers towards the distal end. The dorsal apex of the base (4) and the lateral tubercle of the base (7) can be identified.

A medial view (Figure 6.15d) of the shaft presents similar morphological features as seen on a lateral view. In other words, the shaft is also broader proximally and tapered distally. The dorsal apex of the base (4) and the medial tubercle of the base (3) can be identified from this view.

6.16.2 Head (Figures 6.15a-e)

From a dorsal aspect (Figure 6.15a) the head presents as a narrow strip of rough bone along the distal end of the shaft which then extends proximally to overlap the lateral and medial aspects of the distal third of the shaft. Generally, the head is rough and irregular in shape.

A larger surface area of the rough and irregular-shaped head is seen from a palmar aspect (Figure 6.15b) in comparison to the dorsal view. The head surrounds the periphery of the distal third of the shaft as a broad rather than a narrow strip of bone. The lateral (8) and medial (14) extensions of the head on the shaft are broader than that seen from a dorsal aspect. The lateral and medial extensions tend to taper at their proximal free ends.

On a lateral and medial view (Figure 6.15c) the head is extended in a slightly dorsal direction. This may relate to function or perhaps to the mass of soft tissue padding that causes the distal phalanx of the thumb to be extended at its tip.

A superior view (Figure 6.15e) of the head shows very little with regards to morphological features that can be used for identification purposes. What is visible is an oval-shaped head which has greater width from medial to lateral than from dorsal to palmar surfaces.

6.16.3 Base (Figures 6.15a-d and f)

A dorsal view (Figure 6.15a) shows that the base is wider than the rest of the bone. The proximal articular margin (5) is convex proximally, except at the lateral end which is concave forming a small step inwards. At the point where the base merges with the shaft, a straight margin is formed laterally while at its medial end the margin is convex. Due to the lateral margin projecting more proximally, the lateral part of the shaft including the base on this aspect is extended proximally. The bone thus appears to be tilted on the lateral side which gives the impression that the medial margin of the shaft including its base is set at a higher or

more distal level. The lateral (7) and medial (3) tubercles can be seen at either ends of the base.

When the bone is turned so that the palmar surface of the base is visible (Figure 6.15b), the articular margin of the base (13) is convex proximally. Associated with this margin is a centrally placed oval-shaped articular facet called the palmar articular facet of the base (12) for attachment of flexor pollicis longus (Netter 1989, plate 435, Drake *et al*. 2005). The lateral end of the base is broad, round and projects proximally in contrast to the narrow medial end which curves up in a distal direction. A few foramina may present randomly on the palmar aspect of the base. The lateral (7) and medial (3) tubercles are also visible from this view.

A lateral view of the base (Figure 6.15c) shows a straight lateral articular margin (16) running proximally from the dorsal to the palmar surface of the bone. This results in the palmar end of the margin projecting more proximally than at the dorsal end. This proximal extension makes it difficult to identify the medial articular margin. The dorsal apex of the base projects only slightly proximally thus giving this aspect of the base the appearance of a short and stout “beak” as opposed to an elongated “beak” seen in the index finger.

When the base is viewed from a medial aspect (Figure 6.15d), the medial articular margin (17) is seen as a shallow concavity running at the same level from the dorsal to the palmar surface. The lateral articular margin is also visible from a medial view as it projects further proximally than the medial articular margin.

The articular surface of the base (Figure 6.15f) is oval to round in shape. The palmar articular margin is longer than the dorsal articular margin. The lateral articular margin is straight and longer in comparison to the convex and shorter medial articular margin. The articular surface has a single shallow concavity (18). From this view, the relatively smaller lateral (7) and larger medial (3) tubercles are visible at the lateral and medial ends respectively. The palmar articular margin is interrupted by the presence of a small oval shaped articular facet (12) which is positioned more to the lateral than to the medial end.

6.16.4 Siding

In order to differentiate the right first distal phalanx from the corresponding one on the left side, the bone is orientated with the palmar surface facing down and the dorsal surface facing up or towards one, while the head is placed at the top end and the base at the bottom end (Bass 1995, Matshes *et al*. 2005).

For the purpose of the present study, a list of bony landmarks on the shaft, head and base of the first distal phalanx will now be provided. This is to overcome any problems that may be encountered if only a fragment of the first distal phalanx is found amongst skeletal remains.

Shaft

1. Lateral margin (6) has a longer slope which extends more proximally than medial margin (Figure 6.15a)
2. Medial margin (2) has a shorter slope than the lateral margin (Figure 6.15a)

Head

1. Lateral extension of the head (8) is more proximally placed than the medial extension (14) of the head (Figures 6.15a and b). While the length of the lateral and medial extensions varies in this bone of different individuals, it is a bony landmark that can be used to side this bone.

Base

1. Lateral articular margin (16) which projects more proximally making it difficult to see the medial articular margin (Figure 6.15c)
2. Medial articular margin (17) more distally placed than the more proximally placed lateral articular margin (Figure 6.15d)
3. Palmar articular facet (12) positioned more laterally on the palmar articular margin (Figure 6.15b)

Figure 6.15: Morphology of the right (R) and left (L) first distal phalanx

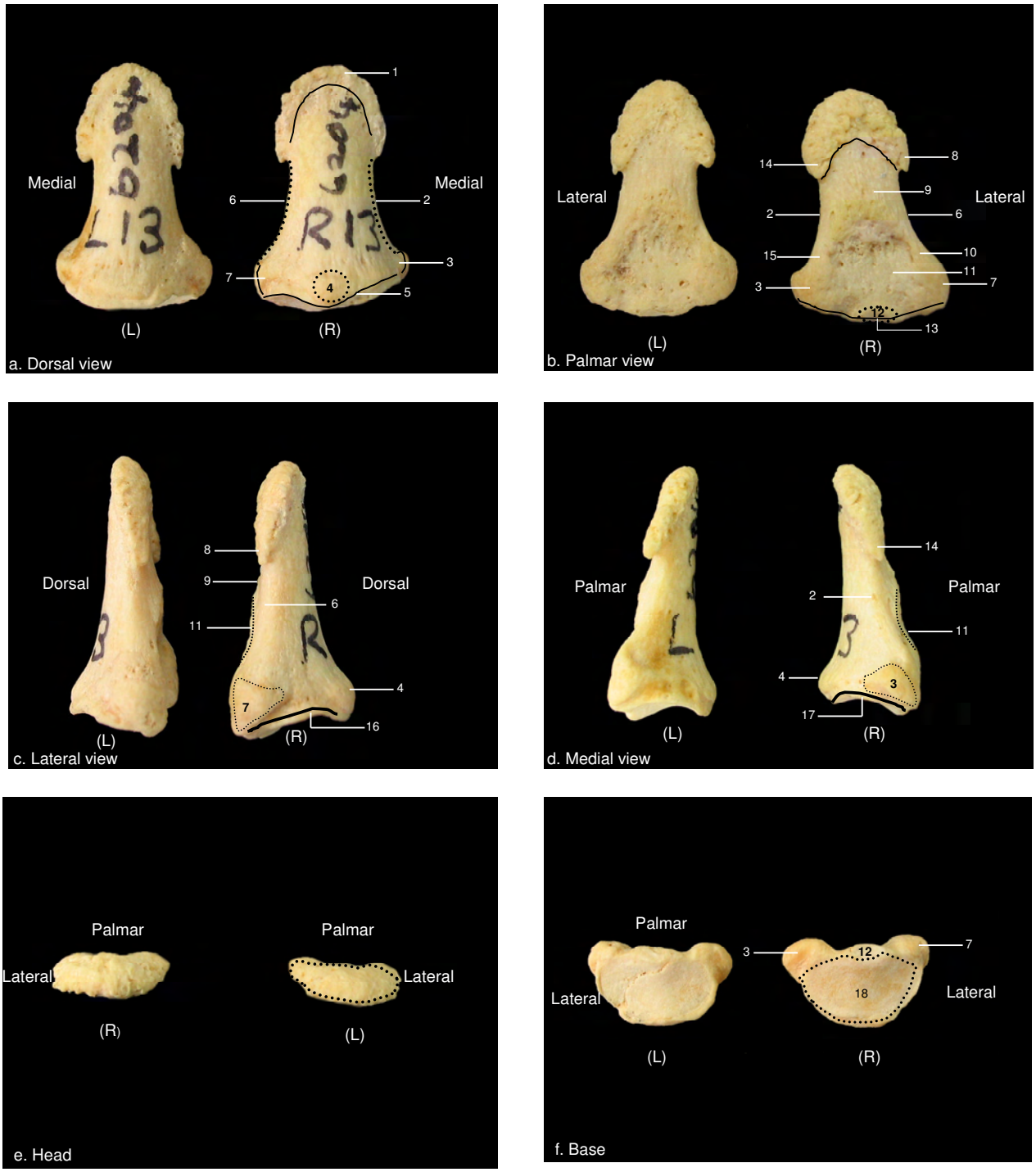

1=head, 2=medial margin of shaft, 3=medial tubercle of base, 4=dorsal apex of base, 5=dorsal articular margin of base, 6=lateral margin of shaft, 7=lateral tubercle of base, 8=palmar lateral extension of head, 9=smooth distal palmar surface of shaft, 10=palmar lateral ridge of shaft, 11=rough proximal palmar concavity of shaft, 12=palmar articular facet of base, 13=palmar articular margin of base, 14=palmar medial extension of head, 15=palmar medial ridge of shaft, 16=lateral articular margin of base, 17=medial articular margin of base, 18=articular facet of base.

6.17 Morphology of the second distal phalanx (Figures 6.16a-f)

6.17.1 Shaft or body (Figures 6.16a-d)

The shaft is convex on its dorsal aspect and concave on the palmar surface (Scheuer & Black 2000). From a dorsal view (Figure 6.16a) the proximal end is broad while the distal end is tapered (Scheuer & Black 2000). The lateral (6) and medial (2) margins are concave. The lateral margin projects further proximally than the medial margin. The dorsal surface is smooth throughout its entire length. Very few, if any, nutrient foramina can be identified on the dorsal aspect.

A view of the palmar surface (Figure 6.16b) shows that the shaft is rough proximally and smooth distally. The rough surface presents as a shallow depression, called the rough palmar concavity (12) which serves as an attachment site for the tendon of flexor digitorum profundus (Gray 1959, Netter 1989, Drake *et al*. 2005). On either side of this rough area, the smooth lateral (11) and medial (16) ridges can be identified. The medial palmar ridge is relatively broader than the lateral palmar ridge. Furthermore, the medial margin at its proximal end tends to curve distally while the lateral margin at its proximal end projects either horizontally or further proximally. Both the lateral and medial margins are concave.

The lateral aspect of the shaft (Figure 6.16c) shows a smooth lateral margin. The greater width is seen at the proximal end. The dorsal surface is concave proximally and convex distally. The proximal end forms a slope as it approaches the base. The rough proximal palmar concavity (12) represents the depression in the middle. Distal to this concavity is the smooth palmar surface of the shaft (10).

Observing the shaft from a medial aspect (Figure 6.16d) reveals a smooth medial margin. Features that are observed from a lateral view can also be seen from a medial view. These include the proximal concavity and distal convexity of the dorsal surface, the rough proximal palmar concavity (12) in the midshaft region and the smooth palmar surface (10) located distal to the proximal palmar concavity (12).

6.17.2 Head (Figures 6.16a-e)

From a dorsal aspect (Figure 6.16a) the head presents as a narrow strip of rough bone along the distal margin which extends proximally to overlap the lateral and medial aspects of the distal third of the shaft.

A larger surface area of the head is seen from a palmar aspect (Figure 6.16b) in comparison to the dorsal view. The head also surrounds the periphery of the distal third of the shaft as a broad region rather than a narrow strip of bone. The lateral and medial extensions of the head on the shaft are broad distally and tapered proximally. Randomly placed nutrient foramina can be identified along the inferior margin of the head.

On a lateral view (Figure 6.16c), the head is flexed rather than extended as in the case of the thumb. Lateral rotation at the distal end of this bone results in both the lateral (9) and medial (15) palmar extensions of the head being visible.

From a medial view (Figure 6.16d), only the medial palmar extension (15) can be identified. Slight flexion of the head, as seen from a lateral view, is also evident from a medial aspect.

The non-articular distal surface (Figure 6.16e) reveals an oval shaped head. No other detail is noted.

6.17.3 Base (Figures 6.16a-d and f)

From a dorsal view (Figure 6.16a), the base is recognized by having a lateral (8) and medial (4) slope which merges to form the dorsal apex (5) of the base. The lateral slope is longer in comparison to the shorter medial slope. The difference in length of the slopes causes the apex of the base to be shifted in a more medial direction. The lateral (7) and medial (3) tubercles can be seen to overlap onto the dorsal surface.

The articular margin of the base as seen from a palmar view (Figure 6.16b) also shows the presence of two slopes. In this case the medial slope (17) is relatively longer than the lateral (13) slope. The point where these two slopes meet is called the palmar apex of the base

(14). The apex of the base is shifted in a more lateral direction as a result of the relatively longer medial slope of the base. The relatively larger medial (3) and smaller lateral (7) tubercles can be seen to overlap onto the palmar aspect.

From a lateral view (Figure 6.16c) the lateral articular margin (18) is concave proximally. The dorsal apex of the base projects further proximally thus increasing the curvature of the lateral articular margin giving it the appearance of an elongated “beak”. The dorsal (5) and palmar (14) apex of the base can be seen from this view.

From a medial view (Figure 6.16d) the medial articular margin (19) is less concave in comparison to the lateral articular margin. In fact, some of the bones observed showed that this margin may be straight for most of its length. That part of the margin closest to the palmar surface tends to curve proximally and this may sometimes give the appearance that the medial articular margin is concave in shape. The dorsal and palmar apex of the base can also be seen from this view.

From an inferior view (Figure 6.16f) the base is oval in shape. The lateral tubercle (7) is relatively larger than the medial tubercle (3) of the base.

6.17.4 Siding

In order to differentiate the right second distal phalanx from the corresponding one on the left side, the bone is orientated with the palmar surface facing down and the dorsal surface facing up or towards one, while the head is placed at the top end and the base at the bottom end (Bass 1995, Matshes *et al.* 2005).

For the purpose of the present study, a list of bony landmarks on the shaft, head and base of the second distal phalanx will now be provided. This is to overcome any problems that may be encountered if only a fragment of the second first distal phalanx is found amongst skeletal remains.

Shaft

1. Lateral margin (6) projects further proximally than the medial margin (Figures 6.16a and b)
2. Medial palmar ridge (16) thicker than lateral palmar ridge (11) (Figure 6.16b)

Head

1. Lateral extension of head (9) broader than medial extension (15) (Figure 6.16a)

Base

1. Longer lateral slope (8) (Figure 6.16a)
2. Shorter medial slope (4) (Figure 6.16a)
3. Dorsal apex (5) shifted more medially (Figure 6.16a)
4. Longer medial slope (17) (Figure 6.16b)
5. Shorter lateral slope (13) (Figure 6.16b)
6. Lateral articular margin (18) concave (Figure 6.16c)
7. Medial articular margin (19) varies from slightly concave to straight (Figure 6.16d)

Figure 6.16: Morphology of the right (R) and left (L) second distal phalanx

1=head, 2=medial margin of shaft, 3=medial tubercle of base, 4=dorsal medial slope of base, 5=dorsal apex of base, 6=lateral margin of shaft, 7=lateral tubercle of base, 8= dorsal lateral slope of base, 9=palmar lateral extension of head, 10=smooth distal palmar surface of shaft, 11=palmar lateral ridge of shaft, 12=rough proximal palmar concavity, 13=palmar lateral slope of base, 14=palmar apex of base, 15=palmar medial extension of head, 16=palmar medial ridge of shaft, 17=palmar medial slope of base, 18=lateral articular margin of base, 19=medial articular margin of base, 20=articular facet of base.

6.18 Morphology of the third distal phalanx (Figures 6.17a-f)

6.18.1 Shaft or body (Figures 6.17a-d)

The distal phalanx of the middle finger is relatively smaller than that of the thumb and index finger, but relatively bigger than that of the ring and little finger. On the dorsal surface (Figure 6.17a), the shaft is smooth throughout its entire length. Proximally, the shaft is broad while distally it is tapered (Scheuer & Black 2000). Lateral (6) and medial (2) margins are concave in shape. There is relatively greater length of the lateral margin as it extends further proximally than the medial margin. Very few, if any, nutrient foramina can be identified at the proximal and distal ends.

On the palmar aspect (Figure 6.17b), the shaft is smooth distally (10). The concave lateral margin (6) extends further proximally than the concave medial margin (2). The proximal depression is referred to as the rough, proximal palmar concavity (12). It is flanked on each side by smooth, lateral (11) and medial (16) ridges. The palmar medial ridge is relatively broader than the palmar lateral ridge. Numerous nutrient foramina can be seen in the proximal palmar concavity. This concavity serves for attachment of the flexor digitorum profundus tendon.

From a lateral view (Figure 6.17c), the dorsal surface is concave proximally and slightly convex distally. The palmar surface, on the other hand, shows the rough proximal concavity (12) while distally, a slope can be identified which represents the smooth palmar surface. The lateral surface is relatively smooth. The shaft is wider proximally and tapered distally.

The medial margin of the shaft, as seen from a medial view (Figure 6.17d), is smooth. The dorsal and palmar surfaces present the same as observed from a lateral view.

6.18.2 Head (Figures 6.17a-e)

From a dorsal aspect (Figure 6.17a), the head presents as a narrow strip of rough bone along the distal margin of the shaft. The head gives off extensions in a proximal direction which overlaps the lateral and medial aspects of the distal third of the shaft with the lateral extension

being relatively broader than the medial extension. The head takes on a round shape similar to that of the index finger. Also noticeable from this view is that the head is pulled into extension and slight lateral rotation.

As is the case in the thumb and index finger, a greater surface area of the head is visible from a palmar (Figure 6.17b) than from a dorsal view. The head forms a broad peripheral band at the distal end of the shaft. The lateral (9) and medial (15) extensions are broader than that observed from the dorsal aspect. The lateral extension projects further proximally than the medial extension. Both the lateral and the medial extensions are tapered at their ends and not attached to either the lateral or medial margins of the shaft. A few foramina can be seen just proximal to the head where it merges with the shaft. The extension of the head, with slight lateral rotation is also seen from this view.

On a lateral view (Figure 6.17c) the medial rotation of the head is not obvious. Instead, the head and distal end of the shaft is aligned in an almost straight line in comparison to the slight extension and flexion seen in the thumb and index fingers respectively. The lateral palmar extension of the head (9) with its tapered free edge can be easily identified from this view.

From a medial view (Figure 6.17d), the alignment of the head and distal end of the shaft is exactly the same as that described from a lateral view. The medial palmar extension of the head (15) with its free tapered edge can also be easily seen.

The non-articular end (Figure 6.17e) reveals a rectangular-shaped head with the greatest width from side to side.

6.18.3 Base (Figures 6.17a-d and f)

From a dorsal view (Figure 6.17a), the dorsal articular margin presents as an irregular convex margin extending from side to side. This margin has two slopes, namely, the dorsal lateral (8) and dorsal medial (4) slope which join to form the dorsal apex of the base (5). These slopes are of equal length.

The articular margin of the base as observed from a palmar view (Figure 6.17b), shows a relatively short lateral (13) and relatively longer medial (17) slope. This difference in length of the slopes may be due to the lateral margin of the shaft and base lifted in a proximal direction while the medial margin of the shaft tends to be pulled distally. Where the two slopes meet, a round apex is formed which is directed slightly laterally. The lateral and medial tubercles overlap onto the palmar surface.

From a lateral view (Figure 6.17c) the lateral articular margin (18) varies from a straight to a slightly concave margin, similar to that observed in the thumb. The apex on the palmar aspect of the base does not extend further proximally as is the case in the thumb. The apex of the dorsal (5) and palmar (14) surfaces of the base can be seen from this view. The elongated lateral tubercle of the base (7) is obliquely positioned just distal to the articular margin.

Features from a medial view (Figure 6.17d) are similar to that seen on a lateral view. The difference is that the medial articular margin (19) is slightly concave and set at a higher or more distal level than the lateral articular margin which makes the lateral margin also visible from a medial view. The medial tubercle (3) of the base is triangular in shape.

The articular surface (20) of the base (Figure 6.17f) is rectangular in shape. The dorsal and palmar margins are relatively longer than the lateral and medial margins. The lateral (7) and medial (3) tubercles can be easily identified on the sides. The apex on the palmar aspect (14) is shifted laterally in comparison to the centrally placed apex on the dorsal surface (5).

6.18.4 Siding

In order to differentiate the right third distal phalanx from the corresponding one on the left side, the bone is orientated with the palmar surface facing down and the dorsal surface facing up or towards one, while the head is placed at the top end and the base at the bottom end (Bass 1995, Matshes *et al*. 2005).

For the purpose of the present study, a list of bony landmarks on the shaft, head and base of the third distal phalanx will now be provided. This is to overcome any problems that

may be encountered if only a fragment of the third distal phalanx is found amongst skeletal remains.

Shaft

1. Lateral margin (6) extends further proximally than the medial (12) margin (Figures 6.17a and b)
2. Palmar medial palmar (16) ridge relatively broader than palmar lateral (11) ridge (Figure 6.17b)

Head

1. The lateral extension (9) is relatively broader than the medial extension (15) (Figure 6.17a)
2. The lateral extension (9) projects further proximally than the medial extension (15) (Figure 6.17b)
2. Head is extended and medially rotated on the shaft (Figure 6.17a and b)

Base

1. Shorter lateral (13) and longer medial (17) slope of palmar articular margin (Figure 6.17b)
2. Lateral tubercle (7) elongated in an oblique manner (Figure 6.17c)
3. Medial tubercle (3) triangular in shape (Figure 6.17d)

Figure 6.17: Morphology of the right (R) and left (L) third distal phalanx

1=head, 2=medial margin of shaft, 3=medial tubercle of base, 4=dorsal medial slope of base, 5=dorsal apex of base, 6=lateral margin of shaft, 7=lateral tubercle of base, 8=dorsal lateral slope of base, 9=palmar lateral extension of head, 10=smooth distal palmar surface of shaft, 11=palmar lateral ridge of shaft, 12=rough proximal palmar concavity of shaft, 13=palmar lateral slope of base, 14=palmar apex of base, 15=palmar medial extension of head, 16=palmar medial ridge of shaft, 17=palmar medial slope of base, 18=lateral articular margin of base, 19=medial articular margin of base, 20=articular facet of base.

6.19 Morphology of the fourth distal phalanx (Figures 6.18a-f)

6.19.1 Shaft or body (Figures 6.18a-d)

The distal phalanx of the ring finger is relatively shorter than that of the middle finger. From a dorsal view (Figure 6.18a) the shaft is smooth along its entire length. The shaft is broadest at the proximal end and tapered distally. The lateral (6) and medial (2) margins are concave. The lateral margin is relatively shorter than the medial margin. Numerous foramina are seen at the distal end compared to the sparsely scattered foramina that can be identified at the proximal end.

The palmar aspect (Figure 6.18b) of the shaft is smooth distally (10) and rough proximally (12). The latter serves for the attachment of the flexor digitorum profundus tendon associated with the ring finger. On either side of this concavity are two ridges, namely the lateral (11) and medial (16) palmar ridges. The bones that were studied showed great variability in the thickness of these ridges. One ridge was not necessarily broader in width than the other. As observed in the thumb, index and middle fingers, the lateral (6) and medial (2) margins are concave with the medial margin extending further proximally than the lateral margin. This feature is more obvious on the palmar than on the dorsal aspect.

On a lateral view (Figure 6.18c) the dorsal surface is convex in the distal third and concave in the proximal two thirds. The palmar surface, on the other hand, forms a slope (10) in the distal half and a concavity (12) in the proximal half.

Morphology of this bone from a medial view (Figure 6.18d), is exactly the same as that described from a lateral view. One distinguishing feature is that the shaft is rotated medially.

6.19.2 Head (Figures 6.18a-e)

From a dorsal aspect (Figure 6.18a), the head presents as a narrow strip of rough bone along the distal margin of the shaft. The head takes on a round shape similar to that of the index and middle fingers.

A greater surface area of the head is seen from a palmar view (Figure 6.18b). The head forms a broad area along the periphery of the shaft's distal end. The head forms lateral (9) and medial (15) extensions along the sides of the distal end of the shaft. Both the lateral and the medial extensions are tapered at their extreme ends. Numerous large nutrient foramina are found scattered on the palmar aspect of the head including its extensions.

On a lateral view (Figure 6.18c) the rotation of the head medially is not as marked as is seen in the middle finger. The non-articulating distal end is only slightly extended. The remainder of the head is positioned obliquely on the distal end of the shaft. The lateral extension (9), with its free tapered end, can be easily identified.

A medial view of the head (Figure 6.18d) is the same as that seen on a lateral view. The difference is that with the head rotated medially, both its medial (15) and lateral (9) extensions can be seen.

A superior view (Figure 6.18e) of the head shows that it is oval-shaped. The lateral end is broader in comparison to the narrow medial end. No additional identifying features can be described from this view.

6.19.3 Base (Figures 6.18a-d and f)

Features of the base from a dorsal view (Figure 6.18a), shows an irregular dorsal articular margin (5). This margin is flanked on each side by a dorsal lateral (8) and dorsal medial (4) slope. The medial slope is relatively longer than the lateral slope. The straight and sloped margins are joined in such a way that it gives the dorsal articular margin a convex shape.

The articular margin on a palmar view (Figure 6.18b), is smooth in comparison to the irregular shaped dorsal articular margin. The palmar articular margin has two slopes, namely, a palmar lateral (13) and palmar medial (17) slope which join each other to form a rounded apex (14). The medial slope is relatively longer than the lateral slope. This difference in length of the slopes may be due to the lateral margin of the shaft and base being pulled in a proximal

direction, creating a deeper lateral curvature of the shaft while the medial of the shaft tends to be pulled distally thus stretching the curvature of the medial margin of the shaft.

From a lateral view (Figure 6.18c) the lateral articular margin (18) is concave and set at a higher or more distal level than the medial articular margin (19). In other words, a lateral view exposes part of the medial articular margin as well. The curvature described for the ring finger is similar to that of the thumb and index finger in that it is concave proximally. The difference comes in the projection of the apices on the dorsal and palmar aspect of the base. For example, in the thumb, the apex on the palmar surface projects further proximally than the apex on its dorsal surface. In the index finger, it is the apex of the dorsal surface that projects further proximally than the apex on its palmar surface. In the ring finger neither the dorsal nor the palmar apex projects further proximally than the other. In other words, the dorsal and palmar apices occur at the same level. The lateral tubercle (7) is located distal to the smooth articular margin and is relatively bigger than the medial tubercle (3).

From a medial view (Figure 6.18d), the articular margin (19) presents as a shallow concavity which is directed proximally. The medial tubercle of the base (3) is distal to the medial articular margin of the base.

The articular end (Figure 6.18f) shows an oval to rectangular shaped base. The palmar articular margin is relatively longer than the dorsal articular margin. The medial and lateral articular margins are convex in shape. The palmar apex (14) separates the relatively longer palmar medial slope from the relatively shorter palmar lateral slope. These slopes are indicated by a solid black line on the figure. The dorsal articular margin (5), lateral (8) and medial (4) slopes gives the dorsal margin a convex shape. The lateral tubercle of the base (7) is relatively larger than the medial tubercle (3). The articular surface (20) is seen as a shallow central depression.

6.19.4 Siding

In order to differentiate the right fourth distal phalanx from the corresponding one on the left side, the bone is orientated with the palmar surface facing down and the dorsal surface

facing up or towards one, while the head is placed at the top end and the base at the bottom end (Bass 1995, Matshes *et al*. 2005).

For the purpose of the present study, a list of bony landmarks on the shaft, head and base of the fourth distal phalanx will now be provided. This is to overcome any problems that may be encountered if only a fragment of the fourth distal phalanx is found amongst skeletal remains.

Shaft

1. Medial margin (2) projects further proximally than the lateral margin (6) (Figures 6.18a and b)

Head

1. Lateral extension (9) is broader and projects more proximally than the medial extension (15) (Figure 6.18b)

Base

1. Medial slope (4) relatively longer than the lateral slope (8) (Figures 6.18a and b)
2. Lateral articular margin (18) has a deep concavity and projects more distally exposing part of the medial articular margin (Figures 6.18c)
3. Medial articular margin (19) has a shallow concavity (Figures 6.18d)
4. Lateral tubercle (7) relatively larger than medial tubercle (3) (Figures 6.18a, b and f)

Figure 6.18: Morphology of the right (R) and left (L) fourth distal phalanx

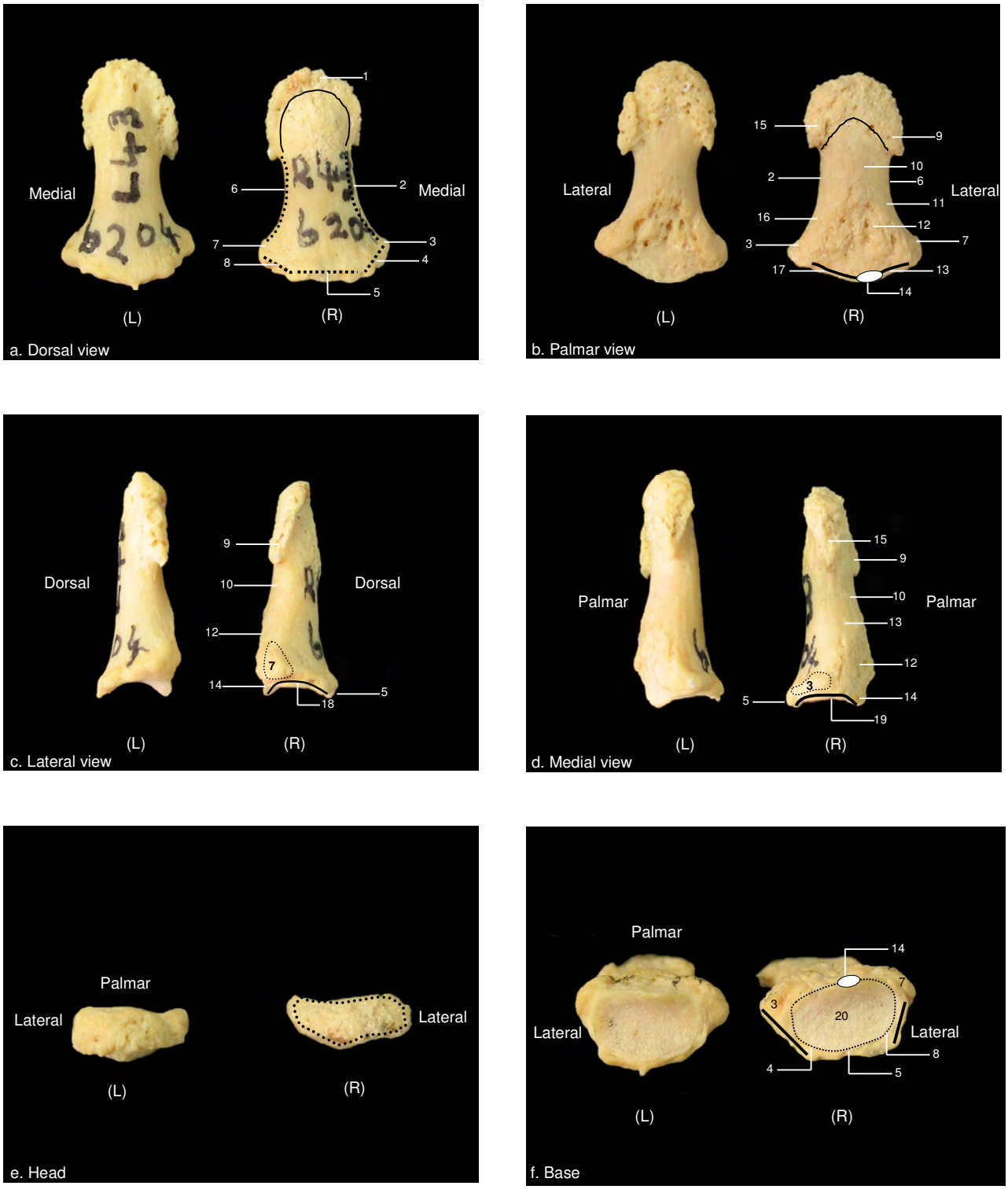

1=head, 2=medial margin of shaft, 3=medial tubercle of base, 4=dorsal medial slope of base, 5=dorsal articular margin of base, 6=lateral margin of shaft, 7=lateral tubercle of base, 8=dorsal lateral slope of base, 9=palmar lateral extension of head, 10=smooth distal palmar surface of shaft, 11=palmar lateral ridge of shaft, 12=rough proximal palmar concavity of shaft, 13=palmar lateral slope of base, 14=palmar apex of base, 15=palmar medial extension of head, 16=palmar medial ridge of shaft, 17=palmar medial slope of base, 18=lateral articular margin of base, 19=medial articular margin of base, 20=articular facet.

6.20 Morphology of the fifth distal phalanx (Figures 6.19a-f)

6.20.1 Shaft or body (Figures 6.19a-d)

In the present study, the shaft of the fifth distal phalanx was the shortest and narrowest in comparison to adjacent distal phalanges. The shaft of this bone, as seen from a dorsal view (Figure 6.19a), is smooth along its entire length. The proximal end is broad in comparison to the tapered distal end. The lateral margin (6) has a deeper concavity in comparison to the more shallow concavity of the medial margin (2). Very few, if any, nutrient foramina are present at the proximal end of the shaft.

The palmar aspect (Figure 6.19b) shows a smooth distal surface (10) and a rough proximal palmar concavity (12). The rough area serves for the attachment of the flexor digitorum profundus tendon associated with the little finger. Two ridges are associated with the rough area, namely, the broader palmar medial (16) and narrow palmar lateral ridges (11). The shaft appears to be tilted to the lateral side due to the shorter lateral and longer medial margins. Not only is the shaft tilted laterally, but it is also medially rotated. Few nutrient foramina can be identified at the proximal end while distally, very few of these foramina are present. In the photograph taken of the right distal phalanx, a single large nutrient foramen was present just proximal to the solid line that outlined the shape of the lateral (9) and medial (15) extensions of the head.

The lateral aspect of the shaft (Figure 6.19c) shows a smooth lateral margin. The distal end of the shaft is pulled into slight flexion in a palmar direction. The smooth lateral margin, broad proximal and tapered distal end of the shaft is a general observation for the lateral views of all distal phalanges. The dorsal surface is convex in the distal half and slightly concave in the proximal half. The palmar surface has a deep concavity distally which is represented by the smooth palmar surface (10) and a rather shallow concavity proximally which is the proximal palmar concavity (12).

Features seen on a medial view (Figure 6.19d), is the same as that identified from a lateral view. What is different between the two views is that medial rotation of the shaft can be

more easily seen from a medial than from a lateral view with a greater part of the palmar surface is exposed.

6.20.2 Head (Figures 6.19a-e)

From a dorsal aspect (Figure 6.19a) the head presents as a narrow strip of rough bone along the distal margin of the shaft. The head is much narrower when compared to that of adjacent fingers. In most of the samples examined, wearing down of the head appears to affect the lateral rather than the medial aspect of the head.

More of the head can be viewed from a palmar aspect (Figure 6.19b) than from the dorsal aspect. Not only does the head form a broad area along the periphery of the distal end of the shaft, it has lateral (9) and medial (15) extensions along the sides of the distal end of the shaft. Both the lateral and the medial extensions are tapered at their extreme ends. The medial extension projects more proximally than the lateral extension. Numerous tiny foramina are found scattered on the palmar aspect of the head, including its extensions.

On a lateral view (Figure 6.19c), the rotation of the head medially is similar to that observed in the middle finger. The head also displays slight flexion from this angle. The lateral palmar extension (9) can be easily identified by its tapered end.

A medial view (Figure 6.19d) shows the medial rotation very clearly as both the lateral (9) and medial (15) extensions of the head are visible. The head also displays slight flexion from this angle, similar to that observed from a lateral view.

The non-articular end (Figure 6.19e) shows a rectangular shaped head. The palmar and dorsal margins are relatively longer than the medial and lateral margins.

6.20.3 Base (Figures 6.19a-d and f)

From a dorsal view (Figure 6.19a) the base is recognized by having a lateral (8) and medial (4) slope which merge to form the dorsal apex (5) of the base. The lateral slope is relatively longer in comparison to the relatively shorter medial slope. This finding was similar to

that observed in the index finger. This difference in length of the slopes causes the apex of the base to be positioned in a more medial direction. Generally, the articular margins are smooth.

The articular margin of the base identified from a palmar view (Figure 6.19b), has two slopes. The lateral (13) and medial (17) slopes, which together form the palmar articular margin, is set at a higher or more distal level than the dorsal lateral and dorsal medial slopes. This results in the dorsal articular margin being visible from a palmar view. This is not the case in the index finger, where the lateral and medial slopes on the palmar and dorsal aspects are at the same level. The medial slope is relatively shorter than the lateral slope. This difference in slope length causes the palmar apex (14) to be more medially placed.

A lateral view (Figure 6.19c) shows that the lateral articular margin (18) forms an oblique line running distally from the dorsal to the palmar surface. The upward slope of this margin results in the medial articular margin also being visible. The lateral tubercle (7) is triangular in shape and relatively smaller than the medial tubercle (3).

From a medial view (Figure 6.19d), the medial articular margin (19) forms a straight line. The medial tubercle (3) is relatively larger than the lateral tubercle.

A view of the articular end (Figure 6.19f), reveals an oval shaped concave surface. The dorsal margin is relatively longer than the palmar margin with the lengths of the lateral and medial margins being the shortest. Both the dorsal and palmar apices are more medially positioned. The dorsal and palmar lateral slopes are relatively longer than the medial slopes on the same surfaces. The medial tubercle (3) of the base is more elongated and projects further medially than the relatively smaller lateral tubercle (7).

6.20.4 Siding

In order to differentiate the right fifth distal phalanx from the corresponding one on the left side, the bone is orientated with the palmar surface facing down and the dorsal surface facing up or towards one, while the head is placed at the top end and the base at the bottom end (Bass 1995, Matshes *et al*. 2005).

For the purpose of the present study, a list of bony landmarks on the shaft, head and base of the fifth distal phalanx will now be provided. This is to overcome any problems that may be encountered if only a fragment of the fifth distal phalanx is found amongst skeletal remains.

Shaft

1. Lateral margin (6) has a deep concavity (Figures 6.19a and b)
2. Medial margin (2) has a shallow concavity that projects more proximally than the lateral margin (Figures 6.19a and b)

Head

Lateral extension (9) slightly broader than the medial extension (15) (Figure 6.19b broken line)

Base

1. Lateral slope of the dorsal and palmar articular margins is relatively long (Figures 6.19a, b and f)
2. Medial slope of the dorsal and palmar articular margins is relatively short (Figures 6.19a, b and f)
3. The palmar articular margin is set at a more distal level than the dorsal articular margin (Figure 6.19b)
4. Medial tubercle (3) relatively larger than lateral tubercle (7)

Figure 6.19: Morphology of the right (R) and left (L) fifth distal phalanx

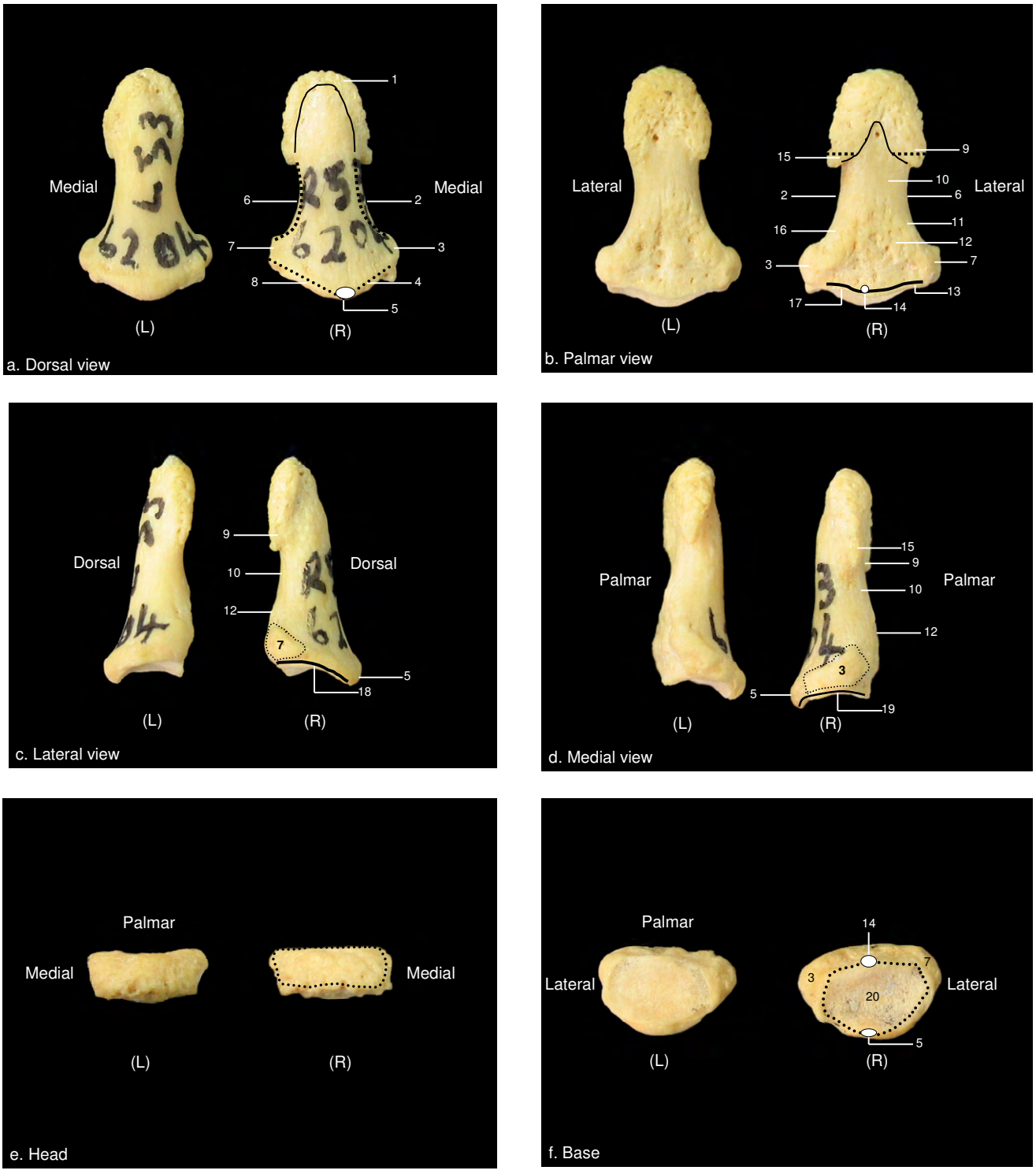

1=head, 2=medial margin of shaft, 3=medial tubercle of base, 4=dorsal medial slope of base, 5=dorsal apex of base, 6=lateral margin of shaft, 7=lateral tubercle of base, 8=dorsal lateral slope of base, 9=palmar lateral extension of head, 10=smooth distal palmar surface of shaft, 11=palmar lateral ridge of shaft, 12=rough proximal palmar concavity of shaft, 13=palmar lateral slope of base, 14=palmar apex of base, 15=palmar medial extension of head, 16=palmar medial ridge of shaft, 17=palmar medial slope of base, 18=lateral articular margin of base, 19=medial articular margin of base, 20=articular facet of base.

CHAPTER 7

RESULTS – MEASUREMENTS

7.1 Intra- and interobserver repeatability tests

An intra- and interobserver repeatability analysis was done to assess the accuracy of the measurements recorded on the hand bones before using them to determine stature and sexual dimorphism. The bones randomly selected from the total sample of 200 for this analysis included the metacarpal, proximal and distal phalanges of the thumb as well as the metacarpal, proximal, middle and distal phalanges of the little finger.

In the first instance, an intra-observer repeatability test was carried out whereby the original observer (O-O) randomly selected a sample of 36 out of the total sample of 200 individuals. The 7 dimensions of the hand bones recorded initially by the original observer on all 200 individuals, were re-measured on the metacarpal, proximal and distal phalanx of the thumb and the metacarpal, proximal, middle and distal phalanx of the little finger on the randomly selected sample of 36. The results for this paired analysis (seen as O-O in Table 7.1) showed no statistically significant differences in any of the seven dimensions for the bones of the thumb and little finger. This indicates that the measurements carried out by the original observer are repeatable.

Secondly, to test for the inter-observer repeatability test, a PhD student in Anthropology served as the second observer. She employed the same method used by the original observer to record the 7 hand bone dimensions on the same randomly selected sample of 36 individuals for all the bones of the thumb and little finger. The results for this paired analysis (O-L) of the original observer (O) and the second observer (L) are shown in Table 7.2. These results indicate that 7 measurements, all related to dimensions of the little finger, were significantly different ($p<0.05$).

The discrepancies in the midshaft region recorded by the second observer may be due to the calliper not being placed exactly at the halfway mark of the shaft. In the case of the base and head measurements, the maximum recording of the width or positioning of the calliper by

the second observer may explain the discrepancies in these readings. The anterior tilting of the head and the numerous ridges on the palmar surface of the head might have affected the method of recording the anteroposterior dimension of the head. It must be taken into account that the hand bones in general are relatively smaller than those of the rest of the skeleton. Furthermore, the dimensions of the little finger are relatively smaller in comparison with adjacent digits, especially the distal phalanx, making mistakes more likely. Special care therefore needs to be taken, especially when measuring the smaller bones.

Table 7.1: Paired *t*-Test statistics for the intra-observer test using the randomly selected bones of the thumb and little finger. All 7 dimensions of these bones are shown below. The measurements recorded by the original observer (O) were repeated by the same observer (O) at a different time

Paired observations for 7 dimensions thumb and little finger	t	df	Sig. (2-tailed)
(O) - (O) First metacarpal (thumb) length	0.86	35	0.40
(O) - (O) First metacarpal (thumb) base mediolateral	0.85	35	0.40
(O) - (O) First metacarpal (thumb) base anteroposterior	1.24	35	0.22
(O) - (O) First metacarpal (thumb) head mediolateral	-1.20	35	0.24
(O) - (O) First metacarpal (thumb) head anteroposterior	-0.30	35	0.76
(O) - (O) First metacarpal (thumb) midshaft mediolateral	-1.68	35	0.10
(O) - (O) First metacarpal (thumb) midshaft anteroposterior	-1.13	35	0.26
(O) - (O) Proximal phalanx (thumb) length	0.99	35	0.33
(O) - (O) Proximal phalanx (thumb) base mediolateral	1.08	35	0.29
(O) - (O) Proximal phalanx (thumb) base anteroposterior	-0.03	35	0.98
(O) - (O) Proximal phalanx (thumb) head mediolateral	-1.25	35	0.22
(O) - (O) Proximal phalanx (thumb) head anteroposterior	-0.22	35	0.83
(O) - (O) Proximal phalanx (thumb) midshaft mediolateral	1.60	35	0.12
(O) - (O) Proximal phalanx (thumb) midshaft anteroposterior	-0.54	35	0.59
(O) - (O) Distal phalanx (thumb) length	0.06	35	0.95
(O) - (O) Distal phalanx (thumb) base mediolateral	0.81	35	0.42
(O) - (O) Distal phalanx (thumb) base anteroposterior	-0.96	35	0.34
(O) - (O) Distal phalanx (thumb) head mediolateral	-0.81	35	0.42
(O) - (O) Distal phalanx (thumb) head anteroposterior	1.58	35	0.12
(O) - (O) Distal phalanx (thumb) midshaft mediolateral	-1.23	35	0.23
(O) - (O) Distal phalanx (thumb) midshaft anteroposterior	-0.67	35	0.51
(O) - (O) Fifth metacarpal (little finger) length	0.65	35	0.52
(O) - (O) Fifth metacarpal (little finger) base mediolateral	0.71	35	0.48
(O) - (O) Fifth metacarpal (little finger) base anteroposterior	0.30	35	0.77
(O) - (O) Fifth metacarpal (little finger) head mediolateral	1.21	35	0.23
(O) - (O) Fifth metacarpal (little finger) head anteroposterior	0.05	35	0.96
(O) - (O) Fifth metacarpal (little finger) midshaft mediolateral	-0.87	35	0.39
(O) - (O) Fifth metacarpal (little finger) midshaft anteroposterior	0.78	35	0.44
(O) - (O) Proximal phalanx (little finger) length	0.17	33	0.86
(O) - (O) Proximal phalanx (little finger) base mediolateral	0.86	34	0.40
(O) - (O) Proximal phalanx (little finger) base anteroposterior	-0.29	34	0.78
(O) - (O) Proximal phalanx (little finger) head mediolateral	0.12	34	0.90
(O) - (O) Proximal phalanx (little finger) head anteroposterior	-0.11	34	0.91
(O) - (O) Proximal phalanx (little finger) midshaft mediolateral	-0.78	34	0.44
(O) - (O) Proximal phalanx (little finger) midshaft anteroposterior	-0.89	34	0.38
(O) - (O) Middle phalanx (little finger) length	-0.86	35	0.40
(O) - (O) Middle phalanx (little finger) base mediolateral	0.70	35	0.49
(O) - (O) Middle phalanx (little finger) base anteroposterior	-2.10	35	0.04
(O) - (O) Middle phalanx (little finger) head mediolateral	0.49	35	0.62
(O) - (O) Middle phalanx (little finger) head anteroposterior	1.20	35	0.24
(O) - (O) Middle phalanx (little finger) midshaft mediolateral	0.10	35	0.92
(O) - (O) Middle phalanx (little finger) midshaft anteroposterior	-0.53	35	0.60
(O) - (O) Distal phalanx (little finger) length	-1.28	35	0.21
(O) - (O) Distal phalanx (little finger) base mediolateral	-0.75	35	0.46
(O) - (O) Distal phalanx (little finger) base anteroposterior	-0.39	35	0.70
(O) - (O) Distal phalanx (little finger) head mediolateral	-0.49	35	0.63
(O) - (O) Distal phalanx (little finger) head anteroposterior	0.04	35	0.97
(O) - (O) Distal phalanx (little finger) midshaft mediolateral	1.22	35	0.23

Table 7.2: Paired *t*-Test statistics for the inter-observer test using the randomly selected bones of the thumb and little finger. All 7 dimensions of these bones are shown below. The measurements recorded by the original observer (O) were repeated by the second observer (L) at a different time. Significant differences are indicated in bold print

Paired observations for 7 dimensions thumb and little finger	t	df	Sig. (2-tailed)
(O) - (L) First metacarpal (thumb) length	0.98	35	0.33
(O) - (L) First metacarpal (thumb) base mediolateral	0.30	35	0.76
(O) - (L) First metacarpal (thumb) base anteroposterior	0.18	35	0.86
(O) - (L) First metacarpal (thumb) head mediolateral	-0.41	35	0.68
(O) - (L) First metacarpal (thumb)head anteroposterior	0.80	35	0.43
(O) - (L) First metacarpal (thumb)midshaft mediolateral	-1.30	35	0.20
(O) - (L) First metacarpal (thumb) midshaft anteroposterior	0.24	35	0.81
(O) - (L) Proximal phalanx (thumb) length	0.52	35	0.61
(O) - (L) Proximal phalanx (thumb) base mediolateral	-0.54	35	0.59
(O) - (L) Proximal phalanx (thumb)base anteroposterior	-1.00	35	0.32
(O) - (L) Proximal phalanx (thumb) head mediolateral	-2.11	35	0.04
(O) - (L) Proximal phalanx (thumb) head anteroposterior	0.80	35	0.43
(O) - (L) Proximal phalanx (thumb) midshaft mediolateral	-0.58	35	0.57
(O) - (L) Proximal phalanx (thumb) midshaft anteroposterior	0.22	35	0.83
(O) - (L) Distal phalanx (thumb) length	-0.21	34	0.83
(O) - (L) Distal phalanx (thumb) base mediolateral	-0.77	34	0.45
(O) - (L) Distal phalanx (thumb) base anteroposterior	-1.02	34	0.31
(O) - (L) Distal phalanx (thumb) head mediolateral	-0.66	34	0.51
(O) - (L) Distal phalanx (thumb) head anteroposterior	-0.49	34	0.63
(O) - (L) Distal phalanx (thumb) midshaft mediolateral	-1.32	34	0.20
(O) - (L) Distal phalanx (thumb) midshaft anteroposterior	-1.77	34	0.08
(O) - (L) Fifth metacarpal (little finger) length	-0.47	35	0.64
(O) - (L) Fifth metacarpal (little finger) base mediolateral	0.38	35	0.71
(O) - (L) Fifth metacarpal (little finger) base anteroposterior	0.87	35	0.39
(O) - (L) Fifth metacarpal (little finger) head mediolateral	0.73	35	0.47
(O) - (L) Fifth metacarpal (little finger) head anteroposterior	0.19	35	0.85
(O) - (L) Fifth metacarpal (little finger) midshaft mediolateral	3.49	35	**0.00**
(O) - (L) Fifth metacarpal (little finger) midshaft anteroposterior	1.51	35	0.14
(O) - (L) Proximal phalanx (little finger) length	-0.87	33	0.39
(O) - (L) Proximal phalanx (little finger) base mediolateral	-5.41	34	**0.00**
(O) - (L) Proximal phalanx (little finger) base anteroposterior	1.34	34	0.19
(O) - (L) Proximal phalanx (little finger) head mediolateral	-1.00	34	0.32
(O) - (L) Proximal phalanx (little finger) head anteroposterior	-0.98	34	0.33
(O) - (L) Proximal phalanx (little finger) midshaft mediolateral	0.43	34	0.67
(O) - (L) Proximal phalanx (little finger) midshaft anteroposterior	-3.00	34	**0.01**
(O) - (L) Middle phalanx (little finger) length	-1.00	35	0.32
(O) - (L) Middle phalanx (little finger) base mediolateral	-3.37	35	**0.00**
(O) - (L) Middle phalanx (little finger) base anteroposterior	-2.02	35	**0.05**
(O) - (L) Middle phalanx (little finger) head mediolateral	-1.28	35	0.21
(O) - (L) Middle phalanx (little finger) head anteroposterior	-1.00	35	0.33
(O) - (L) Middle phalanx (little finger) midshaft mediolateral	-0.16	35	**0.87**
(O) - (L) Middle phalanx (little finger) midshaft anteroposterior	-3.41	35	**0.00**
(O) - (L) Distal phalanx (little finger) length	0.31	35	0.76
(O) - (L) Distal phalanx (little finger) base mediolateral	-0.53	35	0.60
(O) - (L) Distal phalanx (little finger) base anteroposterior	-0.11	35	0.91
(O) - (L) Distal phalanx (little finger) head mediolateral	-0.07	35	0.94
(O) - (L) Distal phalanx (little finger) head anteroposterior	6.59	35	**0.00**
(O) - (L) Distal phalanx (little finger) midshaft mediolateral	0.39	35	0.70

CHAPTER 8

RESULTS - DESCRIPTIVE STATISTICS, PEARSON'S CORRELATION ANALYSIS AND STATURE DETERMINATION

8.1 Introduction

In this section, the results of the basic descriptions as well as the analysis of variance (ANOVA) which were carried out on the hand and long bone data, are given. This analysis was done to establish whether hand and long bone dimensions display differences between males and females as well as between white and black South Africans. The descriptive analysis also gives an indication on whether these differences are statistically significant or not. Should the data not be statistically significant, then pooling of data can be considered.

The means, standard deviations and results of the ANOVA are given for all 7 dimensions of each hand bone and are reported firstly, between males and females (Tables 8.1 to 8.4) and secondly, between whites and blacks (Tables 8.5 to 8.8). The output of the ANOVA for length of five long bones, namely, humerus, radius, ulna, femur and tibia, is given firstly, between white males and white females (Table 8.9), secondly, between black males and black females (Table 8.10) and thirdly, between males in females in the South African population (Table 8.11).

Following a description of the data, a Pearson's correlation analysis is carried out to establish the strength of the relationship that each hand bone has to a long bone. Once a correlation has been established, a regression analysis is constructed and the regression coefficients obtained are then used to calculate a regression equation. The long bone length obtained from this calculation can then be entered into a second regression formula devised by Lundy and Feldesman (1987) and Dayal *et al*. (2008) for estimating stature of an individual.

8.1.1 Descriptive statistics for hand bones of South African males and females

A comparison of all 7 dimensions of each bone in the hand between the sexes is seen in Tables 8.1 to 8.4. The results are reported for metacarpals (Tables 8.1a,b), proximal

phalanges (Tables 8.2a,b), middle phalanges (Tables 8.3a,b) and distal phalanges (Tables 8.4a,b). The mean values (mm) recorded for all 7 dimensions on the metacarpals and phalanges are significantly greater ($p<0.01$) in males than in females. Thus, differences between the sexes are highly significant and constant for the total sample of hand bones measured.

8.1.2 Descriptive statistics for hand bones of South African whites and blacks

A comparison of the 7 dimensions of each hand bone between South African whites and blacks in the male and female group is seen in Tables 8.5 to 8.8. The results are also reported for the following series of hand bones, namely, metacarpals (Tables 8.5a,b), proximal phalanges (Tables 8.6a,b), middle phalanges (Tables 8.7a,b) and distal phalanges (Tables 8.8a,b). In contrast to the findings between the sexes, marked variation occurred when comparisons of the dimensions of the hand bones are made between whites and blacks. Due to these differences, each series of hand bones will be reported independently from each other.

Results for the metacarpals recorded in males (Tables 8.5a,b) indicate that in general, South African whites had significantly larger ($p<0.01$) dimensions than blacks. Out of a total of 35 measurements recorded, 16 were not statistically significant.

Metacarpal measurements for the female group also showed a trend towards significantly greater ($p<0.01$) dimensions in whites than in blacks, with the exception of 13 cases. Of these exceptions, six were significantly different at $p<0.01$ and two at $p<0.05$, namely, the mediolateral (ml) and anteroposterior (ap) midshaft dimension of the first metacarpal, anteroposterior (ap) midshaft dimension of the second and third metacarpals, mediolateral (ml) and anteroposterior (ap) midshaft dimensions of the fourth and fifth metacarpals respectively.

A comparison of the first row of bones in the phalangeal series, namely, the proximal phalanges between whites and blacks (Table 8.6a,b), shows that most dimensions are significantly greater ($p<0.01$) in whites than in blacks, except for three cases in the male group

and eight cases in the female group where the reverse is true. Of these exceptions, none of these differences in males were statistically significant while only two cases in the female group were significantly different ($p<0.01$). These included the length dimensions of the third ($p<0.01$) and fourth ($p<0.05$) proximal phalanges.

A comparison of middle phalangeal dimensions between whites and blacks (Table 8.7a,b) shows the values to be significantly greater in whites than in blacks with a few exceptions. These include two dimensions in the male group which were not statistically significantly different. Of the eight dimensions in females, which were larger in blacks than in whites, only three were significantly different ($p<0.01$). These include the anteroposterior (ap) midshaft dimensions of the third, fourth and fifth middle phalanges ($p<0.01$.

Findings of the distal phalanges (Table 8.8a,b) show all dimensions to be significantly greater in whites than in blacks except for two dimensions in males and 17 dimensions in females. These two dimensions are the anteroposterior (ap) midshaft dimension of the third and fifth distal phalanges.

In summary, all 7 dimensions on each of the hand bones are significantly greater in males than in females. On the other hand, while the same dimensions tended to be greater in whites than in blacks, a large number of cases, especially in the female group, showed the opposite. Many of the observed differences were not significantly different either way. Thus, data for the white and black groups were pooled and only pooled data for males and females will used for further analyses in estimating stature and sexual dimorphism. Furthermore, as the population of origin for single hand bones will not be known in a forensic setting, it gives additional support to pooling of the data.

8.1.3 Descriptive statistics for the humerus, radius, ulna, femur and tibia

A comparison of long bone lengths between the sexes in the white (Table 8.9) and black groups (Table 8.10) indicate significantly greater ($p<0.01$) dimensions in males than in females. Pooling the data for whites and blacks (Table 8.11) also indicate significantly greater

($p<0.01$) long bone lengths in males than in females. For estimation of stature, data on length of long bones for whites and blacks will also be pooled.

8.2 DETERMINATION OF STATURE

The first step in estimating the height of an individual is to determine whether a correlation between the dependent and independent variables exists or not. If a correlation does exist, then the highest correlation value needs to be recorded as this would indicate the strength between the dependent and independent variables. In the present study, the correlation between each hand bone and each of the five long bones, namely, humerus, radius, ulna, femur and tibia will be assessed. Pearson's correlation statistics was employed to carry out this analysis.

8.2.1 Pearson's Correlation Coefficient

Pearson correlation coefficients (r) can only take on values from -1 to +1. If there is a positive sign in front of the value, then it indicates a positive correlation. In other words, as one variable increases, so too does the other one. A negative sign in front of the value indicates a negative correlation. This means that as one variable increases the other decreases. If the sign is ignored, the size of the absolute value should provide an indication of the strength of the relationship between the hand bones to the long bones. The ideal situation is when there is a perfect correlation, indicated by a -1 or +1. In this case the value of one of the variables can be used to accurately determine the value of the other variable. A correlation of zero is an indication that there is no relationship between the two variables under study. In other words, if the value of one variable is known then it cannot be used to predict the value of the other variable (Pallant 2001). The correlation results for males and females of the present study will now be reported.

8.2.1.1 Correlation results for males

In the present study, the relationships between the lengths of the hand bones (metacarpals, proximal, middle and distal phalanges) to the lengths of five long bones of the limbs (humerus, radius, ulna, femur and tibia) were determined. The results for South African males are shown in Table 8.12. Although the results indicate that most of the correlations are statistically significant (indicated by the 2-tailed test of significance), the correlation coefficients for each of the hand bones differ. The length of the first metacarpal is highly correlated to the humeral length (r=0.592) with the lowest correlation to radial length (r=0.459). The length of the second metacarpal is best correlated to radial length (r=0.785) and least correlated to humeral length (r=0.678). The correlation coefficients for the second metacarpal are higher than those observed for the first metacarpal suggesting that the second metacarpal is the bone of choice to regress to the radius. The lengths of the third and fourth metacarpals are best correlated to the tibia (r=0.745 and 0.663) and radius (r=0.744 and 0.619) and least correlated to the femur (r=0.439 and r=0.525 for the third and fourth metacarpals respectively). It is assumed that the hand bones would have a high correlation to upper limb bones as they form part of the same limb, rather than to a lower limb bone. This is clearly not the case with the third and fourth metacarpals. Similar to the results of the second metacarpal, the length of the fifth metacarpal was also best correlated to the radial length (r= 0.628), but least correlated to the femoral length (r=0.401). The results for the metacarpals show great variability, but in general, the best correlations are found with the radius.

With the exception of the first proximal phalanx, all proximal phalanges were best correlated to the tibia (r=0.511, r=0.631, r=0.682, r=0.715, r=0.593 for proximal phalanges two to five). The first proximal phalanx was best correlated to the humerus (r=0.535). In the case of proximal phalanges two to five, a lower limb rather than an upper limb bone seems to be strongly related in males.

The length of the second middle phalanx is best correlated to the femur (r=0.555), the third to the tibia (r=0.0.409), the fourth to the humerus (r=0.504) and the fifth to the tibia (r=0.472) lengths. The long bones found to be the least correlated are the ulna in the case of

the second (r=0.449) and fourth (r=0.279) middle phalanges and the femur in the case of the third (r=0.281) and fifth (r=0.279) middle phalanges.

The length of the first distal phalanx is best correlated to the tibial length (r=0.467) while the lengths of the second (r=0.462), third (r=0.291), fourth (r=0.521) and fifth (r=0.567) distal phalanges are best correlated to humeral length. The lengths of the distal phalanges are least correlated to femoral length in the case of the first (r=0.372) distal phalanx, to radial length in the case of the second (r=0.244), third (r=0.110 for radius and ulna) and fifth (r=0.235) distal phalanges and to tibial length in the case of the fourth (r=0.334) distal phalanx.

In general, the correlations for males are not very high. A correlation value of 0.5 would indicate that 50% of the length of one of the long limb bones, for example, the humerus, can be explained by the length of the fourth metacarpal. In other words, r=0.5 would account for 25% of the explanatory power (r^2). Higher correlation values are seen with the metacarpals and proximal phalanges, while lower correlations are seen in the middle and distal phalanges.

8.2.1.2 Correlation results for females

This section deals with the relationship between the lengths of the hand bones (metacarpals, proximal, middle, and distal phalanges) to the lengths of five long bones of the limbs (humerus, radius, ulna, femur, and tibia) for South African females. These results, which are shown in Table 8.13, are more consistent than those seen in males. The lengths of all hand bones are best correlated to radial length (ranging from r=0.432 to r=0.902). The highest correlation is found in the relationship of the second metacarpal to the radius (r=0.902) and the lowest correlation is seen in the fourth distal phalanx to the humerus (r=0.244).

Generally, correlations were high for the metacarpals, becoming gradually lower from proximal to distal phalanges. The hand bones showed a consistent pattern of being most closely correlated to radial length.

8.3 Regression analysis – direct and stepwise procedures

Once a correlation between the length of a hand bone and the length of a long bone has been established, the next step would be to regress, in a direct and stepwise manner, the length of an independent variable (e.g., a hand bone) to that of a dependent variable (e.g., long limb bone such as the humerus). In the direct approach, all variables are entered in no specific order into the analysis and the output, namely, the regression coefficient, prediction accuracy in percentage and standard error of the estimate (SEE), is given in the same order. In the case of the stepwise analysis, all independent variables are entered into the analysis and the computer generates the best predictor in a stepwise manner (Pallant 2001).

The direct analysis is done if the dimensions of, for example, all the hand bones are entered into the analysis in no specific order and regressed to each of the long bones. The output indicates the regression coefficient value as well as the percentage that the dimensions of the hand bones will contribute to the variation in dimension of a long bone. On the other hand, if only a single hand bone is available to regress to a long bone, then the direct approach can also be used. A stepwise approach is done when all the hand bones are available and these are entered in no specific order in the analysis, then a computer generated output will indicate which hand bone will be the best predictor from the entire series to regress to a long bone.

In both the direct and stepwise outputs, the R, R^2, adjusted R^2 and the standard error of the mean are given. The R value indicates the regression coefficient value. The R^2 value explains the percentage that a dimension contributes to the variation in the dependent variable, although where the R^2 value is reported with small sample sizes it is said to overestimate the true value in a population. The adjusted R^2 corrects this to provide a better estimate of the true population value and is often given when small samples are used (Pallant 2001). In the present study where there is a fairly large sample size, the R^2 rather than the adjusted R^2 value will be reported. In the regression results, some of the slopes will have a positive value which indicates that as the length of a hand bone increases the length of a long bone is also increasing. On the other hand, if the value of the slope is negative, then it

indicates that as the length of a metacarpal increases the length of the long bone is reducing at the same time. Once the regression coefficient, slope, constant and the standard error of estimate is obtained, a regression equation is then calculated.

In the present study, the results for the regression analysis will be given separately for males and females. This will then be followed by the calculation of a regression formula for males and females.

8.3.1 Regression analysis in South African males

8.3.1.1 Metacarpals

Table 8.14 shows the results of the direct and stepwise regression analysis using metacarpal lengths to predict long bone length in South African males. In the direct approach where the lengths of all metacarpals are entered in no particular order into the analysis, the entire group of bones best correlates to the radius and its variation in length (R=0.820, R^2=67.3%), while the same group of hand bones has the weakest correlation to the humerus (R=0.722, R^2=52.1%).

On the other hand, when the metacarpals are entered individually into the analysis a different result is given for each bone. The first metacarpal is best correlated to the humerus (R=0.592, R^2=35.1%), the second metacarpal to the radius (R=0.785, R^2=61.6%), the third (R=0.745, R^2=55.6%) and fourth (R=0.663, R^2=44.0%) metacarpals to the tibia and the fifth metacarpal to the radius (R=0.628, R^2=39.4%). The second metacarpal thus seems to be the bone of preference in the entire series to predict radial or the tibial length if no other metacarpal is present. On the other hand, if the entire series of metacarpals are present, then all the metacarpals should be entered as a single group and regressed to radial length.

In the stepwise model 1 approach, the bone generated by the computer as the best predictor is the second metacarpal which has the highest correlation to the radius (R=0.785, R^2=61.6%). The second metacarpal can also be used to determine length of the humerus, ulna and femur although the correlations are much weaker than with the radius, while the third

metacarpal in the model 1 approach best correlates to the tibia (R=0.745, R^2=55.4%) with percentages less than that for the second metacarpal.

In the stepwise model 2 approach, one has the option of choosing two metacarpals to predict long bone length. While the first and second metacarpals can be used to predict humeral and radial length, the highest correlation value is seen with the radius (R=0.807, R^2=65.1%) rather than with the humerus (R=0.711, R^2=50.5%). The two hand bones that can be used to predict ulna, femoral and tibial length are the second and third metacarpals. These hand bones have the highest correlations to the ulna (R=0.791, R^2=62.5%) and the lowest to the femur (R=0.709, R^2=50.3%).

In the stepwise model 3 approach the option of three hand bones are given which can be used to predict radial, ulna and femoral length. In the case of the radius, it is the first, second and fourth metacarpal (R=0.818, R^2=67%), for the ulna it is the second, third and fourth metacarpal (R=0.803, R^2=64%) while the first, second and third metacarpal can be regressed to the femur (R=0.735, R^2=54%).

Table 8.15 gives the values for the slope and constant of metacarpals which will be used in calculating a regression equation in males. The direct analysis gives an overall indication of positive slope values. In other words, an increase in metacarpal length results in an increase in long bone length. In cases where a negative slope occurs, an inverse relationship of metacarpal length to long bone length takes place. Examples of these are the first metacarpal to the radius, the third metacarpal to the humerus and femur, the fourth metacarpal to all long bones except the femur and lastly, the fifth metacarpal to the femur. The results for individual metacarpals in the direct analysis indicate positive values for all long bones. In the stepwise model 1 analysis, positive slopes are given for the second and third metacarpals. For the stepwise model 2 results, there is a negative value for the third metacarpal to the femur. In the stepwise model 3 analysis, negative slopes are given for the third metacarpal to the femur and for the fourth metacarpal to the radius and ulna.

In conclusion, different metacarpals are linked to different long bones. This indicates great variation in males. However, in the stepwise analyses the second metacarpal seems to

be the ideal bone in the metacarpal series to regress to four of the five long bones in the model 1 results while in the stepwise model two approach it is selected for all five long bones. Additionally, the standard error of the estimate is fairly large (up to 13.9 mm).

8.3.1.2 Proximal phalanges

Table 8.16 shows the results of the direct and stepwise regression analysis using proximal phalangeal lengths to regress to long limb bone lengths in South African males. In the direct approach where all these bones are entered in no particular order into the analysis, the highest correlations are to tibial length (R=0.740, R^2=54.8%) and the lowest to the femur length (R=0.622, R^2=38.7%).

On the other hand, when the proximal phalanges are entered individually into the analysis a different result is obtained for each hand bone. The first proximal phalanx is best correlated to the humerus (R=0.535, R^2=28.7%). The rest of the proximal phalanges are best correlated to the tibia with results of R=0.631, R^2=39.8% (second proximal phalanx), R=0.682, R^2=46.5% (third proximal phalanx), R=0.715, R^2=51.1% (fourth proximal phalanx) and R=0.593, R^2=35.2% (fifth proximal phalanx). The fourth proximal phalanx seems to be the bone of preference in the entire series to regress to the tibial length. On the other hand, if the entire series of proximal phalanges are present, then all of them should be entered as a single group and regressed to tibial length as higher correlations are obtained.

In the stepwise model 1 approach, a different hand bone is generated by the computer as the best predictor for each of the five long bones. For example, the proximal phalanx that best predicts the humerus and femur is the second bone. The correlation values for the humerus are R=0.642, R^2=41.3% which is slightly higher than those of the femur (R=0.618, R^2=38.2%). The third proximal phalanx best predicts the ulna (R=0.648, R^2=42.0%) while the fourth proximal phalanx is linked to the radius (R=0.614, R^2=37.7%) and tibia (R=0.719, R^2=51.7%).

In the stepwise model 2 approach, the two bones generated by the computer as the best predictors for the tibia (R=0.735, R^2=54.0%) are the second and fourth proximal phalanges. The regression coefficient results for proximal phalanges are shown in Table 8.17.

In conclusion, it appears that the second, third and fourth proximal phalanges are the best predictors for long bones. The low correlation values for the first and fifth proximal phalanges indicate that they are not good predictors of any long bone lengths with standard errors of estimate up to 13.9 mm.

8.3.1.3 Middle phalanges

Table 8.18 shows the results of the direct and stepwise regression analysis using lengths of the middle phalanges to regress to long bone lengths in South African males. In the direct approach where the lengths of the entire series are entered in no particular order into the analysis, the group as a whole had the highest correlation to humeral length (R=0.635, R^2=40.3%) while the same group of hand bones had the lowest correlation to ulna length (R=0.558, R^2=31.2%).

When the middle phalanges are entered individually into the analysis a different result is given for each bone. The second middle phalanx is best correlated to the femur (R=0.535, R^2=30.8%), the third (R=0.409, R^2=16.7%) and fifth (R=0.472, R^2=22.2%) middle phalanges to the tibia and the fourth to the humerus (R=0.504, R^2=25.4%). The second middle phalanx seems to be the bone of preference in the entire series to regress to femoral length. On the other hand, if the entire series of middle phalanges are present, then all of them should be entered as a group and regressed to the tibial length as this yields far higher correlations than if just a single bone was entered into the anaysis.

In the stepwise model 1 approach, the hand bone generated by the computer as the best predictor differed for each of the long bones. For example, the second middle phalanx has the highest correlation to the humerus (R=0.575 R^2=33.1%) and femur (R=0.555, R^2=30.9%). The fourth middle phalanx has the highest correlation to the tibia (R=0.528, R^2=27.9%), radius (R=0.493, R^2=24.3%) and ulna (R=0.477, R^2=22.7%).

In the stepwise model 2 approach, the two hand bones generated by the computer as the best predictors for all five long bones are the second and fourth middle phalanges. The regression coefficient results for middle phalanges are shown in Table 8.19.

In conclusion, the second and fourth middle phalanges are the best bones in the middle phalangeal series to regress to that of a long bone. The standard error of the estimate is slightly higher than those of the proximal phalangeal series, reaching values of up to 14.8 mm.

8.3.1.4 Distal phalanges

Table 8.20 shows the results of the direct and stepwise regression analysis using lengths of the distal phalanges to regress to long bone lengths in South African males. In the direct approach where the lengths of the entire series are entered in no particular order into the analysis, the group as a whole presented with the highest correlation to humeral length (R=0.657, R^2=43.1%) while the same group of hand bones has the lowest correlation to tibia length (R=0.541, R^2=29.3%).

When the distal phalanges are entered individually into the analysis a different result is given for each bone. The first distal phalanx is best correlated to the tibia (R=0.467, R^2=21.8%) while the second (R=0.462, R^2=21.3%), third (R=0.291, R^2=0.08%), fourth (R=0.521, R^2=27.2%) and fifth (R=0.567, R^2=32.2%) distal phalanges are best correlated to the humerus. The fifth distal phalanx seems to be the bone of choice to regress to humeral length.

In the stepwise model 1 approach, the bone generated by the computer as the best predictor includes the first and fifth distal phalanges. The first distal phalanx is the best predictor for the radius (R=0.452, R^2=20.4%), ulna (R=0.471, R^2=22.2%), femur (R=0.559, R^2=31.2%) and tibia (R=0.490, R^2=24.0%). Regression coefficient values for the distal phalanges are seen in Table 8.21.

In conclusion, the fifth distal phalanx is selected as the best predictor for the humerus (R=0.600 R^2=36.0%). Futhermore, correlation values of distal phalangeal length to long bone length are low in comparison to the proximal and middle phalanges with standard error of the estimate up to 14.3 mm.

8.3.2 Regression analysis in South African females

8.3.2.1 Metacarpals

Table 8.22 shows the results of the direct and stepwise regression analysis using metacarpal lengths against the lengths of the long limb bones in South African females. In the direct approach where the lengths of all metacarpals are entered in no particular order into the analysis, the entire group of bones has the highest correlation to radial length (R=0.926, R^2=85.7%) while the same group of hand bones has the lowest correlation to humeral length (R=0.797, R^2=63.5%). These results are far higher than those reported for males for the same group of hand bones.

In comparison to the results for males where individual metacarpals were correlated to different long bones, the results in females indicate consistency throughout the analysis in that each metacarpal is best correlated to the radius. The values produced from the regression analysis for the individual metacarpals are R=0.827, R^2=68.4 % (first metacarpal), R=0.902, R^2=81.4 % (second metacarpal), R=0.844, R^2=71.2 % (third metacarpal), R=0.812, R^2=66.0 % (fourth metacarpal) and R=0.806, R^2=65.0 % (fifth metacarpal). From this series of hand bones, the highest percentage recorded is for the second metacarpal. This is also the hand bone that has the highest correlation to the radius. If the entire series of metacarpals are available, then they should be entered as a group and regressed to the radial length.

In the stepwise model 1 approach, the bone generated by the computer as the best predictor for all five long bones is the second metacarpal, which also has the highest correlation value to the radius (R=0.904, R^2=81.7%).

In the stepwise model 2 approach, the two hand bones generated by the computer as the best predictors vary for each long bone. For the humerus (R=0.780, R^2=60.8%) and femur (R=0.790, R^2=62.4.7%) it is the second and fourth metacarpals, for the radius (R=0.924, R^2=85.3%) and ulna (R=0.879, R^2=77.3%) it is the first and second metacarpals, while the second and fifth metacarpals can be used as predictors for the tibia (R=0.849, R^2=72.1%).

In the stepwise model 3 approach, the three hand bones selected also vary for the different long bones. For the humerus (R=0.792, R^2=62.8%), the bones selected are the first, second and fourth metacarpals, for the ulna (R=0.897, R^2=80.5%) it is the first, second and fifth metacarpals. The femur (R=0.841, R^2=70.7%) can be predicted using the second, third and fourth metacarpals while the second, third and fifth metacarpals are selected as predictors for the tibia (R=0.879, R^2=77.3%).

In the stepwise model 4 approach, there is the option of using four metacarpals to predict tibial length (R=0.906, R^2=82.1%). Except for the first metacarpal, all the other metacarpals are selected as predictors for this long bone. The results for the regression coefficients in females are shown in Table 8.23, which generally indicates positive slope values.

In conclusion, while the second metacarpal is correlated to all long bones, the best correlation is to the radius. Given the results on regression coefficients for the metacarpals, it is evident that increases in length of these bones result in a simultaneous increase in the length of a long bone. Fairly large standard errors of estimate up to 12.1 mm were obtained.

8.3.2.2 Proximal phalanges

Table 8.24 sets out the results for the direct and stepwise regression analysis using proximal phalangeal lengths to regress to long bone lengths in South African females. In the direct approach all proximal phalanges are entered into the analysis in no particular order. The highest correlations are obtained for the radius (R=0.788 and R^2=62.2%) and the lowest values for the femur (R=0.533, R^2=28.4%).

Entering the proximal phalanges individually into the direct analysis also produces high correlations to the radius. These high correlation values are given for the first (R=0.706 and R^2=49.9 %), second (R=0.648 and R^2=41.9 %), third (R=0.680 and R^2=46.3 %), fourth (R=0.717 and R^2=51.4 %) and fifth (R=0.597 and R^2=35.7%) proximal phalanges.

In the stepwise model 1 approach, the bone generated by the computer as the best predictor for the humerus (R=0.474, R^2=22.5%) and femur (R=0.461, R^2=21.2%) is the second

proximal phalanx. In the case of the radius (R=0.722, R^2=52.1%), ulna (R=0.695, R^2=48.3%) and tibia (R=0.601, R^2=36.1%) it is the fourth proximal phalanx.

In the stepwise model 2 approach, the two bones generated by the computer as the best predictors for the radius (R=0.777, R^2=60.4%) and ulna (R=0.734, R^2=53.8%) are the first and fourth proximal phalanges. In the case of the femur (R=0.511, R^2=26.1%) it is the first and second proximal phalanges. Regression coefficient values for proximal phalanges are shown in Table 8.25.

In conclusion, while the best correlation of each proximal phalanx varies for each long bone, the stepwise analysis indicates that the first, second and fourth proximal phalanges appear to be the hand bones of choice to predict the length of a long bone. This series of bones has standard errors of estimate up to 13.5 mm.

8.3.2.3 Middle phalanges

Table 8.26 shows the results for the direct and stepwise regression analysis using middle phalangeal lengths to predict long bone lengths in South African females. In the direct approach where the entire series is entered into the analysis in no particular order, the highest correlation is to radial length (R=0.694, R^2=48.1%) and the lowest correlation is to humeral length (R=0.488, R^2=23.8%).

Entering the middle phalanges individually into the direct analysis also gives the highest correlation to the radius in females. These regression values are given for the second (R=0.494, R^2=24.4%), third (R=0.654, R^2=42.7%), fourth (R=0.619, R^2=38.3%), and fifth (R=0.444, R^2=19.7%) middle phalanges. A comparison of these results indicates that the third bone in this series has the highest correlation values.

In the stepwise model 1 approach, the bone generated by the computer as the best one in the series to predict length of long bones is the third middle phalanx with the highest correlation being to the radius (R=0.651 R^2=42.3%).

In the stepwise model 2 approach, the two hand bones generated by the computer as the best predictors for the radius(R=0.682, R^2=46.5%) are the third and fifth middle phalanges.

In the case of the ulna (R=0.620, R^2=38.5%) and tibia (R=0.573, R^2=32.9%) the third and fourth middle phalanges are selected. Regression coefficient results for middle phalanges are shown in Table 8.27.

In conclusion, the third middle phalanx seems to be the ideal bone in the middle phalangeal series to predict radial length in females with standard error of the estimate up to 14.2 mm. On the other hand, if the entire series of middle phalanges is present, then this would be preferred over regression of a single bone.

8.3.2.4 Distal phalanges

Table 8.28 shows the results of the direct and stepwise regression analysis using distal phalangeal lengths to predict long bone lengths in South African females. In the direct approach the entire series of distal phalanges are entered into the analysis in no particular order. The highest correlations were to the radius (R=0.600, R^2=36.0%) and the lowest correlations were reported for the tibia (R=0.442, R^2=19.5%).

Entering the distal phalanges individually into the analysis also indicated high correlations to the radius. The regression values obtained are given for the first (R=0.474, R^2=22.4%), second (R=0.470, R^2=22.1%), third (R=0.507, R^2=25.7%), fourth (R=0.486, R^2=23.6%) and fifth (R=0.432, R^2=18.7%) distal phlanges. The hand bone with the best correlation value and highest percentage to predict radial length in this series of hand bones is the third distal phalanx.

In the stepwise model 1 approach, the bone generated by the computer as the best predictor is the first distal phalanx which has the highest correlation to the radius (R=0.583 R^2=34.0%). Regression coefficient results for distal phalanges are shown in Table 8.29.

In conclusion, the first distal phalanx is the bone of choice to predict any of the five long bones based on the stepwise analysis with the highest correlation being to the radius with standard error estimates up to 14.4 mm. On the other hand, if all five distal phalanges are available and they are entered individually into the analysis, then the third distal phalanx is the

bone of choice. The R values are generally low and standard error of the estimate is high reaching values of up to 14.5 mm.

8.4 Calculation of regression equations

When calculating a regression equation the following steps are followed:

1) The hand bone/s must first be identified
2) The length of the hand bone must then be measured
3) Tables 8.12 and 8.13 are then used to pair the hand bone with the highest correlation to a long bone
4) The regression coefficients (i.e. the slope and constant) and standard error of the estimate are then obtained from the regression tables in this study (Tables 8.14 to 8.21) for the specific hand bone that is to be regressed to a specific long bone
5) The following formula is then used:

y=mx+c

[where, y=length (mm) of a long bone (e.g. humerus), m= length (mm) of hand bone, x= slope and c=constant]

6) Once the length of a hand bone has been regressed to that of a long bone, the value obtained is inserted into a second equation developed by Lundy and Feldesman (1987) or Dayal *et al*. (2008). These authors have devised regression formulae for estimating living stature from long bones of the South African black and white groups.

Example

The hand bone of an unknown individual was found and identified as the first metacarpal. The length measurement of the first metacarpal is then taken, e.g., 45.86 mm. Once the length has been recorded, refer to Tables 8.12 and 8.13 to see which long bone length has the highest correlation value to the first metacarpal. In males (Table 8.12), the first metacarpal would be regressed to humeral length while in females (Table 8.13) it will be to radial length. The next step would be to look up the value of the slope and constant for the first

metacarpal which would be found in Table 8.15 for males and Table 8.23 for females. In males the value of the slope for the first metacarpal (MC1) is 2.717 and the constant is 205,515 (Table 8.15; metacarpal 1; humerus). In females the value of the slope is 3.233 and the constant is 92.970 (Table 8.23; metacarpal 1, radius). Once these values are obtained, then calculation of the regression equation for males and females is as follows:

For males, the formula using the first metacarpal will be:

Y (humeral length) = 45.86 (metacarpal length) x 2.717 (slope) + 205.515 (constant) ± S.E.E

= 330.12 ± 10.618 mm

For females, the formula using the first metacarpal will be:

Y (radial length) = 45.86 (metacarpal length) x 3.233 (slope) + 92.970 (constant) ± S.E.E

= 306.84 ± 5.818 mm

The height of an individual now needs to be calculated. In order to do this, the calculated long bone length (e.g. humeral length), is now inserted into an appropriate formula such as those devised by Lundy and Feldesman (1987) and Dayal et al. (2008).

Note:

The above example is for a single hand bone that is found. Ideally, the entire series such as the entire row of metacarpals is of greater value in that it increases the prediction accuracy.

In a case where all five metacarpals are available, and it is suspected that they belong to a male, the first step would be to measure their lengths (mm). The next step would be to go to Table 8.14. When all five metacarpals are available, they can be used to best predict the length of the radius (R=0.820, R^2=67.3%). Table 8.15 lists the values of the slope, constant and standard error of the estimate.

Measurements

metacarpal (MC) 1 length = 45.86mm (slope = -0.056)

metacarpal (MC) 2 length = 68.19mm (slope = 1.289)

metacarpal (MC) 3 length = 66.28mm (slope = 0.874)

metacarpal (MC) 4 length = 58.88mm (slope = -0.747)

metacarpal (MC) 5 length = 54.32mm (slope = 0.312)

the constant = 138.832

standard error of the estimate (SEE) = 5.16864

Using the following formula:

Y (humeral length) = [MC1 length x (slope)] + [MC2 length x (slope)] + [MC3 length x (slope)] + [MC4 length x (slope)] + [MC5 length x (slope)] + constant ± S.E.E

Insert the appropriate values into the above formula:

Y (radial length) = [45.86 x (-0.056)] + [68.19 x (1.289)] + [66.28 x (0.874)] + [58.88 x (-0.747)] + [54.32 x (0.312)] + 138.832 (constant) ± 5.168 (SEE)

Y (radial length) = [-256.816] + [87.89] + [57.93] - [43.98] + [16.95] + 138.832 (constant) ± 5.168 (SEE)

Y (radial length male) = 257.62 ± 5.168 mm

The calculated long bone length (i.e. radial length), is now inserted into the appropriate formulae of Lundy and Feldesman (1987) and Dayal *et al.* (2008) in order to estimate stature. It should once again be emphasized that it is better to use more than one hand bone as this increases the accuracy for predicting the length of a long bone.

Table 8.1a. Descriptive statistics comparing mean values (mm) of metacarpals (MC) 1 to 3 between males and females in South African whites and blacks

	WHITE				BLACK		
Variable	Sex	Mean	S.D.	P	Mean	S.D.	P
MC1 length	Male	46.21	2.59	0.0000	45.53	3.09	0.0000
	Female	42.64	2.65		42.48	2.75	
MC1 base ml	Male	16.38	1.33	0.0000	16.17	1.46	0.0000
	Female	15.04	1.55		14.37	0.94	
MC1 base ap	Male	16.61	1.73	0.0087	16.27	1.56	0.0000
	Female	15.62	1.91		14.26	1.15	
MC1 head ml	Male	15.91	1.59	0.0000	16.08	1.40	0.0000
	Female	14.30	1.16		14.29	1.10	
MC1 head ap	Male	15.36	1.39	0.0000	14.04	1.36	0.0000
	Female	13.67	1.42		12.66	1.04	
MC1 midshaft ml	Male	13.13	1.06	0.0000	12.85	1.12	0.0000
	Female	11.04	0.96		11.59	1.01	
MC1 midshaft ap	Male	9.19	0.78	0.0000	9.42	0.86	0.0000
	Female	8.01	0.89		8.39	0.81	
MC2 length	Male	68.60	3.63	0.0000	67.80	4.62	0.0000
	Female	64.30	3.25		64.11	4.42	
MC2 base ml	Male	18.70	1.45	0.0000	17.03	1.59	0.0000
	Female	16.30	1.16		15.37	1.40	
MC2 base ap	Male	17.94	1.60	0.0000	17.05	1.44	0.0000
	Female	15.79	1.31		15.38	1.19	
MC2 head ml	Male	15.55	1.50	0.0000	14.49	1.07	0.0000
	Female	13.87	1.11		13.29	0.97	
MC2 head ap	Male	15.36	1.06	0.0000	14.60	0.89	0.0000
	Female	14.01	0.99		13.27	0.91	
MC2 midshaft ml	Male	9.52	0.83	0.0000	9.00	0.71	0.0000
	Female	8.30	0.76		8.28	0.73	
MC2 midshaft ap	Male	9.76	0.81	0.0000	9.90	1.32	0.0000
	Female	8.32	0.79		8.78	0.82	
MC3 length	Male	65.85	3.90	0.0000	66.68	4.38	0.0000
	Female	61.90	3.61		62.80	4.04	
MC3 base ml	Male	14.87	0.84	0.0000	14.05	1.14	0.0000
	Female	13.46	1.16		12.81	0.84	
MC3 base ap	Male	18.14	1.27	0.0000	17.29	1.17	0.0000
	Female	16.04	1.48		15.46	0.90	
MC3 head ml	Male	14.57	1.28	0.0000	14.33	1.09	0.0000
	Female	13.12	1.22		12.95	0.89	
MC3 head ap	Male	15.44	0.99	0.0000	14.72	1.03	0.0000
	Female	13.75	1.04		13.27	0.85	
MC3 midshaft ml	Male	9.42	0.75	0.0000	9.15	0.70	0.0000
	Female	8.37	0.64		8.50	0.75	
MC3 midshaft ap	Male	10.10	0.89	0.0000	10.04	1.09	0.0000
	Female	8.63	0.78		9.06	0.85	

Total sample=200, S.D. = standard deviation, ap = anteroposterior, ml = mediolateral
P = level of significance

Table 8.1b. Descriptive statistics comparing mean values of metacarpals (MC) 4 and 5 between males and females in South African whites and blacks

	WHITE				BLACK		
Variable	Sex	Mean	S.D.	P	Mean	S.D.	P
MC4 length	Male	59.06	2.85	0.0000	58.71	4.25	0.0000
	Female	54.60	3.17		55.73	3.67	
MC4 base ml	Male	12.53	1.04	0.0000	11.46	1.05	0.0000
	Female	11.09	0.93		10.30	0.69	
MC4 base ap	Male	13.29	0.96	0.0000	12.88	1.12	0.0000
	Female	11.42	0.96		11.74	0.93	
MC4 head ml	Male	12.73	0.96	0.0000	12.24	0.89	0.0000
	Female	11.41	1.48		11.42	0.87	
MC4 head ap	Male	13.89	0.90	0.0000	13.27	1.14	0.0000
	Female	12.28	0.89		12.30	0.86	
MC4 midshaft ml	Male	7.88	0.86	0.0000	7.75	0.83	0.0000
	Female	6.63	0.59		6.98	0.68	
MC4 midshaft ap	Male	8.28	0.92	0.0000	8.59	0.88	0.0000
	Female	6.67	0.70		7.78	0.79	
MC5 length	Male	54.35	2.85	0.0000	54.30	3.58	0.0000
	Female	51.10	2.88		50.75	3.71	
MC5 base ml	Male	14.55	1.29	0.0000	13.45	1.29	0.0000
	Female	12.98	1.26		11.83	0.92	
MC5 base ap	Male	12.42	1.20	0.0000	11.66	1.08	0.0000
	Female	10.90	1.01		10.27	0.81	
MC5 head ml	Male	12.47	1.00	0.0000	11.94	0.98	0.0000
	Female	11.01	0.89		10.70	0.87	
MC5 head ap	Male	12.82	0.92	0.0000	12.22	0.78	0.0000
	Female	11.44	0.81		11.16	0.84	
MC5 midshaft ml	Male	8.58	0.88	0.0000	8.58	0.85	0.0000
	Female	7.21	0.71		7.76	0.81	
MC5 midshaft ap	Male	7.83	1.02	0.0000	7.80	1.08	0.0000
	Female	6.42	0.73		6.74	0.74	

Total sample=200, S.D. = standard deviation, ap = anteroposterior, ml = mediolateral
P = level of significance

Table 8.2a. Descriptive statistics comparing mean values (mm) of proximal phalanges (PP) 1 to 3 between males and females in South African whites and blacks

	WHITE				BLACK		
Variable	Sex	Mean	S.D.	P	Mean	S.D.	P
PP1 length	Male	31.24	1.84	0.0000	30.82	2.21	0.0000
	Female	28.32	1.84		28.70	2.54	
PP1 base ml	Male	17.33	1.20	0.0000	16.81	1.10	0.0000
	Female	15.34	0.96		14.83	0.97	
PP1 base ap	Male	12.57	1.03	0.0000	12.33	0.97	0.0000
	Female	10.76	0.77		10.74	0.77	
PP1 head ml	Male	13.43	0.98	0.0000	12.66	0.70	0.0000
	Female	11.91	0.71		11.34	0.71	
PP1 head ap	Male	9.98	1.15	0.0000	9.21	0.99	0.0000
	Female	8.78	1.02		8.00	0.79	
PP1 midshaft ml	Male	10.19	0.86	0.0000	9.46	0.77	0.0000
	Female	8.44	0.74		8.17	0.69	
PP1 midshaft ap	Male	6.86	0.61	0.0000	6.65	0.56	0.0000
	Female	5.50	0.53		5.70	0.54	
PP2 length	Male	40.97	2.42	0.0000	40.29	2.91	0.0004
	Female	38.37	2.28		38.16	2.86	
PP2 base ml	Male	17.26	1.47	0.0000	16.61	0.90	0.0000
	Female	15.51	1.11		14.93	1.10	
PP2 base ap	Male	12.67	0.80	0.0000	12.18	0.82	0.0000
	Female	11.32	0.72		10.96	0.69	
PP2 head ml	Male	12.33	0.86	0.0000	11.23	0.69	0.0000
	Female	11.07	0.79		10.30	0.65	
PP2 head ap	Male	8.99	0.79	0.0000	8.09	0.62	0.0000
	Female	7.86	0.65		7.33	0.55	
PP2 midshaft ml	Male	10.69	1.00	0.0000	9.84	0.81	0.0000
	Female	8.89	0.68		8.62	0.71	
PP2 midshaft ap	Male	7.19	0.64	0.0000	6.74	0.67	0.0000
	Female	6.06	0.62		5.86	0.46	
PP3 length	Male	45.63	2.33	0.0000	45.72	2.90	0.0003
	Female	42.34	2.16		43.49	3.07	
PP3 base ml	Male	17.27	1.02	0.0000	16.56	0.90	0.0000
	Female	15.50	0.93		14.82	0.93	
PP3 base ap	Male	13.37	0.73	0.0000	13.24	1.04	0.0000
	Female	11.80	0.67		11.92	0.63	
PP3 head ml	Male	12.84	0.72	0.0000	11.98	0.72	0.0000
	Female	11.53	0.82		11.03	0.76	
PP3 head ap	Male	9.15	0.65	0.0000	8.55	0.65	0.0000
	Female	8.18	0.91		7.69	0.62	
PP3 midshaft ml	Male	11.00	0.95	0.0000	10.34	0.98	0.0000
	Female	9.24	0.72		9.04	0.77	
PP3 midshaft ap	Male	7.87	0.84	0.0000	7.36	0.61	0.0000
	Female	6.68	0.66		6.56	0.58	

Total sample=200, S.D. = standard deviation, ap = anteroposterior, ml = mediolateral
P = level of significance

Table 8.2b. Descriptive statistics comparing mean values (mm) of proximal phalanges (PP) 4 and 5 between males and females in South African whites and blacks

	WHITE				BLACK		
Variable	Sex	Mean	S.D.	P	Mean	S.D.	P
PP4 length	Male	42.59	2.30	0.0000	43.05	2.81	0.0003
	Female	39.55	2.27		40.83	3.15	
PP4 base ml	Male	15.67	0.99	0.0000	14.92	1.03	0.0000
	Female	14.09	0.96		13.40	0.81	
PP4 base ap	Male	12.40	0.74	0.0000	12.21	0.80	0.0000
	Female	11.00	0.71		11.02	0.61	
PP4 head ml	Male	11.93	0.70	0.0000	11.27	0.65	0.0000
	Female	10.74	0.84		10.50	1.48	
PP4 head ap	Male	8.66	0.66	0.0000	7.94	0.67	0.0000
	Female	7.61	0.76		7.34	0.62	
PP4 midshaft ml	Male	10.32	0.92	0.0000	9.60	0.88	0.0000
	Female	8.57	0.80		8.42	0.75	
PP4 midshaft ap	Male	7.15	0.78	0.0000	6.88	0.63	0.0000
	Female	6.10	0.82		6.10	0.53	
PP5 length	Male	33.53	2.64	0.0000	33.58	2.59	0.0001
	Female	30.54	1.43		31.22	2.92	
PP5 base ml	Male	14.96	1.21	0.0000	14.38	0.85	0.0000
	Female	13.48	0.75		12.80	0.78	
PP 5 base ap	Male	10.99	0.83	0.0000	10.76	1.07	0.0000
	Female	9.64	0.60		9.51	0.66	
PP5 head ml	Male	10.10	0.77	0.0000	9.58	0.68	0.0000
	Female	8.82	0.65		8.62	0.58	
PP5 head ap	Male	7.42	0.92	0.0000	6.88	0.57	0.0000
	Female	6.30	0.61		6.00	0.51	
PP5 midshaft ml	Male	8.88	0.85	0.0000	8.47	0.80	0.0000
	Female	7.25	0.74		7.24	0.68	
PP5 midshaft ap	Male	5.88	0.68	0.0000	5.69	0.48	0.0000
	Female	4.77	0.48		4.96	0.51	

Total sample=200, S.D. = standard deviation, ap = anteroposterior, ml = mediolateral
P = level of significance

Table 8.3a. Descriptive statistics comparing mean values (mm) of middle phalanges (MP) 2 to 4 between males and females in South African whites and blacks

	WHITE				BLACK		
Variable	Sex	Mean	S.D.	P	Mean	S.D.	P
MP2 length	Male	24.63	1.84	0.0000	23.86	2.08	0.0024
	Female	22.68	1.51		22.52	2.15	
MP2 base ml	Male	14.07	0.99	0.0000	13.41	0.92	0.0000
	Female	12.64	0.83		11.91	0.69	
MP2 base ap	Male	9.85	0.63	0.0000	9.50	0.62	0.0000
	Female	8.72	0.58		8.56	0.50	
MP2 head ml	Male	10.42	0.89	0.0000	9.65	0.70	0.0000
	Female	9.53	0.81		8.83	0.54	
MP2 head ap	Male	6.62	0.83	0.0000	6.02	0.81	0.0000
	Female	6.09	0.83		5.33	0.55	
MP2 midshaft ml	Male	8.60	0.81	0.0000	8.06	0.80	0.0000
	Female	7.21	0.65		7.03	0.63	
MP2 midshaft ap	Male	5.14	0.53	0.0000	4.99	0.44	0.0000
	Female	4.34	0.42		4.44	0.36	
MP3 length	Male	29.36	1.69	0.0000	29.17	2.09	0.0002
	Female	27.40	1.93		27.57	2.06	
MP3 base ml	Male	14.71	1.00	0.0000	14.33	0.97	0.0000
	Female	13.43	0.93		13.09	1.14	
MP3 base ap	Male	10.54	0.70	0.0000	10.31	0.74	0.0000
	Female	9.50	0.73		9.48	0.58	
MP3 head ml	Male	10.89	0.85	0.0000	10.55	0.64	0.0000
	Female	10.05	0.84		9.59	0.58	
MP3 head ap	Male	6.86	0.75	0.0019	6.48	0.66	0.0000
	Female	6.35	0.83		5.88	0.59	
MP3 midshaft ml	Male	9.23	0.85	0.0000	8.83	0.81	0.0000
	Female	7.79	0.59		7.69	0.71	
MP3 midshaft ap	Male	5.62	0.59	0.0000	5.58	0.43	0.0000
	Female	4.65	0.50		4.93	0.41	
MP4 length	Male	28.17	1.85	0.0000	27.62	2.27	0.0338
	Female	26.11	2.67		26.66	2.16	
MP4 base ml	Male	13.85	0.93	0.0000	13.42	1.06	0.0000
	Female	12.56	0.88		12.25	0.78	
MP4 base ap	Male	9.99	0.60	0.0000	9.81	0.63	0.0000
	Female	8.86	0.67		8.98	0.57	
MP4 head ml	Male	10.49	0.95	0.0000	10.03	0.83	0.0000
	Female	9.53	0.69		9.32	0.60	
MP4 head ap	Male	6.48	0.64	0.0000	6.01	0.72	0.0006
	Female	5.68	0.76		5.48	0.79	
MP4 midshaft ml	Male	8.84	0.81	0.0000	8.21	0.85	0.0000
	Female	7.34	0.59		7.32	0.72	
MP4 midshaft ap	Male	5.32	0.92	0.0000	5.18	0.47	0.0000
	Female	4.22	0.44		4.61	0.44	

Total sample=200, S.D. = standard deviation, ap = anteroposterior, ml = mediolateral
P = level of significance

Table 8.3b. Descriptive statistics comparing mean values (mm) of the fifth middle phalanx (MP) between males and females in South African whites and blacks

	WHITE				BLACK		
Variable	Sex	Mean	S.D.	P	Mean	S.D.	P
MP5 length	Male	20.19	1.73	0.0011	20.49	1.97	0.0000
	Female	18.68	2.54		18.71	1.80	
MP5 base ml	Male	12.06	1.12	0.0000	11.55	0.95	0.0000
	Female	10.88	1.07		10.23	0.77	
MP5 base ap	Male	8.61	0.61	0.0000	8.45	0.62	0.0000
	Female	7.62	0.75		7.50	0.58	
MP5 head ml	Male	9.38	0.63	0.0000	8.83	0.61	0.0000
	Female	8.48	0.83		7.97	0.61	
MP5 head ap	Male	5.63	0.60	0.0000	5.14	0.49	0.0000
	Female	4.97	0.67		4.52	0.44	
MP5 midshaft ml	Male	7.64	0.66	0.0000	7.17	0.64	0.0000
	Female	6.35	0.69		6.22	0.57	
MP5 midshaft ap	Male	4.45	0.43	0.0000	4.52	0.39	0.0000
	Female	3.65	0.49		3.93	0.37	

Total sample=200, S.D. = standard deviation, ap = anteroposterior, ml = mediolateral
P = level of significance

Table 8.4a. Descriptive statistics comparing mean values (mm) of distal phalanges (DP) 1 to 3 between males and females in South African whites and blacks

	WHITE				BLACK		
Variable	Sex	Mean	S.D.	P	Mean	S.D.	P
DP1 length	Male	23.41	1.68	0.0000	23.11	1.24	0.0000
	Female	21.07	1.24		20.88	1.87	
DP1 base ml	Male	15.78	1.58	0.0000	15.19	1.02	0.0000
	Female	13.99	1.11		13.25	1.09	
DP1 base ap	Male	9.67	0.86	0.0000	9.27	0.82	0.0000
	Female	8.32	0.66		8.05	0.70	
DP1 head ml	Male	11.17	1.35	0.0000	10.51	1.09	0.0000
	Female	9.50	1.24		9.01	0.67	
DP1 head ap	Male	4.27	0.42	0.0000	4.11	0.48	0.0000
	Female	3.57	0.50		3.68	0.39	
DP1 midshaft ml	Male	8.78	0.91	0.0000	8.21	0.81	0.0000
	Female	7.66	0.92		7.28	0.64	
DP1 midshaft ap	Male	4.71	0.55	0.0000	4.87	0.56	0.0000
	Female	3.98	0.73		4.05	0.48	
DP2 length	Male	18.31	1.12	0.0000	17.51	1.32	0.0000
	Female	16.26	1.11		16.29	1.36	
DP2 base ml	Male	10.99	1.02	0.0000	10.89	0.98	0.0000
	Female	9.98	1.11		9.47	0.63	
DP2 base ap	Male	7.03	1.29	0.0027	6.50	0.81	0.0000
	Female	6.30	1.00		5.70	0.37	
DP2 head ml	Male	8.22	0.93	0.0000	7.75	1.08	0.0000
	Female	7.22	0.93		6.88	0.76	
DP2 head ap	Male	3.90	0.49	0.0000	3.73	0.60	0.0000
	Female	3.38	0.40		3.27	0.35	
DP2 midshaft ml	Male	5.56	0.69	0.0000	5.32	0.70	0.0000
	Female	4.77	0.55		4.79	0.53	
DP2 midshaft ap	Male	3.87	0.42	0.0000	3.87	0.40	0.0000
	Female	3.32	0.38		3.39	0.36	
DP3 length	Male	19.26	1.15	0.0000	18.68	1.23	0.0003
	Female	17.31	1.29		17.70	1.36	
DP3 base ml	Male	11.80	0.98	0.0000	11.48	0.92	0.0000
	Female	10.33	0.91		10.34	0.77	
DP3 base ap	Male	7.34	0.94	0.0000	6.96	0.81	0.0000
	Female	6.37	0.74		6.43	0.72	
DP3 head ml	Male	8.98	0.94	0.0000	8.60	1.09	0.0000
	Female	7.75	1.10		7.67	0.96	
DP3 head ap	Male	4.45	0.48	0.0000	4.29	0.51	0.0006
	Female	3.80	0.47		3.94	0.47	
DP3 midshaft ml	Male	5.85	0.66	0.0000	5.70	0.81	0.0014
	Female	5.00	0.64		5.22	0.61	
DP3 midshaft ap	Male	4.06	0.42	0.0000	4.04	0.42	0.0001
	Female	3.41	0.42		3.70	0.42	

Total sample=200, S.D. = standard deviation, ap = anteroposterior, ml = mediolateral
P = level of significance

Table 8.4b. Descriptive statistics comparing mean values (mm) of distal phalanges (DP) 4 and 5 between males and females in South African whites and blacks

	WHITE				BLACK		
Variable	Sex	Mean	S.D.	P	Mean	S.D.	P
DP4 length	Male	19.29	1.20	0.0000	18.59	1.26	0.0008
	Female	17.30	1.44		17.65	1.39	
DP4 base ml	Male	11.64	0.88	0.0000	11.25	1.04	0.0000
	Female	10.46	1.16		10.04	0.67	
DP4 base ap	Male	7.07	0.76	0.0000	6.73	0.92	0.0012
	Female	6.40	0.85		6.20	0.63	
DP4 head ml	Male	8.84	0.84	0.0000	8.31	1.12	0.0000
	Female	7.75	0.94		7.40	0.85	
DP4 head ap	Male	4.43	0.44	0.0000	4.18	0.55	0.0065
	Female	3.88	0.44		3.90	0.43	
DP4 midshaft ml	Male	5.75	0.60	0.0000	5.49	0.73	0.0000
	Female	4.91	0.55		4.93	0.55	
DP4 midshaft ap	Male	4.05	0.77	0.0000	3.94	0.37	0.0000
	Female	3.45	0.49		3.57	0.32	
DP5 length	Male	17.74	0.99	0.0000	16.70	1.27	0.0000
	Female	15.44	1.28		15.21	1.28	
DP5 base ml	Male	10.01	0.77	0.0000	9.74	0.74	0.0000
	Female	8.84	1.05		8.52	0.59	
DP 5 base ap	Male	6.36	0.68	0.0000	6.03	0.76	0.0000
	Female	5.74	0.99		5.27	0.50	
DP5 head ml	Male	6.79	0.78	0.0000	6.24	0.92	0.0005
	Female	5.80	0.92		5.63	0.69	
DP5 head ap	Male	3.87	0.46	0.0000	3.66	0.40	0.0000
	Female	3.35	0.44		3.29	0.30	
DP5 midshaft ml	Male	4.37	0.55	0.0000	4.31	0.58	0.0000
	Female	3.74	0.50		3.79	0.41	
DP5 midshaft ap	Male	3.43	0.34	0.0000	3.48	0.36	0.0000
	Female	2.90	0.34		3.08	0.31	

Total sample=200, S.D. = standard deviation, ap = anteroposterior, ml = mediolateral
P = level of significance

Table 8.5a. Descriptive statistics comparing mean values (mm) of metacarpals (MC) 1 to 3 between whites and blacks in South African males and females

	MALE				FEMALE		
Variable	Group	Mean	S.D.	P	Mean	S.D.	P
MC1 length	White	46.21	2.59	0.2405	42.64	2.65	0.0769
	Black	45.53	3.09		42.48	2.75	
MC1 base ml	White	16.38	1.33	0.4492	15.04	1.55	0.0112
	Black	16.17	1.46		14.37	0.94	
MC1 base ap	White	16.61	1.73	0.3023	15.62	1.91	0.0004
	Black	16.27	1.56		14.26	1.15	
MC1 head ml	White	15.91	1.59	0.5763	14.30	1.16	0.9605
	Black	16.08	1.40		14.29	1.10	
MC1 head ap	White	15.36	1.39	0.0000	13.67	1.42	0.0001
	Black	14.04	1.36		12.66	1.04	
MC1 midshaft ml	White	13.13	1.06	0.0000	11.04	0.96	0.0071
	Black	12.85	1.12		11.59	1.01	
MC1 midshaft ap	White	9.19	0.78	0.0000	8.01	0.89	0.0283
	Black	9.42	0.86		8.39	0.81	
MC2 length	White	68.60	3.63	0.3403	64.30	3.25	0.8166
	Black	67.80	4.62		64.11	4.42	
MC2 base ml	White	18.70	1.45	0.0000	16.30	1.16	0.0006
	Black	17.03	1.59		15.37	1.40	
MC2 base ap	White	17.94	1.60	0.0044	15.79	1.31	0.1036
	Black	17.05	1.44		15.38	1.19	
MC2 head ml	White	15.55	1.50	0.0000	13.87	1.11	0.0073
	Black	14.49	1.07		13.29	0.97	
MC2 head ap	White	15.36	1.06	0.0002	14.01	0.99	0.0002
	Black	14.60	0.89		13.27	0.91	
MC2 midshaft ml	White	9.52	0.83	0.0011	8.30	0.76	0.9061
	Black	9.00	0.71		8.28	0.73	
MC2 midshaft ap	White	9.76	0.81	0.5117	8.32	0.79	0.0045
	Black	9.90	1.32		8.78	0.82	
MC3 length	White	65.85	3.90	0.3193	61.90	3.61	0.2452
	Black	66.68	4.38		62.80	4.04	
MC3 base ml	White	14.87	0.84	0.0000	13.46	1.16	0.0018
	Black	14.05	1.14		12.81	0.84	
MC3 base ap	White	18.14	1.27	0.0008	16.04	1.48	0.0211
	Black	17.29	1.17		15.46	0.90	
MC3 head ml	White	14.57	1.28	0.3154	13.12	1.22	0.4833
	Black	14.33	1.09		12.95	0.89	
MC3 head ap	White	15.44	0.99	0.0006	13.75	1.04	0.0144
	Black	14.72	1.03		13.27	0.85	
MC3 midshaft ml	White	9.42	0.75	0.0739	8.37	0.64	0.3707
	Black	9.15	0.70		8.50	0.75	
MC3 midshaft ap	White	10.10	0.89	0.7833	8.63	0.78	0.0103
	Black	10.04	1.09		9.06	0.85	

Total sample=200, S.D. = standard deviation, ap = anteroposterior, ml = mediolateral
P = level of significance

Table 8.5b. Descriptive statistics comparing mean values (mm) of metacarpals (MC) 4 and 5 between whites and blacks in South African males and females

	MALE				FEMALE		
Variable	Group	Mean	S.D.	P	Mean	S.D.	P
MC4 length	White	59.06	2.85	0.6314	54.60	3.17	0.1039
	Black	58.71	4.25		55.73	3.67	
MC4 base ml	White	12.53	1.04	0.0000	11.09	0.93	0.0000
	Black	11.46	1.05		10.30	0.69	
MC4 base ap	White	13.29	0.96	0.0488	11.42	0.96	0.0952
	Black	12.88	1.12		11.74	0.93	
MC4 head ml	White	12.73	0.96	0.0094	11.41	1.48	0.9675
	Black	12.24	0.89		11.42	0.87	
MC4 head ap	White	13.89	0.90	0.0031	12.28	0.89	0.9228
	Black	13.27	1.14		12.30	0.86	
MC4 midshaft ml	White	7.88	0.86	0.4474	6.63	0.59	0.0077
	Black	7.75	0.83		6.98	0.68	
MC4 midshaft ap	White	8.28	0.92	0.0843	6.67	0.70	0.0000
	Black	8.59	0.88		7.78	0.79	
MC5 length	White	54.35	2.85	0.9391	51.10	2.88	0.6095
	Black	54.30	3.58		50.75	3.71	
MC5 base ml	White	14.55	1.29	0.0000	12.98	1.26	0.0000
	Black	13.45	1.29		11.83	0.92	
MC5 base ap	White	12.42	1.20	0.0013	10.90	1.01	0.0010
	Black	11.66	1.08		10.27	0.81	
MC5 head ml	White	12.47	1.00	0.0095	11.01	0.89	0.0906
	Black	11.94	0.98		10.70	0.87	
MC5 head ap	White	12.82	0.92	0.0006	11.44	0.81	0.0939
	Black	12.22	0.78		11.16	0.84	
MC5 midshaft ml	White	8.58	0.88	0.9855	7.21	0.71	0.0006
	Black	8.58	0.85		7.76	0.81	
MC5 midshaft ap	White	7.83	1.02	0.8965	6.42	0.73	0.0334
	Black	7.80	1.08		6.74	0.74	

Total sample=200, S.D. = standard deviation, ap = anteroposterior, ml = mediolateral
P = level of significance

Table 8.6a. Descriptive statistics comparing mean values (mm) of proximal phalanges (PP) 1 to 3 between whites and blacks in South African males and females

	MALE				FEMALE		
Variable	Group	Mean	S.D.	P	Mean	S.D.	P
PP1 length	White	31.24	1.84	0.3065	28.32	1.84	0.3913
	Black	30.82	2.21		28.70	2.54	
PP1 base ml	White	17.33	1.20	0.0255	15.34	0.96	0.0101
	Black	16.81	1.10		14.83	0.97	
PP1 base ap	White	12.57	1.03	0.2367	10.76	0.77	0.8749
	Black	12.33	0.97		10.74	0.77	
PP1 head ml	White	13.43	0.98	0.0000	11.91	0.71	0.0001
	Black	12.66	0.70		11.34	0.71	
PP1 head ap	White	9.98	1.15	0.0005	8.78	1.02	0.0057
	Black	9.21	0.99		8.00	0.79	
PP1 midshaft ml	White	10.19	0.86	0.0000	8.44	0.74	0.0672
	Black	9.46	0.77		8.17	0.69	
PP1 midshaft ap	White	6.86	0.61	0.0774	5.50	0.53	0.0667
	Black	6.65	0.56		5.70	0.54	
PP2 length	White	40.97	2.42	0.2126	38.37	2.28	0.6807
	Black	40.29	2.91		38.16	2.86	
PP2 base ml	White	17.26	1.47	0.0091	15.51	1.11	0.0104
	Black	16.61	0.90		14.93	1.10	
PP2 base ap	White	12.67	0.80	0.0037	11.32	0.72	0.0137
	Black	12.18	0.82		10.96	0.69	
PP2 head ml	White	12.33	0.86	0.0000	11.07	0.79	0.0000
	Black	11.23	0.69		10.30	0.65	
PP2 head ap	White	8.99	0.79	0.0000	7.86	0.65	0.0000
	Black	8.09	0.62		7.33	0.55	
PP2 midshaft ml	White	10.69	1.00	0.0000	8.89	0.68	0.0606
	Black	9.84	0.81		8.62	0.71	
PP2 midshaft ap	White	7.19	0.64	0.0009	6.06	0.62	0.0716
	Black	6.74	0.67		5.86	0.46	
PP3 length	White	45.63	2.33	0.8737	42.34	2.16	0.0329
	Black	45.72	2.90		43.49	3.07	
PP3 base ml	White	17.27	1.02	0.0004	15.50	0.93	0.0005
	Black	16.56	0.90		14.82	0.93	
PP3 base ap	White	13.37	0.73	0.4651	11.80	0.67	0.3701
	Black	13.24	1.04		11.92	0.63	
PP3 head ml	White	12.84	0.72	0.0000	11.53	0.82	0.0025
	Black	11.98	0.72		11.03	0.76	
PP3 head ap	White	9.15	0.65	0.0000	8.18	0.91	0.0028
	Black	8.55	0.65		7.69	0.62	
PP3 midshaft ml	White	11.00	0.95	0.0010	9.24	0.72	0.1767
	Black	10.34	0.98		9.04	0.77	
PP3 midshaft ap	White	7.87	0.84	0.0007	6.68	0.66	0.3309
	Black	7.36	0.61		6.56	0.58	

Total sample=200, S.D. = standard deviation, ap = anteroposterior, ml = mediolateral
P = level of significance

Table 8.6b. Descriptive statistics comparing mean values (mm) of proximal phalanges (PP) 4 and 5 between whites and blacks in males and females

	MALE				FEMALE		
Variable	Group	Mean	S.D.	P	Mean	S.D.	P
PP4 length	White	42.59	2.30	0.3776	39.55	2.27	0.0220
	Black	43.05	2.81		40.83	3.15	
PP4 base ml	White	15.67	0.99	0.0003	14.09	0.96	0.0002
	Black	14.92	1.03		13.40	0.81	
PP4 base ap	White	12.40	0.74	0.2372	11.00	0.71	0.9246
	Black	12.21	0.80		11.02	0.61	
PP4 head ml	White	11.93	0.70	0.0000	10.74	0.84	0.3234
	Black	11.27	0.65		10.50	1.48	
PP4 head ap	White	8.66	0.66	0.0000	7.61	0.76	0.0555
	Black	7.94	0.67		7.34	0.62	
PP4 midshaft ml	White	10.32	0.92	0.0001	8.57	0.80	0.3325
	Black	9.60	0.88		8.42	0.75	
PP4 midshaft ap	White	7.15	0.78	0.0522	6.10	0.82	0.9869
	Black	6.88	0.63		6.10	0.53	
PP5 length	White	33.53	2.64	0.9216	30.54	1.43	0.1559
	Black	33.58	2.59		31.22	2.92	
PP5 base ml	White	14.96	1.21	0.0073	13.48	0.75	0.0000
	Black	14.38	0.85		12.80	0.78	
PP 5 base ap	White	10.99	0.83	0.2430	9.64	0.60	0.2995
	Black	10.76	1.07		9.51	0.66	
PP5 head ml	White	10.10	0.77	0.0006	8.82	0.65	0.1056
	Black	9.58	0.68		8.62	0.58	
PP5 head ap	White	7.42	0.92	0.0008	6.30	0.61	0.0084
	Black	6.88	0.57		6.00	0.51	
PP5 midshaft ml	White	8.88	0.85	0.0141	7.25	0.74	0.9450
	Black	8.47	0.80		7.24	0.68	
PP5 midshaft ap	White	5.88	0.68	0.0999	4.77	0.48	0.0554
	Black	5.69	0.48		4.96	0.51	

Total sample=200, S.D. = standard deviation, ap = anteroposterior, ml = mediolateral
P = level of significance

Table 8.7a. Descriptive statistics comparing mean values (mm) of middle phalanges (MP) 2 to 4 between whites and blacks in South African males and females

	MALE				FEMALE		
Variable	Group	Mean	S.D.	P	Mean	S.D.	P
MP2 length	White	24.63	1.84	0.0562	22.68	1.51	0.6737
	Black	23.86	2.08		22.52	2.15	
MP2 base ml	White	14.07	0.99	0.0009	12.64	0.83	0.0060
	Black	13.41	0.92		11.91	0.69	
MP2 base ap	White	9.85	0.63	0.0069	8.72	0.58	0.1331
	Black	9.50	0.62		8.56	0.50	
MP2 head ml	White	10.42	0.89	0.0000	9.53	0.81	0.0000
	Black	9.65	0.70		8.83	0.54	
MP2 head ap	White	6.62	0.83	0.0004	6.09	0.83	0.0000
	Black	6.02	0.81		5.33	0.55	
MP2 midshaft ml	White	8.60	0.81	0.0012	7.21	0.65	0.1559
	Black	8.06	0.80		7.03	0.63	
MP2 midshaft ap	White	5.14	0.53	0.1283	4.34	0.42	0.2027
	Black	4.99	0.44		4.44	0.36	
MP3 length	White	29.36	1.69	0.6263	27.40	1.93	0.6625
	Black	29.17	2.09		27.57	2.06	
MP3 base ml	White	14.71	1.00	0.0562	13.43	0.93	0.1114
	Black	14.33	0.97		13.09	1.14	
MP3 base ap	White	10.54	0.70	0.1237	9.50	0.73	0.8897
	Black	10.31	0.74		9.48	0.58	
MP3 head ml	White	10.89	0.85	0.0234	10.05	0.84	0.0020
	Black	10.55	0.64		9.59	0.58	
MP3 head ap	White	6.86	0.75	0.0079	6.35	0.83	0.0018
	Black	6.48	0.66		5.88	0.59	
MP3 midshaft ml	White	9.23	0.85	0.0176	7.79	0.59	0.4586
	Black	8.83	0.81		7.69	0.71	
MP3 midshaft ap	White	5.62	0.59	0.6710	4.65	0.50	0.0028
	Black	5.58	0.43		4.93	0.41	
MP4 length	White	28.17	1.85	0.1883	26.11	2.67	0.2780
	Black	27.62	2.27		26.66	2.16	
MP4 base ml	White	13.85	0.93	0.0333	12.56	0.88	0.0684
	Black	13.42	1.06		12.25	0.78	
MP4 base ap	White	9.99	0.60	0.1507	8.86	0.67	0.3336
	Black	9.81	0.63		8.98	0.57	
MP4 head ml	White	10.49	0.95	0.0116	9.53	0.69	0.1152
	Black	10.03	0.83		9.32	0.60	
MP4 head ap	White	6.48	0.64	0.0011	5.68	0.76	0.2142
	Black	6.01	0.72		5.48	0.79	
MP4 midshaft ml	White	8.84	0.81	0.0002	7.34	0.59	0.8714
	Black	8.21	0.85		7.32	0.72	
MP4 midshaft ap	White	5.32	0.92	0.3662	4.22	0.44	0.0000
	Black	5.18	0.47		4.61	0.44	

Total sample=200, S.D. = standard deviation, ap = anteroposterior, ml = mediolateral
P = level of significance

Table 8.7b. Descriptive statistics comparing mean values (mm) of the fifth middle phalanx (MP) between whites and blacks in South African males and females

	MALE				FEMALE		
Variable	Group	Mean	S.D.	P	Mean	S.D.	P
MP5 length	White	20.19	1.73	0.4401	18.68	2.54	0.9472
	Black	20.49	1.97		18.71	1.80	
MP5 base ml	White	12.06	1.12	0.0178	10.88	1.07	0.0009
	Black	11.55	0.95		10.23	0.77	
MP5 base ap	White	8.61	0.61	0.1917	7.62	0.75	0.3928
	Black	8.45	0.62		7.50	0.58	
MP5 head ml	White	9.38	0.63	0.0000	8.48	0.83	0.0008
	Black	8.83	0.61		7.97	0.61	
MP5 head ap	White	5.63	0.60	0.0000	4.97	0.67	0.0002
	Black	5.14	0.49		4.52	0.44	
MP5 midshaft ml	White	7.64	0.66	0.0006	6.35	0.69	0.3516
	Black	7.17	0.64		6.22	0.57	
MP5 midshaft ap	White	4.45	0.43	0.3855	3.65	0.49	0.0023
	Black	4.52	0.39		3.93	0.37	

Total sample=200, S.D. = standard deviation, ap = anteroposterior, ml = mediolateral
P = level of significance

Table 8.8a. Descriptive statistics comparing mean values (mm) of distal phalanges (DP) 1 to 3 between whites and blacks in South African males and females

	MALE				FEMALE		
Variable	Group	Mean	S.D.	P	Mean	S.D.	P
DP1 length	White	23.41	1.68	0.3101	21.07	1.24	0.5634
	Black	23.11	1.24		20.88	1.87	
DP1 base ml	White	15.78	1.58	0.0288	13.99	1.11	0.0012
	Black	15.19	1.02		13.25	1.09	
DP1 base ap	White	9.67	0.86	0.0187	8.32	0.66	0.0466
	Black	9.27	0.82		8.05	0.70	
DP1 head ml	White	11.17	1.35	0.0087	9.50	1.24	0.0168
	Black	10.51	1.09		9.01	0.67	
DP1 head ap	White	4.27	0.42	0.0863	3.57	0.50	0.2063
	Black	4.11	0.48		3.68	0.39	
DP1 midshaft ml	White	8.78	0.91	0.0013	7.66	0.92	0.0206
	Black	8.21	0.81		7.28	0.64	
DP1 midshaft ap	White	4.71	0.55	0.0468	3.98	0.73	0.6017
	Black	4.87	0.56		4.05	0.48	
DP2 length	White	18.31	1.12	0.0016	16.26	1.11	0.9080
	Black	17.51	1.32		16.29	1.36	
DP2 base ml	White	10.99	1.02	0.0600	9.98	1.11	0.0078
	Black	10.89	0.98		9.47	0.63	
DP2 base ap	White	7.03	1.29	0.0181	6.30	1.00	0.0002
	Black	6.50	0.81		5.70	0.37	
DP2 head ml	White	8.22	0.93	0.0227	7.22	0.93	0.0529
	Black	7.75	1.08		6.88	0.76	
DP2 head ap	White	3.90	0.49	0.1324	3.38	0.40	0.1621
	Black	3.73	0.60		3.27	0.35	
DP2 midshaft ml	White	5.56	0.69	0.0972	4.77	0.55	0.8159
	Black	5.32	0.70		4.79	0.53	
DP2 midshaft ap	White	3.87	0.42	0.9375	3.32	0.38	0.4099
	Black	3.87	0.40		3.39	0.36	
DP3 length	White	19.26	1.15	0.0202	17.31	1.29	0.1482
	Black	18.68	1.23		17.70	1.36	
DP3 base ml	White	11.80	0.98	0.1046	10.33	0.91	0.9552
	Black	11.48	0.92		10.34	0.77	
DP3 base ap	White	7.34	0.94	0.0364	6.37	0.74	0.6893
	Black	6.96	0.81		6.43	0.72	
DP3 head ml	White	8.98	0.94	0.0703	7.75	1.10	0.7293
	Black	8.60	1.09		7.67	0.96	
DP3 head ap	White	4.45	0.48	0.1165	3.80	0.47	0.1457
	Black	4.29	0.51		3.94	0.47	
DP3 midshaft ml	White	5.85	0.66	0.3126	5.00	0.64	0.0772
	Black	5.70	0.81		5.22	0.61	
DP3 midshaft ap	White	4.06	0.42	0.8437	3.41	0.42	0.0012
	Black	4.04	0.42		3.70	0.42	

Total sample=200, S.D. = standard deviation, ap = anteroposterior, ml = mediolateral
P = level of significance

Table 8.8b. Descriptive statistics comparing mean values (mm) of distal phalanges (DP) 4 and 5 between whites and blacks in South African males and females

	MALE				FEMALE		
Variable	Group	Mean	S.D.	P	Mean	S.D.	P
DP4 length	White	19.29	1.20	0.0070	17.30	1.44	0.2445
	Black	18.59	1.26		17.65	1.39	
DP4 base ml	White	11.64	0.88	0.0489	10.46	1.16	0.0334
	Black	11.25	1.04		10.04	0.67	
DP4 base ap	White	7.07	0.76	0.0571	6.40	0.85	0.1881
	Black	6.73	0.92		6.20	0.63	
DP4 head ml	White	8.84	0.84	0.0111	7.75	0.94	0.0684
	Black	8.31	1.12		7.40	0.85	
DP4 head ap	White	4.43	0.44	0.0182	3.88	0.44	0.8642
	Black	4.18	0.55		3.90	0.43	
DP4 midshaft ml	White	5.75	0.60	0.0572	4.91	0.55	0.8867
	Black	5.49	0.73		4.93	0.55	
DP4 midshaft ap	White	4.05	0.77	0.3987	3.45	0.49	0.1586
	Black	3.94	0.37		3.57	0.32	
DP5 length	White	17.74	0.99	0.0000	15.44	1.28	0.4164
	Black	16.70	1.27		15.21	1.28	
DP5 base ml	White	10.01	0.77	0.0920	8.84	1.05	0.0886
	Black	9.74	0.74		8.52	0.59	
DP 5 base ap	White	6.36	0.68	0.0301	5.74	0.99	0.0054
	Black	6.03	0.76		5.27	0.50	
DP5 head ml	White	6.79	0.78	0.0024	5.80	0.92	0.3272
	Black	6.24	0.92		5.63	0.69	
DP5 head ap	White	3.87	0.46	0.0203	3.35	0.44	0.3971
	Black	3.66	0.40		3.29	0.30	
DP5 midshaft ml	White	4.37	0.55	0.5727	3.74	0.50	0.5555
	Black	4.31	0.58		3.79	0.41	
DP5 midshaft ap	White	3.43	0.34	0.4361	2.90	0.34	0.0092
	Black	3.48	0.36		3.08	0.31	

Total sample=200, S.D. = standard deviation, ap = anteroposterior, ml = mediolateral
P = level of significance

Table 8.9: Descriptive statistics comparing mean values (mm) of long bone lengths between males and females in South African whites

Variable	Sex	Mean	SD	t	Sig. (2-tailed) P
Humeral length maximum	Male	338.73	17.55	7.15	0.00
	Female	314.76	14.95		
Radial length	Male	254.09	13.13	9.41	0.00
	Female	229.16	12.53		
Ulna length	Male	272.42	13.17	9.95	0.00
	Female	245.90	12.68		
Femur length maximum	Male	471.93	36.45	4.98	0.00
	Female	441.51	21.39		
Tibial length	Male	390.06	21.01	6.77	0.00
	Female	361.00	20.58		

Total sample=200, S.D.=standard deviation, P = level of significance

Table 8.10: Descriptive statistics comparing mean values (mm) of long bone lengths between males and females in South African blacks

Variable	Sex	Mean	SD	t	Sig. (2-tailed) P
Humeral length maximum	Male	327.53	30.15	5.68	0.00
	Female	300.34	15.29		
Radial length	Male	259.44	12.64	10.12	0.00
	Female	232.44	13.85		
Ulna length	Male	278.57	11.14	10.59	0.00
	Female	250.90	14.58		
Femur length maximum	Male	460.00	20.66	6.24	0.00
	Female	433.05	22.29		
Tibial length	Male	393.84	19.63	6.97	0.00
	Female	362.22	25.11		

Sample size=200, S.D.=standard deviation, P = level of significance

Table 8.11: Descriptive statistics comparing mean values (mm) of long bone lengths between males and females for the South African population

Variable	Sex	Mean	SD	t	Sig. (2-tailed) P
Humeral length maximum	Male	332.89	25.43	8.25	0.00
	Female	307.47	16.70		
Radial length	Male	256.88	13.09	13.74	0.00
	Female	230.82	13.25		
Ulna length	Male	275.63	12.48	14.32	0.00
	Female	248.42	13.83		
Femur length maximum	Male	465.71	29.75	7.57	0.00
	Female	437.24	22.15		
Tibial length	Male	392.03	20.28	9.76	0.00
	Female	361.62	22.87		

Sample size=200, S.D.=standard deviation, P = level of significance

Table 8.12: Pearson's correlation coefficients between the bones of the hand (metacarpals and phalanges) and the long bones (humerus, radius, ulna, femur, tibia) in South African males

		Humerus	Radius	Ulna	Femur	Tibia
Metacarpal 1 (n=94)	Pearson Correlation	.592(**)	.459(**)	.510(**)	.511(**)	.480(**)
	Sig. (2-tailed)	.000	.000	.000	.000	.000
Metacarpal 2 (n=94)	Pearson Correlation	.678(**)	.785(**)	.772(**)	.684(**)	.742(**)
	Sig. (2-tailed)	.000	.000	.000	.000	.000
Metacarpal 3 (n=94)	Pearson Correlation	.512(**)	.744(**)	.719(**)	.439(**)	.745(**)
	Sig. (2-tailed)	.000	.000	.000	.000	.000
Metacarpal 4 (n=94)	Pearson Correlation	.561(**)	.619(**)	.600(**)	.525(**)	.663(**)
	Sig. (2-tailed)	.000	.000	.000	.000	.000
Metacarpal 5 (n=93)	Pearson Correlation	.549(**)	.628(**)	.623(**)	.401(**)	.619(**)
	Sig. (2-tailed)	.000	.000	.000	.000	.000
Proximal Phalanx 1 (n=94)	Pearson Correlation	.535(**)	.457(**)	.491(**)	.482(**)	.511(**)
	Sig. (2-tailed)	.000	.000	.000	.000	.000
Proximal Phalanx 2 (n=92)	Pearson Correlation	.581(**)	.530(**)	.572(**)	.594(**)	.631(**)
	Sig. (2-tailed)	.000	.000	.000	.000	.000
Proximal Phalanx 3 (n=94)	Pearson Correlation	.546(**)	.594(**)	.619(**)	.531(**)	.682(**)
	Sig. (2-tailed)	.000	.000	.000	.000	.000
Proximal Phalanx 4 (n=94)	Pearson Correlation	.535(**)	.607(**)	.615(**)	.441(**)	.715(**)
	Sig. (2-tailed)	.000	.000	.000	.000	.000
Proximal Phalanx 5 (n=90)	Pearson Correlation	.514(**)	.498(**)	.498(**)	.412(**)	.593(**)
	Sig. (2-tailed)	.000	.000	.000	.000	.000
Middle Phalanx 2 (n=92)	Pearson Correlation	.535(**)	.450(**)	.449(**)	.555(**)	.482(**)
	Sig. (2-tailed)	.000	.000	.000	.000	.000
Middle Phalanx 3 (n=94)	Pearson Correlation	.364(**)	.390(**)	.306(**)	.281(**)	.409(**)
	Sig. (2-tailed)	.000	.000	.003	.006	.000
Middle Phalanx 4 (n=93)	Pearson Correlation	.504(**)	.455(**)	.424(**)	.429(**)	.496(**)
	Sig. (2-tailed)	.000	.000	.000	.000	.000
Middle Phalanx 5 (n=90)	Pearson Correlation	.329(**)	.444(**)	.442(**)	.279(**)	.472(**)
	Sig. (2-tailed)	.002	.000	.000	.008	.000
Distal Phalanx 1 (n=94)	Pearson Correlation	.445(**)	.418(**)	.442(**)	.372(**)	.467(**)
	Sig. (2-tailed)	.000	.000	.000	.000	.000
Distal Phalanx 2 (n=91)	Pearson Correlation	.462(**)	.244(*)	.282(**)	.372(**)	.228(*)
	Sig. (2-tailed)	.000	.020	.007	.000	.029
Distal Phalanx 3 (n=90)	Pearson Correlation	.291(**)	.110	.110	.211(*)	.145
	Sig. (2-tailed)	.005	.303	.304	.046	.173
Distal Phalanx 4 (n=89)	Pearson Correlation	.521(**)	.360(**)	.360(**)	.430(**)	.334(**)
	Sig. (2-tailed)	.000	.001	.001	.000	.001
Distal Phalanx 5 (n=88)	Pearson Correlation	.567(**)	.235(*)	.258(*)	.505(**)	.299(**)
	Sig. (2-tailed)	.000	.028	.015	.000	.005

** Correlation is significant at the 0.01 level (2-tailed).
* Correlation is significant at the 0.05 level (2-tailed).

Table 8.13: Pearson's correlation coefficients between the bones of the hand (metacarpals and phalanges) and the long bones (humerus, radius, ulna, femur, tibia) in South African females.

		Humerus	Radius	Ulna	Femur	Tibia
Metacarpal 1 (n=98)	Pearson Correlation	0.612(**)	.827(**)	.790(**)	.594(**)	.631(**)
	Sig. (2-tailed)	.000	.000	.000	.000	.000
Metacarpal 2 (n=98)	Pearson Correlation	.713(**)	.902(**)	.858(**)	.724(**)	.771(**)
	Sig. (2-tailed)	.000	.000	.000	.000	.000
Metacarpal 3 (n=98)	Pearson Correlation	.573(**)	.844(**)	.773(**)	.650(**)	.714(**)
	Sig. (2-tailed)	.000	.000	.000	.000	.000
Metacarpal 4 (n=98)	Pearson Correlation	.448(**)	.812(**)	.698(**)	.456(**)	.584(**)
	Sig. (2-tailed)	.000	.000	.000	.000	.000
Metacarpal 5 (n=97)	Pearson Correlation	.581(**)	.806(**)	.660(**)	.574(**)	.485(**)
	Sig. (2-tailed)	.000	.000	.000	.000	.000
Proximal Phalanx 1 (n=97)	Pearson Correlation	.420(**)	.706(**)	.646(**)	.466(**)	.500(**)
	Sig. (2-tailed)	.000	.000	.000	.000	.000
Proximal Phalanx 2 (n=98)	Pearson Correlation	.482(**)	.648(**)	.562(**)	.459(**)	.513(**)
	Sig. (2-tailed)	.000	.000	.000	.000	.000
Proximal Phalanx 3 (n=97)	Pearson Correlation	.338(**)	.680(**)	.634(**)	.412(**)	.522(**)
	Sig. (2-tailed)	.001	.000	.000	.000	.000
Proximal Phalanx 4 (n=97)	Pearson Correlation	.362(**)	.717(**)	.678(**)	.404(**)	.592(**)
	Sig. (2-tailed)	.000	.000	.000	.000	.000
Proximal Phalanx 5 (n=95)	Pearson Correlation	.381(**)	.597(**)	.561(**)	.403(**)	.441(**)
	Sig. (2-tailed)	.000	.000	.000	.000	.000
Middle Phalanx 2 (n=95)	Pearson Correlation	.372(**)	.494(**)	.459(**)	.447(**)	.407(**)
	Sig. (2-tailed)	.000	.000	.000	.000	.000
Middle Phalanx 3 (n=97)	Pearson Correlation	.433(**)	.654(**)	.599(**)	.497(**)	.557(**)
	Sig. (2-tailed)	.000	.000	.000	.000	.000
Middle Phalanx 4 (n=95)	Pearson Correlation	.378(**)	.619(**)	.567(**)	.414(**)	.510(**)
	Sig. (2-tailed)	.000	.000	.000	.000	.000
Middle Phalanx 5 (n=94)	Pearson Correlation	.330(**)	.444(**)	.400(**)	.313(**)	.361(**)
	Sig. (2-tailed)	.001	.000	.000	.002	.000
Distal Phalanx 1 (n=98)	Pearson Correlation	.354(**)	.474(**)	.420(**)	.419(**)	.337(**)
	Sig. (2-tailed)	.000	.000	.000	.000	.001
Distal Phalanx 2 (n=95)	Pearson Correlation	.328(**)	.470(**)	.410(**)	.349(**)	.314(**)
	Sig. (2-tailed)	.001	.000	.000	.001	.002
Distal Phalanx 3 (n=95)	Pearson Correlation	.257(*)	.507(**)	.381(**)	.286(**)	.322(**)
	Sig. (2-tailed)	.012	.000	.000	.005	.001
Distal Phalanx 4 (n=92)	Pearson Correlation	.244(*)	.486(**)	.395(**)	.259(*)	.281(**)
	Sig. (2-tailed)	.019	.000	.000	.013	.007
Distal Phalanx 5 (n=86)	Pearson Correlation	.398(**)	.432(**)	.345(**)	.402(**)	.354(**)
	Sig. (2-tailed)	.000	.000	.001	.000	.001

** Correlation is significant at the 0.01 level (2-tailed).
* Correlation is significant at the 0.05 level (2-tailed).

Table 8.14: Direct and stepwise regression showing the sequence of variable entry of metacarpals (MC) 1 to 5 into the analysis and standard error of the estimates (SEE) (mm), *R* and R^2 to estimate the length (mm) of a long bone in South African males

		Humerus	Radius	Ulna	Femur	Tibia
All MC	R	0.722	0.820	0.811	0.749	0.782
Direct	R^2	0.521	0.673	0.658	0.560	0.612
	SEE	9.20442	5.16864	5.57831	10.55606	7.11019
MC 1	R	0.592	0.459	0.510	0.511	0.480
	R^2	0.351	0.211	0.260	0.261	0.230
	SEE	10.61863	7.81528	7.97720	13.31537	9.75856
MC 2	R	0.678	0.785	0.772	0.684	0.742
	R^2	0.460	0.616	0.596	0.467	0.550
	SEE	9.68835	5.44944	5.89334	11.30427	7.45728
MC 3	R	0.512	0.744	0.719	0.439	0.745
	R^2	0.262	0.553	0.518	0.192	0.556
	SEE	11.32250	5.88279	6.44281	13.91958	7.41296
MC 4	R	0.561	0.619	0.600	0.525	0.663
	R^2	0.315	0.383	0.360	0.275	0.440
	SEE	10.90682	6.90868	7.42137	13.18625	8.32086
MC 5	R	0.549	0.628	0.623	0.401	0.619
	R2	0.302	0.394	0.388	0.160	0.383
	SEE	10.86055	6.87769	7.29371	14.26282	8.76542
Stepwise	R	0.679	0.785	0.774	0.683	0.745
Model 1	R^2	0.461	0.616	0.599	0.467	0.554
	SEE	9.54258	5.47883	5.90967	11.36334	7.45098
Predictors		MC2	MC2	MC2	MC2	MC3
Stepwise	R	0.711	0.807	0.791	0.709	0.782
Model 2	R^2	0.505	0.651	0.625	0.503	0.611
	SEE	9.1975	5.25089	5.73948	11.03407	6.99847
Predictors		MC2	MC2	MC2	MC2	MC3
		MC1	MC1	MC3	MC3	MC2
Stepwise	R		0.818	0.803	0.735	
Model 3	R^2		0.669	0.644	0.540	
	SEE		5.14431	5.62622	10.67212	
Predictors			MC2	MC2	MC2	
			MC1	MC3	MC3	
			MC4	MC4	MC1	

Table 8.15: Direct and stepwise regression coefficients (slope and constant) and standard error of the estimates (SEE) (mm) of metacarpals (MC) 1 to 5 to estimate the length (mm) of a long bone in South African males

	Humerus	Radius	Ulna	Femur	Tibia
Direct					
MC 1	1.304	-0.056	0.364	1.407	0.080
MC 2	1.854	1.289	1.320	3.173	1.048
MC 3	-0.651	0.874	0.793	-1.322	1.108
MC 4	-0.061	-0.747	-0.901	0.748	-0.150
MC 5	0.503	0.312	0.398	-1.172	0.121
Constant	163.470	138.832	145.394	292.368	244.747
SEE	9.20442	5.16864	5.57831	10.55606	7.11019
Metacarpal 1					
Slope	2.717	1.407	1.648	2.755	1.857
Constant	205.515	190.611	197.857	339.951	306.009
SEE	10.61863	7.81528	7.97720	13.31537	9.75856
Metacarpal 2					
Slope	2.100	1.624	1.684	2.489	1.939
Constant	186.949	144.347	158.571	296.522	258.864
SEE	9.68835	5.44944	5.89334	11.30427	7.45728
Metacarpal 3					
Slope	1.580	1.533	1.563	1.591	1.942
Constant	225.486	153.476	169.769	360.865	262.361
SEE	11.32250	5.88279	6.44281	13.91958	7.41296
Metacarpal 4					
Slope	1.981	1.459	1.491	2.176	1.976
Constant	213.542	169.199	185.683	338.180	274.777
SEE	10.90682	6.90868	7.42137	13.18625	8.32086
Metacarpal 5					
Slope	2.155	1.674	1.753	1.881	2.085
Constant	213.493	164.265	178.233	364.301	278.030
SEE	10.86055	6.87769	7.29371	14.26282	8.76542
Stepwise Model 1					
MC 1					
MC 2	2.068	1.625	1.691	2.493	
MC 3					1.939
MC 4					
MC 5					
Constant	189.320	144.260	158.045	296.213	262.555
SEE	9.54258	5.47883	5.90967	11.36334	7.45098
Stepwise Model 2					
MC 1	1.233				
MC 2	1.601	1.098	1.204	3.432	1.051
MC 3		0.652	0.602	-1.161	1.097
MC 4					
MC 5					
Constant	164.506	136.961	151.304	309.207	246.707
SEE	9.1975	5.25089	5.73948	11.03407	6.99847
Stepwise Model 3					
MC 1				1.386	
MC 2		1.322	1.447	3.086	
MC 3		0.908	0.879	-1.384	
MC 4		-0.609	-0.658		
MC 5					
Constant		140.545	155.180	283.808	
SEE		5.14431	5.62622	10.67212	

Table 8.16: Direct and stepwise regression showing the sequence of variable entry of proximal phalanges (PP) 1 to 5 into the analysis and standard error of the estimate (SEE) (mm), *R* and R^2 to estimate the length (mm) of a long bone in South African males

		Humerus	Radius	Ulna	Femur	Tibia
All PP Direct	R	0.664	0.631	0.659	0.622	0.740
	R^2	0.440	0.398	0.435	0.387	0.548
	SEE	10.22718	7.07855	7.30164	12.75499	7.70705
PP 1	R	0.535	0.457	0.491	0.482	0.511
	R^2	0.287	0.209	0.241	0.232	0.261
	SEE	11.13048	7.82358	8.08167	13.57384	9.55929
PP 2	R	0.581	0.530	0.572	0.594	0.631
	R^2	0.337	0.281	0.327	0.352	0.398
	SEE	10.84185	7.48127	7.65327	12.56490	8.68560
PP 3	R	0.546	0.594	0.619	0.531	0.682
	R^2	0.299	0.353	0.383	0.282	0.465
	SEE	11.03811	7.07720	7.28345	13.12682	8.13681
PP 4	R	0.535	0.607	0.615	0.441	0.715
	R^2	0.287	0.368	0.378	0.194	0.511
	SEE	11.13017	6.99215	7.31734	13.90157	7.77650
PP 5	R	0.514	0.498	0.498	0.412	0.593
	R^2	0.264	0.248	0.248	0.169	0.352
	SEE	11.33092	7.69598	8.17271	14.38101	8.94246
Stepwise Model 1	R	0.642	0.614	0.648	0.618	0.719
	R^2	0.413	0.377	0.420	0.382	0.517
	SEE	10.23072	7.02791	7.22319	12.50968	7.77657
Predictors		PP2	PP4	PP3	PP2	PP 4
Stepwise Model 2	R					0.735
	R^2					0.540
	SEE					7.62945
Predictors						PP4 PP2

Table 8.17: Direct and stepwise regression coefficients (slope and constant) and standard error of the estimate (SEE) (mm) of the proximal phalanges (PP) 1 to 5 to estimate the length (mm) of a long bone in South African males

	Humerus	Radius	Ulnar	Femur	Tibia
Direct					
PP 1	0.779	-0.096	0.110	0.855	-0.362
PP 2	3.316	0.242	0.253	3.419	0.643
PP 3	-1.483	0.847	1.269	-0.103	0.993
PP 4	0.408	1.033	0.780	-0.227	1.551
PP 5	0.588	0.214	0.129	-0.045	0.416
Constant	202.401	158.006	163.918	317.433	250.282
SEE	10.22718	7.07855	7.30164	12.75499	7.70705
Proximal Phalanx 1					
Slope	3.411	1.946	2.201	3.606	2.747
Constant	224.443	194.827	205.227	354.524	306.006
SEE	11.13048	7.82358	8.08167	13.57384	9.55929
Proximal Phalanx 2					
Slope	2.828	1.712	1.951	3.392	2.583
Constant	215.441	185.669	194.332	328.775	286.352
SEE	10.84185	7.48127	7.65327	12.56490	8.68560
Proximal Phalanx 3					
Slope	2.730	1.982	2.178	3.117	2.874
Constant	205.474	164.567	173.925	323.896	259.800
SEE	11.03811	7.07720	7.28345	13.12682	8.13681
Proximal Phalanx 4					
Slope	2.715	2.055	2.194	2.628	3.059
Constant	213.861	167.069	179.444	353.754	260.042
SEE	11.13017	6.99215	7.31734	13.90157	7.77650
Proximal Phalanx 5					
Slope	2.557	1.667	1.771	2.448	2.486
Constant	244.725	199.021	213.882	384.493	307.464
SEE	11.33092	7.69598	8.17271	14.38101	8.94246
Stepwise Model 1					
PP 1				3.620	
PP 2	3.156				
PP 3			2.324		
PP 4		2.146			3.156
PP 5					
Constant	202.480	163.076	167.077	319.822	255.767
SEE	10.23072	7.02791	7.22319	12.50968	7.77657
Stepwise Model 2					
PP 1					
PP 2					1.046
PP 3					
PP 4					2.267
PP 5					
Constant					251.364
SEE					7.62945

Table 8.18: Direct and stepwise regression showing the sequence of variable entry of middle phalanges (MP) 2 to 5 into the analysis and standard error of the estimate (SEE) (mm), *R* and R^2 to estimate the length (mm) of a long bone in South African males

		Humerus	Radius	Ulna	Femur	Tibia
All MP	R	0.635	0.567	0.558	0.623	0.601
Direct	R^2	0.403	0.322	0.312	0.388	0.362
	SEE	10.39432	7.48465	7.88246	12.40385	9.26484
MP 2	R	0.535	0.450	0.449	0.555	0.482
	R^2	0.286	0.203	0.202	0.308	0.232
	SEE	11.16954	7.91818	8.35206	12.79881	9.82609
MP 3	R	0.364	0.390	0.306	0.281	0.409
	R^2	0.133	0.152	0.094	0.079	0.167
	SEE	12.27303	8.10256	8.83124	14.86691	10.14807
MP 4	R	0.504	0.455	0.424	0.429	0.496
	R^2	0.254	0.207	0.180	0.184	0.246
	SEE	11.44316	7.83989	8.40615	14.06331	9.67028
MP 5	R	0.329	0.444	0.442	0.279	0.472
	R^2	0.108	0.197	0.196	0.078	0.222
	SEE	12.35341	7.96941	8.33353	14.80081	9.98934
Stepwise	R	0.575	0.493	0.477	0.555	0.528
Model 1	R^2	0.331	0.243	0.227	0.309	0.279
	SEE	10.81078	7.76637	8.20483	12.95552	9.67440
Predictors		MP2	MP4	MP4	MP2	MP4
Stepwise	R	0.619	0.562	0.550	0.593	0.597
Model 2	R^2	0.384	0.315	0.302	0.352	0.356
	SEE	10.43734	7.43129	7.84252	12.61879	9.19406
Predictors		MP2	MP4	MP4	MP2	MP4
		MP4	MP2	MP2	MP4	MP2

Table 8.19: Direct and stepwise regression coefficients (slope and constant) and standard error of the estimates (SEE) (mm) of the middle phalanges (MP) 2 to 5 to estimate the length (mm) of a long bone in South African males

	Humerus	Radius	Ulna	Femur	Tibia
Direct					
MP 2	3.403	1.197	1.451	4.170	1.636
MP 3	-0.546	0.280	-0.365	-0.979	0.196
MP 4	2.697	1.226	1.332	3.369	1.773
MP 5	-1.172	0.404	0.649	-1.827	0.567
Constant	212.675	175.624	198.801	337.369	284.821
SEE	10.39432	7.48465	7.88246	12.40385	9.26484
Middle Phalanx 2					
Slope	3.520	1.986	2.089	4.243	2.686
Constant	245.227	207.057	222.914	363.875	326.152
SEE	11.16954	7.91818	8.35206	12.79881	9.82609
Middle Phalanx 3					
Slope	2.505	1.789	1.480	2.266	2.373
Constant	257.023	202.861	230.227	400.150	321.820
SEE	12.27303	8.10256	8.83124	14.86691	10.14807
Middle Phalanx 4					
Slope	3.160	1.894	1.862	3.159	2.614
Constant	242.184	202.481	221.702	378.383	318.461
SEE	11.44316	7.83989	8.40615	14.06331	9.67028
Middle Phalanx 5					
Slope	2.287	2.097	2.185	2.284	2.840
Constant	284.403	212.784	229.382	420.661	333.695
SEE	12.35341	7.96941	8.33353	14.80081	9.98934
Stepwise Model 1					
MP 2	3.818			4.347	
MP 3					
MP 4		2.276	2.300		3.108
MP 5					
Constant	238.389	191.667	209.405	361.676	304.373
SEE	10.81078	7.76637	8.20483	12.95552	9.67440
Stepwise Model 2					
MP 2	2.952	1.383	1.476	3.423	1.831
MP 3					
MP 4	1.803	1.573	1.549	1.923	2.176
MP 5					
Constant	208.816	177.821	194.630	330.141	286.047
SEE	10.43734	7.43129	7.84252	12.61879	9.19406

Table 8.20: Direct and stepwise regression showing the sequence of variable entry of distal phalanges (DP) 1 to 5 into the analysis and standard error of the estimates (SEE) (mm), *R* and R^2 to estimate the length (mm) of a long bone in South African males

		Humerus	Radius	Ulna	Femur	Tibia
All DP	R	0.657	0.568	0.587	0.604	0.541
Direct	R^2	0.431	0.323	0.344	0.364	0.293
	SEE	10.04404	7.64473	8.09223	12.34664	9.86875
DP 1	R	0.445	0.418	0.442	0.372	0.467
	R^2	0.198	0.175	0.196	0.139	0.218
	SEE	11.79925	7.99286	8.32004	14.37616	9.83274
DP 2	R	0.462	0.244	0.282	0.372	0.228
	R^2	0.213	0.060	0.080	0.139	0.098
	SEE	11.71338	8.54028	9.01645	14.10518	13.09722
DP 3	R	0.291	0.110	0.110	0.211	0.145
	R^2	0.084	0.012	0.012	0.044	0.021
	SEE	12.68089	8.92948	9.40688	14.92736	11.09677
DP 4	R	0.521	0.360	0.360	0.430	0.334
	R2	0.272	0.129	0.130	0.185	0.112
	SEE	11.08863	8.42090	8.86729	13.44774	10.64633
DP 5	R	0.567	0.235	0.258	0.505	0.299
	R^2	0.322	0.055	0.066	0.255	0.090
	SEE	10.72367	8.64931	9.13573	13.39970	10.69489
Stepwise	R	0.600	0.452	0.471	0.559	0.490
Model 1	R^2	0.360	0.204	0.222	0.312	0.240
	SEE	10.38900	8.07774	8.59156	12.51951	9.97223
Predictors		DP5	DP1	DP1	DP1	DP1

Table 8.21: Direct and stepwise regression coefficients (slope and constant) and standard error of the estimates (SEE) (mm) of distal phalanges (DP) 1 to 5 to estimate the length (mm) of a long bone in South African males

	Humerus	Radius	Ulna	Femur	Tibia
Direct					
DP 1	0.466	3.097	3.371	0.046	4.147
DP 2	2.230	0.389	1.001	1.968	-0.449
DP 3	-4.194	-3.413	-3.817	-4.356	-3.245
DP 4	2.394	3.973	4.059	2.377	2.772
DP 5	4.909	-1.848	-2.052	6.055	-0.215
Constant	229.809	197.976	208.443	364.321	316.325
SEE	10.04404	7.64473	8.09223	12.34664	9.86875
Distal Phalanx 1					
Slope	3.996	2.503	2.792	3.924	3.536
Constant	237.264	196.919	208.521	375.088	308.907
SEE	11.79925	7.99286	8.32004	14.37616	9.83274
Distal Phalanx 2					
Slope	4.977	1.755	2.164	4.615	2.091
Constant	241.253	223.903	234.804	384.188	353.971
SEE	11.71338	8.54028	9.01645	14.10518	13.09722
Distal Phalanx 3					
Slope	3.233	0.828	0.870	2.704	1.364
Constant	269.334	239.558	257.164	415.907	365.752
SEE	12.68089	8.92948	9.40688	14.92736	11.09677
Distal Phalanx 4					
Slope	5.394	2.587	2.729	5.107	3.010
Constant	228.302	206.222	221.909	370.186	334.464
SEE	11.08863	8.42090	8.86729	13.44774	10.64633
Distal Phalanx 5					
Slope	6.024	1.704	1.987	6.388	2.736
Constant	226.816	225.964	239.340	356.548	344.321
SEE	10.72367	8.64931	9.13573	13.39970	10.69489
Stepwise					
Model 1					
DP 1		2.781	3.120		3.813
DP 2					
DP 3					
DP 4					
DP 5	6.167			6.680	
Constant	224.540	190.879	201.226	352.085	303.167
SEE	10.38900	8.07774	8.59156	12.51951	9.97223

Table 8.22: Direct and stepwise regression showing the sequence of variable entry of metacarpals (MC) 1 to 5 into the analysis and standard error of the estimates (SEE) (mm), *R* and R^2 to estimate the length (mm) of a long bone in South African females

		Humerus	Radius	Ulna	Femur	Tibia
All MC	R	0.797	0.926	0.907	0.846	0.910
Direct	R^2	0.635	0.857	0.823	0.717	0.828
	SEE	7.32868	4.00888	4.97223	8.05951	5.77430
MC 1	R	0.612	0.827	0.790	0.594	0.631
	R^2	0.374	0.684	0.624	0.353	0.399
	SEE	9.34768	5.81861	7.07333	11.86070	10.60585
MC 2	R	0.713	0.902	0.858	0.724	0.771
	R^2	0.508	0.814	0.736	0.524	0.595
	SEE	8.28382	4.45926	5.92749	10.17291	8.70401
MC 3	R	0.573	0.844	0.773	0.650	0.714
	R^2	0.329	0.712	0.597	0.422	0.509
	SEE	9.67949	5.55472	7.32097	11.20616	9.58143
MC 4	R	0.448	0.812	0.698	0.456	0.584
	R^2	0.201	0.660	0.487	0.208	0.341
	SEE	10.56093	6.03318	8.26321	13.12046	11.09916
MC 5	R	0.581	0.806	0.660	0.574	0.485
	R^2	0.337	0.650	0.436	0.329	0.235
	SEE	9.65938	6.13491	8.67872	12.13626	11.90087
Stepwise	R	0.713	0.904	0.859	0.724	0.776
Model 1	R^2	0.508	0.817	0.738	0.524	0.602
	SEE	8.32248	4.43651	5.91711	10.22371	8.58358
Predictors		MC2	MC2	MC2	MC2	MC2
Stepwise	R	0.780	0.924	0.879	0.790	0.849
Model 2	R^2	0.608	0.853	0.773	0.624	0.721
	SEE	7.47180	3.98971	5.53297	9.12976	7.22912
Predictors		MC2	MC2	MC2	MC2	MC2
		MC4	MC1	MC1	MC4	MC5
Stepwise	R	0.792		0.897	0.841	0.879
Model 3	R^2	0.628		0.805	0.707	0.773
	SEE	7.31940		5.15711	8.10085	6.54756
Predictors		MC2		MC2	MC2	MC2
		MC4		MC1	MC4	MC5
		MC1		MC5	MC3	MC3
Stepwise	R					0.906
Model 4	R^2					0.821
	SEE					5.84479
Predictors						MC2
						MC5
						MC3
						MC4

Table 8.23: Direct and stepwise regression coefficients (slope and constant) and standard error of the estimates (SEE) (mm) of metacarpals (MC) 1 to 5 to estimate the length (mm) of a long bone in South African females

	Humerus	Radius	Ulna	Femur	Tibia
Direct					
MC 1	0.942	1.120	1.507	0.624	0.669
MC 2	3.104	1.503	2.579	3.644	3.882
MC 3	0.688	0.286	1.055	3.246	3.157
MC 4	-2.760	0.045	-0.984	-4.626	-2.238
MC 5	0.101	0.058	-1.352	-0.716	-3.491
Constant	171.617	63.212	73.930	264.666	188.928
SEE	7.32868	4.00888	4.97223	8.05951	5.77430
Metacarpal 1					
Slope	2.729	3.233	3.443	3.310	3.262
Constant	190.697	92.970	99.766	295.021	223.231
SEE	9.34768	5.81861	7.07333	11.86070	10.60585
Metacarpal 2					
Slope	2.204	2.443	2.589	2.793	2.760
Constant	165.358	73.681	80.026	256.580	184.866
SEE	8.28382	4.45926	5.92749	10.17291	8.70401
Metacarpal 3					
Slope	1.787	2.303	2.352	2.528	2.574
Constant	195.445	86.967	99.657	278.278	201.586
SEE	9.67949	5.55472	7.32097	11.20616	9.58143
Metacarpal 4					
Slope	1.561	2.479	2.374	1.984	2.356
Constant	220.706	93.838	115.365	326.407	232.108
SEE	10.56093	6.03318	8.26321	13.12046	11.09916
Metacarpal 5					
Slope	2.091	2.535	2.316	2.578	2.003
Constant	200.375	101.492	128.361	304.606	260.173
SEE	9.65938	6.13491	8.67872	12.13626	11.90087
Stepwise Model 1					
MC 2	2.202	2.439	2.585	2.792	2.750
Constant	165.498	73.999	80.374	256.694	185.707
SEE	8.32248	4.43651	5.91711	10.22371	8.58358
Stepwise Model 2					
MC 1		1.205	1.320		
MC 2	3.815	1.784	1.867	4.814	-2.744
MC 4	-2.129			-2.669	
MC 5					4.763
Constant	179.312	64.843	70.342	274.015	196.126
SEE	7.47180	3.98971	5.53297	9.12976	7.22912
Stepwise Model 3					
MC 1	1.032		1.542		
MC 2	3.383		2.646	3.614	3.703
MC 3				3.096	1.935
MC 4	-2.299			-4.660	
MC 5			-1.226		-3.606
Constant	172.577		73.317	267.830	187.462
SEE	7.31940		5.15711	8.10085	6.54756
Stepwise Model 4					
MC 2					4.100
MC 3					3.239
MC 4					-2.201
MC 5					-3.429
Constant					193.024
SEE					5.84479

Table 8.24: Direct and stepwise regression showing the sequence of variable entry of proximal phalanges (PP) 1 to 5 into the analysis and standard error of the estimates (SEE) (mm), *R* and R^2 to estimate the length (mm) of a long bone in South African females

		Humerus	Radius	Ulna	Femur	Tibia
All PP	R	0.565	0.788	0.735	0.533	0.615
Direct	R^2	0.319	0.622	0.540	0.284	0.378
	SEE	9.93376	6.58907	8.06088	12.71758	11.00904
PP 1	R	0.420	0.706	0.646	0.466	0.500
	R^2	0.177	0.499	0.417	0.217	0.250
	SEE	10.74584	7.36507	8.83879	13.11484	11.90683
PP 2	R	0.482	0.648	0.562	0.459	0.513
	R^2	0.232	0.419	0.315	0.211	0.263
	SEE	10.35382	7.88511	9.54503	13.10113	11.73771
PP 3	R	0.338	0.680	0.634	0.412	0.522
	R^2	0.114	0.463	0.401	0.170	0.273
	SEE	11.14588	7.62583	8.95944	13.50146	11.72385
PP 4	R	0.362	0.717	0.678	0.404	0.592
	R^2	0.131	0.514	0.459	0.163	0.351
	SEE	11.05382	7.22629	8.52704	13.53318	11.02685
PP 5	R	0.381	0.597	0.561	0.403	0.441
	R^2	0.145	0.357	0.315	0.162	0.195
	SEE	10.81125	8.34223	9.53232	13.33132	12.17230
Stepwise	R	0.474	0.722	0.695	0.461	0.601
Model 1	R^2	0.225	0.521	0.483	0.212	0.361
	SEE	10.36161	7.24506	8.35507	13.04313	10.91264
Predictors		PP2	PP4	PP4	PP2	PP4
Stepwise	R		0.777	0.734	0.511	
Model 2	R^2		0.604	0.538	0.261	
	SEE		6.63097	7.94253	12.70439	
Predictors			PP4	PP4	PP2	
			PP1	PP1	PP1	

Table 8.25: Direct and stepwise regression coefficients (slope and constant) and standard error of the estimates (SEE) (mm) of proximal phalanges (PP) 1 to 5 to estimate the length (mm) of a long bone in South African females

	Humerus	Radius	Ulna	Femur	Tibia
Direct					
PP 1	0.653	1.591	1.623	1.442	0.935
PP 2	3.482	0.774	0.067	2.359	0.562
PP 3	-1.554	0.379	0.358	-0.106	-0.380
PP 4	-1.030	0.725	1.617	-1.140	2.553
PP 5	1.800	0.439	0.102	1.562	-0.244
Constant	207.522	96.508	113.768	306.438	235.050
SEE	9.93376	6.58907	8.06088	2.71758	11.00904
Proximal Phalanx 1					
Slope	2.250	1.946	3.384	3.119	3.107
Constant	242.711	194.827	149.687	346.918	273.431
SEE	10.74584	7.36507	8.83879	13.11484	11.90683
Proximal Phalanx 2					
Slope	2.226	2.622	2.535	2.648	2.746
Constant	221.630	130.172	149.223	334.514	256.924
SEE	10.35382	7.88511	9.54503	13.10113	11.73771
Proximal Phalanx 3					
Slope	1.514	2.678	2.778	2.312	2.718
Constant	241.910	115.653	127.044	336.709	245.490
SEE	11.14588	7.62583	8.95944	13.50146	11.72385
Proximal Phalanx 4					
Slope	1.576	2.732	2.889	2.199	2.979
Constant	243.570	120.755	130.231	347.614	242.561
SEE	11.05382	7.22629	8.52704	13.53318	11.02685
Proximal Phalanx 5					
Slope	1.913	2.669	2.774	2.521	2.570
Constant	247.211	147.793	160.181	357.375	282.136
SEE	10.81125	8.34223	9.53232	13.33132	12.17230
Stepwise Model 1					
PP 2	2.315			2.808	
PP 4		2.747	2.935		2.978
Constant	218.203	119.890	128.047	328.304	242.200
SEE	10.36161	7.24506	8.35507	13.04313	10.91264
Stepwise Model 2					
PP 1		1.844	1.674	1.861	
PP 2				1.731	
PP 4		1.724	2.006		
Constant		108.508	117.717	316.457	
SEE		6.63097	7.94253	12.70439	

Table 8.26: Direct and stepwise regression showing the sequence of variable entry of middle phalanges (MP) 2 to 5 variables into the analysis and standard error of the estimates (SEE) (mm), *R* and R^2 to estimate the length (mm) of a long bone in South African females

		Humerus	Radius	Ulna	Femur	Tibia
All MP	R	0.488	0.694	0.635	0.544	0.582
Direct	R^2	0.238	0.481	0.403	0.295	0.339
	SEE	10.51108	7.62308	9.06152	12.77742	11.37170
MP 2	R	0.372	0.494	0.459	0.447	0.407
	R^2	0.138	0.244	0.211	0.199	0.166
	SEE	10.93960	9.01284	10.17761	13.09190	12.40922
MP 3	R	0.433	0.654	0.599	0.497	0.557
	R^2	0.188	0.427	0.359	0.247	0.310
	SEE	10.69703	7.87079	9.27629	12.86394	11.42045
MP 4	R	0.378	0.619	0.567	0.414	0.510
	R^2	0.143	0.383	0.322	0.172	0.260
g	SEE	10.78037	8.19651	9.54919	13.48752	11.74718
MP 5	R	0.330	0.444	0.400	0.313	0.361
	R^2	0.109	0.197	0.160	0.098	0.130
	SEE	11.30222	9.22123	10.59255	14.21647	12.86149
Stepwise	R	0.423	0.651	0.589	0.498	0.543
Model 1	R^2	0.179	0.423	0.347	0.248	0.295
	SEE	10.71605	7.89318	9.31015	12.96420	11.54082
Predictors		MP3	MP3	MP3	MP3	MP3
Stepwise	R		0.682	0.620		0.573
Model 2	R^2		0.465	0.385		0.329
	SEE		7.64659	9.09013		11.32428
Predictors			MP3	MP3		MP3
			MP5	MP4		MP4

Table 8.27: Direct and stepwise regression coefficients (slope and constant) and standard error of the estimates (SEE) (mm) of middle phalanges (MP) 2 to 5 to estimate the length (mm) of a long bone in South African females

	Humerus	Radius	Ulna	Femur	Tibia
Direct					
MP 2	1.275	0.625	0.851	1.779	0.642
MP 3	1.080	2.193	1.946	2.040	2.257
MP 4	0.283	0.621	0.791	0.264	0.983
MP 5	0.899	0.730	0.639	0.825	0.656
Constant	223.876	126.065	140.647	316.813	247.182
SEE	10.51108	7.62308	9.06152	12.77742	11.37170
Middle Phalanx 2					
Slope	2.361	2.760	2.837	3.523	2.980
Constant	253.355	168.094	181.994	356.014	294.527
SEE	10.93960	9.01284	10.17761	13.09190	12.40922
Middle Phalanx 3					
Slope	2.597	3.437	3.507	3.721	3.867
Constant	235.355	136.055	149.880	333.534	255.753
SEE	10.69703	7.87079	9.27629	12.86394	11.42045
Middle Phalanx 4					
Slope	1.822	2.671	2.721	2.540	2.883
Constant	258.928	160.162	174.586	368.930	286.259
SEE	10.78037	8.19651	9.54919	13.48752	11.74718
Middle Phalanx 5					
Slope	1.808	2.095	2.119	2.145	2.283
Constant	272.890	191.293	206.545	395.548	319.230
SEE	11.30222	9.22123	10.59255	14.21647	12.86149
Stepwise					
Model 1					
MP 3	2.558	3.456	3.468	3.808	3.811
Constant	236.322	135.545	150.882	330.764	257.194
SEE	10.71605	7.89318	9.31015	12.96420	11.54082
Stepwise					
Model 2					
MP 3		3.018	2.333		2.523
MP 4			1.318		1.495
MP 5		1.036			
Constant		128.168	147.276		253.105
SEE		7.64659	9.09013		11.32428

Table 8.28: Direct and stepwise regression showing the sequence of variable entry of distal phalanges (DP) 1 to 5 into the analysis and standard error of the estimates (SEE) (mm), *R* and R^2 to estimate the length (mm) of a long bone in South African females

		Humerus	Radius	Ulna	Femur	Tibia
All DP	R	0.495	0.600	0.536	0.513	0.442
Direct	R^2	0.245	0.360	0.287	0.263	0.195
	SEE	10.75109	9.02764	10.14532	13.32497	13.00060
DP 1	R	0.354	0.474	0.420	0.419	0.337
	R^2	0.125	0.224	0.176	0.175	0.113
	SEE	11.09019	9.12218	10.35052	13.54571	12.91585
DP 2	R	0.328	0.470	0.410	0.349	0.314
	R^2	0.108	0.221	0.168	0.122	0.098
	SEE	11.23967	9.22203	10.42380	13.93184	13.09722
DP 3	R	0.244	0.507	0.381	0.286	0.322
	R^2	0.059	0.257	0.145	0.082	0.104
	SEE	11.48434	9.01562	10.74986	14.49094	13.09369
DP 4	R	0.398	0.486	0.395	0.259	0.281
	R^2	0.159	0.236	0.156	0.067	0.079
	SEE	10.97460	9.22789	10.65546	14.47203	13.20502
DP 5	R	0.398	0.432	0.345	0.402	0.354
	R^2	0.159	0.187	0.119	0.162	0.125
	SEE	10.97460	9.49433	10.86264	13.57887	12.91634
Stepwise	R	0.435	0.583	0.532	0.486	0.427
Model 1	R^2	0.189	0.340	0.283	0.237	0.182
	SEE	10.84039	8.91060	9.89631	13.18908	12.74598
Predictors		DP1	DP1	DP1	DP1	DP1

Table 8.29: Direct and stepwise regression coefficients (slope and constant) and standard error of the estimates (SEE) (mm) of distal phalanges (DP) 1 to 5 to estimate the length (mm) of a long bone in South African females

	Humerus	Radius	Ulna	Femur	Tibia
Direct					
DP 1	3.746	3.521	4.107	5.599	3.692
DP 2	-1.125	-0.336	0.757	-0.852	-0.318
DP 3	-1.997	1.730	0.425	-0.256	-0.128
DP 4	-0.131	0.270	-0.062	-1.570	-0.479
DP 5	3.392	-0.183	-0.690	2.318	1.876
Constant	230.396	129.224	151.322	326.972	270.336
SEE	10.75109	9.02764	10.14532	13.32497	13.00060
Distal Phalanx 1					
Slope	2.664	3.112	3.038	3.961	2.929
Constant	250.838	165.159	182.598	352.549	300.466
SEE	11.09019	9.12218	10.35052	13.54571	12.91585
Distal Phalanx 2					
Slope	3.129	3.936	3.752	4.159	3.463
Constant	256.059	166.482	185.353	368.337	305.812
SEE	11.23967	9.22203	10.42380	13.93184	13.09722
Distal Phalanx 3					
Slope	2.263	3.936	3.292	3.213	3.310
Constant	266.577	161.447	188.455	379.051	303.654
SEE	11.48434	9.01562	10.74986	14.49094	13.09369
Distal Phalanx 4					
Slope	2.019	3.595	3.209	2.715	2.702
Constant	271.169	167.699	190.337	387.947	314.885
SEE	10.97460	9.22789	10.65546	14.47203	13.20502
Distal Phalanx 5					
Slope	3.695	3.526	3.092	4.628	3.788
Constant	248.982	175.845	198.308	363.706	302.880
SEE	10.97460	9.49433	10.86264	13.57887	12.91634
Stepwise					
Model 1					
DP 1	3.730	4.566	4.431	5.237	4.288
Constant	227.139	133.869	152.588	324.354	270.735
SEE	10.84039	8.91060	9.89631	13.18908	12.74598

CHAPTER 9

RESULTS - SEX DETERMINATION

9.1 Introduction

Seven measurements were recorded on each of the hand bones, the details of which are set out in the chapter on materials and methods. These measurements included the length dimension, anteroposterior (ap) and mediolateral (ml) head dimensions, anteroposterior (ap) and mediolateral (ml) midshaft dimensions, anteroposterior (ap) and mediolateral (ml) base dimensions.

In the present study, discriminant function analysis using a stepwise and direct approach, was conducted on the pooled data which was based on results from the descriptive analysis. From this, canonical discriminant function coefficients for the stepwise and direct procedures as well as sexing accuracies were obtained. The canonical discriminant coefficients will be discussed in detail with the metacarpals where examples will be given on how to incorporate these values into the equation to estimate sex. For the phalanges, reference will be made to the table. The calculations for the phalanges are exactly the same as that for the metacarpals.

In the first step, the stepwise discriminant function procedure is performed using Wilk's lambda with F=3.84 to enter and F=2.71 to remove. In other words, Wilk's lambda determines the order in which the variables are selected to enter into the function. Multivariate analysis of variance (MANOVA) is used to compare the group means on a combination of variables. In the present study, the groups would be male and female while the variables are the seven dimensions of each hand bone. The value of interest in the results generated by the computer is Wilk's lambda. These values are arranged from the highest to the lowest confidence scores. Lambda can be described almost as an inverse measure. In other words, if its values are near zero then it denotes a high discrimination between the groups. If the values are further away from zero, then it denotes a low discrimination between the groups. In addition to the Wilk's lambda scores, the values for the exact F-ratio are also provided. These values are also

graded from the highest to the lowest and interpreted in the same manner as the Wilk's lambda. Thus, the Wilk's lambda will be described for each series of hand bones.

Wilk's lambda is also used to test the significance of the discriminant function as a whole. The larger the lambda value the more likely that the discriminant function is significant. A significant lambda means that one can reject the null hypothesis that two groups have the same discriminant function score. One can therefore conclude that the variable entered is discriminating. In other words, either one or all seven hand bone dimensions are significantly different between males and females.

The stepwise discriminant function analysis generates the output in a stepwise manner. Stepwise selects the one parameter that provides the best discrimination first, and then sees what has not already been "covered" by that parameter, thereby selecting the second best discriminator until it has chosen the best possible combination of variables.

In the present study, the (model) stepwise Wilk's lambda was run initially to generate the discriminant functions that would yield the highest lambda scores for each series of hand bones and to list them in a stepwise manner. Lambda varies from zero to one, with zero indicating a difference in the group mean values. A value of one indicates all the group means are the same. The F test of lambda shows which variable has a significant contribution.

In order to carry out the direct Wilk's lambda analysis, the discriminant function with the highest lambda score from the stepwise procedure was used. The reason for doing this is that a vast number of combinations of all variables are possible. In other words, the statistics would become overwhelming considering that there are seven dimensions for each hand bone and that there are four hand bone series, namely, metacarpals, proximal, middle and distal phalanges.

For practical reasons, a stepwise analysis was carried out firstly, using all measurements per hand bone. Secondly, the direct analysis was run using the "best" measurement per hand bone only.

In the statistical analysis there is an F- test of significance of the ratio between two Wilk's lambdas. The second lambda is divided by the first lambda where there are fewer

predictors, and an approximate F value for this ratio is calculated (Tabachnick & Fidell 2007). This F- ratio also assesses the improvement in classification when using sequential discriminant analysis. In the present study, the Wilk's lambda will be reported with comments on the level of significance.

In the second output, canonical discriminant function coefficients are generated. Canonical analysis is a multivariate technique that determines the relationship between groups of variables in a data set. In this analysis, values for the unstandardized and standardized coefficients as well as the structure coefficients are given. The sum of the unstandardized discriminant coefficients and the constant with the observations yields the discriminant scores. Unstandardized discriminant function coefficients and standardized discriminant coefficients are partial coefficients that are used to assess the relative classifying importance of the independent variables (e.g. seven hand bone dimensions).

The group centroids are the mean discriminant scores of each dependent variable categories (e.g. male and female) for each of the discriminant scores (e.g. seven hand bone dimensions). A two-group discriminant analysis will have two centroids, one for each group. The indication that the discriminant function is clearly discriminating is when the mean values are distinctly different. If the mean values are close to each other, the likelihood of more errors of classification exists. The midpoint between the two centroids is the sectioning point.

In the third output, discriminant analysis with cross-validation, which is done only for those cases in the analysis, is then used to assess classification accuracy. In cross-validation, each case is classified by the functions derived from all cases other than that case.

The ultimate goal in this chapter is to develop discriminant function formulae using metacarpals, proximal, middle, and distal phalanges for the South African population. This information will contribute to existing data on different parts of the skeleton recorded by other researchers on the South African population. Each series of hand bones will be reported on independently.

9.2 Metacarpals (Tables 9.1 to 9.3)

The results of the discriminant function analysis of metacarpals are shown in Table 9.1). When all seven variables were entered for metacarpal 1, only five variables were selected in a stepwise manner and two were excluded. The order of selection was mediolateral (ml) midshaft, mediolateral (ml) head, mediolateral (ml) base, anteroposterior (ap) midshaft and length variables. The variable with the largest Wilk's lambda score was the mediolateral (ml) midshaft dimension. This variable will yield a high sexing accuracy with the least amount of error. The variable with the lowest Wilk's lambda score was the length dimension. This variable, on the other hand, will yield a low sexing accuracy and have a high error. The variable with the largest Wilk's lambda score also had the largest univariate F-ratios. The range of F-ratios for first metacarpals was from 38.88 to 125.78. Results for the first metacarpal were highly significant ($p<0.01$). To run the direct analysis, only the mediolateral midshaft dimension was entered into the computer. The results also indicated a high Willk's lambda score for this variable, similar to that of the computed with the stepwise procedure.

Stepwise discriminant function analysis for the second metacarpal selected three variables. The order of their selection were anteroposterior (ap) base, anteroposterior (ap) midshaft and mediolateral (ml) base dimensions. The variable with the highest Wilk's lambda score and exact F-ratio was the anteroposterior (ap) base dimension. In other words, this variable has a high sexing accuracy with the least amount of error. The mediolateral (ml) base has the lowest Wilk's lambda score and is expected to have the highest error in sexing accuracy. While the univariate F-ratio's for second metacarpals were slightly less (range = 53.41 to 87.16) than those of the first metacarpal, they were statistically significant ($p<0.01$). A direct discriminant analysis using the anteroposterior (ap) base dimension yielded a high Wilk's lambda score and exact F-ratio with a lambda value close to the same variable computed through the stepwise analysis.

An analysis in a stepwise manner for the third metacarpal showed that the first two out of the three variables selected are exactly the same as those selected for the second metacarpal. These are the anteroposterior (ap) base which had the highest Wilk's lambda

score, followed by the anteroposterior (ap) midshaft dimension. The variable with the lowest Wilk's lambda score and exact F-ratio was the anteroposterior (ap) head dimension. The range recorded for the univariate F-ratio's was 53.90 to 116.972. The direct discriminant analysis for the anteroposterior (ap) base dimension generated a Wilk's lambda score close to that of the same variable generated in the stepwise analysis. All results were highly significant ($p<0.01$).

Results for the fourth metacarpal also yielded three variables similar to that of the second and third metacarpals. These variables are the anteroposterior (ap) and mediolateral (ml) base and anteroposterior (ap) midshaft dimensions. The first selected variable with the highest lambda score and F-ration was the anteroposterior (ap) base. The variable with the lowest Wilk's lambda score was the anteroposterior (ap) midshaft dimension. Univariate F-ratio's recorded for fourth metacarpals ranged from 42.958 to 108.914.

The last bone in the series yielded five variables in the stepwise analysis. Except for the anteroposterior (ap) head dimension, all the dimensions selected are similar to those of the first metacarpal. The sequence of the selection, however, differs from that of the first metacarpal. The variable with the highest Wilk's lambda score and F-ratio in the fifth metacarpal is the anteroposterior (ap) head dimension. As is the case of the first metacarpal, the variable with the lowest Wilk's lambda score is length. The range for the univariate F-ratio's is recorded from 33.940 to 97.384.

An overview of the metacarpal results indicate that the base is the preferred dimension for metacarpals two, three, and four while the midshaft and head are the dimensions selected for the first and fifth metacarpals respectively. Moreover, anteroposterior rather than mediolateral width dimensions are considered the best sex determinants in the metacarpal series. The lengths of metacarpals do not have a role in sexing accuracies.

In the second part of the discrimant analysis, canonical discriminant coefficients produced by the stepwise and direct analyses are generated (Table 9.2). The output reflects the values for the unstandardized coefficients, standardardized coefficients, structure coefficients and group centroids. The unstandardized (raw) coefficients are used to calculate the discriminant function formulae. The standard coefficient provides information on the

contribution of that variable to the overall classification, while the structure coefficient assesses the product-moment correlation between the variables and the discriminant function respectively. The sectioning point is the midpoint between the two centroids and is calibrated to zero if the samples are of equal size. If the calculated value falls below the sectioning point, the bone is female. On the other hand, if the value is above, then the bone is male.

9.3 Calculation of discriminant scores

Before calculating a discriminant score the following steps need to be followed:

1) The hand bone/s must first be identified
2) Seven dimensions must be recorded on each hand bone
3) A discriminant function analysis must then be run on the data
4) A stepwise and direct analysis must be carried out
5) Look for the variable with the highest Wilk's lambda value and establish in the output the significance level. A high lambda is indicative of the best discriminator for sex
6) Analyze the output with the canonical discriminant function coefficients as these will be entered into the following formula:

DS = unstandardized (raw) coefficient x dimension + c

[Where DS=discriminating score, c=constant]

7) Calculate the sectioning point
8) Compare the discriminating score to the sectioning point to confirm whether the bone is male or female
9) Establish sexing accuracies for the original and cross-validated samples

Example

The hand bone of an unknown individual was found and identified as the second metacarpal. The following measurements are obtained for this hand bone:

VARIABLE	MEASUREMENT
mediolateral (ml) head	= 15.67 mm
anteroposterior (ap) head	= 15.16 mm

mediolateral (ml) midshaft = 13.46 mm

anteroposterior (ap) midshaft = 9.40 mm

mediolateral (ml) base = 15.96 mm

anteroposterior (ap) base = 15.08 mm

length = 46.97 mm

Discriminant score (DS) = (unstandardized coefficient x base ap) + (unstandardized coefficient x midshaft ap) + (unstandardized coefficient x base ml) + constant (see Table 9.2)

DS = (0.3046 x 15.08) + (0.5284 x 9.40) + (0.2756 x 15.96) + (-14.5365)

DS = 4.593368 + 4.96696 + 4.398576 – 14.5365

DS = -0.577596 (This value is smaller than the sectioning point, indicating a female)

While the results thus far have been reported for an intact bone, it may happen that only a fragment of a hand bone is available. The first step in such cases would be to identify the hand bone to which this fragment belongs. Following the stepwise procedures for the descriptions of hand bones, let us say that the fragment was the base of a second metacarpal. This variable with its dimension is then entered into the direct discriminant analysis.

DS = (unstandardized coefficient x base ap) + constant

DS = (0.7002 x 15.08) + (-11.5789)

DS = 10.559016 – 11.5789

DS = -1.019884 (This value is smaller than the sectioning point, indicating a female)

However, because only one dimension is available, a demarking point rather than the discriminating score can be used to make assessment easier. The demarking point is obtained from the group means. In this example, it would be the mean value between the two group means. The mean value of the male and female is added and then divided by two. For example:

ap base dimension mean value in males = 17.4763

ap base dimension mean value in females = 15.5860

then, 17. 4763 + 15.5860 = 33.0623 / 2 = 16.53115 (= demarking point)

The ap base measurement of 15.08 mm is smaller than the demarking point, thus also indicating a female. The accuracies of the discriminant functions are shown in Table 9.3.

Metacarpal results for classification accuracy are seen in Table 9.3. For metacarpal one, 85 males and females out of a total original sample of 100 and 99 in the stepwise analysis were correctly classified. In the cross-validated sample, which is based on the “leave one out” classification, 84 males and 85 females out of a sample of 100 and 99 were correctly classified. The results indicate that only one case in the male was dropped in the cross-validation analysis. In the direct analysis, using a single variable, the percentage accuracy was reduced. Seventy five males and 78 females out of a total sample of 100 and 99 respectively, were assigned to the correct sex. The cross-validated results indicate no difference in accuracy when compared to the results of the original sample.

In general, the analyses with multiple variables exhibited better classification accuracies than those of single variables. The rows marked “original” refers to the percentage of individuals predicted to belong to either the male or female group; whereas the cross-validation classification test determines the accuracy of assignment of a bone to either a male or female category. This was achieved by re-classifying each case to see whether that individual case was attributed to the same group membership as during the first classification. Subsequently, the test allows an observation of the number of specimens classified versus the number of specimens in the sample. When using multiple variables, the average range of accuracies is from 76.0 – 85.9% and 83.8 – 86.7% for males and females respectively. This drops to 71.0 – 78.0 % and 78.8 – 86.7% for males and females when single variables are used. The sexing accuracy for metacarpals was thus fairly high in both the original (correct group membership) and cross-validation testing.

9.3 Proximal phalanges (Tables 9.4 to 9.6)

The results of the discriminant function analysis of proximal phalanges are shown in Table 9.4. After entering all seven variables for the first proximal phalanx, three variables were selected in the stepwise procedure. The order of selection was anteroposterior (ap) midshaft, anteroposterior (ap) base and mediolateral (ml) midshaft. The variable with the largest Wilk's lambda score was the mediolateral (ap) midshaft dimension which means that this variable will yield a high sexing accuracy with the least amount of error. While this variable showed the highest lambda score, it was the lowest in the proximal phalangeal series. The range of F-ratios for the first proximal phalanges was 86.5000 to 204.3969. Results for these hand bones were highly significant ($p<0.01$). To run the direct analysis, only the anteroposterior (ap) midshaft dimension was entered into the computer. While the results also indicated a high Willk's lambda score for this variable, similar to that of the computed with the stepwise procedure, it was the lowest in the first proximal phalangeal series of bones.

Stepwise discriminant function analysis for the second proximal phalanx also selected three variables. The order of their selection was midshaft mediolateral (ml), midshaft anteroposterior (ap) and base anteroposterior (ap) dimensions. The variable with the highest Wilk's lambda score and exact F-ratio was the midshaft mediolateral (ml) dimension. While the univariate F-ratio's for second proximal phalanges were slightly less (range = 63.0925 to 148.1646) than those of irst proximal phalanges, they were nonetheless, statistically significant ($p<0.01$). A direct discriminant analysis using the midshaft mediolateral (ml) dimension yielded a high Wilk's lambda score and exact F-ratio with a lambda value equivalent to that for the same variable computed through the stepwise analysis.

Two variables were selected in the stepwise procedure for the third and fourth proximal phalanges, namely, anteroposterior (ap) base and mediolateral (ml) midshaft dimensions, while midshaft (ml) and base (ap) were selected for the fifth proximal phalanx. The unstandardized, standard and structure coefficients as well as the sectioning points are shown in Table 9.5.

The sexing accuracy indicated high percentages for the third proximal phalanx (Table 9.6). An overview of the stepwise procedure for this bone shows that in the original output, 81 cases out of a sample of 100 (81.0%) was correctly assigned as male and 87 out of 98 cases (88.8%) were correctly assigned as female. In the cross-validated analysis, only one case was dropped for both the male and female sample yielding accuracies of 80.0% and 83.8% for male and females respectively. A comparison between the average percentages recorded for the original (84.8%) and cross-validated (83.8%) analysis showed slight differences. Results for the direct analysis using the best selected single variable of the third proximal phalanx, reveals the same values as for the original and cross-validated stepwise analysis. In other words, 82 cases out of a total sample of 100 (82.0%) in males and 86 out of 98 (87.8%) cases in females was the third proximal phalanx correctly assigned. Sexing accuracy averages for the original and cross-validated results was the same, namely, 84.8%.

In general, the analyses with multiple variables provided better classification accuracies than for single variables of the proximal phalangeal series. The average range of accuracies using multiple variables is from 80.6 – 84.0% and 85.9 – 88.8% for male and females respectively. In comparison, these results drops slightly when using single variables with accuracies reported as 74.5 – 85.0% for males while in females the classification accuracies are similar to that for multiple variables, namely, 86.6 – 88.8% (Table 9.6).

An overview of this series of hand bones is that the base and midshaft are the preferred areas of proximal phalanges for sexing a bone. Width measurements of the midshaft and anteroposterior (ap) of the base presented with high lambda scores. The length dimension was not selected for any of the proximal phalanges. Average sexing accuracies for this series of hand bones ranged 81.7% to 86.9% which are fairly high percentages.

9.4 Middle phalanges (Tables 9.7 to 9.9)

Table 9.7 shows the discriminant function analysis for all middle phalanges. While three variables were selected for the second middle phalanx, only two were chosen for the third,

fourth and fifth middle phalanges. The one variable that appears in all middle phalanges is the width of the midshaft. The anteroposterior (ap) dimension of the midshaft is selected for the second, third and fifth middle phalanges. The anteroposterior (ap) dimension of the base is selected for the first and fourth middle phalanges. In terms of priority listing, the highest Wilk's lambda score in the second middle phalanx is the anteroposterior (ap) base dimension (0.5714) in comparison to the mediolateral (ml) midshaft dimension of the third (0.5805), fourth (0.5976) and fifth (0.5831) middle phalanges. The first selected variable generated by the stepwise procedure and entered into the direct analysis, indicates a lambda value similar to that. The lambda value for the fourth middle phalanx, however, was higher than that obtained for the stepwise analysis. This indicates that a single variable can be used to assign sex to a bone. The unstandardized, standard and structure coefficients as well as the sectioning points are shown in Table 9.8.

Classification accuracies for the middle phalangeal series of bones are shown in Table 9.9. For the second middle phalanx 76 out of 98 original cases (77.6%) in males and 82 out of 96 (85.4%) for females, were correctly classified. When the stepwise results are compared to that of the cross-validated output, there was no change in the male group and only one case was dropped in the female group yielding a percentage of 83.3%. The average sexing accuracy was recorded as 81.4% (original) and 80.9% (cross-validated). Entering a single variable for the direct analysis drops the number of cases in males to 71 out of 98 (72.4%) and in females to 80 out of 96 (83.3%) with an average for the two groups being 77.8%.

Average classification accuracies using the third middle phalanx were the highest in the middle phalangeal series and reported as 85.9% using multiple variables and 81.8% using a single variable. Furthermore, none of the cases dropped during cross-validation.

Using multiple variables in the case of the fourth middle phalanx, 77 out of 99 original cases (77.8%) in males and 83 out of 96 cases (86.5%) for females, were correctly classified. There was no change in the cross-validated results with average accuracies reported as 82.1%. These results dropped slightly when single variables were used as 71 out of 99 original cases (71.7%) in males and 82 out of 96 cases (85.4%) for females, were correctly classified.

On cross-validation one case was dropped in males while in females the results stayed the same.

Average classification accuracies using the fifth middle phalanx were the second highest in the middle phalangeal series and reported as 84.8% using multiple variables and 81.7% with single variables.When compared to using multiple variables, the number of cases using single variables dropped to 76 (79.2%) and 80 (84.2%) for males and females respectively with an average accuracy range of 84.3 – 84.8%. When comparing accuracies for the original and cross-validated analysis using single variables, none of the cases were dropped.

In conclusion, using single variables in the middle phalangeal series of bones will reduce the overall sexing accuracy in comparison to using as many variables as possible. However, the computed statistics for the middle phalangeal series of bones indicates that single variables of the third and fifth bones yields fairly high sexing accuracies.

9.5 Distal phalanges (Tables 9.10 to 9.12)

Results of the discriminant analysis for the distal phalangeal series of bones are shown in Table 9.10. For the first distal phalanx, three variables selected in a stepwise manner were, base (ap), length, and midshaft (ap) of which the base (ap) dimension had the highest lambda score (0.59698). Direct analysis on the anteroposterior (ap) base dimension revealed a lambda value (0.5970) close to that given in the stepwise approach. While three variables were also selected for the second distal phalanx, they were slightly different to that of the first bone, namely, midshaft (ap), length and base (ml) dimensions. The midshaft (ap) dimension had the highest lambda score (0.69351) with a corresponding high F-ratio (84.411). This variable was entered into the direct analysis yielding a lambda value (0.6935) close to that reported in the stepwise procedure with a similar F-ratio (84.4112). For distal phalanges 3 and 4, the same three variables were selected, namely, base (ml), length and midshaft (ap) dimensions. The base (ml) dimension had the highest lambda score of 0.65801 (distal phalanx 3) and 0.71977

(distal phalanx 4) and a corresponding high F-ratio of 98.230 (distal phalanx 3) and 72.025 (distal phalanx 4). Entering these variables entered into the direct analysis yielded similar results to that of the direct analysis. Four variables were selected for the fifth distal phalanx, namey, length, base (ml), midshaft (ap), and head (ml). The length dimension had the highest lambda score (0.63854) and F-ratio (101.328). Generally, the lambda scores and F-ratios using multiple and single variables were similar. The unstandardized, standard and structure coefficients as well as the sectioning points are shown in Table 9.11.

Classification accuracies using distal phalanges are shown in Table 9.12. For the first distal phalanx, 84 out of 100 males (84.0%) and 84 out of 99 females (84.8%) were correctly sexed. On cross-validation, only one case was dropped for males resulting in 83.0% sexing accuracy with no change in the number of female cases. Average accuracies with multiple variables were 84.4% (original) and 83.9% (cross-validated). When using a single variable the number of cases in males dropped in that 81 out of 100 cases (81.0%) were correctly classified while the numbers of female cases increased slightly in that 86 out of 99 (83.9%) females were correctly classified. Average accuracies for multiple and single variables was 84.4% and 83.9% respectively.

For the second distal phalanx, 76 out of 97 males (78.4%) and 80 out of 96 females (83.3%) were correctly assigned. On cross-validation, one case was dropped in males (77.3%) and in females (82.3%). Average accuracies for multiple variables were 80.8% (original) and 79.8 (cross-validated). The number of cases dropped slightly when using single variables as compared to multiple variables. In other words, 71 out of 96 (73.2%) male and 75 out of 96 (78.1%) female cases were correctly assigned. No cases were dropped on cross-validation with single variables. The average accuracy reported for single variables was 75.6%.

In the third distal phalanx, 77 of 96 cases in males (80.2%) and 80 out of 95 cases for females (84.2%) were correctly assigned. On cross-validation, one case was dropped in males (79.2%) and two in females (82.1%). The average sexing accuracies were 82.2% (original) and 80.6% (cross-validated). When only a single variable is entered, the results indicate a drop in accuracies in that 74 cases (77.1%) in males and 74 cases (77.1%) in females were only

correctly assigned. On cross-validation, no cases were dropped for either males or females. Average sexing accuracies using single variables was 77.1%.

Sexing accuracies for the fouth distal phalanx indicate that 77 out of 95 males (81.1%) and 74 out of 93 females (79.6%) cases were correctly assigned. On cross-validation, the number of male cases stayed the same while one case was dropped from the female sample (78.5%). Average accuracies were recorded as 80.3% (original) and 79.8% (cross-validated). Using single variables, there is a drop in the number of cases to 73 (76.8%) in males and 73 (79.6%) in females. No cases were dropped on cross-validation when using single variables and average accuracies were reported as 78.2%.

Generally, the fifth distal phalanx gave the highest sexing accuracy. When multiple variables are used, 80 out of 94 (85.1%) males and 73 out of 87 (93.9%) females were accurately sexed. On cross-validation, one case was dropped in males (81.9%) and one in females (82.8%). Average sexing accuracies for males and females was 84.5% (original) and 82.3% (cross-validated). When using single variables, 75 out of 94 (79.8%) males and 70 out of 87 (80.5%) females were correctly assigned. Cross-validated results showed that only one case was dropped in females with an overall average classification accuracy of 79.0 – 80.1%.

In conclusion, the sexing accuracies for distal phalanges are fairly high using multiple and single variables with the fifth distal phalanx as the best selected bone in this series.

Table 9.1: Discriminant function analysis of metacarpals 1 to 5 for South Africans

Function	Step	Variable	Wilk's lambda	Exact F-ratio	d.f
Metacarpal 1					
Stepwise	1	midshaft ml	0.610	125.780	1.197
	2	head ml	0.563	75.929	2.196
	3	base ml	0.537	56.142	3.195
	4	midshaft ap	0.514	45.769	4.194
	5	length	0.498	38.878	5.193
Direct	1	midshaft ml	0.610	125.780	1.197
Metacarpal 2					
Stepwise	1	base ap	0.693	87.165	1.197
	2	midshaft ap	0.590	68.004	2.196
	3	base ml	0.549	53.409	3.195
Direct	1	base ap	0.693	87.165	1.197
Metacarpal 3					
Stepwise	1	base ap	0.627	116.972	1.197
	2	midshaft ap	0.575	72.568	2.196
	3	head ap	0.547	53.900	3.195
Direct	1	base ap	0.627	116.972	1.197
Metacarpal 4					
Stepwise	1	base ap	0.643	108.914	1.196
	2	base ml	0.547	53.611	3.194
	3	midshaft ap	0.529	42.958	4.193
Direct	1	base ap	0.641	110.344	1.197
Metacarpal 5					
Stepwise	1	head ap	0.667	97.384	1.195
	2	midshaft ml	0.592	66.738	2.194
	3	base ml	0.570	48.479	3.193
	4	midshaft ap	0.550	39.220	4.192
	5	length	0.530	33.940	5.191
Direct	1	head ap	0.667	97.384	1.195

ap=anteroposterior, ml=mediolateral, df-degrees of freedom

Table 9.2: Canonical discriminant function coefficients of metacarpals (MC) 1 to 5 for South Africans

Function	Step	Variable	Unstandardized coefficient	Standard coefficient	Structure coefficient	Group centroids
MC1 Stepwise	1	midshaft ml	0.2861	0.3016	0.7962	M=0.9935
	2	head ml	0.2566	0.3384	0.6470	F=-1.0036
	3	base ml	0.2121	0.2879	0.5766	
	4	midshaft ap	0.3822	0.3239	0.6573	
	5	length	0.0982	0.2730	0.5938	
		(Constant)	-18.3415			
		Sectioning point	-0.00505			
Direct	1	midshaft ml	0.9485	1	1	M=0.7910
		(Constant)	-11.5287			F=-0.7990
		Sectioning point	-0.0040			
		Demarking point	Males>12.15>Females			
MC2 Stepwise	1	base ap	0.3046	0.4350	0.7338	M=0.8974
	2	midshaft ap	0.5284	0.5153	0.7301	F=-0.9064
	3	base ml	0.2756	0.4294	0.7093	
		(Constant)	-14.5365			
		Sectioning point	-0.00450			
Direct	1	base ap	0.7002	1	1	M=0.6585
		(Constant)	-11.5789			F=-0.6652
		Sectioning point	-0.0033			
		Demarking point	Males>16.53>Females			
MC3 Stepwise	1	base ap	0.3324	0.4219	0.8462	M=0.9015
	2	midshaft ap	0.4283	0.3942	0.7375	F=-0.9106
	3	head ap	0.4124	0.4216	0.8353	
		(Constant)	-15.5067			
		Sectioning point	-0.00455			
Direct	1	base ap	0.7879	1	1	M=0.7628
		(Constant)	-13.1813			F=-0.7705
		Sectioning point	-0.0038			
		Demarking point	Males>16.72>Females			
MC4 Stepwise	1	base ap	0.4163	0.4200	0.8003	M=0.9174
	2	base ml	0.4627	0.4861	0.6529	F=-0.9361
	3	midshaft ap	0.5275	0.4849	0.7145	
		(Constant)	-14.5196			
		Sectioning point	-0.00935			
Direct	1	base ap	0.9935	1	1	M=0.7409
		(Constant)	-12.2514			F=-0.7484
		Sectioning point	-0.0037			
		Demarking point	Males>12.33>Females			
MC5 Stepwise	1	midshaft ml	0.3723	0.3096	0.7072	M=0.9291
	2	base ml	0.2954	0.3909	0.6371	F=-0.9386
	3	midshaft ap	0.4857	0.4411	0.7288	
	4	length	0.1157	0.3786	0.5560	
		(Constant)	-16.4791			
		Sectioning point	-0.00475			
Direct	1	midshaft ml	1.1567	1	1	M=0.6995
		(Constant)	-13.7773			F=-0.7067
		Sectioning point	-0.0036			
		Demarking point	Males>11.91>Females			

ap=anteroposterior, ml=mediolateral

Table 9.3: Sexing accuracy of metacarpals 1 to 5 of South Africans. Percentage of correct group membership and cross-validation

Function		N (Total)	Male Count	%	Female Count	%	Average Accuracy
Metacarpal 1							
Stepwise	Original	199	85/100	85.0	85/99	85.9	85.4
	Cross-validated	199	84/100	85.0	85/99	85.9	84.9
Direct-MC1 midshaft ml	Original	199	75/100	75.0	78/99	78.8	76.9
	Cross-validated	199	75/100	75.0	78/99	78.8	76.9
Metacarpal 2							
Stepwise	Original	199	76/100	76.0	83/99	83.8	79.9
	Cross-validated	199	76/100	76.0	82/99	82.8	79.4
Direct-MC2 base ap	Original	199	71/100	71.0	80/99	80.8	75.9
	Cross-validated	199	71/100	71.0	80/99	80.8	75.9
Metacarpal 3							
Stepwise	Original	199	80/100	80.0	83/99	83.8	81.9
	Cross-validated	199	79/100	79.0	83/99	83.8	81.4
Direct-MC3 base ap	Original	199	72/100	72.0	84/99	84.8	78.4
	Cross-validated	199	72/100	72.0	83/99	83.8	77.9
Metacarpal 4							
Stepwise	Original	198	80/100	80.0	85/98	86.7	83.3
	Cross-validated	198	77/100	77.0	85/98	86.7	81.8
Direct-MC4 base ap	Original	199	78/100	78.0	79/99	79.8	78.9
	Cross-validated	199	78/100	78.0	79/99	79.8	78.9
Metacarpal 5							
Stepwise	Original	197	78/99	78.8	84/98	85.7	82.2
	Cross-validated	197	78/99	78.8	84/98	85.7	82.2
Direct-MC5 head ap	Original	199	76/99	76.8	82/98	83.7	80.2
	Cross-validated	199	76/99	76.8	82/98	83.7	80.2

Table 9.4: Discriminant function analysis of proximal phalanges 1 to 5 for South Africans

Function	Step	Variables	Wilks lambda	Exact F-ratio	d.f
Proximal Phalanx 1					
Stepwise	1	midshaft ap	0.4895	204.3969	1.196
	2	base ap	0.4426	122.7989	2.195
	3	midshaft ml	0.4278	86.5000	3.194
Direct	1	midshaft ap	0.4895	204.3969	1.196
Proximal Phalanx 2					
Stepwise	1	midshaft ml	0.5682	148.1646	1.195
	2	midshaft ap	0.5169	90.6562	2.194
	3	base ap	0.5049	63.0925	3.193
Direct	1	midshaft ml	0.5682	148.1646	1.197
Proximal Phalanx 3					
Stepwise	1	base ap	0.5423	165.3920	1.196
	2	midshaft ml	0.4696	110.1276	2.195
Direct	1	base ap	0.5423	165.3920	1.196
Proximal Phalanx 4					
Stepwise	1	base ap	0.5503	160.1438	1.196
	2	midshaft ml	0.5005	97.2858	2.195
Direct	1	base ap	0.5503	160.1438	1.196
Proximal Phalanx 5					
Stepwise	1	midshaft ml	0.5405	161.5076	1.190
	2	base ap	0.4808	102.0623	2.189
Direct	1	midshaft ml	0.5398	163.6591	1.192

ap=anteroposterior, ml=mediolateral, df=degrees of freedom

Table 9.5: Canonical discriminant function coefficients of proximal phalanges (PP) 1 to 5 for South Africans

Function	Step	Variable	Unstandardized coefficient	Standard coefficient	Structure coefficient	Group centroids
PP1 Stepwise	1	midshaft ap	0.8641	0.4899	0.8830	M=1.1391
	2	base ap	0.4285	0.3820	0.8268	F=-1.1624
	3	midshaft ml	0.3856	0.3132	0.8035	
		(Constant)	-13.8089			
		Sectioning point	-0.0116			
Direct	1	midshaft ap	1.7640	1	1	M=1.0058
		(Constant)	-10.9009			F=-1.0263
		Sectioning point	-0.0102			
		Demarking point	Males>6.18>Females			
PP2 Stepwise	1	midshaft ml	0.6104	0.5261	0.8802	M=0.9903
	2	midshaft ap	0.5790	0.3634	0.8017	F=-0.9803
	3	base ap	0.3790	0.2980	0.8241	
		(Constant)	-13.9989			
		Sectioning point	-0.0050			
Direct	1	midshaft ml	1.1601	1	1	M=0.8717
		(Constant)	-11.0219			F=-0.8628
		Sectioning point	-0.0044			
		Demarking point	Males>9.50>Females			
PP3 Stepwise	1	base ap	0.8285	0.6526	0.8643	M=1.0468
	2	midshaft ml	0.6094	0.5457	0.7989	F=-1.0681
		(Constant)	-16.4649			
		Sectioning point	-0.01065			
Direct	1	base ap	1.2695	1	1	M=0.9048
		(Constant)	-15.9796			F=-0.9232
		Sectioning point	-0.0092			
		Demarking point	Males>12.59>Females			
PP4 Stepwise	1	base ap	0.9061	0.6504	0.9049	M=0.9839
	2	midshaft ml	0.5638	0.4959	0.8297	F=-1.0039
		(Constant)	-15.7711			
		Sectioning point	-0.0100			
Direct	1	base ap	1.3931	1	1	M=0.8903
		(Constant)	-16.2481			F=-0.9085
		Sectioning point	-0.0091			
		Demarking point	Males>11.66>Females			
PP5 Stepwise	1	midshaft ml	0.8834	0.6898	0.8872	M=1.0338
	2	base ap	0.6148	0.5019	0.7732	F=-1.0338
		(Constant)	-13.3100			
		Sectioning point	0.0000			
Direct	1	midshaft ml	1.2839	1	1	M=0.9185
		(Constant)	-10.2171			F=-0.9185
		Sectioning point	0.0000			
		Demarking point	Males>7.96>Females			

ap=anteroposterior, ml=mediolateral

Table 9.6: Sexing accuracy using the proximal phalanges 1 to 5. Percentage of correct group membership and cross-validation

Function		N (Total)	Male Count	%	Female Count	%	Average Accuracy
Proximal phalanx 1							
Stepwise	Original	198	84/100	84.0	87/98	88.8	86.4
	Cross-validated	198	84/100	84.0	86/98	87.8	85.9
Direct midshaft ap	Original	198	85/100	85.0	87/98	88.8	86.9
	Cross-validated	198	85/100	85.0	87/98	88.8	86.9
Proximal phalanx 2							
Stepwise	Original	197	79/98	80.6	85/99	85.9	83.2
	Cross-validated	197	79/98	80.6	85/99	85.9	83.2
Direct midshaft ml	Original	197	73/98	74.5	88/99	88.9	81.7
	Cross-validated	197	73/98	74.5	88/99	88.9	81.7
Proximal phalanx 3							
Stepwise	Original	198	81/100	81.0	87/98	88.8	84.8
	Cross-validated	198	80/100	80.0	86/98	87.8	83.8
Direct base ap	Original	198	82/100	82.0	86/98	87.8	84.8
	Cross-validated	198	82/100	82.0	86/98	87.8	84.8
Proximal phalanx 4							
Stepwise	Original	198	81/100	81.0	86/98	87.8	84.3
	Cross-validated	198	80/100	80.0	86/98	87.8	83.8
Direct base ap	Original	198	77/100	77.0	85/98	86.7	84.8
	Cross-validated	198	77/100	77.0	85/98	86.7	83.3
Proximal phalanx 5							
Stepwise	Original	193	81/97	83.5	83/96	86.5	85.0
	Cross-validated	193	81/97	83.5	83/96	86.5	85.0
Direct midshaft ml	Original	194	78/97	80.4	84/97	86.6	83.5
	Cross-validated	194	77/97	79.4	84/97	86.6	83.0

Table 9.7: Discriminant function analysis of middle phalanges 2 to 5 for South Africans

Function	Step	Variables	Wilk's lambda	Exact F-ratio	d.f
Middle Phalanx 2					
Stepwise	1	base ap	0.5714	143.9917	1.192
	2	midshaft ml	0.5252	86.3415	2.191
	3	midshaft ap	0.5132	60.0775	2.190
Direct	1	base ap	0.5714	143.9917	1.192
Middle Phalanx 3					
Stepwise	1	midshaft ml	0.5805	141.6487	1.196
	2	midshaft ap	0.5169	91.1227	2.195
Direct	1	midshaft ml	0.5805	141.6487	1.196
Middle Phalanx 4					
Stepwise	1	midshaft ml	0.5976	129.3029	1.192
	2	base ap	0.5475	78.9273	2.191
Direct	1	midshaft ml	0.6325	112.1567	1.193
Middle Phalanx 5					
Stepwise	1	midshaft ml	0.5831	135.1478	1.189
	2	midshaft ap	0.5227	85.8365	2.188
Direct	1	midshaft ml	0.5831	135.1478	1.189

ap=anteroposterior, ml=mediolateral, df=degrees of freedom

Table 9.8: Canonical discriminant function coefficients of middle phalanges (MP) 2 to 5 for South Africans

Function	Step	Variable	Unstandardized coefficient	Standard coefficient	Structure coefficient	Group centroids
MP2						
Stepwise	1	base ap	0.8555	0.5134	0.8892	M=0.9589
	2	midshaft ml	0.5193	0.3896	0.8262	F=-0.9789
	3	midshaft ap	0.6306	0.2810	0.7887	
		(Constant)	-14.8327			
		Sectioning point	-0.0100			
Direct	1	base ap	1.6665	1	1	M=0.8527
		(Constant)	-15.2669			F=-0.8705
		Sectioning point	-0.0089			
		Demarking point	Males>9.16>Females			
MP3						
Stepwise	1	midshaft ml	0.7944	0.6022	0.8794	M=0.9522
	2	midshaft ap	1.1185	0.5509	0.8539	F=-0.9716
		(Constant)	-12.4827			
		Sectioning point	-0.4761			
Direct	1	midshaft ml	1.3192	1	1	M=0.8373
		(Constant)	-11.0683			F=-0.8544
		Sectioning point	-0.0086			
		Demarking point	Males>8.39>Females			
MP4						
Stepwise	1	midshaft ml	0.8256	0.6140	0.9027	M=0.8951
	2	base ap	0.8356	0.5181	0.8602	F=-0.9138
		(Constant)	-14.4151			
		Sectioning point	-0.0094			
Direct	1	midshaft ml	1.2843	1	1	M=0.7468
		(Constant)	-10.1807			F=-0.7702
		Sectioning point	-0.0117			
		Demarking point	Males>7.93>Females			
MP5						
Stepwise	1	midshaft ml	0.9311	0.6168	0.8849	M=0.9456
	2	midshaft ap	1.2454	0.5374	0.8451	F=-0.9556
		(Constant)	-11.5301			
		Sectioning point	-0.0050			
Direct	1	midshaft ml	1.5095	1	1	M=0.8368
		(Constant)	-10.3340			F=-0.8456
		Sectioning point	-0.0044			
		Demarking point	Males>6.85>Females			

ap=anteroposterior, ml=mediolateral, df=degrees of freedom

Table 9.9: Sexing accuracy of middle phalanges 2 to 5 of South Africans. Percentage of correct group membership and cross-validation

Function		N (Total)	Male Count	%	Female Count	%	Average Accuracy
Middle phalanx 2							
Stepwise	Original	194	76/98	77.6	82/96	85.4	81.4
	Cross-validated	194	76/98	77.6	81/96	84.4	80.9
Direct base ap	Original	194	71/98	72.4	80/96	83.3	77.8
	Cross-validated	194	71/98	72.4	80/96	83.3	77.8
Middle phalanx 3							
Stepwise	Original	198	85/100	85	85/98	86.7	85.9
	Cross-validated	198	85/100	85	85/98	86.7	85.9
Direct midshaft ml	Original	198	79/100	79	83/98	84.7	81.8
	Cross-validated	198	79/100	79	83/98	84.7	81.8
Middle phalanx 4							
Stepwise	Original	195	77/99	77.8	83/96	86.5	82.1
	Cross-validated	195	77/99	77.8	83/96	86.5	82.1
Direct midshaft ml	Original	195	71/99	71.7	82/96	85.4	78.5
	Cross-validated	195	70/99	70.7	82/96	85.4	77.9
Middle phalanx 5							
Stepwise	Original	191	80/96	83.3	82/95	86.3	84.8
	Cross-validated	191	79/96	82.3	82/95	86.3	84.3
Direct midshaft ml	Original	191	76/96	79.2	80/95	84.2	81.7
	Cross-validated	191	76/96	79.2	80/95	84.2	81.7

Table 9.10: Discriminant function analysis of distal phalanges 1 to 5 for South Africans

Function	Step	Variables	Wilk's lambda	Exact F-ratio	d.f
Distal phalanx 1					
Stepwise	1	base ap	0.59698	132.992	1.197
	2	length	0.53326	85.777	2.196
	3	midshaft ap	0.49236	67.017	3.195
Direct	1	base ap	0.5970	132.9919	1.197
Distal phalanx 2					
Stepwise	1	midshaft ap	0.69351	84.411	1.191
	2	length	0.59236	65.377	2.190
	3	base ml	0.56810	47.895	3.189
Direct	1	midshaft ap	0.6935	84.4112	1.191
Distal phalanx 3					
Stepwise	1	base ml	0.65801	98.230	1.189
	2	length	0.61597	58.604	2.188
	3	midshaft ap	0.59285	42.808	3.187
Direct	1	base ml	0.6551	100.0504	1.190
Distal phalanx 4					
Stepwise	1	base ml	0.71977	72.025	1.185
	2	length	0.66666	46.001	2.184
	3	midshaft ap	0.63901	34.460	3.183
Direct	1	base ml	0.7216	71.7534	1.186
Distal phalanx 5					
Stepwise	1	length	0.63854	101.328	1.179
	2	base ml	0.56018	69.877	2.178
	3	midshaft ap	0.52757	52.833	3.177
	4	head ml	0.51527	41.392	4.176
Direct	1	length	0.6385	101.3285	1.179

ap=anterposterior, ml=mediolateral, df=degrees of freedom

Table 9.11: Canonical discriminant function coefficients of distal phalanges (DP) 1 to 5 for South Africans

Function	Step	Variable	Unstandardized coefficient	Standard coefficient	Structure coefficient	Group centroids
DP1 Stepwise	1	length	0.2945	0.4485	0.7397	M=1.0052
	2	base ap	0.6361	0.4965	0.8092	F=-1.0154
	3	midshaft ap	0.6961	0.4094	0.6508	
		(Constant)	-15.1960			
		Sectioning point	-0.0051			
Direct	1	base ap	1.2811			M=0.8134
		(Constant)	-11.3104			F=-0.8216
		Sectioning point	-0.0207			
		Demarking point	Males>8.83>Females			
DP2 Stepwise	1	length	0.4210	0.5314	0.7431	M=0.86291
	2	base ml	0.3684	0.3565	0.7196	F=-0.8719
	3	midshaft ap	1.1747	0.4572	0.7624	
		(Constant)	-15.2461			
		Sectioning point	-0.0045			
Direct	1	midshaft ap	2.5693			M=0.6579
		(Constant)	-9.2838			F=-0.6648
		Sectioning point	-0.0035			
		Demarking point	Males>3.61>Females			
DP3 Stepwise	1	length	0.2943	0.3765	0.6887	M=0.8201
	2	base ml	0.6481	0.5843	0.8699	F=-0.8287
	3	midshaft ap	0.7872	0.3381	0.6874	
		(Constant)	-15.4935			
		Sectioning point	-0.0043			
Direct	1	base ml	1.1106			M=0.7219
		(Constant)	-12.2026			F=-0.7219
		Sectioning point	O			
		Demarking point	Males>10.99>Females			
DP4 Stepwise	1	DP4 length	0.3288	0.4263	0.7213	M=0.7357
	2	DP4 base ml	0.5743	0.5568	0.8302	F=-0.7597
	3	DP4 midshaft ap	0.7003	0.3606	0.6384	
		(Constant)	-14.8560			
		Sectioning point	-0.0120			
Direct	1	DP4 base ml	1.0328			M=0.6113
		(Constant)	-11.2036			F=-0.6244
		Sectioning point	-0.0066			
		Demarking point	Males>10.85>Females			
DP5 Stepwise	1	length	0.4142	0.5236	0.7757	M=0.9279
	2	base ml	0.6993	0.5631	0.7731	F=-1.0026
	3	head ml	-0.3525	-0.3005	0.4865	
	4	midshaft ap	1.2803	0.4415	0.6901	
		(Constant)	-15.2340			
		Sectioning point	-0.0374			
Direct	1	length	0.7911			M=0.7198
		(Constant)	-12.8945			F=-0.7777
		Sectioning point	-0.0289			
		Demarking point	Males>16.30>Females			

ap=anteroposterior, ml=mediolateral

Table 9.12: Sexing accuracy of distal phalanges 1 to 5 of South Africans. Percentage of correct group membership and cross-validation

Function		N (Total)	Male Count	%	Female Count	%	Average Accuracy
Distal phalanx 1							
Stepwise	Original	199	84/100	84	84/99	84.8	84.4
	Cross-validated	199	83/100	83	84/99	84.8	83.9
Direct base ap	Original	199	81/100	81	86/99	86.9	83.9
	Cross-validated	199	81/100	81	86/99	86.9	83.9
Distal phalanx 2							
Stepwise	Original	193	76/97	78.4	80/96	83.3	80.8
	Cross-validated	193	75/97	77.3	79/96	82.3	79.8
Direct midshaft ap	Original	193	71/96	73.2	75/96	78.1	75.6
	Cross-validated	193	71/96	73.2	75/96	78.1	75.6
Distal phalanx 3							
Stepwise	Original	191	77/96	80.2	80/95	84.2	82.2
	Cross-validated	191	76/96	79.2	78/95	82.1	80.6
Direct base ml	Original	192	74/96	77.1	74/96	77.1	77.1
	Cross-validated	192	74/96	77.1	74/96	77.1	77.1
Distal phalanx 4							
Stepwise	Original	188	77/95	81.1	74/93	79.6	80.3
	Cross-validated	188	77/95	81.1	73/93	78.5	79.8
Direct base ml	Original	188	73/95	76.8	74/93	79.6	78.2
	Cross-validated	188	73/95	76.8	74/93	79.6	78.2
Distal phalanx 5							
Stepwise	Original	181	80/94	85.1	73/87	83.9	84.5
	Cross-validated	181	77/94	81.9	72/87	82.8	82.3
Direct length	Original	181	75/94	79.8	70/87	80.5	80.1
	Cross-validated	181	75/94	79.8	68/87	78.2	79.0

CHAPTER 10

DISCUSSION

10.1 Introduction

Descriptions of hand bones in anatomical textbooks are of limited value to forensic anthropologists in that insufficient detail with regard to identification and siding on individual bones is given. Instead, these textbooks are designed to assist students studying anatomy to distinguish between different series of hand bones, namely, metacarpals and phalanges. Additional information given in these books, such as details of the base, shaft, and head, allow students to relate attachments of soft tissues or neurovascular structures to these bony landmarks. However, the information given in these textbooks is insufficient with regard to identification and siding of individual hand bones for forensic purposes. Recent studies on adults (Case & Heilman 2006) and juveniles (Scheuer & Black 2000) have provided morphological descriptions of hands for purposes of identification with some features for siding of these bones. The results from the work carried out by these authors were applied to the present study. The detailed description given in this study can be used both for identification and siding purposes and it is hoped that this would be of value to forensic anthropologists.

Stature is an important characteristic used in identifying human remains. Various methods are employed in order to derive an individual's height. While methods used to estimate stature are standard and can be applied to different populations, regression formulae developed by these methods for one population cannot be used on a different group. Regression formulae are thus population specific. Estimation of stature does not only include the more commonly used long limb bones, but hand bones have also been considered in these studies (Scheuer & Elkington 1993). A number of forensic anthropological studies have been carried out on South Africans in order to develop regression formulae specific for this population (e.g., Lundy 1983, 1984, 1985, 1988, Lundy & Feldesman 1987, Dayal 2002, Bidmos & Asala 2005, Bidmos 2006, Chibba & Bidmos 2006, Steyn & Smith 2007, Ryan & Bidmos 2007, Bidmos 2008). Hand bones of the South African population, however, have not

been included in these studies. The present study therefore attempted to fill this gap by regressing the length of each hand bone to that of a long bone. Reasons for adopting this indirect approach will be discussed under stature estimation.

Sexually dimorphic features on various bones of the skeleton are known to be of value in forensic cases (Dwight 1905, Pearson 1917-1919, Reynolds 1947, Washburn 1948, Bainbridge & Genoves 1956, Jit & Singh 1956, Thieme & Schull 1957, Steel 1963, Singh & Singh 1972a,b, Singh & Singh 1974, Singh 1975, Singh & Singh 1976, Black 1978, Flander 1978, Kelly 1978, DiBennardo & Taylor 1979, 1982, Jit *et al*. 1980, Weaver 1980, Kimura 1982a,b, İşcan & Derrick 1984, İşcan & Miller-Shaivitz 1984a,b,c, Dittrick & Suchey 1986, Kieser *et al*. 1992, Steyn & İşcan 1997). This also includes the hand bones (e.g., Scheuer and Elkington 1993, Barrio *et al*. 2006, Falsetti 1995). In the present study, the mediolateral and anteroposterior width of the hand bones displayed greater sexual dimorphism than the length dimension.

Of interest is the age at which a hand bone dimension exhibits sexual dimorphism. Developmental studies have shown that while ossification of the skeleton occurs at about the 6th week of intrauterine development, sexual differentiation is said to be evident at about the 8th week (Komar & Buikstra 2008). The high percentage of correct sex classification for adult hand bones reported in the present study is a further indication of the value of hand bones in establishing sex from an unknown skeleton.

10.2 Research sample

This study was comprised of three aspects, namely, the morphological description of the hand bones, estimation of stature and sex determination. In order to carry out a non-metrical analysis or description of the hand bones, a large enough sample was needed to establish standard criteria that would include key morphological features of each hand bone. An initial sample of 80 sets of hands removed from cadavers allocated to medical and dental students for their dissections were used. These hands were collected over a period of two years as only 48 cadavers are dissected each year by the medical and dental students in the

Department of Anatomy at the University of Pretoria. The mean age for the total sample was 59 years with an average age for males and females recorded as 64 and 55 years respectively. This initial sample was sufficient to identify morphological similarities and differences of bones belonging to one hand and to compare it with those of the opposite hand.

In a descriptive study of bones, one would expect age changes such as osteoporosis to obscure the morphology of a bone. Very few hand bones in this study presented with degenerative changes. Relatively small artefacts were sometimes located on the distal articular surfaces or head region of a bone, but these did not mask bone morphology.

In any osteometric study, the size of the sample is crucial and queries often arise in osteometric and forensic studies as to what constitutes an adequate sample size (St.Hoyme & İşcan 1986, Lundy 1986). In metric studies, if the sample is too small it may not be representative of the population under study (Barrier & L'Abbé 2008) and may not yield the desired results from a statistical analysis. Thus, once a list of key bony landmarks for identification and siding purposes of each hand bone was established in the present study using 80 sets of hand bones, the size of the sample had to be increased. This additional sample was obtained from the Pretoria skeletal collection, bringing the total sample to 200 sets of hand bones with equal numbers of males (50 whites and 50 blacks) and females (50 whites and 50 blacks). A sample size of 50 for each sex and population group was chosen as this best represented an adequate number for statistical analyses. It may be worthwhile mentioning that the Pretoria Bone Collection normally receives more skeletal material of black than white individuals which includes males and females (L'Abbé *et al*. 2005). However, the collection was big enough to randomly select equal numbers of both sexes from the two population groups for this study.

All osteometric studies using relatively large sample sizes may be influenced by secular trends. This is a tendency towards a change in body size or shape which occurs over a certain time period, as well as through successive generations when compared to past generations (Kieser *et al*. 1987, Garn 1987). This change occurs very slowly throughout time and can present either as a positive or negative secular change. A positive secular trend is an increase

in dimensions as opposed to a negative secular trend, where dimensions are reduced over a certain time period (Tobias 1975, 1985; Tobias & Netscher 1977, Cameron *et al.* 1989). Explanations given for an increase in size include improved nutritional status and optimum medical care for individuals. A healthier environment has a major impact on the size of an individual as it influences growth and development (Henneberg & George 1993, Jantz 2001). A positive secular trend for stature in the American population was noted from 1940 to 1989 which has been attributed to economic recovery (Bogin 1988). According to Cameron *et al.* (1989) environmental factors, which are said to play a key role in positive secular trends, were absent in the mid-20th century.

There are researchers who have documented weak positive trends in stature in the South African population (Henneberg & van den Berg 1990, Steyn & Smith 2007). Studies on the crania and femora, on the other hand, showed a reversal of a positive trend (Tobias & Netscher 1977) which was also documented in the South African population (Tobias 1985). Tobias (1985) presented data on growth and stature from the 20th century for generations that were subjected to deteriorating economic conditions and political unrest. Data on the black South African population of the late 19th century indicated a decline in stature (Tobias 1975). This decrease in stature was associated with a decline in the economic, social, and political environments for black South Africans prior to and during the apartheid era.

The period between 1880 and 1970 showed that South African whites had an increase in mean height of 4.5 mm per decade compared to 2.4 mm per decade for South African blacks (Henneberg & van den Berg 1990). White South Africans were said to be predominantly Dutch in origin which accounted for their increase in stature. However, their increase in stature was still below that of the Dutch population, namely, 15 mm per decade (Bogin 1988). The year 1945 was a period which depicted the end of World War II which was followed by improvements in the industrial sector amongst other changes. This period was considered to be a time when secular trends may have had a great impact on a number of different populations (Henneberg & van den Berg 1990). While Kalichman *et al.* (2008) provided evidence for a secular trend in the size of hand bones in males and females they found this to

be the case only with length dimensions that increased in younger individuals, while midshaft width dimensions remained the same in individuals of different ages.

Dimensions of the cranium and dentition in black South Africans were thought to have shown a positive secular trend (Kieser *et al*. 1987). The finding of a positive secular trend in the dentition is interesting as one would expect a reduction rather than an increase in the size of the teeth. However, these authors reported an increase in the mesiodistal rather than in the buccolingual diameters of the dental arcades of living black South Africans which they compared to that recorded in black crania taken from a skeletal collection.

The Pretoria Bone collection, which houses skeletal material dating from 1987, would also be subjected to the effects of secular trends, either positively or negatively. However, the hand bones that were studied came from the more recent skeletal additions to this collection, and represent the currently living people. It can thus be expected that the influence of secular trend on hand bone dimensions would not be significant.

10.2.1 Non-metric analysis

One of the biggest problems of the descriptive phase of this study was to establish standard identification and siding criteria that could be applied to any bone of the hand. Unfortunately, many of the skeletal elements of the hands that are housed in boxes in the Pretoria Bone Collection were not labelled in terms of hand bone series that they belonged to, namely, metacarpal, proximal, middle, or distal phalanges. In a few boxes the hand bones were not present. As a result of unlabelled and missing hand bones in these skeletal collection boxes, great difficulty was encountered in trying to establish similarities and differences in the bones of the hand. Thus, the only way to describe the bones of the hand as accurately as possible was to use undissected or partially dissected hands. The source for undissected or partially dissected hands was from cadavers assigned to medical and dental students. Removal of the hands from these cadavers had to done only after the students had completely dissected the entire upper limb region. While the sex-population groups were not important for the descriptive aspect of this study, equal numbers of males and females from white and black

South African population groups was necessary to include all possible variations in hand morphology. Both right and left hands were cleaned so that the features of one hand could be compared to that of the other hand.

Once it was decided to start the descriptive part of this study with cadaver material, another problem arose. Separating the hands from the rest of the cadaver's body was not easy. The concern of the technical staff was that the hand bones would not be re-united with the same individual in the Bone Collection at the end of this study. The solution to this problem was to liaise with the technical staff involved with the maceration process. This meant keeping a record of cadaver numbers so that when the maceration process was complete, and the skeleton of each cadaver was ready to be added to the Pretoria Bone Collection, the number assigned to the skeletal box was also kept on record. At the end of the study the hands were re-united with the rest of its skeleton, and all administrative papers had to be signed off by the researcher as well as the clinical anatomy and forensic anthropology technical staff.

Cleaning and careful separation of individual bones of the hand was time-consuming as every effort was made not to mix them. This was crucial as not only was the descriptive part of this study depended on this phase, but the list of key morphological features developed in this phase had to be used to identify and side the hand bones from the collection in order to increase the sample size. Furthermore, in the event of hand bones being recovered from amongst the human remains in a forensic case, these features would need to be accurate in order to correctly assign a hand bone to a digit and a hand.

10.2.2 Metric analysis

A descriptive analysis was run initially on the entire sample to ascertain whether there were statistically significant differences firstly, between whites and blacks, and secondly, between males and females. As the statistical results for the hand bones indicated few statistically significant differences between whites and blacks, the data for these groups were pooled. Additionally, the ancestry will not be known if a sample hand bone is found, therefore it will make little sense to separate the bones of the two ancestral groups. Descriptive statistics

carried out between males and females showed significant differences indicating that hand bone dimensions displayed sexual dimorphism. It was on the basis of these results that all other metric analyses were carried out for males and females.

With the repeatability measurements, the dimension that presented with problems for the second observer was measuring the midshaft area of the smaller hand bones. As some of the hand bones differ in morphology at their proximal and distal ends, trying to visually establish the midshaft region can be difficult. This problem was overcome by measuring the maximum length of the hand bone, and finding the halfway mark which indicated the midpoint between the head and base of the hand bone.

10.3 Morphology of the hand bones

Forensic anthropologists apply osteological techniques to assist them during analyses of decomposed or skeletonized remains known to be human in origin. Their techniques are aimed at providing information that would be useful in identifying these unknown remains, which could also lead to the possible cause of death of an individual. Forensic anthropologists are thus reliant on the knowledge and methods used in the subdisciplines of biological anthropology and archaeology (Brickley & Fellini 2007, Rich *et al*. 2005, Komar & Buikstra 2008, Byers 2005). The bones of the hand are seldomly, if ever, used together with the rest of the skeleton in contributing to the forensic process. Descriptions of hand bones, accompanied by photographs and line diagrams in a number of textbooks are generally aimed at students who need a basic knowledge of hand bones and not designed for forensic purposes (Gray 1959, Bass 1995, Romanes 1991, White 2000). Furthermore, these textbooks do not list sufficient identification and siding criteria which forensic anthropologists could use. This observation is supported by comments made by Case and Heilman (2006), who stated that a superficial description of hand bones as given in anatomical textbooks can only be applied in cases of clinical pathology while anthroplogical, forensic and palaeopathological studies require greater morphological detail. This further emphasizes the need for detailed hand bone descriptions.

In forensic anthropology, the first step when the skeleton or parts thereof is recovered from human remains is the identification of the bones. With regard to the hand bones, osteology textbooks typically classify the metacarpals according to the digit that they belong to which is helpful to some extent in identifying these bones. Phalanges, on the other hand, are classified according to a series, namely, proximal, middle, and distal phalanges. While it may be useful to know where the base, shaft and head of a hand bone is located, this information in textbooks is insufficient should a fragment of the bone be recovered that has to be linked to the correct digit and hand.

According to some authors (Steele & Bramlett 1988, Bass 1995, White 2000), being able to single out a hand bone or a part of it becomes a challenge especially if bones of the feet, in particular, the metatarsals and phalanges, are present. One would assume from this that the morphology of hand and foot bones is similar which would make it difficult to identify them from each other which further emphasizes the need to develop specific standard methods of identification and siding of hand bones. In the present study, this was accomplished.

Researchers have attempted to develop such standard methods. For example, Scheuer and Black (2000) proposed relative length ratios as a guide for correct ray placement of the phalangeal bones. These authors concluded that to carry out an accurate ray placement requires detailed knowledge of hand bone morphology while Smith (1996) suggests that to develop the skill for correct ray placement practice is needed. Thus, the study carried out by Scheuer and Black (2000), which concentrated on ray placement, was not only to identify a bone, but also to side it.

Accuracy in the identification of human hand bones in a forensic investigation is important, as all the findings are of medicolegal significance. In fact, Scheuer and Black (2000) have stated that correct identification of individual hand bones is as critical to a forensic case as are long bones. Once a bone can be successfully identified, the next step would be to side it. This cannot be achieved without prior knowledge of the location or position of the bone (Case & Heilman 2006). Individual metacarpals are far easier to recognise when found isolated

in comparison to the phalanges, because each metacarpal has marked differences that can be easily observed. Phalanges, on the other hand, show similar morphological features that require the presence of all the phalanges as a group (Douglas *et al*. 1997, Kilgore *et al*. 1997), or as a series (Oxenham *et al*. 2005). This was initially also the case with the present study as all the phalanges had to be examined as a group after which they were then separated into their respective series of proximal, middle, and distal phalanges. The distal phalanges, in the present study, were found to be the most difficult of all the phalanges to identify and side.

Additional indicators such as the quality and condition of a bone are also of help in forensic cases (Komar & Buikstra 2008). Distinctive features of bones, which assist in their identification, are said to be related to forces placed on these bones. Age-related studies incorporating the effect of mechanical loading during different developmental periods on the upper limbs, including the hands, of humans and cross-sectional areas of femora from archaeological samples have been investigated (Ruff *et al*. 1994). The femur has been shown to adapt over time to loads of weight bearing by increasing its cortical bone growth and the changes were more marked in the diaphyseal rather than at the articular ends (Ruff *et al*. 1994). While the hands are not subjected to the effects of weight bearing, their functional role in manipulating the environment may bring about subtle morphological changes leaving an imprint or landmark on the bone. One example of such an imprint is the presence of prominent ridges on the palmar aspect of the medial and lateral side of the middle phalanges which serve for the attachment of the flexor digitorum superficialis muscle. The relevance of this information to the present study was that these imprints were used as bony landmarks in the identification and siding process.

The shape of a bone is thought to relay patterns of adaptation, health, activity and life history between past and present human populations (Lazenby 1998). One of the bones of the hand, namely, the second metacarpal, is thought to provide these various patterns of evolutionary changes. Evidence for this is seen in radiogrammetric studies, which have shown that the second metacarpal can be used as a measure of normal and abnormal bone growth, aging and functional asymmetry (Lazenby 1998). With regard to the present study, the shape

of the lateral and medial margins of the shaft depicted certain aspects of the morphology which was used to also identify and side a hand bone.

When siding a hand bone the accuracy of the method used is of importance. Ricklan (1988), in his study on the morphology of the hand bones of early and recent South African hominids, identified asymmetrical features on either side of the midline of the phalangeal bones and scored them. He reported siding accuracies of 83.0% (first proximal phalanx), 82.0% (second proximal phalanx), 80.0% (third proximal phalanx) and 98.0% (fifth proximal phalanx). For the middle phalangeal row, he reported siding accuracies of 93.0% (second middle phalanx) and 85.0% (third middle phalanx). For the distal row he recorded 91.0% (second distal phalanx), 77.0% (third distal phalanx), 57.0% (fourth distal phalanx) and 89.0% (fifth distal phalanx) siding accuracy. Case and Heilman (2006) reported siding accuracies ranging from 88.0-100% for proximal phalanges, 96.0-98.0% for middle phalanges and 52.0-94.0% for the distal phalanges. The second, third and fourth distal phalanges from their studies, however, gave poor results and had to be re-evaluated. While the accuracy of siding was not tested in the present study, emphasis was placed on the method used to describe the hand bones. The only way to carry out this objective was to place all 80 sets of right and left hands out on tables and the descriptions had to done from one view at a time. A feature noted on one bone was then followed through to all other bones, and in each case, similarities and differences were noted. Furthermore, if similar features were observed on bones from both the right and left hands, the surface or margin associated with that specific feature was used also in the siding technique. Thus, although accuracy was not tested formally in the present study, the criteria developed during the initial phase using cadaver material were used to identify and side the hands from the Pretoria Bone Collection. It was felt by the researcher that this could be done accurately. Thus a detailed description accompanied by fully labelled diagrams for each hand bone was accomplished.

In forensic analysis, the methods employed need to reliable, and if the hand bones are to be incorporated into such cases, then the methods used for hand bone identification should also be as accurate as possible. Thus, while the reported accuracies given by Case and

Heilman (2006) are relatively high, these authors admit that there was no guarantee that all the phalanges came from the same individual. The reason for this was that some of their samples on which their studies were based, came from an anatomical supplier. The method used in the present study is reliable as the sets of right and left hands that were observed came from the same individual. In this way, control was exercised when similarities and differences were noted on these hand bones. Differences described in this study, as well as the methods that were used, now need to be tested on an independent sample in order to determine their accuracy.

The illustrations and key landmarks provided by Ricklan (1988) and Case and Heilman (2006) for the phalanges, were quite useful for the present study. Generally, these authors provided two features (see Tables 2.1 and 2.2) for siding each of the phalangeal rows as seen by different views. The problem with the two features given is that they were not constant for each proximal phalanx. For example, the features for the first three proximal phalanges were described from a palmar view, the fourth phalanx was described from a proximal view and the fifth one from a dorsal view. In the present study, all descriptions were carried out from the same direction, namely, dorsal, palmar, lateral, medial, proximal, and distal views of the shaft, head and base for each hand bone. This was to standardize all descriptions based on the direction in which a bone was held. The descriptions given for the head, shaft and base in the present study, were done so as to be able to identify a hand bone if only a fragment of it was recovered amongst human remains. Thus, a more comprehensive description was attempted with all hand bones in the present study.

Case and Heilman (2006) also referred to a bilateral mass at the base of a proximal phalanx. On closer observations of the hand bones in the present study, the mass was associated with the medial and lateral tubercles and named as such. For the middle phalanges, Case and Heilman (2006) again listed two features (see Tables 2.1 and 2.2 and Figures 2.5 and 2.6) to side each of these bones. These features, amongst others, were also observed in the present study. All illustrations given by these authors for the distal phalanges also showed two distinct features (see Tables 2.1 and 2.2 and Figures 2.5 and 2.6) for the first

to the fourth distal phalangeal bones and a single feature for the fifth distal phalanx. The problem encountered with all the illustrations given by Case and Heilman (2006), is that the figures were not labelled with regard to their orientation. In other words, it is not certain as to what was medial and lateral for right and left hand bones. The diagrams were carefully looked at in conjuction with the individual bones of the hand used in the present study. The orientation with regards to direction is especially crucial when referring to a smaller sized facet at the proximal end, which is used to side the bone. These authors, however, were able to show at least two features on all phalanges which can be used to side these bones. The present study attempted to improve on this list by not only providing a comprehensive description which can be used to identify a bone, but more than two key bony landmarks were also given.

In descriptions of hand bones, nutrient foramina are sometimes also mentioned. The earliest study on the location of nutrient foramina was by Bass (1995) who noted these foramina at the proximal rather than at the distal ends of the shaft of hand bones. On the other hand, studies by Patake and Mysorekar (1977) on nutrient vessels associated with the skeletal system have shown that nutrient foramina are normally present in the midshaft region of metacarpals and concentrated on the medial aspect of the first and second metacarpal and on the lateral side of the remaining metacarpal bones The number of foramina per hand bone also appears to be restricted in that the first metacarpal is reported to have a single foramen (Patake & Mysorekar 1977) while the second metacarpal has two foramina (Singh 1959). The number and location of these nutrient foramina are known to present with numerous variations which explains why they are not used in defining an isolated segment of a bone (Steele 1970). In the present study, the number and location of these nutrient foramina were not constant and although mentioned when present, they were not listed amongst the criteria for identification and siding of hand bones. When nutrient foramina are absent, it has been suggested that the periosteal vessels become the main supply of blood rather than the nutrient artery (Lütken 1950, Mysorekar *et al*. 1967). In a study relating the number of foramina to the length of a long bone, Patake & Mysorekar (1977) found no association between these two variables.

In summary, while descriptions in anatomical textbooks on morphology of the hand bones are far less than those of the rest of the skeleton, some recent research on this subject was published. The present study was also able to show that these bones have more than just a base, shaft and head region. This detail would be of benefit to students and researchers who need more than just a superficial overview of the hand bones. The list of key morphological traits listed at the end of each bone's description, is to provide a quick reference to identify and side a particular hand bone. The different views from which the bones were described as well as the layout of these descriptions under the subsections of head, base and shaft, may assist the forensic anthropologist who recovers either an intact of fragmented hand bone. The photographs provided with each description were done in a way where the main landmarks were emphasized. The layout of the descriptions and photographs could possibly also serve as a field manual. Future research would entail establishing the praticality of using such information in a forensic anthropological setting. In comparison to descriptions of these bones in anatomy textbooks, this research has attempted to provide slightly more detail in a practical manner.

10.4 Stature determination

One of the purposes of the present study was to assess the value of hand bones in the estimation of stature when other long bones are unavailable. This brings into question as to what constitutes an adequate sample size. Generally, a greater sample size tends to yield better results and the regression formulae devised from such a sample best represents the population under study. Sample sizes in hand bone studies vary amongst researchers. For example, Meadows and Jantz (1992) measured metacarpal lengths of right and left hands taken from the same 212 individuals. In contrast, Musgrave and Harneja (1978) recorded metacarpal lengths from 20 left hands and 26 right hands which came from two different female samples. Grieshaber (2001) found statistical calculations problematic with regard to use of the metacarpals in stature estimations and concluded that an original equation for stature estimation from metacarpals could not be devised based on their small sample size

and that these bones were not well preserved. In the present study, the total sample of hands from 200 individuals which included males and females of two South African population groups (whites and blacks), compared well with the sample size recorded by Meadows and Jantz (1992), but is far greater than those of Musgrave and Harneja (1978).

The earliest arguments against the use of the same formulae across populations were recorded by a number of researchers (Pearson 1899, Allbrook 1961). Later studies by Trotter and Gleser (1952, 1958) and Trotter (1970) also stated that regression equations are population and sex-specific and should be limited to the population and sex groups from which the equations were derived. Numerous current studies followed this pattern of thought (Lundy 1983, Lundy & Feldesman 1987, Dayal 2002, Bidmos 2008). Thus, new stature regression equations had to be derived from the bones of the hand specifically for the South African population.

While sample size is crucial, methods used in estimating stature are just as important. Various methods of estimating stature can be used depending on the case under study (Konigsberg *et al*. 1998). One way of reconstructing stature is to use all the skeletal elements from the calcaneus to the skull, according to the anatomical method that was devised by Fully (1956). Although this method is commonly used in anthropological and forensic studies, it does not emphasize explicit methods for carrying out the procedure (Raxter *et al*. 2006). For example, Raxter *et al*. (2006) tested Fully's method for accuracy and applicability and reported that the correction factors used by Fully to convert summed skeletal height to living stature were too small. In using Fully's method, these authors found that stature was underestimated by 2.4 cm. They thus provided new correction factors to account for soft tissue. Nevertheless, this method is tedious and also requires a near complete skeleton. On the other hand, one advantage of the anatomical method is that it measures body proportions accurately (Lundy 1988).

The mathematical method is another way of estimating stature (Lundy 1988). Formulae devised by Lundy and Feldesman (1978) and Dayal (2002) specifically for the South African population, are currently being used by forensic anthropologists doing research in this country.

In forensic anthropology, direct measurements from a complete skeleton of human remains are not always possible. Stature is therefore predicted from the lengths of the long bones, preferably those of the lower limb region (Aiello 1992). In cases where fragments, rather than intact long limb bones are recovered, there are various ways in which stature can be estimated as accurately as possible. The total length of a long bone can also be estimated from its fragments. The estimated length of the long bone can then be inserted into an appropriate regression formula to estimate living height. Wilbur (1998) used metacarpals to estimate femur length, which in turn was used to estimate stature. This indirect method of determining stature was also adopted in the present study, using all hand bones and five long limb bones. The maximum long bone length dimensions of Lundy and Feldesman (1978) and Dayal (2002) were employed for the long limb and hand bones of the present study.

Another indirect approach is where the measured values of long bone fragments are substituted into the regression formula (Simmons *et al*. 1990). Steele and McKern (1969) demarcated segments of the humerus, radius, and tibia as percentages that can then be used to estimate the length of each of these long bones. The calculated length values are then inserted into an appropriate regression formula to get to the final estimated stature.

Parts of the ulna and tibia have been used to determine the entire length of these bones (Mysorekar *et al*. 1984). The distal end of a femur and proximal end of a radius have also been used to determine stature (Mysorekar *et al*. 1984). Mysorekar *et al*. (1984) identified anatomical landmarks at the proximal end of a long bone which they then subtracted from the total length in order to give the length of the distal fragment.

In the present study, while seven dimensions were recorded, only the maximum length, and not the width dimensions at the proximal, distal and midshaft regions, of each hand bone was used to estimate the length of a long limb bone.

Studies estimating adult stature directly from metacarpal bone length (Musgrave & Harneja 1978, Meadows & Jantz 1992, Wilbur 1998), often employ the use of radiographs taken of hands from adult patients (Gupta *et al*. 2000, Himes *et al*. 1977, Musgrave & Harneja 1978) in comparison to the present study where measurements were recorded directly from

the bones of the hand. The problem with radiographic images is that a correction factor needs to be included. Thus a direct approach where measurements can be recorded from the bone itself is advantageous compared to an indirect measurement.

In some anthropological studies, regression formulae are devised for combined groups within the same population. For example, Byers *et al*. (1989) combined data for Afro-American and Euro-American males to derive a common regression equation for males. These authors did the same for their female samples. However, Byers *et al*. (1989) did not provide any descriptive statistics or motivation as to why they combined their ancestral groups.

A study by Bidmos (2008) on an indigenous South African sample, which actually constitutes different “tribes”, was also computed as a single group in the regression analysis. Bidmos’ motivation for combining these “tribes” were as a result of research carried out by De Villiers (1968) and Lundy (1983), who proved that no statistically significant intertribal differences exist in the osteometric dimensions of South African groups.

In the present study, descriptive statistics were provided firstly, for white and black groups (sexes combined) and secondly, for males and females (white and black groups combined). Very few statistically significant differences in hand bone dimensions were noted between the white and black groups in contrast to that obtained for males and females, where most of these differences were statistically significant. Based on these findings, data for the South African population used in the present study, were combined into two groups, namely, males and females rather than into four groups of white males, white females, black males and black females. In other words, all regression analyses were carried out for South African males and females.

When carrying out studies on stature, correlation analyses are also done. This was done in the present study as it was important to assess whether all hand bones are equally correlated to all long limb bones or only to specific long limb bones. Furthermore, correlations between the length of a single long limb bone or combination of bones with stature forms a crucial part in any study concerned with estimating height of an individual. While correlation

values are known to differ depending on the skeletal element used to estimate stature, the best correlation values are those that are close to a value of one.

Lengths of metatarsals have been shown to be significantly correlated with stature in Euro- and Afro-Americans with values ranging from 0.6 to 0.8 (Byers *et al*. 1989). In their study of South African black females, Lundy and Feldesman (1987) reported correlation values of 0.896 (femur), 0.873 and 0.896 (tibia), 0.864 and 0.879 (fibula), 0.816 and 0.803 (ulna), 0.839 and 0.814 (radius), 0.805 and 0.792 (humerus). In summary, their lowest and highest correlation values were 0.538 and 0.956 respectively.

Dayal (2002) carried out her study on South African white males and females and produced correlation coefficients of 0.92 and 0.93 (femur), 0.87 and 0.90 (fibula), 0.83 (ulna), 0.85 and 0.84 (radius), 0.83 and 0.84 (humerus), In summary, the lowest and highest correlation values for Dayal's study were 0.56 and 0.96 respectively.

Correlation values for metacarpals reported by various authors ranged from 0.565 to 0.828 (Meadows & Jantz 1992), and 053 to 067 (Musgrave & Harneja 1978). Correlation values of individual hand bones for males and females in the present study were 0.785 and 0.902 (metacarpals), 0.715 and 0.717 (proximal phalanges), 0.654 and 0.567 (middle phalanges) and 0.567 and 0.507 (distal phalanges) respectively. The lowest and highest correlation values can be summed as 0.567 and 0.785 (males) and 0.507 and 0.902 (females). The metacarpals showed the highest values (0.902) in comparison to the distal phalanges where the correlation values were the lowest (0.507). These results are similar to those reported by Meadows & Jantz (1992) and Musgrave & Harneja (1978).

Correlation values of the long limb bones in the present study for males and females were similar to those given by Lundy and Feldesman (1987) and Dayal (2002) and summarized as 0.678 and 0.713 (humerus), 0.785 and 0.902 (radius), 0.772 and 0.790 (ulna), 0.684 and 0.724 (femur), and 0.745 and 0.771 (tibia). The values for females were slightly higher than those for males which may be an indication that females present with less osteological variation than their male counterparts. The radius was also found to be the best correlated bone in females when compared to the other long limb bones. This is possibly due

to a direct relation of the radius to the wrist and hand bones. The correlation results for males, on the other hand, proved to be inconsistent when compared to those of females in that no single long limb bone was highly correlated to any of the hand bones. In a practical situation, therefore, this means that if any hand bone of a female is recovered, then it could be said with a certain degree of confidence that the radius would be the best bone to select when estimating stature indirectly.

In studies on estimation of stature, long limb bones are regressed directly to stature. In comparison, to estimate the height of an individual in the present study, the value obtained for a long limb bone that was calculated from regression of one of seven hand bone dimensions, namely length, would have to be inserted into a second regression formula devised by Lundy and Feldesman (1987) and Dayal (2002). This indirect approach of estimating stature was adopted because the cadaver lengths or antemortem stature found in the skeletal records of the Petoria Bone Collection were either unreliable or not recorded. One disadvantage of the indirect method is that the total skeletal height (TSH) of an individual would have to be calculated by the length of either a single long limb bone or a combination of bones which in turn would have to be calculated from a hand bone. Thereafter, a correction factor for soft tissues would have to be added. Not only is this a longer process, but the standard errors would also be expected to be higher when compared to a direct approach. An indirect approach such as the one adopted in the present study is not new. Wilbur (1998) used metacarpals to estimate femur length which in turn was then used to estimate stature.

It is important in stature estimation that standard errors should be minimal as reliability of a regression equation is based on the standard error of estimates. A low standard error of estimate indicates a high accuracy as opposed to a low accuracy obtained with high standard error of estimate (Ryan & Bidmos 2007, Bidmos 2006). The reason why intact long limb bones are commonly used when estimating stature is because they yield high accuracies and low standard error of estimates (Simmons *et al*. 1990, Holland 1992). Authors have reported standard errors for upper limb bones ranging from 3.3 – 5.0 (Trotter & Gleser 1952, Steele

1970), lower limbs from 3.3 – 6.2 (Trotter & Gleser 1952, Steele 1970), and metatarsals 4.2 – 7.0 (Byers *et al*. 1989).

In their study on estimating stature from metacarpals of a male and female Euro-American sample, Musgrave and Harneja (1978) reported average standard errors ranging from 5.5 to 7.2 cm (metacarpal 1), 4.7 to 5.8 cm (metacarpal 2), 4.7 to 6.6 cm (metacarpal 3), 5.0 to 7.6 cm (metacarpal 4), and 4.7 to 8.3 cm (metacarpal 5). These standard errors are far greater than the rest of the skeleton including those reported by Byers *et al*. (1989) for metatarsals of the foot.

Standard errors recorded for metacarpals and phalanges in the present study were far greater than those reported by the above-mentioned authors. Even when all the metacarpals in the present study were combined, the standard errors were still high. Standard errors obtained where hand bone dimensions were linked to each of the five long limb bones differed for individual bones. Grouped metacarpals showed the lowest standard errors for the radius (5.2 cm), and ulna (5.6 cm) and the highest for the tibia (7.1 cm), humerus (9.2 cm) and femur (10.6 cm). For proximal phalanges, the lowest standard errors were 7.1 cm (radius), 7.3 cm (ulna), and 7.7 cm (tibia) compared to 10.2 cm (humerus) and 12.8 (femur). For the middle phalanges, the lowest standard errors were 7.5 cm (radius) and 7.9 cm (ulna) compared to 9.3 cm (tibia), 10.4 cm (humerus), and 12.4 cm (femur). The lowest standard errors for the distal phalanges were 7.6 cm (radius) compared to 8.1 cm (ulna), 9.9 cm (tibia), 10.0 cm (humerus), and 12.3 cm (femur).

In summary, the lowest standard error of estimates in the present study was above 5.0 cm. This indicates that intact long limb bones still remain the best skeletal components for adult stature estimation as regression equations derived from them have relatively lower standard errors of estimate compared to those obtained from hand bones. Alternatively, if hand bones are the only available skeletal elements, then this study has proposed methods that could be employed to use these hand bones to indirectly estimate stature. This study further emphasizes that the ideal situation would be to use all the hand bones as a group as this would yield better results than only a single hand bone.

There are studies indicating that using a combination of variables results in lower standard errors and therefore higher prediction accuracies (Trotter & Gleser 1952, Lundy 1983, Lundy & Feldesman 1987, Holland 1992, Dayal 2002, Bidmos & Asala 2005). Byers *et al*. (1998) reported that metatarsals 2 and 4 contributed greatly to the accuracy of calculated stature when included with metatarsal 1. The results of the present study indicate that different combinations of hand bones yielded greater prediction accuracies than using only a single hand bone. Ideally, if all hand bones were used, the prediction accuracy would increase. In the present study it was found that in males, for example, a combination of metacarpals 1, 2, 3, and 4, proximal phalanges 2, 3, and 4, middle phalanges 2 and 4 and distal phalanges 1 and 5 were the hand bone combinations selected which increased the accuracy for predicting long limb bones. In females, a combination of all five metacarpals, all proximal phalanges with the exception of the third bone, all middle phalanges with the exception of the second bone and only distal phalanx 1 were selected. While these results indicate great variability between the sexes, the bones of the second (index finger) and fourth (ring finger) digit, with the exception of the distal phalanges, appear to be the best selected hand bones to regress to a long limb bone.

While certain hand bones were selected in the present study as the best predictors for long bone lengths, the standard error of estimates were high, especially for individual rather than for grouped hand bones. Furthermore, the standard error of estimates in males in the present study were slightly higher than for females for the metacarpals and proximal phalanges as a group, while for the middle and distal phalanges, those of females were higher than those of males. If the standard error is higher in one sex, the total skeletal height together with the soft tissue correction factor may lead to a wider range of estimated living statures with the identification process being less accurate.

While the literature has shown that population and individual variation does and will always exist, probable errors will tend to prevail irrespective of how accurate or precise regression equations are devised in order to estimate stature (Sjøvold 2000). All evidence recovered at a site where human remains are uncovered should be investigated, and this

includes the bones of the hand. It has been suggested that the relationship between metacarpals to stature, is far stronger than long bone fragments to stature, which support the use of this series of bones in estimating height of an individual (Musgrave & Harneja 1978). The present study has shown that this is not true. Further support for consideration of hand bones in stature estimation studies would be endorsed by the following quotation given by Sjøvold (2000) “It is self-evident that an undamaged bone facilitates further investigation” (p. 276).

10.5 SEX DETERMINATION

In forensic anthropology, estimation of sex is crucial in that other estimates, such as stature and age, are dependent on it (Scheuer 2002). Determining sex depends greatly on the degree of sexual dimorphism in that specific bone (Novotny *et al*. 1993, Kemkes-Grottenthaler 2001). Sexual dimorphism is defined as observed physical traits, such as size and shape or architecture, within a group that distinguishes males from females (Eckert 1980, Loth & Henneberg 1996, Steyn & İşcan 1999, Loth & İşcan 2000, Asala 2001, Mall *et al*. 2001, Bidmos & Asala 2003, Bidmos & Dayal 2003, Byers 2005). It is generally known that males tend to be relatively larger in overall body dimensions as well as more robust than females. This is attributed to a number of factors that affect the shape and strength of a bone over a certain time period (Ruff 1987, Asala 2001, Byers 2005). In fact, females are said to be 92.0% the size of males, which is a size difference of approximately 8.0% (Byers 2005). Thus, the ability to ascertain the size and shape or architectural differences from skeletal elements greatly contributes to sexing of individuals (Byers 2005).

As shape or architectural differences between males and females are especially evident in the pelvis (Byers 2005, Komar & Buikstra 2008), this bone has been frequently used in sexing individuals (Byers 2005, Komar & Buikstra 2008). In the present study, the measurements recorded on hand bones rather than the shape of these bones, were crucial steps for determining whether the hands, and in particular, the dimensions of each hand bone, could be used by forensic anthropologists to accurately determine sex.

Dimensions of other bones of the skeleton are commonly used in sex determination studies for various population groups. For example, sex differences in the femur and tibia have been documented for American blacks and whites (Black 1978, DiBennardo & Taylor 1982, İşcan & Miller-Shaivitz 1984, Holland 1992), Japanese (Hanihara 1958, İşcan *et al.* 1994), Asian Indians (Singh & Singh 1972, Singh *et al*. 1975), British (Steel 1972), Czechs (Cerny & Komenda 1980), French (Godycki 1957), and Italians (Pettener *et al*. 1980).

Studies on sexual dimorphism in South Africa have steadily increased due to the overwhelming rate of crime in this country. As sexual dimorphism is population specific irrespective of whether metric or non-metric (morphological) methods are used (Novotny *et al.* 1993, İşcan & Shihai 1995), the South African population needed to have its own formulae. The femur and tibia as well as other parts of the human skeleton have thus been used to establish discriminant function formulae. These include the cranium (Ricklan 1987, Steyn & İşcan 1998), mandible (Steyn & İşcan 1998), patella (Dayal 2005), talus (Bidmos & Dayal 2003), humerus (Steyn & İşcan 1999), radius and ulna (Barrier & L'Abbé 2008), calcaneus (Bidmos 2004) and pelvis (Patriquin *et al*. 2005).

As metric variations of different parts of the skeleton are known to occur with time (Borgognini *et al*. 1986, Henneberg 1988), the techniques for establishing sexual dimorphism in a specific population must be derived from a contemporary skeletal collection otherwise this can lead to inaccurate classification of an unknown individual (İşcan 1988). One such study where sexual dimorphism was studied from skeletal material that was not obtained from a contemporary collection was that carried out by Lazenby in 1994. In his observations on second metacarpals, which came from a 19th century skeletal collection, Lazenby (1994) correctly identified the known males, while the females in his sample were misidentified. Conclusions drawn from this is that the source of the skeletal material is crucial as it is known that the bones show a certain degree of sexual dimorphism not only within populations, but also within the same individual (Scheuer & Black 2000). Furthermore, secular changes in populations are known to occur from one generation to the next which can influence results (Bogin 1988, Riggs *et al*. 2004, Marshall *et al*. 2006). The cadaver and skeletal sample used in

the present study came from a contemporary collection and would be expected to truly be representative of the current South African population.

Not only is the source of the sample important but the size of the sample must also be adequate. As explained under the discussion of stature, the white and black population groups were pooled on the basis of the descriptive studies which indicated few statistically significant differences in hand bone dimensions between whites and blacks. The pooled data were thus subjected to discriminant function analysis in this study. The sample size of equal numbers of males (100) and females (100) was appropriate for the statistical analysis. When considering using skeletal elements to discriminate sex, a percentage baseline for assigning individuals to the correct sex must be established. According to Scheuer and Elkington (1993), any method devised to sex individuals using hand bones, can only be useful if it yields an accuracy of 80.0%.

The accuracy in classifying sex from human remains is crucial as it reduces the total number of unknown forensic cases considerably (Loth & İşcan 2000). The degree to which sexing can be accurately carried out also depends on which bone or combination of bones have been selected. Percentage accuracies recorded when an entire skeletion is available is said to be 90.0 - 100%, with pelvis only 90.0 - 95%, skull 80.0 - 90.0% and with long limb bones it reduces to 80.0% (Krogman 1962, Steele 1970, Krogman & İşcan 1986). This information relays the importance of selecting a bone for estimating sex of an individual. However, practical situations and differential preservations may necessitate the use of bones that do not have such high accuracies. The evidence recovered at a crime scene may not necessarily be the bones that are known to be highly sexually dimorphic. While it is known that percentage accuracies drop to 80.0% for lower limbs, one would assume that the upper limbs would have similar percentage accuracies as sex determinants. Barrier and L'Abbé (2008) studied sexual dimorphism in forearm bones of a South African population. Her results for the radius yielded accuracies ranging from 80.0 - 86.0% for males and 82.0 - 88.0% for females, and for the ulna, the accuracies ranged from 76.0 - 87.0% for males and 83.0 - 89.0% for

females. These results indicate that upper limb bones are just as sexually dimorphic as lower limb bones.

Not only is there motivation for the use of forearm bones in contributing to the discriminant process, the use of hand bones is also gaining recognition. For example, metacarpals have been used to establish sex differences (Kimura 1990, Scheuer & Elkington 1993). Scheuer and Elkington (1993) reported that the second metacarpal provided the highest probable correct sexing accuracy (79.0%) and the third metacarpal the lowest (75.0%). In the present study, the first metacarpal for males (85.0%) and females (85.9%) presented with the highest accuracies in the stepwise analysis. These accuracies are slightly higher than those reported by Scheuer and Elkington (1993). It is interesting that the metacarpal of the thumb, rather than the index finger as reported by Scheuer and Elkington, was selected was selected as the most accurate in the present study. The percentages reported for the present study as well as that given by Scheuer and Elkington (1993) are similar to those reported by Barrier and L'Abbé (2008) for the forearm bones which further supports the use of the upper limbs including the hand bones to discriminate sex.

Just as it would be ideal to have a complete skeleton to estimate sex, an intact rather than a fragmented long limb or hand bone is also preferred. However, fragments of bone may be the only remnants recovered during an investigation process. Of interest to the forensic anthropologists in such cases is whether different parts of a hand bone can be used to estimate sex. Most studies have used the proximal and distal ends, such as the head of the humerus and femur, with resultant accuracies equal to or greater than 86.0% (İşcan & Shihai 1995, King *et al*. 1998). Breadth and height of the patella, talus, and calcaneus, although reported to be less accurate than those of the femur and tibia, with percentages ranging from 69.0 - 92.0%, are said to be of value when incomplete or fragmented bones are recovered (Riepert *et al*. 1996, Introna *et al*. 1998, Bidmos & Asala 2003, Asala *et al*. 2004). There are researches who have indicated that only the distal breadth of the radius and ulna is a good indicator for sex discrimination and it is shown to yield classification accuracies ranging from 72.0 - 92.0% (Allen *et al*. 1987; Holman & Benett 1991, Mall *et al*. 2001, Sakaue 2004).

As far as single measurements are concerned, maximum midshaft dimensions of metacarpals were listed by Scheuer and Elkington (1993,) as the variable with the highest correct sexing accuracy, namely, 76.0% (probability) and 80.0% (actual). Himes and Malina (1977) reported that metacarpal diaphyseal diameters were relatively larger in males than in females. The best discriminators in the present study generally included the measurements recorded at the base (anteroposterior) and midshaft (mediolateral) regions. These results were reported for the stepwise analysis for almost all of the hand bones with sexing accuracies ranging from 75.9 - 84.8% for the base and 75.6 - 86.9% for the midshaft dimensions. For distal phalanges, the base and midshaft measurements were also selected as the best discrimating variables, except that the mediolateral dimension of the base was selected for the third and fourth digits and the anteroposterior variable of the midshaft for the second bone.

An earlier study by Black (1978) showed that the width of a long bone has been reported to be more sexually dimorphic than the length. This was also true for the present study. The length dimension was selected only for the fifth distal phalanx in the stepwise analysis, with a classification accuracy of 85.1% for males and 84.5% for females. These results suggest that length is not as important as the width dimensions in distinguishing between the sexes. There are a number of studies that support the fact that maximum length of a long bone is not necessarily selected as the best discriminating variable (Thieme & Schull 1957, İşcan & Shihai 1995, İşcan *et al*. 1998, King *et al*. 1998; Mall *et al*. 2001, Purkait & Chandra 2002). The study by Barrier and L'Abbé (2008) on forearm bones, reported a 4.0% drop in classification accuracies when the length variable was removed from the male sample. The conclusion drawn by these authors is that the length dimension is only moderately sexually dimorphic.

In the present study, the dimensions of the head (or distal end) of a hand bone, similar to that of length, were also not selected as the best discriminating variable with the exception of the fifth metacarpal. In this bone, the anteroposterior dimension of the head was selected as the best discriminating variable in the stepwise analyses, with a classification accuracy of 76.8% for males and 80.2% for females when used on its own. One can thus conclude that

head dimensions especially the mediolateral width, is a moderate discriminator of sex, similar to that of length. It can be concluded that the statistically significant differences of hand bone dimensions between males and females observed in this study compare well with those reported on other aspects of the skeleton for the South African population (Asala *et al.* 1998, Asala 2001, Bidmos 2006, Patriquin *et al*. 2005).

Barrio and L'Abbé (2008), in their study on a Spanish sample of European origin, used eight metacarpal dimensions. The additional dimension in their study was the epicondylar diameter of the head. It may be argued that the maximum mediolateral dimension which these authors measured excluded the medial and lateral tubercles of the head. Instead, they recorded the distance between these tubercles, namely, epicondylar diameter of the head, as a separate entity. These anatomical landmarks were found to be part of the maximum side to side (mediolateral) dimension in the present study. Furthermore, these authors also reported separate findings for the right and left hand as well as for a pooled sample. Their results, as well as those of other authors (Di Bennardo & Taylor 1979, Ruff 1987), indicate that transverse dimensions are more dimorphic than longitudinal measurements. Barrio *et al*. (2006) also noted differences in transverse measurements for the epiphyses and shaft, with the mediolateral of the former and anteroposterior dimension of the latter displaying the greatest dimorphism.

The accuracies reported by Barrio *et al*. (2006) were higher than that reported by Stojanowski (1999) for two to five variables where a range of 79.0 - 85.0% was obtained and lower than that reported by Falsetti (1995), who gave a range of 84.0 - 92.0% for the metacarpal series as a group. Falsetti (1995) looked at metacarpals two, four and five and reported sexing accuracies in males as 100% for metacarpal five, 84.6% for metacarpal four and 83.3% for metacarpal two. For females the reverse pattern occurred. In other words, 100% accuracy was recorded for metacarpal five, 90.9% for metacarpal two, and 81.8% for metacarpal five. Comparing the results of Falsetti's (1995) study to those of Scheuer and Elkington (1993), it seems the bone of choice in males is the fifth metacarpal while in females it varies between the second and third metacarpals. In the present study, the fourth metacarpal

in males and the first metacarpal in females were the bones selected for the South African population.

Smith (1996) used maximum measurements at the head, base, and midshaft of all the metacarpals, while maximum and interarticular lengths were applied to metacarpals one to three and only the maximum length of four, and five was recorded. Smith (1996) recorded correct classification of metacarpals 86.8% for the right hand and 89.4% for the left hand.

Burrows *et al*. (2003) assessed the validity of metacarpals as sex discriminators by employing the methods proposed by Scheuer and Elkington (1993), Falsetti (1995) and Stojanowski (1999). They concluded that the methods proposed by all three authors were valid and produced high accuracies.

While Scheuer and Elkington (1993) proposed the testing of their equations on other populations, reported results from various other authors indicated that these equations are population specific and should be tested from a sample obtained from the same population. It was on this basis that discriminating equations for metacarpals and phalanges of the human hand for a South African population was derived.

Studies on the use of proximal phalanges as sex discriminators are rare. Scheuer and Elkington (1993) reported an actual correct sexing accuracy for the first proximal phalanx as 78.0%. Smith (1996) results for the various phalangeal rows showed that the designation of individuals to their correct sex and population groups using proximal phalanges was 76.0 - 79.0%, with middle phalanges it was 72.0 - 79.0% and for distal phalanges the percentages were recorded as 81.0 - 83.0%. Smith was able to show that metacarpals displayed higher discriminating values (87.0 - 89.0%) when compared to phalanges.

Percentage accuracies recorded for metacarpals and phalanges in the present study were similar and as high as those reported by Scheuer and Elkington (1993). The phalanges selected as the best discriminators differed for each series. In the proximal phalangeal series, the first proximal phalanx in males and females (84.0% and 88.8% respectively) and third proximal phalanx in females (88.8%) was selected. For the middle phalangeal series, the third middle phalanx for males (85.0%) and females (86.7%) was selected. The fifth distal phalanx

for males (85.1%) and first distal phalanx for females (84.4%) was listed for the distal phalangeal row. Average percentage accuracies for combined data of males and females, listed proximal phalanx one (86.4%), middle phalanx three (85.9%) and distal phalanx five (84.4%) as the three most dimorphic hand bones. These high percentage accuracies recorded for the phalanges may well place these hand bones on the same level as those of, for example, the femur or pelvis, as useful determinants for sex.

Burrows *et al*. (2003) tested three formulae published by Scheuer and Elkington (1993), Smith (1996) and Steele (1970) in order to establish the validity of hand bones, which included the metacarpals and phalanges, as sex determinants. These authors applied the three formulae to a totally different population which yielded poor classification results. They found that the classification accuracies for males were 100%, when compared to that of females of 10%. The study by these authors further emphasizes the fact that hand bones are no different to the rest of the skeleton in that discrimant formulae devised for hands are population specific.

When discriminant functions are tested they generally tend to deviate from the predicted accuracies (Case & Ross 2007). In the case of the study carried out by Burrows *et al*. (2003), the tested accuracies deviated from predicted accuracies by 10.0%. These authors also reported that 60.0% of the discriminant functions deviated by 5.0 - 10.0%. Based on these results, Burrows *et al*. (2003) suggested using single rather than multiple dimensions in order to obtain better predictive accuracies. From this viewpoint, Case and Ross (2007) then based their study on the findings by Burrows *et al*. (2003) and measured the maximum axial length dimension of both right and left sides of hand and foot bones to establish its accuracy as a sex determinant. They reported that the left hand yielded better results than the right hand, and that hands are to be selected rather than feet. They further concluded that the phalanges are better sex discriminators than metacarpals and metatarsals. In the present study, single and combinations of hand bones yielded high classification accuracies. Also, the classification accuracies for each series of hand bones were similar and this includes the metacarpals, proximal, middle and distal phalanges.

With regard to the different phalangeal series of bones, Case and Ross (2007) found that classification accuracies increased in a distal direction meaning that distal phalanges are preferred over those of the proximal and middle rows. These authors also reported that sexing accuracies using phalanges are far better than using metacarpals or metatarsals. One problem which they encountered was the correct siding of the third digit's middle and distal phalanges and suggested that articulated hand bones would be far easier than an isolated phalangeal bone. To overcome this problem, it is hoped that the key identification and siding features listed in the present study would contribute to the methods devised for sexing hand bones.

In the present study, the anteroposterior measurement of the first proximal phalanx in males was the best discriminator (84.0%). In females, the anteroposterior dimension of the first proximal phalanx (88.8%) and the anteroposterior dimension of the base of the third proximal phalanx (88.8%) were the best discriminators. For the middle phalanges, the mediolateral dimension of the third middle phalanx (85.0% and 86.7% for males and females respectively) is the best discriminator. Thus, the percentages for middle phalanges are slightly higher than for proximal phalanges. These results are similar to those reported by Case and Heilman (2006). For distal phalanges, the length of the fifth distal phalanx in males was the best discriminator (85.1%) while in females it was the anteroposterior dimension of the first distal phalanx (84.8%). These results are in agreement with the high percentages reported by Smith (1996). When compared to the findings of the metacarpals in the present study, length was the least selected dimension.

In summary, these results have shown that individual and combination of hand bones are as sexually dimorphic as those of the lower and rest of the upper extremities. The statistically significant differences between males and females observed in this study compare well to those reported on other aspects of the skeleton for the South African population (Asala 2001, Asala *et al.* 1998, Bidmos 2006, Patriquin *et al*. 2005).

Further research on assessing sexual dimorphism of hand bones with age changes may shed light on how the variables selected for accuracy would change, if at all, at different time periods for the South African population. Another aspect for further investigation would be

to perhaps split the South African population into its two groups, namely, whites and blacks, to establish whether the sexually dimorphic variables selected from this study, would also be applicable to these groups.

In summary, Scheuer and Elkington (1993) have proposed that accuracies of discriminant function formulae need to be above 80% to be usable. In this study most of the formulae yielded accuracies above 80%, with all of them being above 75%. It is hoped that the discriminant function tables and formulae that have been devised for the bones of the hand in a South African population, will contribute to the current and ever-growing osteometric standards initiated by various researchers who have already contributed to these standard techniques for South Africans (Washburn 1949, Keen 1950, De Villiers, 1968, Lundy & Feldesman 1987, Macho 1990, Kieser *et al*. 1992, Loth & Henneberg 1996, Steyn & İşcan 1997, İşcan & Steyn 1999, Loth & İşcan. 2000, Oettle & Steyn 2000, Asala 2001, Partriquin *et al*. 2003).

CHAPTER 11

CONCLUSIONS

11.1 Morphology of the hand bones

From the results on descriptions of the hand bones, the following conclusions can be made:

- The bones of the human hand do have specific features which can be used to identify them.
- Some of these features are unique, which makes it possible to assign a metacarpal or phalanx either to the right or the left hand.
- The morphological detail provided for the shaft, body and base of each hand bone can be applied if fragments of hand bones are recovered.

11.2 STATURE DETERMINATION

From the results on determination of stature, the following conclusions can be made:

- It is possible to regress the length of a hand bone to that of a long limb bone.
- Correlation of hand bones to long bone lengths in males varied in that they were not all correlated to one long limb bone whereas in females, all hand bones were highly correlated to the radius length.
- Regression formulae for hand bones of the South African population were created
- Standard errors, however, were high in comparison to those reported for long limb bones.
- In addition, the estimated long bone length would have to be inserted into a second formula, either that of Lundy and Feldesman (1987) or Dayal *et al*. (2008). This, however, may result in an increase in the standard error of estimates which further emphasises the provisional nature of any stature estimate based on the hands.
- Cadaver lengths recorded in the Pretoria Bone Collection, may need to be re-looked with regard to the manner in which they were measured as some of these recorded dimensions were inaccurate or missing.

- Better results may be obtained if the direct method could be used. In other words, the length of a hand bone is regressed directly against cadaver length. This was, unfortunately, impossible since the cadaver lengths are unreliable.

11.3 SEX DETERMINATION

From the results on determination of sex, the following conclusions can be made:

- The hand bones of South Africans are sexually dimorphic for base and midshaft dimensions rather than for head dimensions.
- Width dimensions are more sexually dimorphic than length measurements.
- South African males were more often misclassified than their female counterparts possibly because males display greater variability in the skeleton than females.
- Metacarpals and first proximal phalangeal bones for the South African population are as sexually dimorphic as hand bones and lower limb bones reported in the literature for other populations.
- Classification accuracies using hand bones were moderately high with percentages recorded for metacarpals as 75.9 - 80.2% and 79.9 - 85.4%, proximal phalanges as 81.7 - 86.9% and 83.2 - 86.4%, middle phalanges as 77.8 - 81.8% and 81.4 - 85.9%, and distal phalanges as 75.6 - 83.9% and 80.3 - 84.5% for single and multiple variables respectively. Average accuracies for males and females generally ranged from 75.9 - 86.9%.
- As the hands used in this study came from a contemporary sample, one would expect that secular trends would have a minimal effect.